Advanced Echocardiography and Clinical Surrogates to Risk Stratify and Manage Patients With Structural Heart Disease

Philippe Debonnaire

Advanced Echocardiography and Clinical Surrogates to Risk Stratify and Manage Patients With Structural Heart Disease
The studies described in this thesis were performed at the Department of Cardiology of Leiden University Medical Center (LUMC), Leiden, The Netherlands

Cover: Philippe Debonnaire
Layout and Printing: Optima Grafische Communicatie, Rotterdam, the Netherlands

ISBN: 978-94-6169-808-7

Advanced Echocardiography and Clinical Surrogates to Risk Stratify and Manage Patients With Structural Heart Disease

Proefschrift

Ter verkrijging van de graad van Doctor aan de Universiteit Leiden,
op gezag van Rector Magnificus prof. mr. C.J.J.M. Stolker,
volgens besluit van het College voor Promoties te verdedigen op
donderdag 28 april 2016 klokke 15.00 uur

door

Philippe Jean Marc Rita Debonnaire
Geboren te Turnhout, België, in 1980

Promotor
Prof. Dr. J.J. Bax

Co-promotores
Dr. V. Delgado
Dr. N. Ajmone Marsan

Leden promotiecommissie:
Prof. Dr. M.J. Schalij
Prof. Dr. R.J. Klautz
Prof. Dr. D.E. Atsma
Dr. E.E. Holman
Prof. Dr. I.C. van Gelder, (University Medical Center Groningen, the Netherlands)
Prof. Dr. J. Van Cleemput (University Hospitals Leuven, Belgium)
Prof. Dr. J.L. Zamorano (University Complutense, Hospital Ramón y Cajal, Madrid, Spain)

To my wife Charlotte, my kids Ralph,
Anaïs and James and to my parents,
the unconditional wind beneath my wings.

TABLE OF CONTENTS

PART II — ECHOCARDIOGRAPHIC DEFORMATION IMAGING

Chapter 1

General Introduction and Outline of the Thesis

Structural heart disease comprises a spectrum of non-coronary based cardiac pathologies, including valvular heart disease and primary hypertrophic cardiomyopathy (HCM). Valvular heart disease involves myopathy secondary to pressure loading (e.g. aortic stenosis) or volume loading (e.g. mitral regurgitation). In primary HCM the myocardium is primarily affected by mutation of sarcomeric protein encoding genes. Both forms of structural heart disease are characterized by structural and functional myocardial changes that ultimately impose a risk of arrhythmia, heart failure and (sudden) death, if left untreated.[1, 2] Thorough risk stratification has therefore become mainstay for decision making concerning the need, timing, and type of therapeutic interventions. In addition adequate patient selection is crucial as these interventions tend to become less invasive, including transcatheter approaches. In this regard, the myriad of non-invasive cardiac imaging modalities and techniques, as well as clinical surrogates, provides unique opportunities for risk stratification and patient selection.

Due to its wide availability, versatility and non-invasive nature, echocardiography remains the first line modality for risk stratification and patient selection for transcatheter therapies. 3-Dimensional (3D) echocardiography offers superior valvular anatomical and structural information compared to 2-dimensional echocardiography and its accuracy to quantify left ventricular ejection fraction is superior to 2-dimensional echocardiography when compared to magnetic resonance imaging as reference standard.[3, 4] Echocardiographic deformation imaging (strain, strain rate) can depict early and preclinical functional alterations of the myocardium.[5] With the advent of advanced automatization, increasing measurement reproducibility, both advanced echocardiographic techniques may fuel further advances to establish their role in the clinical arena of structural heart disease management.[6]

PATIENT SELECTION FOR TRANSCATHETER VALVE THERAPIES: RISK SCORES AND 3-DIMENSIONAL ECHOCARDIOGRAPHY

Significant valvular heart disease, mainly aortic stenosis and mitral regurgitation, affects 3% of the general population, and is associated with increased morbidity and mortality.[7] The coincidence of population ageing with valvular heart disease prevalence raising over 8% in patients older than 65 years, makes that the global burden of valvular heart disease is expected to grow significantly.[7] Due to inherent clustering of co-morbidities, however, many of these patients are at high or even prohibitive risk for conventional valve surgery, the gold standard treatment. Surveys have confirmed that such patients are often denied surgery, associated with dismal outcome.[8, 9] Transcatheter valve therapies provide a valuable therapeutic

alternative for symptomatic patients with severe valvular heart disease that are at high or prohibitive surgical risk. Transcatheter aortic valve implantation (TAVI) comprises the insertion of a self or balloon-expandable bioprosthetic valve within the stenotic native aortic valve via percutaneous route. (Figure 1) Percutaneous mitral valve repair using Mitra-Clip involves placement of a cobalt-chromium clip to attach both mitral leaflets at the origin of the regurgitant jet. This procedure significantly reduces mitral regurgitation severity by creating a double orifice valve and is performed via transfemoral venous access. (Figure 2) Both therapies relief symptoms and are associated with improved functional status, quality of life, reduced heart failure hospitalizations and, in case of TAVI, improved survival when compared to optimal medical therapy.[10-12] Although an attractive option for many patients, the outcome of transcatheter therapies critically depends on adequate patient selection (including risk stratification and technical eligibility assessment) and procedural guidance. Clinical evaluation and 3D cardiac imaging have become key for this purpose.

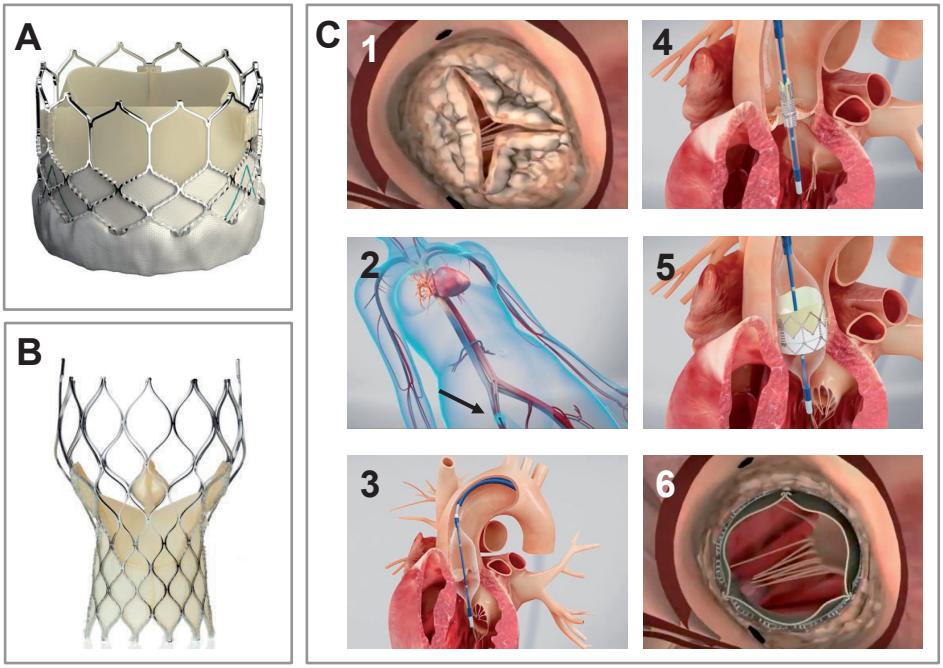

Figure 1.1
Transcatheter aortic valve implantation (TAVI). Panel A: The balloon-expandable Sapien 3 prosthesis (Edwards Lifesciences). Panel B: The self-expandable Evolut R Corevalve prosthesis (Medtronic). Panel C: Procedural principles of TAVI.1: degenerative calcified aortic valve stenosis. 2: arterial transfemoral access. 3: balloon dilatation of diseased native aortic valve. 4: meticulous positioning of a balloon-expandable prosthesis. 5: balloon expansion of the prosthesis within diseased native valve. 6: normal opening of the bioprosthesis.

Risk scores

Surgical risk scores including EuroSCORE and Society of Thoracic Surgeons (STS) score have been widely adopted as a simple tool to calculate 30 day surgical mortality risk and categorize patients into high or prohibitive risk for conventional surgery.[13, 14] Importantly, however, being at increased surgical risk does not imply beneficial outcome when transcatheter therapy is provided. In addition, these surgical risk scores have not been developed nor validated for patients undergoing percutaneous valvular interventions. Apart from procedural related factors, patient related factors including advanced age, renal dysfunction and frailty amongst others may independently relate to outcome after transcatheter therapies. Clinical risk scores, based on preprocedural patient related factors, to predict outcome in case of transcatheter valve therapy are an unmet clinical need that may represent a valuable additional tool for decision making and patient management.[2]

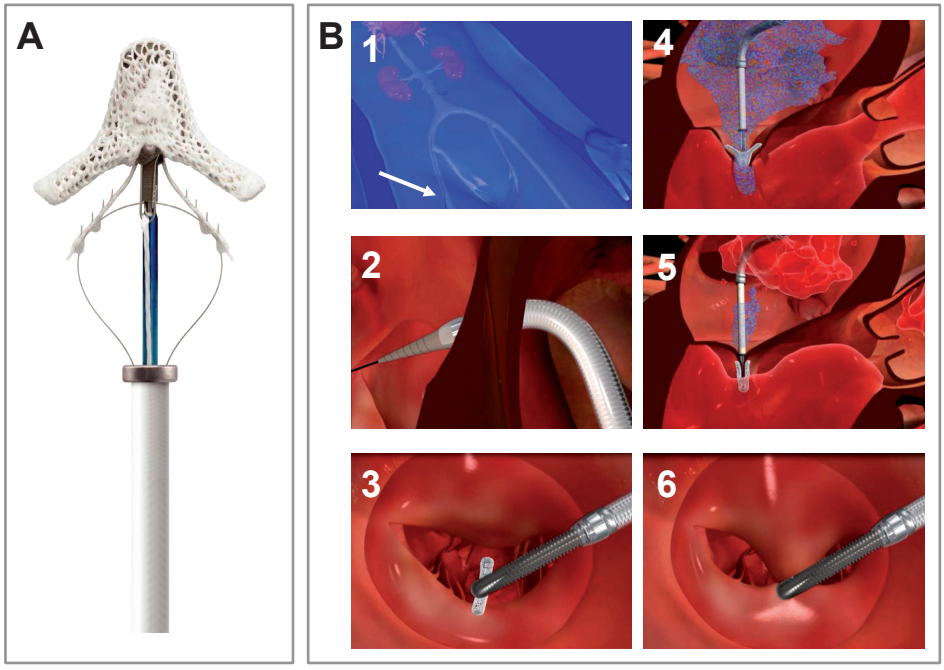

Figure 1.2
Transcatheter mitral valve repair (Mitra-Clip). Panel A: The cobalt-chromium Mitra-Clip (Abbott Vascular). Panel B: Procedural principles of Mitra-Clip.1: venous transfemoral access. 2: transseptal insertion of clip delivery system. 3: Mitra-Clip positioning perpendicular to coaptation line of dysfunctional mitral valve. 4: insertion of clip into left ventricle at site of maximal regurgitation. 5: grasping and clipping of both anterior and posterior mitral valve leaflet with significant regurgitation reduction. 6: double orifice mitral valve.

3-dimensional echocardiography

Tremendous advances have been made by the introduction of matrix-array transducers that allow for acquisition of a 3D pyramidal volume during one or more cardiac cycles while holding breath. Apart from more accurate and reliable semi-automated quantification of ventricular volumes, mass, and ejection fraction compared to conventional echocardiography, 3D-echocardiography has revolutionized cardiac valve assessment, in particular of the mitral valve.[4, 15] The technique permits simultaneous visualization of multiple transsections through a region of interest (multi-plane imaging), allows to cut and examine the 3D volume at any desired level or plane and, even more important, provides the surgical or en face view of the valve. These properties translate into unique, superior and reproducible morphological and structural evaluation of the diseased mitral valve, even for novice readers.[4, 16] (Figure 3) In addition quantification of valve area and (functional) regurgitation can be performed more reliably.[4] Further software analysis also permits to create 3D models of the mitral valve complex to derive a multitude of geometric indices and measures, thereby providing unique pathophysiological insights into mitral valve disease.[4] (Figure 3) Of note, acquisition quality of 3D datasets to avoid artifacts or low temporal resolution, subject to learning curve, is critical for reliable use.

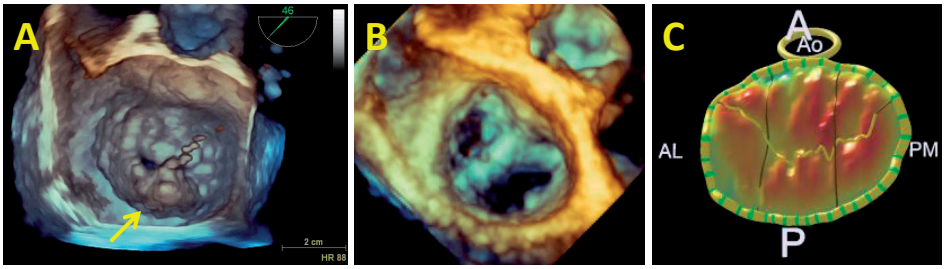

Figure 1.3
Three-dimensional echocardiography of the mitral valve. Panel A: Surgical view with P2 scallop flail (arrow) due to chordal rupture. Panel B: Double orifice valve after central Mitra-Clip. Panel C: 3-dimensional model of complex Barlow disease with diffuse prolapse (red). A: anterior, AL: anterolateral, Ao: aortic valve, P: posterior, PM: posteromedial.

In patients undergoing transcatheter valve therapies, including TAVI and Mitra-Clip, 3D-echocardiography is becoming mainstream for patient selection and procedural guiding.[17] 3D-imaging by echocardiography or computed tomography shows the typical oval shape of the aortic annulus which critically determines the choice of adequate valve prosthesis size in patients undergoing TAVI. In addition 3D transesophageal echocardiography may be useful to assist in adequate positioning of the valve prosthesis during the procedure, an important outcome

determinant.[18] 3D-echocardiography is even more indispensible in patients undergoing Mitra-Clip therapy.[17] Technical eligibility for Mitraclip includes a multitude of anatomic criteria that can easily be assessed by 3D-echocardiography: central (non-commissural) jet origin, mitral valve area > 3.5-4.0 cm^2, no calcification, cleft or significant leaflet thickening in the grasping area, non rheumatic disease, sufficient mobile leaflet length, minimal residual leaflet coaptation length and non extensive tethering (coaptation depth) for functional regurgitation and non extensive flail width and gap for organic regurgitation.[19] Equally important 3D-echocardiography is the cornerstone during procedural guidance as, contrary to TAVI, fluoroscopic imaging has a very limited role to depict the mitral valve.

DEFORMATION IMAGING IN STRUCTURAL HEART DISEASE: ECG AND ECHOCARDIOGRAPHIC SURROGATES OF CARDIAC FIBROSIS

Myocardial Fibrosis

Myocardial fibrosis refers to increased collagen content in the myocardium. *Focal fibrosis* comprises myocardial cell loss replaced by collagen (replacement fibrosis, scar), while *diffuse fibrosis* represents increased interstitial collagen without notable cell loss (interstitial fibrosis).[20, 21] Diffuse fibrosis often precedes focal fibrosis and is predominantly found in non-ischemic mitral regurgitation patients.[22] Focal fibrosis to a variable extent is found in 30-60% of patients with aortic stenosis and in 42-71% of primary HCM patients.[23-27] Presence of fibrosis adversely affects myocardial diastolic and later systolic function due to reduced myocardial compliance and increased stiffness and relates to structural remodeling. Moreover, it provides a substrate for re-entry tachyarrhythmia. Fibrosis has been linked to clinical translates such as symptom and arrhythmia onset, heart failure and even (sudden) death.[23, 27] Identification of fibrosis therefore provides an attractive target that may hold the key for early risk stratification and hence decision-making in patients with structural heart disease.

ECG and fibrosis

Fragmentation of QRS complexes on surface ECG (comprising various RSR' patterns) has been related to fibrosis in both ischemic and non-ischemic cardiomyopathy.[28, 29] Moreover its presence was shown to be associated with adverse outcome in a variety of cardiomyopathies such as ischemic cardiomyopathy, arrhythmogenic right ventricular dysplasia, Brugada syndrome and idiopathic dilated cardiomyopathy.[30-32] Abnormal ECG findings are noted in 75 up to 95% of primary HCM patients, however, no such abnormalities have consistently shown a

relationship to poor outcome in these patients. The presence and potential clinical value of QRS fragmentation, as a surrogate marker of fibrosis, has been poorly explored in this patient population.

Deformation imaging and fibrosis

Speckle tracking echocardiography involves frame by frame tracking of natural acoustic markers present in B-mode images, so called 'speckles', during the cardiac cycle. This technique measures displacement of myocardial segments and allows semi-automated quantification of velocity, relative myocardial length changes (strain) and the speed of these changes (strain rate) in longitudinal, circumferential and radial direction, due to its angle independency.[33] In addition the wringing motion of the left ventricle with clockwise rotation of the base and anticlockwise movement of the apex, due to the helical myocardial architecture, can be assessed as rotation and twist (net rotation difference between base and apex).[33] It is a robust imaging technique, validated against sono-micrometry, that offers great opportunities to study the complex myocardial atrial and ventricular function, far more sensitive than ejection fraction.[34] The average peak systolic strain value of all segments of the left ventricle is expressed as global longitudinal strain and often represented by a color-coded bull's eye plot. (Figure 4)

Longitudinal deformation is predominantly determined by endocardial fibers and explored most as the subendocardium is most vulnerable and early affected in the vast majority of cardiomyopathies. Longitudinal deformation is determined by intrinsic myocardial contractility, chamber structure, geometry, loading conditions and, importantly, fibrosis extent.[35] Therefore it represents a valuable and sensitive marker yielding great potential as a biological signal related to multiple clinical endpoints in patients with structural heart disease, often regarded as a surrogate marker of fibrosis. As longitudinal dysfunction precedes overt left ventricular dysfunction in terms of reduced ejection fraction, it represents an ideal tool to detect subclinical dysfunction. Indeed, impaired left ventricular longitudinal deformation despite preserved left ventricular ejection has been consistently shown in patients with significant aortic stenosis, mitral regurgitation and hypertrophic cardiomyopathy.[36-38] In valvular heart disease (early) impaired longitudinal deformation relates to symptom onset, heart failure, decreased survival and worse postoperative outcome.[38-40] In primary HCM a relation with decreased survival and tachyarrhytmia has been shown.[41] Although atrial remodeling is present in both mitral regurgitation and primary HCM, related to dismal outcome, the clinical value of left atrial function, assessed by deformation imaging, is far less elucidated. (Figure 4)

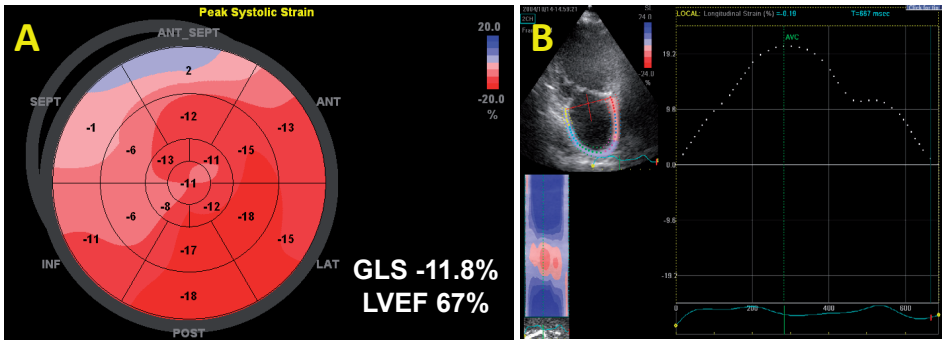

Figure 1.4
Left ventricular and atrial longitudinal strain. Panel A: Bull's eye plot showing reduced left ventricular global longitudinal strain (GLS) despite normal left ventricular ejection fraction (LVEF) in a patient with primary hypertrophic cardiomyopathy. Maximal hypertrophy in septal and anteroseptal region corresponds to most impaired longitudinal deformation (blue and pink). Panel B: Left atrial longitudinal strain assessment.

Objectives and outline of the thesis

In this thesis we explore the risk stratification and management of patients with structural heart disease, focusing on valvular heart disease and primary HCM. In particular the potential clinical role of advanced echocardiography including 3D-echocardiography and deformation imaging (strain), as well as clinical surrogates are studied. Although risk often comprises a continuum rather than a dichotomous phenomenon, its assessment is a prerequisite for clinical decision making in daily practice.

Part I focuses on the potential role of 3-dimensional echocardiography. At first a clinical risk score model for prediction of outcome in patients undergoing TAVI is presented (Chapter 2). Second the role of 3D-echocardiography is explored in depth in patients with mitral valve disease. Different non-invasive cardiac imaging modalities to evaluate mitral valve function and anatomy are described and the use of 3D-echocardiography is put into perspective (Chapter 3). We then evaluate the role of the latter to gain insights in patients with functional mitral regurgitation (Chapter 4), to select patients and guide procedures regarding percutaneous mitral valve repair using Mitra-Clip (Chapter 5) and to assess the effect of Mitra-Clip on the mitral valve (Chapter 6).

In Part II we further elaborate the potential role of risk stratification by ECG and myocardial deformation imaging (strain), as surrogate markers of fibrosis. Surface ECG fragmentation in primary HCM is first evaluated (Chapter 7). The important future role of fibrosis imaging in valvular heart disease patients is then reviewed (Chapter 8). Finally the role of left atrial structure and function is evaluated in patients with mitral regurgitation (Chapter 9) and primary HCM (Chapter 10, 11).

REFERENCES

1. Authors/Task Force members, Elliott PM, Anastasakis A, et al. 2014 ESC Guidelines on diagnosis and management of hypertrophic cardiomyopathy: the Task Force for the Diagnosis and Management of Hypertrophic Cardiomyopathy of the European Society of Cardiology (ESC). *Eur Heart J.* 2014;35:2733-2779.
2. Joint Task Force on the Management of Valvular Heart Disease of the European Society of Cardiology, European Association for Cardio-Thoracic Surgeons, Vahanian A, et al. Guidelines on the management of valvular heart disease (version 2012). *Eur Heart J.* 2012;33:2451-2496.
3. Lang RM, Badano LP, Mor-Avi V, et al. Recommendations for cardiac chamber quantification by echocardiography in adults: an update from the american society of echocardiography and the European association of cardiovascular imaging. *Eur Heart J Cardiovasc Imaging.* 2015;16:233-271.
4. Lang RM, Tsang W, Weinert L, et al. Valvular heart disease. The value of 3-dimensional echocardiography. *J Am Coll Cardiol.* 2011;58:1933-1944.
5. Mor-Avi V, Lang RM, Badano LP, et al. Current and evolving echocardiographic techniques for the quantitative evaluation of cardiac mechanics: ASE/EAE consensus statement on methodology and indications endorsed by the Japanese Society of Echocardiography. *J Am Soc Echocardiogr.* 2011;24:277-313.
6. Voigt JU, Pedrizzetti G, Lysyansky P, et al. Definitions for a common standard for 2D speckle tracking echocardiography: consensus document of the EACVI/ASE/Industry Task Force to standardize deformation imaging. *Eur Heart J Cardiovasc Imaging.* 2015;16:1-11.
7. Nkomo VT, Gardin JM, Skelton TN, et al. Burden of valvular heart diseases: a population-based study. *Lancet.* 2006;368:1005-1011.
8. Mirabel M, Iung B, Baron G, et al. What are the characteristics of patients with severe, symptomatic, mitral regurgitation who are denied surgery? *Eur Heart J.* 2007;28:1358-1365.
9. Iung B, Baron G, Butchart EG, et al. A prospective survey of patients with valvular heart disease in Europe: The Euro Heart Survey on Valvular Heart Disease. *Eur Heart J.* 2003;24:1231-1243.
10. Leon MB, Smith CR, Mack M, et al. Transcatheter aortic-valve implantation for aortic stenosis in patients who cannot undergo surgery. *N Engl J Med.* 2010;363:1597-1607.
11. Mauri L, Foster E, Glower DD, et al. 4-year results of a randomized controlled trial of percutaneous repair versus surgery for mitral regurgitation. *J Am Coll Cardiol.* 2013;62:317-328.
12. Swaans MJ, Bakker AL, Alipour A, et al. Survival of transcatheter mitral valve repair compared with surgical and conservative treatment in high-surgical-risk patients. *JACC Cardiovasc Interv.* 2014;7:875-881.
13. O'Brien SM, Shahian DM, Filardo G, et al. The Society of Thoracic Surgeons 2008 cardiac surgery risk models: part 2--isolated valve surgery. *Ann Thorac Surg.* 2009;88:S23-42.
14. Nashef SA, Roques F, Sharples LD, et al. EuroSCORE II. *Eur J Cardiothorac Surg.* 2012;41:734-744; discussion 744-735.
15. Lang RM, Mor-Avi V, Dent JM, et al. Three-dimensional echocardiography: is it ready for everyday clinical use? *JACC Cardiovasc Imaging.* 2009;2:114-117.
16. Tsang W, Weinert L, Sugeng L, et al. The value of three-dimensional echocardiography derived mitral valve parametric maps and the role of experience in the diagnosis of pathology. *J Am Soc Echocardiogr.* 2011;24:860-867.

17. Zamorano JL, Badano LP, Bruce C, et al. EAE/ASE recommendations for the use of echocardiography in new transcatheter interventions for valvular heart disease. *Eur Heart J*. 2011;32:2189-2214.
18. Smith LA, Dworakowski R, Bhan A, et al. Real-time three-dimensional transesophageal echocardiography adds value to transcatheter aortic valve implantation. *J Am Soc Echocardiogr*. 2013;26:359-369.
19. Feldman T, Foster E, Glower DD, et al. Percutaneous repair or surgery for mitral regurgitation. *N Engl J Med*. 2011;364:1395-1406.
20. Krenning G, Zeisberg EM, Kalluri R. The origin of fibroblasts and mechanism of cardiac fibrosis. *J Cell Physiol*. 2010;225:631-637.
21. Mewton N, Liu CY, Croisille P, et al. Assessment of myocardial fibrosis with cardiovascular magnetic resonance. *J Am Coll Cardiol*. 2011;57:891-903.
22. Fuster V, Danielson MA, Robb RA, et al. Quantitation of left ventricular myocardial fiber hypertrophy and interstitial tissue in human hearts with chronically increased volume and pressure overload. *Circulation*. 1977;55:504-508.
23. Weidemann F, Herrmann S, Stork S, et al. Impact of myocardial fibrosis in patients with symptomatic severe aortic stenosis. *Circulation*. 2009;120:577-584.
24. Dweck MR, Joshi S, Murigu T, et al. Midwall fibrosis is an independent predictor of mortality in patients with aortic stenosis. *J Am Coll Cardiol*. 2011;58:1271-1279.
25. Debl K, Djavidani B, Buchner S, et al. Delayed hyperenhancement in magnetic resonance imaging of left ventricular hypertrophy caused by aortic stenosis and hypertrophic cardiomyopathy: visualisation of focal fibrosis. *Heart*. 2006;92:1447-1451.
26. Ho CY, Lopez B, Coelho-Filho OR, et al. Myocardial fibrosis as an early manifestation of hypertrophic cardiomyopathy. *N Engl J Med*. 2010;363:552-563.
27. Chan RH, Maron BJ, Olivotto I, et al. Prognostic value of quantitative contrast-enhanced cardiovascular magnetic resonance for the evaluation of sudden death risk in patients with hypertrophic cardiomyopathy. *Circulation*. 2014;130:484-495.
28. Das MK, Khan B, Jacob S, et al. Significance of a fragmented QRS complex versus a Q wave in patients with coronary artery disease. *Circulation*. 2006;113:2495-2501.
29. Das MK, Suradi H, Maskoun W, et al. Fragmented wide QRS on a 12-lead ECG: a sign of myocardial scar and poor prognosis. *Circ Arrhythm Electrophysiol*. 2008;1:258-268.
30. Das MK, Maskoun W, Shen C, et al. Fragmented QRS on twelve-lead electrocardiogram predicts arrhythmic events in patients with ischemic and nonischemic cardiomyopathy. *Heart Rhythm*. 2010;7:74-80.
31. Morita H, Kusano KF, Miura D, et al. Fragmented QRS as a marker of conduction abnormality and a predictor of prognosis of Brugada syndrome. *Circulation*. 2008;118:1697-1704.
32. Peters S, Trummel M, Koehler B. QRS fragmentation in standard ECG as a diagnostic marker of arrhythmogenic right ventricular dysplasia-cardiomyopathy. *Heart Rhythm*. 2008;5:1417-1421.
33. Blessberger H, Binder T. Non-invasive imaging: Two dimensional speckle tracking echocardiography: basic principles. *Heart*. 2010;96:716-722.
34. Amundsen BH, Helle-Valle T, Edvardsen T, et al. Noninvasive myocardial strain measurement by speckle tracking echocardiography: validation against sonomicrometry and tagged magnetic resonance imaging. *J Am Coll Cardiol*. 2006;47:789-793.
35. Bijnens BH, Cikes M, Claus P, et al. Velocity and deformation imaging for the assessment of myocardial dysfunction. *Eur J Echocardiogr*. 2009;10:216-226.

36. Serri K, Reant P, Lafitte M, et al. Global and regional myocardial function quantification by two-dimensional strain: application in hypertrophic cardiomyopathy. *J Am Coll Cardiol*. 2006;47:1175-1181.
37. Ng AC, Delgado V, Bertini M, et al. Alterations in multidirectional myocardial functions in patients with aortic stenosis and preserved ejection fraction: a two-dimensional speckle tracking analysis. *Eur Heart J*. 2011;32:1542-1550.
38. Witkowski TG, Thomas JD, Debonnaire PJ, et al. Global longitudinal strain predicts left ventricular dysfunction after mitral valve repair. *Eur Heart J Cardiovasc Imaging*. 2013;14:69-76.
39. Kusunose K, Goodman A, Parikh R, et al. Incremental prognostic value of left ventricular global longitudinal strain in patients with aortic stenosis and preserved ejection fraction. *Circ Cardiovasc Imaging*. 2014;7:938-945.
40. Yingchoncharoen T, Gibby C, Rodriguez LL, et al. Association of myocardial deformation with outcome in asymptomatic aortic stenosis with normal ejection fraction. *Circ Cardiovasc Imaging*. 2012;5:719-725.
41. Saito M, Okayama H, Yoshii T, et al. Clinical significance of global two-dimensional strain as a surrogate parameter of myocardial fibrosis and cardiac events in patients with hypertrophic cardiomyopathy. *Eur Heart J Cardiovasc Imaging*. 2012;13:617-623.

Part I

3-Dimensional echocardiography

Chapter 2

Value of the *'TAVI$_2$-SCORe'* versus Surgical Risk Scores for Prediction of One Year Mortality in 511 Patients Undergoing Transcatheter Aortic Valve Implantation

Philippe Debonnaire, Laura Fusini, Ron Wolterbeek, Vasileios Kamperidis, Philippe van Rosendael, Frank van der Kley, Spyridon Katsanos, Emer Joyce, Gloria Tamborini, Manuela Muratori, Paola Gripari, Jeroen J Bax, Nina Ajmone Marsan, Mauro Pepi, Victoria Delgado

Am J Cardiol, 2015 Jan 15;115(2):234-242.

ABSTRACT

Objectives

A bed-side available transcatheter aortic valve implantation (TAVI)-dedicated prognostic risk score is an unmet clinical need. We aimed to develop such a risk score predicting 1-year mortality post-TAVI and to compare it to the performance of the logistic EuroSCORE I (LES-I) and II (LES-II) and the Society of Thoracic Surgeons (STS) score.

Methods and Results

Baseline variables of 511 consecutive patients undergoing TAVI that were independently associated with 1-year mortality post-TAVI were included in the *$TAVI_2$-SCORe*. Discrimination and calibration abilities of the novel score were assessed and compared to surgical risk scores. One-year mortality was 17.0% (n=80/471). Porcelain **T**horacic aorta (HR 2.56), **A**nemia (HR 2.03), left **V**entricular dysfunction (HR 1.98), recent myocardial **I**nfarction (HR 3.78), male **S**ex (HR 1.81), **C**ritical aortic valve stenosis (HR 2.46), **O**ld age (HR 1.68) and **Re**nal dysfunction (HR 1.76) formed the *$TAVI_2$-SCORe (all p<0.05)*. According to number of points assigned (1 for each variable and 2 for infarction), patients were stratified into 5 risk categories: 0, 1 (HR 2.6), 2 (HR 3.6), 3 (HR 10.5) and ≥4 (HR 17.6). *$TAVI_2$-SCORe* showed best discrimination ability (Harrells`C statistic 0.715) compared to LES-I, LES-II and STS scores (0.609, 0.633 and 0.50, respectively). Cumulative 1-year survival was 54% versus 88% for patients with *$TAVI_2$-SCORE* ≥3 versus <3 points, respectively (p<0.001). Contrary to surgical risk scores, there was no significant difference between observed and expected 1-year mortality for all *$TAVI_2$-SCORe* risk strata (all p>0.05, Hosmer-Lemeshow statistic 0.304), suggesting superior calibration performance.

Conclusions

The *$TAVI_2$-SCORe* is an accurate, simple and bed-side available score predicting 1-year mortality post-TAVI, outperforming conventional surgical risk scores for this endpoint.

INTRODUCTION

Current guidelines recommend transcatheter aortic valve implantation (TAVI) to improve symptoms and/or survival in symptomatic patients with severe aortic valve stenosis and high or prohibitive risk for surgical aortic valve replacement.[1] Candidate selection for TAVI is based on the heart-team decision.[1] Current surgical risk scores, including the logistic EuroSCORE I (LES-I), the logistic EuroSCORE II (LES-II) or the Society of Thoracic Surgeons (STS) score predict 30 day survival after conventional surgery and are used to identify high or prohibitive surgical risk patients.[1, 2] These risk scores, however, are not designed nor validated to assess mortality risk for TAVI. In particular, a few studies that have evaluated the value of conventional surgical risk scores to predict 1-year mortality after TAVI concluded that the heart-team evaluation remains the cornerstone in decision-making in the absence of a TAVI-dedicated risk score that might have superior discrimination or calibration properties than conventional surgical risk scores.[3-6] Accordingly, a risk score to predict outcome after TAVI and thereby optimize the selection of patients remains an unmet clinical need.[7, 8] The aim of the current study was to test and compare the performance of LES-I, LES-II and STS score to a newly developed TAVI-dedicated clinical risk score to predict 1-year mortality post-TAVI. We hypothesized that a TAVI-dedicated risk score based on baseline preprocedural patient characteristics might be superior to conventional surgical risk scores in predicting survival.

METHODS

Patient population

Patients with symptomatic severe aortic stenosis (valve area <1.0 cm^2 and/or <0.6 cm^2/m^2 and/or mean gradient ≥40 mmHg) who underwent TAVI at the Leiden University Medical Center (Leiden, the Netherlands) and Centro Cardiologico Monzino IRCCS (Milan, Italy) between November 2007 and November 2012 were included. All patients were considered to be at high or prohibitive surgical risk, according to the heart-team decision. Baseline patient demographic data, cardiovascular risk factors, symptoms, medication, laboratory variables and 2-dimensional transthoracic echocardiographic data were retrospectively analyzed.

Echocardiography

Baseline transthoracic 2-dimensional echocardiography was performed using commercially available ultrasound systems (Vivid 7 and E9, GE Medical Systems, Horten, Norway and iE33, Philips Medical systems). Standard gray-scale and Dop-

pler ECG-triggered cine-loop images were acquired and transferred to a workstation for off-line analysis (EchoPAC version 110.0.0 or 112.0.0). Left ventricular (LV) assessment was performed as recommended, including LV linear dimensions measured at the parasternal long-axis view and LV mass calculated using the Devereux's formula and indexed to body surface area.[9] LV volumes and ejection fraction were measured according to the Simpson's method. Similarly, left atrial volume was determined. All volumes were indexed to the body surface area. Early mitral inflow velocity (E) was measured on pulsed wave Doppler recordings with the sample volume located at the tips of the mitral leaflets and the early septal mitral annular velocity (E') was assessed on apical 4-chamber tissue-Doppler acquisitions.[10] Subsequently the E/E' ratio was calculated. Mitral, aortic and tricuspid valve regurgitation were evaluated using spectral and color-Doppler images and semi-quantitatively graded as trivial, mild, moderate and severe, as recommended.[11] Aortic valve area was assessed using the continuity equation and indexed to the body surface area.[12] On continuous wave Doppler acquisitions in the apical 5-chamber view the mean transaortic valve gradient was measured.[12] Maximal tricuspid regurgitant jet velocity combined with inferior caval vein respiratory variation was used to calculate systolic pulmonary arterial pressure.[13]

Mortality risk factors

Baseline patient data were used to calculate individual values of conventional surgical risk scores that assess the probability of 30 day mortality after cardiac surgery: LES-I, LES-II and STS score. Parameters were entered according to the website definitions. Additional baseline factors, potentially relating to increased risk of mortality after TAVI, were also collected. These included laboratory findings such as hemoglobin, C-reactive protein (CRP), serum albumin, aspartate transaminase (AST), alanin aminotransferase (ALT) and total bilirubin. Poor mobility and neurologic dysfunction were defined in accordance with website definitions applied in the LES-II. Frailty was present when evidence existed of a syndrome of decreased reserve and resistance to stressors, resulting from multiple declines across multiple physiologic systems, leading to vulnerability to adverse outcomes.[14, 15] Cognitive dysfunction or dementia was noted if mentioned in the medical history. Porcelain aorta and hostile chest were defined in accordance with recent VARC-2 consensus definitions.[16] Urgent procedural need comprised patients requiring intervention on current admission for medical reasons.

TAVI procedure

The vast majority of TAVI procedures (n=499, 98%) were performed using a balloon-expandable Edwards-Sapien prosthesis (Edwards Lifesciences, Irvine, CA)

of 23, 26, or 29 mm. A minority of patients (n=12, 2%) received a self-expandable CoreValve prosthesis (Medtronic, Minneapolis, USA), using similar sizes. Prosthesis sizing was based on aortic annulus measurements using 3-dimensional imaging techniques (multidetector row computed tomography [preferably] or transesophageal echocardiography). The transfemoral route was used in 268 patients (52%), while a transapical route was chosen in 243 subjects (48%) because of unsuitable anatomy or intervention/surgery of the arterial vascular tree or in case of porcelain aorta.[7] All procedures were performed during general anaesthesia under fluoroscopic and transesophageal echocardiography guidance.

Study endpoint

All-cause mortality 1-year after TAVI was the primary study endpoint. Survival and causes of death were assessed for all patients by consulting the patient's medical files and the official Dutch National Survival Registry.

Statistical analysis

Continuous variables, reported as mean ± SD if normally distributed and as median with interquartile range if non-normally distributed, were compared with the Student-T test and Mann Whitney U test, respectively. Categorical data are given as percentages and compared by χ^2-test or Fisher exact test as appropriate. First, performance of conventional surgical risk score models to predict 1-year mortality was evaluated.[17, 18] Discrimination (ability to correctly identify high versus low mortality risk) was evaluated by Harrell`s C statistic. The cumulative survival was assessed with the Kaplan Meier method dichotomizing the patients into high versus low mortality risk, using >20% versus ≤20% for LES-I, >8% versus ≤8% for LES-II and >10% versus ≤10% for STS-score, respectively.[19] Calibration (ability to match patients' expected versus observed mortality) was determined by binomial testing of expected versus observed overall mortality and according to risk score quartiles. In addition Hosmer-Lemeshow goodness of fit statistic was calculated for all surgical risk scores. A value <0.05 indicates significant difference in expected versus observed mortality.

Second, a new TAVI-dedicated 1-year mortality risk prediction model was developed, restricted to demographic, clinical, biochemical and echocardiographic patient factors present at baseline. Exploratory categorizing of baseline parameters into nominal variables by different cut-off levels was performed and tested at univariate Cox regression analysis. Categorical baseline parameters available in approximately all study patients and achieving univariate significance level of $p<0.05$, were entered in a multivariate Cox regression model, using a backward elimination approach. Multivariate analysis identified risk factors independently

related to 1-year mortality after TAVI. These risk factors were assigned 1 or 2 points, proportional to their respective hazard ratios, to create a simple scoring system, the *TAVI$_2$-SCORe* (porcelain *T*horacic aorta, *A*nemia, *V*entricular dysfunction, recent myocardial *I*nfarction, male *S*ex category, *C*ritical aortic valve stenosis, *O*ld age and *Re*nal dysfunction). According to the number of points assigned, patients were divided into different risk categories.

Third, the performance of the newly developed *TAVI$_2$-SCORe* model was evaluated using identical discrimination and calibration statistics as described above. In addition internal validation of the model's discriminatory power was performed by bootstrap validation of Harrell`s C statistic on 100 samples drawn from the patient cohort. The mean difference in performance between each bootstrap sample and its corresponding performance in the original patient sample (optimism) was used to correct the initial Harrell's C statistic of the original patient cohort for the *TAVI$_2$-SCORe* model.

Fourth, the performance of the new *TAVI$_2$-SCORe* to predict 1-year mortality after TAVI versus that of the conventional surgical risk scores was evaluated based on available results of discrimination and calibration for the respective scores.

SPSS version 20.0. (SPSS Inc., Chicago, Illinois) was used for statistical analysis. A p-value of <0.05 was considered statistically significant for all tests that were 2-sided.

RESULTS

A total of 511 patients (median age 82 [77-86] years, 38% male) were included, of which 207 (41%) were treated in Leiden and 304 (59%) in Milan. A total of 36 patients were excluded because of incomplete data to calculate respective conventional surgical risk scores. Baseline characteristics are listed in Table 1. All patients were at high or prohibitive surgical risk as indicated by mean LES-I, LES-II and STS score. No patients were lost to follow-up for evaluation of the study endpoint. Within 30 days, 29 (5.7%) died, mainly from cardiovascular causes (n=25, 86%), as summarized in Table 2. Peri-procedural death occurred in 12 patients. In addition 51 individuals died between 30 days and 1-year, resulting in overall 1-year mortality of 17.0% (n=80/471). Mortality between 30 days and 1-year was attributed to cardiovascular cause in 47% (n=24) of patients. One year mortality rates were similar between both centers (p=0.88). Patients were further dichotomized based on 1-year mortality status, as shown in Table 1. Patients who died within 1-year after TAVI showed significantly higher LES-I and LES-II than patients who survived and tended to have higher STS score.

Table 2.1
Baseline characteristics of overall study population and stratified according to survival status one year post transcatheter aortic valve implantation.

		At One Year		
Variable	Overall n=511	Alive (n=391)	Dead (n=80)	p value
Age (years)	82 (77-86)	82 (77-86)	83 (78-87)	0.28
Men	194 (38%)	135 (35%)	40 (50%)	0.009
Body surface area (m^2)	1.77±0.21	1.76±0.20	1.77±0.23	0.68
Body mass index (kg/m^2)	26±4	26±4	25±4	0.16
Sinus rhythm	393 (77%)	303 (78%)	58 (73%)	0.34
Hypertension	423 (83%)	319 (82%)	66 (83%)	0.85
Diabetes mellitus II	141 (28%)	106 (27%)	23 (29%)	0.76
Smoker	175 (35%)	134 (34%)	23 (30%)	0.34
Hypercholesterolemia	309 (61%)	225 (58%)	50 (63%)	0.41
Medications				
β-blocker	267 (52%)	201 (51%)	42 (53%)	0.86
Diuretics	375 (73%)	285 (73%)	64 (80%)	0.19
Spironolactone	102 (20%)	76 (19%)	21 (26%)	0.17
Angiotenisn converting enzyme inhibitor and/or angiotensin II receptor blocker	302 (59%)	240 (61%)	44 (55%)	050
Statin	247 (48%)	180 (46%)	41 (51%)	0.40
Insulin	77 (15%)	55 (14%)	14 (18%)	0.43
Inotrope(s)	22 (4%)	17 (4%)	4 (5%)	0.77
New York Heart Association class				0.009
I	17 (3%)	14 (4%)	1 (1%)	
II	132 (26%)	106 (27%)	12 (15%)	
III	252 (50%)	196 (50%)	40 (5%)	
IV	109 (21%)	75 (19%)	27 (34%)	
Syncope	105 (21%)	83 (21%)	16 (20%)	0.81
Angina pectoris	180 (35%)	140 (36%)	26 (33%)	0.57
Logistic Euroscore I (%)	18.3 (12.1-27.7)	17.8 (12.1-26.1)	22.6 (14.3-34.5)	0.002
Logistic Euroscore II (%)	6.4 (4.0-10.6)	6.1 (3.9-10.1)	9.1 (5.5-14.1)	<0.001
STS score (%)	16.6 (12.5-22.1)	16.4 (12.5-21.9)	17.8 (12.9-23.5)	0.14
Dialysis	4 (0.8%)	4 (1%)	0 (0%)	1.00
Chronic obstructive pulmonary disease	148 (29%)	107 (27%)	31 (39%)	0.042
Peripheral artery disease	242 (47%)	179 (46%)	44 (55%)	0.13
Porcelain aorta	58 (11%)	36 (9%)	17 (21%)	0.002
Prior stroke/transient ischemic attack	74 (14%)	58 (15%)	9 (11%)	0.40
Recent myocardial infarction (<90 days)	12 (2%)	6 (2%)	5 (6%)	0.025
Prior cardiac surgery	127 (25%)	92 (24%)	22 (28%)	0.45

Table 2.1 (continued)

Variable	Overall n=511	At One Year		p value
		Alive (n=391)	Dead (n=80)	
Prior percutaneous coronary intervention	121 (24%)	90 (23%)	20 (25%)	0.84
Poor mobility	140 (28%)	110 (28%)	24 (30%)	0.75
Neurologic dysfunction	42 (8%)	35 (9%)	7 (9%)	0.95
Frailty	98 (21%)	74 (20%)	20 (26%)	0.22
Cognitive dysfunction/dementia	55 (11%)	43 (11%)	12 (15%)	0.31
Ascites	4 (1%)	2 (1%)	2 (3%)	0.14
Cirrosis	15 (3%)	11 (3%)	4 (5%)	0.30
Hostile chest	93 (18%)	70 (18%)	14 (18%)	0.92
Creatinine clearance (ml/kg/min)	49 (36-61)	49 (36-61)	44 (31-58)	0.07
Hemoglobin (g/dl)	12.1±1.6	12.1±1.6	11.7±1.6	0.047
C reactive protein (mg/dl)	4.0 (2-10)	3.4 (1.8-8.8)	7.0 (2.7-15.1)	0.010
Albumin (g/dl)	3.8±0.5	3.8±0.5	3.6±0.6	0.030
Total bilirubin (μmol/l)	0.81 (0.63-1.20)	0.80 (0.61-1.10)	0.98 (0.67-1.40)	0.009
Aspartate transaminase (U/l)	23 (18-29)	22 (18-28)	25 (20-34)	0.009
Alanin aminotransferase (U/l)	17 (13-23)	17 (13-22)	19 (14-26)	0.06
Left ventricular end-diastolic diameter (mm)	48±8	48±8	48±8	0.78
Left ventricular end-systolic diameter (mm)	31±9	31±9	32±10	0.53
Left ventricular mass index (g/m^2)	145±40	146 ± 40	150±41	0.37
Left ventricular end-diastolic volume index (ml/m^2)	52 (42-68)	53 (42-68)	50 (41-70)	0.45
Left ventricular end-systolic volume index (ml/m^2)	21 (15-34)	21 (15-34)	24 (15-37)	0.37
Left ventricular ejection fraction (%)	58 (46-66)	58 (48-66)	54 (39-61)	0.008
Left atrial volume index (ml/m^2)	54±23	55±24	52±16	0.32
E/e`	26 (18-37)	26 (17-37)	32 (20-40)	0.18
Systolic pulmonary arterial pressure (mmHg)	39 (30-46)	39 (31-46)	42 (32-49)	0.009
Aortic regurgitation ≥ grade 3	25 (5%)	19 (5%)	1 (4%)	1.00
Mitral regurgitation ≥ grade 3	33 (7%)	26 (7%)	5 (7%)	1.00
Tricuspid regurgitation ≥ grade 3	32 (6%)	22 (6%)	7 (9%)	0.29
Aortic valve mean gradient (mmhg)	47±17	48±16	47±20	0.43
Aortic valve area indexed (cm^2/m^2)	0.38±0.10	0.38±0.10	0.38±0.09	0.87
Urgent procedural need	45 (9%)	28 (7%)	14 (18%)	0.003

Hypertension: history of high blood pressure and/or on antihypertensive treatment. Hypercholesterolemia: history of hypercholesterolemia and/or on statin therapy.

Table 2.2
Causes of death post transcatheter aortic valve implantation.

Variable	first 30 days n=29	30 days - one year n=51	overall n=80
Cardiovascular	25 (86%)	24 (47%)	49 (61%)
Cardiogenic shock/heart failure	11 (38%)	10 (20%)	21 (26%)
Vascular access problems	7 (24%)	0	7 (14%)
iliac dissection	3 (10%)	0	3 (4%)
aortic dissection	4 (14%)	0	4 (5%)
Sudden death	2 (7%)	3 (6%)	5 (6%)
Stroke	0	5 (10%)	5 (6%)
Myocardial infarction	0	1 (2%)	1 (1%)
Aortic annulus rupture	1 (3%)	0	1 (1%)
Left main coronary occlusion	1 (3%)	0	1 (1%)
Interventricular septum rupture	1 (3%)	0	1 (1%)
Acute bowel ischemia	1 (3%)	1 (2%)	2 (3%)
Intestinal bleeding	1 (3%)	2 (4%)	2 (3%)
Pulmonary embolism	0	2 (4%)	2 (3%)
Non cardiovascular	4 (14%)	27 (53%)	31 (39%)
Infection	1 (3%)	6 (12%)	7 (9%)
Traffic accident	1 (3%)	1 (2%)	2 (3%)
Unknown	2 (3%)	11 (22%)	13 (16%)
Renal failure	0	2 (4%)	2 (3%)
Respiratory failure	0	2 (4%)	2 (3%)
Liver failure	0	2 (4%)	2 (3%)
Femur fracture	0	1 (2%)	1 (1%)
Oncologic	0	2 (4%)	2 (3%)

Surgical risk scores and 1-year mortality

The Harrell's C statistic for LES-I, LES-II and STS score to predict 1-year mortality after TAVI was 0.609 (p=0.002), 0.633 (p<0.001) and 0.500 (p=0.14), respectively. Kaplan Meier survival analysis showed significantly worse cumulative 1-year survival in patients with LES-I >20% compared to ≤20% (79 versus 89%, p=0.002) and LES-II >8% versus ≤8% (77 versus 89%, p=0.001), but not when stratified by STS score >10% versus ≤10% (84 % versus 89%, p=0.36) (Figure 1). These results suggest that LES-II has overall reasonable ability to discriminate between patients at high versus low risk for 1-year mortality after TAVI, and better compared to LES-I and STS score.

Overall the STS score showed good calibration with no significant difference between the number of predicted and observed deaths during 1-year follow-up

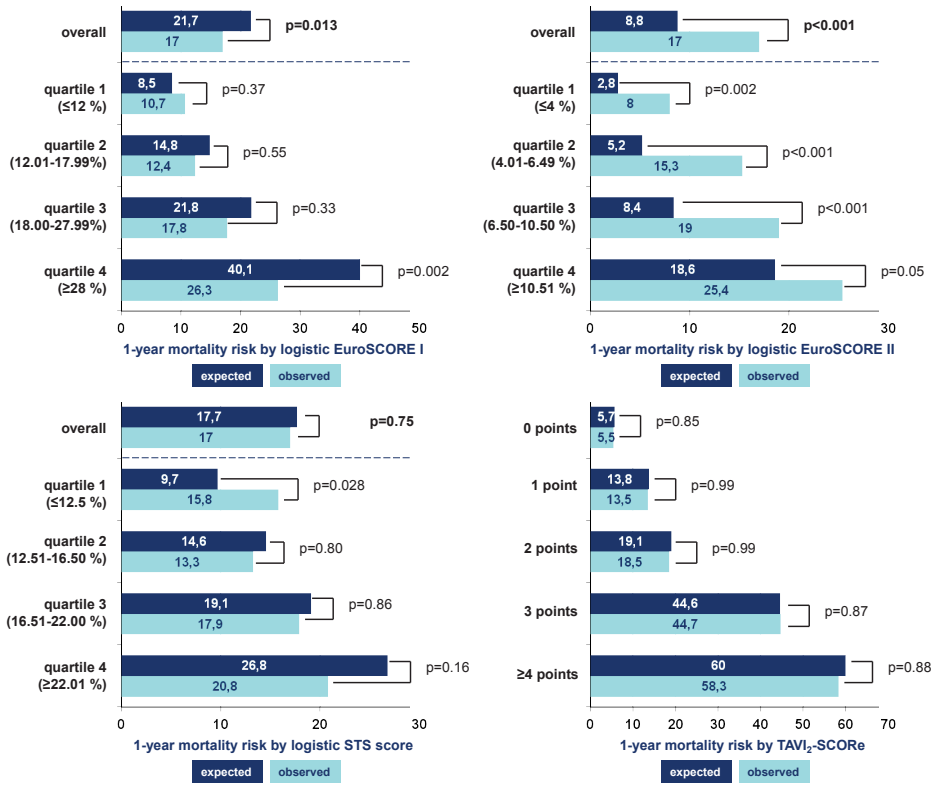

Figure 2.1
Percentage of expected versus observed mortality 1-year after TAVI for surgical risk scores (and quartiles) and *$TAVI_2$-SCORe* risk strata (calibration ability). See text for details.

(Figure 2). The STS-score however, significantly overestimated 1-year mortality for the lowest risk category (first STS score quartile). In contrast, the LES-I and LES-II showed significant differences in predicting 1-year mortality compared to the observed deaths. In particular, LES-I overestimated mainly high risk patients (fourth quartile) and LES-II significantly overestimated survival within all risk categories (all 4 quartiles). Hosmer-Lemeshow statistics (8 degrees of freedom) confirmed the superior calibration ability of the STS score (0.844) compared to the LES-I (0.457) versus LES-II (0.185).

Development of the *$TAVI_2$-SCORe*

Several baseline parameters that are included in the conventional surgical risk scores were associated with 1-year mortality after TAVI (Table 3 and in supplemental Table 1). Interestingly, other baseline parameters, not included in LES-I, LES-II or STS score, were also associated with 1-year mortality post-TAVI: porcelain

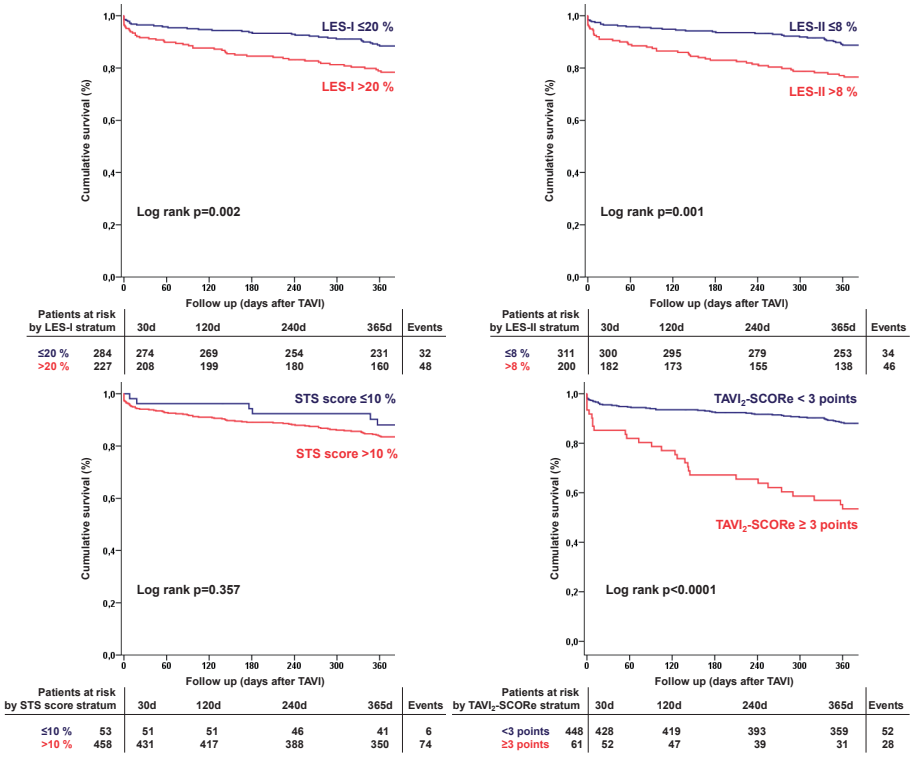

Figure 2.2
Cumulative 1-year survival after TAVI stratified into high versus low risk categories of surgical risk scores and *$TAVI_2$-SCORe* (discrimination ability).

thoracic aorta, hemoglobin <10 g/dl (anemia), CRP >10 mg/dl, serum albumin <3.0 g/dl, total bilirubin level and mean aortic valve gradient ≥70 mmHg (critical aortic valve stenosis). Univariate baseline predictors available in the vast majority of the study population (509/511 patients) were entered in the multivariate analysis that identified 8 baseline parameters with independent relation to 1-year mortality after TAVI: porcelain *T*horacic aorta, *A*nemia, *V*entricular dysfunction (LV ejection fraction <35%), recent myocardial *I*nfarction (<90 days prior to TAVI), male *S*ex category, *C*ritical aortic valve stenosis, *O*ld age (>85 years) and *Re*nal dysfunction (creatinine clearance <30 ml/kg/min). These parameters comprise the *$TAVI_2$-SCORe*. All parameters were individually weighted by assignment of 1 point for the majority of the variables and 2 points for recent myocardial infarction, proportional to hazard ratios noted. According to the number of points assigned (0, 1, 2, 3 or ≥4), patients were divided into 5 different risk categories (Figure 3).

Table 2.3
Univariate and multivariate cox regression analysis. Baseline parameters available in the majority of study patients (n=509/511) and reaching significance level <0.05 at univariate level only are shown. Results of univariate analysis including all factors tested is available as supplemental file.

	Univariate			Multivariate		
	HR	p value	95% CI	HR	p value	95% CI
Age >85 years	1.63	0.035	1.04-2.56	1.68	0.030	1.05-2.69
Male gender	1.70	0.018	1.10-2.64	1.81	0.012	1.14-2.87
New York Heart Association class III or IV	2.24	0.008	1.23-4.05	1.82	0.06	0.98-3.38
Chronic obstructive pulmonary disease	1.62	0.037	1.03-2.53	1.54	0.08	0.96-2.47
Porcelain aorta	2.39	0.001	1.34-4.08	2.56	0.001	1.46-4.48
Recent myocardial infarction (<90 days)	3.58	0.006	1.15-8.87	3.78	0.005	1.50-9.54
Creatinine clearance <30 ml/kg/min	1.95	0.011	1.16-3.26	1.76	0.036	1.04-2.97
Hemoglobin <10 g/dl	1.89	0.031	1.06-3.36	2.03	0.022	1.11-3.73
Left ventricular ejection fraction <35 %	2.05	0.015	1.15-3.66	1.98	0.028	1.08-3.63
Systolic pulmonary arterial pressure >45 mmHg	1.58	0.049	1.01-2.49	1.39	0.19	0.85-2.28
Aortic valve mean gradient ≥70 mmHg	2.10	0.012	1.18-1.73	2.46	0.004	1.33-4.56
Urgent procedure	2.22	0.007	1.25-3.96	1.67	0.10	0.91-3.05

Abbreviations: CI: confidence interval; HR: hazard ratio

TAVI$_2$-SCORe and 1-year mortality

The Harrell's C statistic for prediction of 1-year mortality after TAVI in the original patient cohort applying the *TAVI$_2$-SCORe* was 0.720 (p<0.001). Internal bootstrap validation indicated limited optimism of the model (0.005), an expected low value for a single predictor model. The final corrected Harrell's C statistic therefore was 0.715, indicating high discriminatory performance. In addition, the Kaplan Meier analysis indicated highly significant differences in cumulative survival for patients when stratified according to different *TAVI$_2$-SCORe* risk strata (Figure 3). In particular, a *TAVI$_2$-SCORe* of ≥3 points versus <3 indicates significantly worse 1-year cumulative survival after TAVI (54 versus 88%, p<0.0001). Figure 4 indicates that a *TAVI$_2$-SCORe* of 3 or ≥4 points, compared to 0 points, was associated with a respective 10-fold and 17-fold increased mortality risk within 1-year after TAVI. These data indicate that the *TAVI$_2$-SCORe* is accurate in discriminating patients at high versus low risk for 1-year mortality after TAVI.

In addition, no significant difference in expected versus observed mortality 1-year after TAVI was observed for the *TAVI$_2$-SCORe*, stratified according to the different risk categories. Hosmer-Lemeshow statistic for the *TAVI$_2$-SCORe* was 0.304 (2 degrees of freedom). These data underscore accurate calibration of the *TAVI$_2$-SCORe* model.

TAVI$_2$-SCORe versus LES-I, LES-II and STS score

Higher bootstrap validation corrected Harrell`s C statistic and the Kaplan Meier survival analyses showed that the *TAVI$_2$-SCORe* had better discriminatory performance to predict 1-year mortality after TAVI than conventional surgical risk scores. Moreover, no significant difference between observed and expected 1-year mortality for all *TAVI$_2$-SCORe* risk strata suggested better calibration performance compared to LES-I, LES-II and STS score.

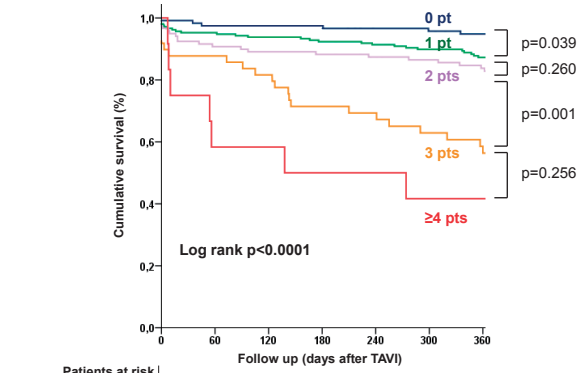

Patients at risk by TAVI$_2$-SCORe stratum		30d	120d	240d	365d	Events
0 points	119	118	116	108	103	6
1 points	210	200	197	185	167	26
2 points	119	110	106	100	90	20
3 points	49	43	40	33	26	21
≥4 points	12	9	7	6	5	7

Figure 2.3
Cumulative 1-year survival after TAVI, stratified according to the different *TAVI$_2$-SCORe* risk strata. Different risk strata were compared by Cox regression. Pt(s): point(s).

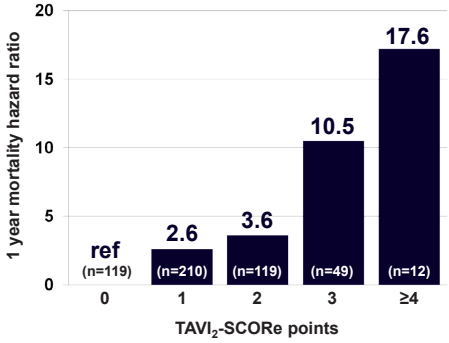

Figure 2.4
Hazard ratio for 1-year mortality after TAVI according to different *TAVI$_2$-SCORe* risk strata. Ref: reference category.

DISCUSSION

This study indicates that *TAVI$_2$-SCORe* is a simple and novel risk model for accurate prediction of 1-year mortality after TAVI, based on preprocedural baseline patient characteristics. Moreover, the *TAVI$_2$-SCORe* outperforms discriminatory and calibration abilities of conventional surgical risk scores, including LES-I, LES-II and STS-score.

Surgical risk scores and TAVI outcome

Cumulative 30 day and 1-year mortality observed in our registry is in line with the respective mortality of 7.4-9.7% and 24% reported in the 2 largest real-world registries including >3000 patients treated with TAVI.[19, 20] In addition, the high LES-I and STS scores in our series, comparable to the scores previously reported, reflect appropriate selection of patients for TAVI that were at high or prohibitive surgical risk.[1, 8, 19, 20] Estimation of operative risk with the LES-I, LES-II, and STS scores are used worldwide.[21-23] These scores however, have not been developed to predict the operative risk of elderly patients with symptomatic severe aortic stenosis and associated co-morbidities who are currently referred for TAVI. In addition, these scores, and recently more TAVI-dedicated risk scores, are intended to predict 30 day mortality.[8] Although this is an important acute clinical endpoint, 1-year mortality might be preferred for purposes of patient selection and evaluation of cost-benefits for a given treatment. A limited number of studies have reported on the value of conventional surgical risk scores to predict 1-year mortality after TAVI and have compared the performance of different surgical risk scores.[3-6, 19] Predictive performance of a risk model relies both on discrimination (ability to identify patients at high versus low mortality risk) and calibration (ability to match observed versus expected mortality).[17, 18] Both characteristics are not mutual exclusive and should be reported to assess the value of a prognostic risk model.[17] In patients undergoing TAVI, higher LES-I and STS score have been associated with increased 1-year mortality risk.[6, 19] Another study including 426 TAVI patients suggested that STS score but not LES-I or LES-II were independently related to this endpoint.[3] Furthermore, Sedaghat et al. reported on model performance statistics of different conventional surgical risk scores to predict 1-year mortality after TAVI in 206 patients undergoing TAVI with CoreValve prosthesis.[4] The authors showed better discrimination abilities for LES-I compared to LES-II and STS score with Harrell's C statistic of 0.72, 0.70 and 0.70 respectively. In addition both LES-I and LES-II were well calibrated for 1-year mortality contrary to STS score with a Hosmer-Lemeshow statistic of 0.36, 0.32 and 0.08, respectively. In contrast, the present study showed reasonable discrimination abilities for LES-II score (≤8 % low risk versus >8 % high risk) and superior and good calibration for STS score, despite mortality underestimation for the lowest risk category.

TAVI$_2$-SCORe and TAVI outcome

Based on preprocedural patients' baseline characteristics that showed independent association with 1-year mortality after TAVI, we developed the *TAVI$_2$-SCORe*. LV systolic dysfunction, recent myocardial infarction, sex, age and renal dysfunction, incorporated in conventional surgical risk scores, also showed a relation to outcome after TAVI in several reports.[14, 21-27] Porcelain thoracic aorta and anemia might represent risk factors more specifically related to outcome after TAVI.[28] Interestingly, several additional factors such as hypoalbuminemia and a rise of inflammatory markers (CRP) were related to the study endpoint. These factors should be explored in larger patient cohorts and might prove to be useful to further refine the *TAVI$_2$-SCORe*. The present study demonstrated accurate and superior discrimination and calibration properties of the *TAVI$_2$-SCORe* compared to conventional surgical risk scores.

LIMITATIONS

Some important limitations should be acknowledged. First, prospective validation of the *TAVI$_2$-SCORe* in a large external cohort of patients treated with TAVI is needed. Second, the current study findings cannot be extrapolated to patients treated with TAVI prosthesis other than the Edwards SAPIEN system. Third, procedural and postprocedural factors, including the access (transfemoral versus transapical, direct aortic or transsubclavian) and paravalvular leak post-TAVI also determine outcome post-TAVI and might further improve predictive performance, but do not allow for clinical decision making prior to the TAVI procedure.[20, 26, 29, 30] Finally, frailty, a potential key factor in TAVI outcome, did not relate to the study endpoint in the current series. A more objective definition to define frailty by using multidimensional geriatric assessment including prospective assessment of mobility, cognitive function, nutritional status and instrumental and basic daily live activities might be more appropriate.

CONCLUSION

TAVI$_2$-SCORe is a risk score predicting 1-year mortality after TAVI, based on preprocedural baseline patient characteristics. Simplicity, bed-side availability and better predictive ability compared to conventional surgical risk scores are the main strengths. Awaiting prospective external validation, *TAVI$_2$-SCORe* might become a valuable clinical tool for decision making and patient selection for TAVI.

SUPPLEMENTAL TABLE

Univariate 1-year mortality cox regression analysis for all baseline parameters tested and categorized to their best performing cut-off values.

	Available in N patients	HR	p value	95% CI
Age (years)	511	1.01	0.56	0.98-1.05
Age >85 years	511	1.63	0.035	1.04-2.56
Male gender	511	1.70	0.018	1.10-2.64
Body surface area (m^2)	511	1.13	0.82	0.39-3.31
Body mass index (kg/m^2)	511	0.96	0.17	0.91-1.02
Body mass index >25 kg/m^2	511	0.76	0.22	0.49-1.18
Sinus rhythm	511	0.78	0.32	0.48-1.27
Hypertension	511	1.01	0.97	0.57-1.80
Diabetes mellitus II	511	1.09	0.73	0.67-1.77
Smoker	500	0.78	0.32	0.48-1.27
Hypercholesterolemia	511	1.13	0.59	0.72-1.78
β-blocker	511	1.04	0.88	0.67-1.60
Diuretics	511	1.48	0.16	0.86-2.56
Spironolactone	511	1.44	0.15	0.87-2.37
Angiotensin converting enzyme inhibitor and/or angiotensin II receptor blocker	511	0.81	0.36	0.52-1.26
Statin	511	1.19	0.45	0.76-1.84
Insulin	510	1.26	0.44	0.71-2.24
Inotrope(s)	511	1.17	0.76	0.73-3.21
New York Heart Association class III-IV	511	2.24	0.008	1.23-4.05
Syncope	511	0.94	0.82	0.54-1.62
Angina	511	0.89	0.63	0.58-1.42
Angina pectoris class IV	511	1.46	0.52	0.46-4.64
Dialysis	511	0.05	0.58	0.00-1882
Chronic obstructive pulmonary disease	511	1.62	0.037	1.03-2.53
Peripheral artery disease	511	1.39	0.14	0.89-2.16
Porcelain aorta	510	2.39	0.001	1.34-4.08
Prior stroke/transient ischemic attack	511	0.73	0.37	0.36-1.46
Recent myocardial infarction (<90 days)	511	3.58	0.006	1.15-8.87
Prior cardiac surgery	511	1.20	0.74	0.73-196
Prior percutaneous coronary intervention	511	1.10	0.72	0.66-1.82
Poor mobility	510	1.11	0.67	0.69-1.79
Neurologic dysfunction	511	1.07	0.86	0.49-2.33
Frailty	478	1.38	0.22	0.83-2.30
Cognitive dysfunction/dementia	511	1.52	0.18	0.82-2.81
Ascites	511	3.09	0.12	0.76-12.6
Cirrosis	511	1.63	0.34	0.60-4.45

(continued)

	Available in N patients	HR	p value	95% CI
Hostile chest	509	0.92	0.77	0.52-1.64
Creatinine clearance (ml/kg/min)	511	0.99	0.13	0.98-1.01
Creatinine clearance ≤ 30 ml/kg/min	511	1.95	0.011	1.16-3.26
Hemoglobin (g/dl)	510	0.87	0.038	0.76-0.99
Hemoglobin <10 g/dl	510	1.89	0.031	1.06-3.36
C reactive protein (mg/dl)	327	1.01	0.38	0.99-1.01
C reactive protein >10 mg/dl	327	2.03	0.013	1.16-3.53
Albumin (g/dl)	373	0.63	0.023	0.43-0.94
Albumin <3.0 g/dl	373	3.45	0.001	1.71-7.13
Total bilirubin (µmol/l)	433	1.45	0.021	1.06-2.00
Total bilirubin >2.0 µmol/l	433	1.95	0.12	0.84-4.49
Aspartate transaminase (U/l)	464	1.01	0.19	0.99-1.01
Aspartate transaminase >70 U/l (2x ULN)	464	2.66	0.06	0.97-7.29
Alanin aminotransferase (U/l)	464	1.01	0.62	0.96-1.01
Alanin aminotransferase >90 U/l (2x ULN)	464	1.74	0.44	0.73-7.08
Left ventricular end-diastolic diameter (mm)	502	0.99	0.91	0.97-1.03
Left ventricular end-systolic diameter (mm)	429	1.01	0.47	0.99-1.03
Left ventricular mass index (g/m^2)	502	1.01	0.30	0.99-1.01
Left ventricular mass index >130 g/m^2	502	1.43	0.15	0.88-2.31
Left ventricular end-diastolic volume index (ml/m^2)	511	0.99	0.67	0.99-1.01
Left ventricular end-diastolic volume index ≥75 ml/m^2	511	1.24	0.46	0.71-2.17
Left ventricular end-systolic volume index (ml/m^2)	511	1.01	0.30	0.99-1.02
Left ventricular end-systolic volume index ≥31 ml/m^2	511	1.43	0.13	0.90-2.25
Left ventricular ejection fraction (%)	511	0.98	0.004	0.96-0.99
Left ventricular ejection fraction <35 %	511	2.05	0.015	1.15-3.66
Left atrial volume index (ml/m^2)	505	0.99	0.38	0.98-1.01
Left atrial volume index >34 ml/m^2	505	1.41	0.38	0.65-3.07
E/e`	185	1.01	0.26	0.99-1.02
Systolic pulmonary artery pressure (mmHg)	511	1.02	0.039	1.01-1.04
Systolic pulmonary artery pressure >45 mmhg	511	1.58	0.049	1.01-2.49
Aortic regurgitation ≥grade 3	511	0.74	0.61	0.23-2.35
Mitral regurgitation ≥grade 3	511	1.03	0.95	0.42-2.55
Tricuspid regurgitation ≥grade 3	511	1.52	0.29	0.70-3.30
Aortic valve mean gradient (mmHg)	511	0.99	0.48	0.98-1.01
Aortic valve mean gradient >70 mmhg	511	2.10	0.012	1.18-1.73
Aortic valve index (cm^2/m^2)	511	0.58	0.65	0.06-5.78
Aortic valve index <0.6 cm^2/m^2	511	20.7	0.41	0.02-2.63
Urgent procedural need	511	2.22	0.007	1.25-3.96

REFERENCES

1. Joint Task Force on the Management of Valvular Heart Disease of the European Society of Cardiology, European Association for Cardio-Thoracic Surgeons, Vahanian A, Alfieri O, Andreotti F et al. Guidelines on the management of valvular heart disease (version 2012). *Eur Heart J.* 2012;33:2451-2496.
2. Mack MJ. Risk scores for predicting outcomes in valvular heart disease: how useful? *Curr Cardiol Rep.* 2011;13:107-112.
3. Hemmann K, Sirotina M, De Rosa S et al. The STS score is the strongest predictor of long-term survival following transcatheter aortic valve implantation, whereas access route (transapical versus transfemoral) has no predictive value beyond the periprocedural phase. *Interact Cardiovasc Thorac Surg.* 2013;17:359-364.
4. Sedaghat A, Sinning JM, Vasa-Nicotera M et al. The revised EuroSCORE II for the prediction of mortality in patients undergoing transcatheter aortic valve implantation. *Clin Res Cardiol.* 2013; 102:821-829.
5. Thomas M, Schymik G, Walther T et al. One-year outcomes of cohort 1 in the Edwards SAPIEN Aortic Bioprosthesis European Outcome (SOURCE) registry: the European registry of transcatheter aortic valve implantation using the Edwards SAPIEN valve. *Circulation.* 2011;124:425-433.
6. Wenaweser P, Stortecky S, Schwander S et al. Clinical outcomes of patients with estimated low or intermediate surgical risk undergoing transcatheter aortic valve implantation. *Eur Heart J.* 2013;34:1894-1905.
7. Vahanian A, Alfieri O, Al-Attar N et al. Transcatheter valve implantation for patients with aortic stenosis: a position statement from the European Association of Cardio-Thoracic Surgery (EACTS) and the European Society of Cardiology (ESC), in collaboration with the European Association of Percutaneous Cardiovascular Interventions (EAPCI). *Eur Heart J.* 2008;29:1463-1470.
8. Iung B, Laouenan C, Himbert D et al. Predictive factors of early mortality after transcatheter aortic valve implantation: individual risk assessment using a simple score. *Heart.* 2014;100:1016-1023.
9. Lang RM, Bierig M, Devereux RB et al. Recommendations for chamber quantification: a report from the American Society of Echocardiography's Guidelines and Standards Committee and the Chamber Quantification Writing Group, developed in conjunction with the European Association of Echocardiography, a branch of the European Society of Cardiology. *J Am Soc Echocardiogr.* 2005;18:1440-1463.
10. Nagueh SF, Appleton CP, Gillebert TC et al. Recommendations for the evaluation of left ventricular diastolic function by echocardiography. *J Am Soc Echocardiogr.* 2009;22:107-133.
11. Zoghbi WA, Enriquez-Sarano M, Foster E et al. American Society of Echocardiography. Recommendations for evaluation of the severity of native valvular regurgitation with two-dimensional and Doppler echocardiography. *J Am Soc Echocardiogr.* 2003;16:777-802.
12. Baumgartner H, Hung J, Bermejo J et al. Echocardiographic assessment of valve stenosis: EAE/ASE recommendations for clinical practice. *J Am Soc Echocardiogr.* 2009;22:1-23.
13. Rudski LG, Lai WW, Afilalo J et al. Guidelines for the echocardiographic assessment of the right heart in adults: a report from the American Society of Echocardiography endorsed by the European Association of Echocardiography, a registered branch of the European Society of Cardiology, and the Canadian Society of Echocardiography. *J Am Soc Echocardiogr.* 2010;23:685-713; quiz 786-688.

14. Rodes-Cabau J, Webb JG, Cheung A et al. Long-term outcomes after transcatheter aortic valve implantation: insights on prognostic factors and valve durability from the Canadian multicenter experience. *J Am Coll Cardiol.* 2012;60:1864-1875.
15. Fried LP, Tangen CM, Walston J et al. Cardiovascular Health Study Collaborative Research Group. Frailty in older adults: evidence for a phenotype. *J Gerontol A Biol Sci Med Sci.* 2001;56:M146-156.
16. Kappetein AP, Head SJ, Genereux P et al. Valve Academic Research Consortium. Updated standardized endpoint definitions for transcatheter aortic valve implantation: the Valve Academic Research Consortium-2 consensus document. *J Thorac Cardiovasc Surg.* 2013;145:6-23.
17. Cook NR. Use and misuse of the receiver operating characteristic curve in risk prediction. *Circulation.* 2007;115:928-935.
18. Steyerberg EW, Vickers AJ, Cook NR et al. Assessing the performance of prediction models: a framework for traditional and novel measures. *Epidemiology.* 2010;21:128-138.
19. Gilard M, Eltchaninoff H, Iung B et al. Registry of transcatheter aortic-valve implantation in high-risk patients. *N Engl J Med.* 2012;366:1705-1715.
20. Di Mario C, Eltchaninoff H, Moat N et al. Transcatheter Valve Treatment Sentinel Registry Investigators of the ERPotESoC. The 2011-12 pilot European Sentinel Registry of Transcatheter Aortic Valve Implantation: in-hospital results in 4,571 patients. *EuroIntervention.* 2013;8:1362-1371.
21. O'Brien SM, Shahian DM, Filardo G et al. Society of Thoracic Surgeons Quality Measurement Task Force. The Society of Thoracic Surgeons 2008 cardiac surgery risk models: part 2--isolated valve surgery. *Ann Thorac Surg.* 2009;88:S23-42.
22. Roques F, Michel P, Goldstone AR et al. The logistic EuroSCORE. *Eur Heart J.* 2003;24:881-882.
23. Nashef SA, Roques F, Sharples LD et al. EuroSCORE II. *Eur J Cardiothorac Surg.* 2012;41:734-744; discussion 744-735.
24. Moat NE, Ludman P, de Belder MA et al. Long-term outcomes after transcatheter aortic valve implantation in high-risk patients with severe aortic stenosis: the U.K. TAVI (United Kingdom Transcatheter Aortic Valve Implantation) Registry. *J Am Coll Cardiol.* 2011;58:2130-2138.
25. Seiffert M, Schnabel R, Conradi L et al. Predictors and outcomes after transcatheter aortic valve implantation using different approaches according to the valve academic research consortium definitions. *Catheter Cardiovasc Interv.* 2012; DOI 10.1002/ccd.24751.
26. Tamburino C, Capodanno D, Ramondo A et al. Incidence and predictors of early and late mortality after transcatheter aortic valve implantation in 663 patients with severe aortic stenosis. *Circulation.* 2011;123:299-308.
27. Zahn R, Gerckens U, Linke A et al. German Transcatheter Aortic Valve Interventions - Registry I. Predictors of one-year mortality after transcatheter aortic valve implantation for severe symptomatic aortic stenosis. *Am J Cardiol.* 2013;112:272-279.
28. Gotzmann M, Thiessen A, Lindstaedt M et al. Left atrial diameter, aortic mean gradient, and hemoglobin for risk stratification in patients undergoing transcatheter aortic valve implantation. *Clin Cardiol.* 2013;36:228-234.
29. Toggweiler S, Humphries KH, Lee M et al. 5-year outcome after transcatheter aortic valve implantation. *J Am Coll Cardiol.* 2013;61:413-419.
30. Khatri PJ, Webb JG, Rodes-Cabau J et al. Adverse effects associated with transcatheter aortic valve implantation: a meta-analysis of contemporary studies. *Ann Intern Med.* 2013;158:35-46.

Chapter 3

Contemporary imaging of normal mitral valve anatomy and function

Philippe Debonnaire, Meindert Palmen, Nina Ajmone Marsan, Victoria Delgado

Curr Opin Cardiol, 2012 Sep 15;27(5):455-464.

ABSTRACT

Objectives

Mitral valve (MV) disease is highly prevalent. Accurate characterization of normal anatomy and function of the MV is crucial to understand the pathophysiology of MV disease. This review summarizes recent advances on noninvasive cardiac imaging to assess normal MV anatomy and function and provides an overview of the clinical applications of these novel imaging techniques in the evaluation of patients with MV disease.

Summary

Echocardiography remains the first imaging technique for evaluation of the anatomy and function of the MV. However, advances in minimally invasive and transcatheter valve repair/replacement procedures demand high spatial resolution images to accurately assess the anatomy of the MV and its surrounding structures. Three-dimensional echocardiography improves 2-dimensional echocardiography morphological and functional MV evaluation. Furthermore, computed tomography provides high spatial resolution 3-dimensional data and may constitute the modality of choice for additional morphological or geometrical study of the MV and surrounding structures. In addition, cardiac magnetic resonance (CMR) permits accurate assessment of anatomy and function of the mitral valve and is considered the method of reference to quantify mitral flow.

Conclusions

Any abnormality in any of the components of the MV (annulus, leaflets, subvalvular apparatus, left ventricle and left atrium) may lead to MV dysfunction. Current noninvasive cardiac imaging modalities permit accurate assessment of MV anatomy and function. These imaging techniques refine our diagnostic performance, provide additional (patho)physiological insights and help to design new strategies for interventional or surgical treatment of diseased MV.

INTRODUCTION

Mitral valve (MV) disease is one of the most prevalent valvular heart diseases. Despite the dramatic decrease in rheumatic valve disease in industrialized countries, the increased lifespan of the population has led to an increase in degenerative MV disease, fueling the number of MV interventions.[1,2] Echocardiography is used as a first-line imaging technique to study MV disease. However, more recently, advanced imaging techniques such as 3-dimensional (3D) echocardiography, multidetector row computed tomography (MDCT) and cardiac magnetic resonance (CMR) were added to the diagnostic armentarium to study the MV.[3,4] These imaging techniques are sequentially applied (1) to identify MV dysfunction, (2) to study the etiology, morphological lesions and mechanism of MV dysfunction (Carpentier triad), (3) to assess hemodynamic, morphological and functional cardiac consequences of MV disease and (4) to select, guide and evaluate the therapeutical approach.[5,6] To answer all these questions, thorough knowledge of the normal morphological, geometrical and functional appearance of the MV is crucial. Moreover, this knowledge is basic to design and develop novel treatment strategies for MV dysfunction that aim at restoring normal MV anatomy and function.

This review focuses on the use and clinical value of different imaging modalities to assess normal MV anatomy and function.

IMAGING NORMAL MITRAL VALVE

The normal MV is a functional complex that consists of mitral annulus, leaflets, subvalvular apparatus, left ventricle (LV) and left atrium (LA).[7,8] Any abnormality in any of these components may cause MV dysfunction (stenosis/regurgitation). Structural MV abnormalities are referred to as organic MV disease. Functional MV dysfunction is secondary to LV remodeling with normal structural MV. (Key points table)

Key points table.

KEY POINTS	
1	The normal MV is a functional complex that relies on normal morphology, geometry and function of all its constituents.
2	3D-echocardiography improves morphological MV evaluation and mitral annular structural and functional evaluation.
3	MDCT allows in-depth study of mitral anatomy and CMR provides an alternative for quantitative mitral functional evaluation.

Mitral annulus

The mitral annulus consists of a discontinuous fibrous D-shaped ring between the LV and LA to which the MV leaflets are anchored.[7,8] The anterior part of the mitral annulus is in close relationship with the aortic annulus at the level of the left and non-coronary aortic valve cusps. This part is enforced by a fibrous continuity, so-called aorto-mitral valvular continuity, which ends laterally in the left and right fibrous trigones (Figure 1, panel A).[7-9] In contrast, the posterior part of the mitral annulus is

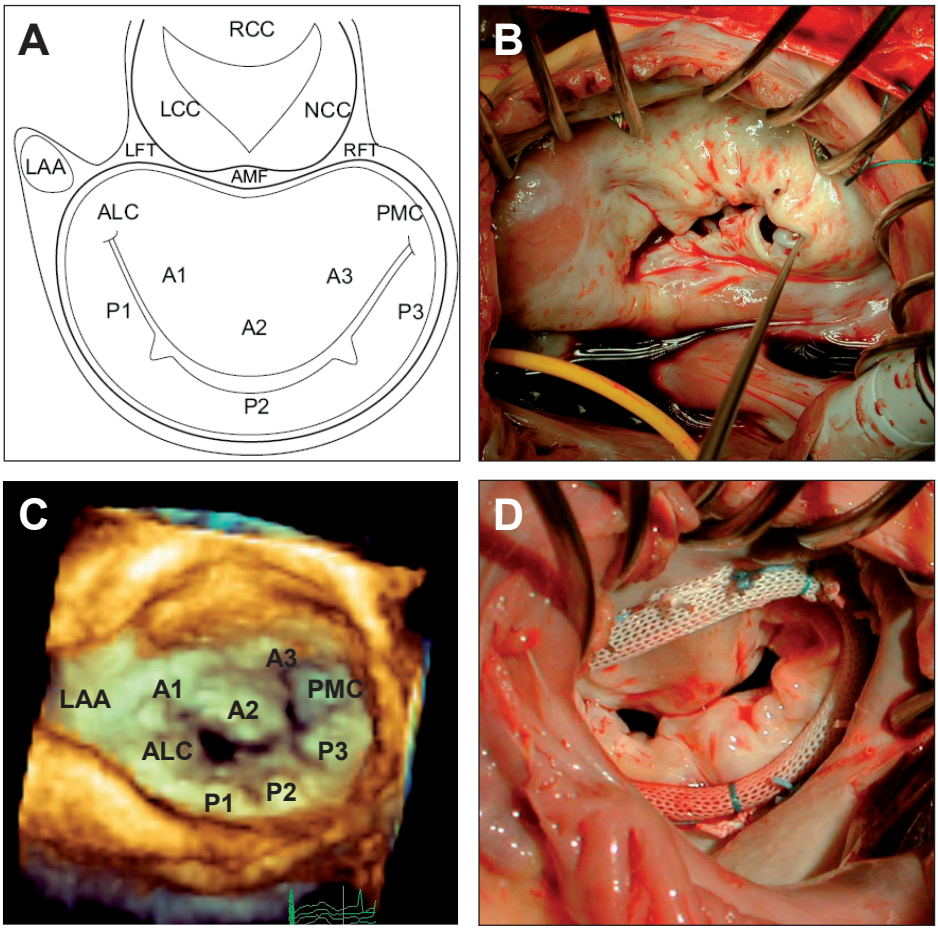

Figure 3.1
Surgical view of the mitral valve. Panel A: Schematic representation of mitral valve anatomy (with permission from reference [9]). Panel B: Surgical exposition of Barlow degenerated mitral valve. Panel C: 3-Dimensional echocardiography of structural normal mitral valve. Panel D: Same patient as panel C, now post mitral annuloplasty for functional mitral regurgitation. Note the morphologic resemblance of the valve on 3-dimensional echocardiography and peroperatively. A: anterior mitral valve with scallops A1, A2 and A3, ALC: antero-lateral commissure, AMF: aortic-mitral fibrosa, LAA: left atrial appendage, LCC: left coronary cusp of aortic valve, LFT: left fibrous trigone, NCC: non coronary cusp of aortic valve, P: posterior mitral valve leaflet with scallops P1, P2 and P3, PMC: postero-medial commissure, RCC: right coronary cusp of aortic valve, RFT: right fibrous trigone.

more muscular and lacks a firm fibrous cord. Consequentially, this site is prone to dilatation and calcification.[8] The 3D-shape of the mitral annulus resembles a saddle with peaks located anteriorly and posteriorly and nadirs at the postero-medial and antero-lateral commissures.[10] This 3D-geometry optimizes stress distribution over the mitral leaflets.[10] Assessment of mitral annular dimensions is important to determine appropriate annuloplasty ring or mitral prosthesis size.

Noninvasive imaging modalities permit end-systolic quantification of the maximal antero-posterior diameter (minor axis) and the inter-commissural diameter (major axis) in appropriate reconstruction planes, characterizing the planar D-shaped morphology of the mitral annulus (Table 1).[5,11] Based on 2-dimenisonal (2D) echocardiographic measurements, an antero-posterior annular diameter >35 mm measured at end-systole or an annular to end-diastolic anterior mitral leaflet length ratio >1.3 define mitral annulus dilatation.[12] 3D-imaging modalities permit accurate alignment of multiplanar reformation planes through the mitral annulus and increase the accuracy of the measurements of the annular dimensions.[11,13,14] In a series of 17 patients undergoing 2D transthoracic echocardiography and MDCT, mitral annulus measurements performed on conventional 2D echocar-

Table 3.1
Geometric indices of clinical interest for the functional mitral valve complex. See text for explanation.

Annulus
Antero-posterior diameter (minor axis)
Inter-commissural diameter (major axis)
Annular area and circumference
Annular width-to-height-ratio
Aortic-mitral annular angle
Left atrium
Left atrial diameter
Leaflets
Coaptation depth
Coaptation length
Tenting area or volume
Posterior and anterior mitral leaflet angle (A2-P2 level)
Posterior and anterior mitral leaflet length (A2-P2 level)
Subvalvular apparatus
Chordal length
Interpapillary muscle distance
Papillary muscle tethering length
Papillary muscle anterior and posterior angle
Left ventricle
Sphericity index (length-to-width ratio)

diographic views overestimated the antero-posterior diameter by 23% and underestimated the inter-commissural diameter by 12% compared with MDCT. In contrast, echocardiographic measurements performed on correct anatomical views resulted in improved agreement with MDCT measurements with an underestimation of the antero-posterior diameter by 1% and an overestimation of the inter-commissural diameter by 0.9%.[11] Subsequently, head-to-head comparison between 3D-transesophageal echocardiography (TEE) and MDCT measurements of mitral annular dimensions showed good agreement between both techniques.[14] These 3D-imaging techniques have refined the analysis of mitral annular geometry and have provided several parameters (annular height, minimal and maximal width, height-to-commissural-width ratio, annular circumference, annular area and aortic-mitral annular angle) that may help to understand the pathophysiology of MV disease and to design tailored MV repair techniques (Figure 2).[13,15,16]

In percutaneous MV interventions, the assessment of the anatomic relationship of the mitral annulus and its surrounding structures is crucial, especially the coronary circumflex artery and the coronary sinus with MDCT and CMR (Figure 3).[17-20] This is of major interest as the coronary sinus is a new target for percutaneous indirect annuloplasty devices that aim to reduce the antero-posterior diameter of the mitral annulus.[5] In patients with structurally normal hearts and in patients with heart failure and mitral regurgitation, MDCT and CMR showed that the coronary sinus is frequently located above the mitral annulus.[18,19] In addition, the circumflex coronary artery was located between the coronary sinus and the mitral annulus in 68 to 80% of patients.[18-20] These findings highlight the limited patients` eligibility for percutaneous indirect annuloplasty: the technique may be ineffective in reducing mitral regurgitation if the coronary sinus is not aligned with the mitral annulus or may imply a high risk of myocardial ischemia if the coronary sinus courses above the circumflex artery.[21] Furthermore, MDCT provides the highest spatial resolution to characterize mitral annulus calcification, a potential limitation for coronary sinus-based annuloplasty procedures.

Additionally to the anatomical characterization, the function of the mitral annulus can be studied. The mitral annular area decreases approximately 25% at mid-systole due to atrial and ventricular myocardial forces imposed upon the mitral annulus and its normal translational motion towards the LV apex.[10] Mitral-aortic valvular coupling can be studied by evaluating changes of the aortic-mitral angle throughout the cardiac cycle.[15] These 3D dynamic properties of the mitral annulus reduce MV leaflet stress, enhance mitral leaflet coaptation and contribute to atrial and ventricular performance by optimizing filling and ejection flow dynamics.[7,10] Assessment of mitral annular function may help to optimize surgical techniques and design devices for mitral valve repair.

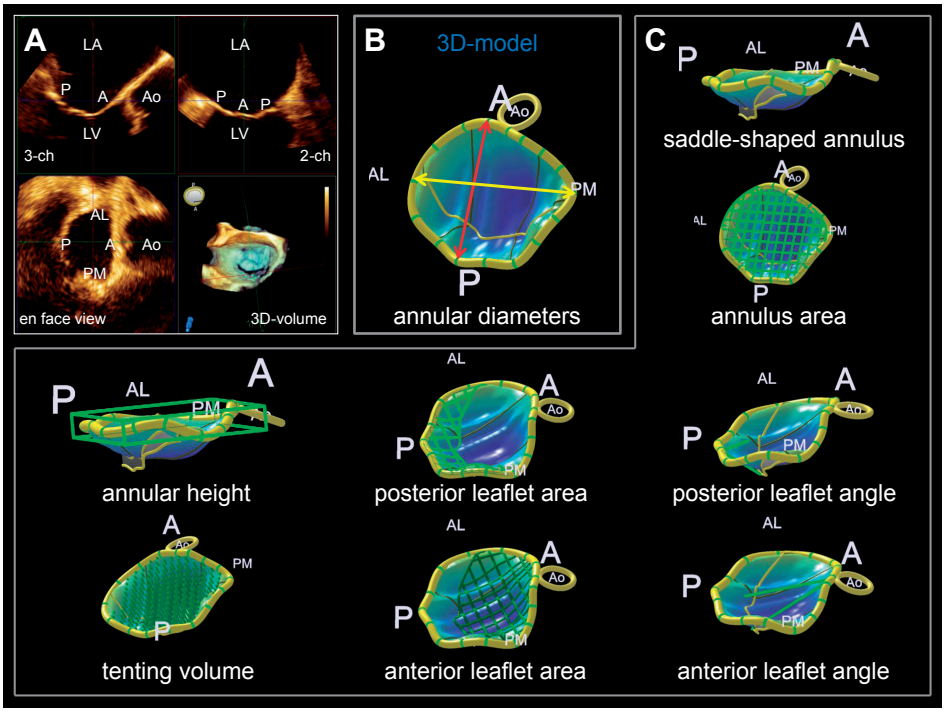

Figure 3.2
Real time three-dimensional echocardiography to assess mitral valve geometry. Panel A: Indication of anatomic landmarks on 3-dimensional reformation planes is performed, using Mitral Valve Quantification software. Panel B: A 3-dimensional model of the mitral valve is generated by the software. The saddle-like shape of mitral annulus is appreciated. Panel C: Several geometric indices of clinical interest can be measured. A: anterior, AL: antero-lateral, Ao: aorta, LA: left atrium, LV: left ventricle, P: posterior, PM: postero-medial, 2-ch: two-chamber, 3-ch: three-chamber, 3D: three-dimensional. Red arrow: antero-posterior annular diameter (minor axis), Yellow arrow: inter-commissural annular diameter (major axis).

Mitral leaflets

The MV consists of the anterior and the posterior leaflets that converge at the antero-lateral and postero-medial commissures (Figure 1). The anterior mitral leaflet is rounded and occupies one third of the annular circumference whereas the posterior mitral leaflet is elongated and narrow and is hinged to the remaining two thirds of the annulus. Despite having comparable surface areas, this anatomic fact explains that the anterior mitral leaflet forms the greatest part of the atrial floor (Figure 2). Based on the presence of 2 indentations, the posterior mitral leaflet is usually divided into a lateral P1 scallop (close to the left atrial appendage), a bigger central P2 and a medial P3 scallop.[22] The opposing segments of the anterior mitral leaflet are similarly named A1, A2 and A3 scallop.[7-9] Of note, indentations between the leaflets never reach the mitral annulus in normal MV.[7]

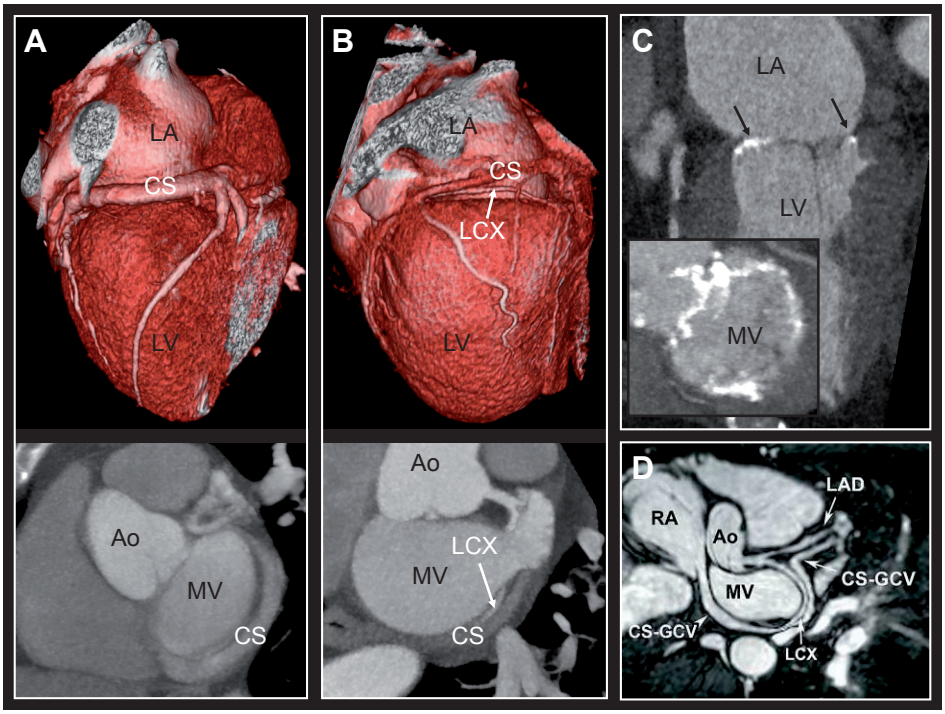

Figure 3.3
Peri-annular anatomy by computed tomography and cardiac magnetic resonance. Panels A-C: computed tomography, panel D: cardiac magnetic resonance. Panel A: Volume-rendered reconstruction showing presence of coronary sinus (CS) in atrio-ventricular groove close to the mitral annulus (upper panel). Short axis view of mitral annulus showing close proximity of CS (lower panel). Anatomic eligibility for percutaneous indirect mitral annuloplasty is likely. Panel B: CS courses superiorly of mitral annulus and left circumflex coronary artery (LCX) runs inferior of CS (upper panel). Short axis view points out risk of LCX impingement in case of percutaneous indirect mitral annuloplasty (lower panel). Panel C: Mitral annular calcification is seen on long-axis view of the left ventricle (arrows) and short axis mitral annular view (detail). Panel D: LCX partly overlaps with CS at level of mitral annulus (with permission form reference 20). Ao: aorta, LA: left atrium, CS-GCV: coronary sinus-great cardiac vein, LAD: left anterior descendens coronary artery, LV: left ventricle, MV: mitral valve, RA: right atrium.

The segmental anatomical identification is of paramount importance when studying and reporting on the morphology and function of the MV.[6] The location and extent of prolapsing segments in organic mitral regurgitation or the exact localization of the restriction characteristic of functional mitral regurgitation (usually postero-medial segments) are essential for therapeutic management strategies.[5,12] Protocols for standardized approach using 2D- and 3D-transthoracic or TEE, MDCT and CMR have been reported.[3,12,13,23,24] 3D-echocardiography provides the possibility of simultaneous 3D-display "en face" view of the MV leaflets from the ventricular or atrial perspective ('surgical view') (Figure 1 and 4). This increases the accuracy of MV evaluation by novice readers, improves the evaluation of the commissural regions and provides a common communication platform between

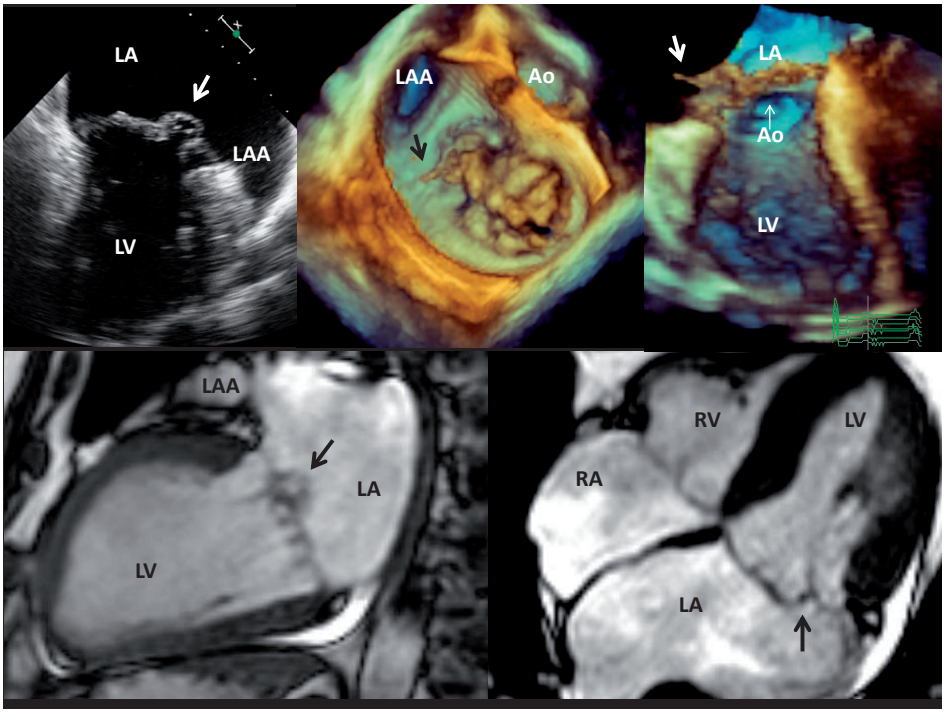

Figure 3.4
Multimodality morphologic study of a patient with Barlow degenerated mitral valve leaflet. Panel A: 2-Dimensional echocardiographic 2-chamber view shows thickened leaflets and prolapse of anterior mitral valve leaflet (arrow). Panel B: 3-Dimensional echocardiography surgical view illustrates complex Barlow degeneration with A2-A3 scallop prolapse and flail A1 scallop (arrow) Panel C: 3-Dimensional long-axis view indicates flail anterior leaflet. Panel D: cardiac magnetic resonance (CMR) reveals prolapse of mitral valve on 2-chamber view. Panel E: CMR suggests A2 prolapse on 4-chamber view, although caution is warranted when diagnosing prolapse in this view because misinterpretation may occur due to the saddle-shaped mitral annulus. Ao: aorta, LA: left atrium, LAA: left atrial appendage, LV: left ventricle, RA: right atrium, RV: right ventricle

the cardiac surgeon/interventionalist and cardiac imager.[13,25] 2D-TEE, 3D-TEE and MDCT provide the best spatial resolution to study mitral leaflet morphology and geometry.[3] Attempts using CMR steady state free precession (cine) images are increasingly reported with reasonable results, but they suffer from suboptimal spatial resolution (Figure 4).[26-28]

Normal leaflet length can be assessed in mid-diastole from the hinge point at the mitral annulus towards the leaflet tips. Its assessment can be used for indexation of geometric MV measurements in functional MV disease and can influence surgical management strategies in hypertrophic cardiomyopathy patients with increased LV outflow tract gradient and systolic anterior movement of the anterior mitral leaflet, causing mitral regurgitation.[29]

The parasternal and apical long-axis views of the left ventricle allow quantification of the MV leaflet geometry (Table 1). At mid-systole the coaptation distance or height (4-6 mm from coaptation point to mitral annulus plane) and the anterior and posterior angles formed between the mitral annulus plane and the respective anterior and posterior mitral leaflets can be measured at the A1-P1, A2-P2 or A3-P3 level (Figure 5).[3,12,30] A triangular tenting area or volume comprised between the mitral annulus plane, the leaflet surfaces and the coaptation line can be identified.[12] Increased tenting area and increased posterior and distal anterior leaflet angle are important determinants of mitral regurgitation severity and are related to adverse outcome after mitral surgery for functional mitral regurgitation.[12,31,32] The coaptation length refers to the length between the tips of the leaflets and their coaptation point that is formed by the systolic overlap of the leaflets (6-10 mm at A2-P2 level), providing a coaptation reserve, essential to maintain normal

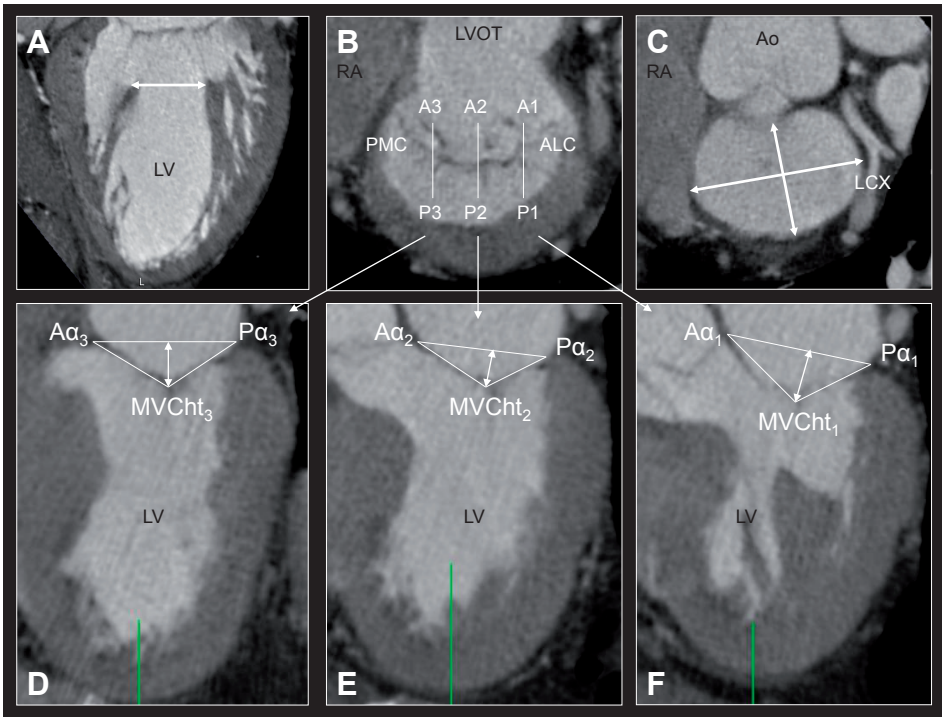

Figure 3.5
Segmental anatomy and geometric indices of mitral valve by computed tomography. Panel A: Interpapillary muscle distance on 2-chamber plane. Panel B: Short-axis view of mitral valve with A1-A2-A3 scallops, P1-P2-P3 scallops, antero-lateral commissure (ALC) and postero-medial commissure (PMC). Panel C: Short-axis view at level of mitral annulus to measure minor and major axis annular diameters (arrows). Panels D, E, F: Reconstruction planes at A1-P1, A2-P2 and A3-P3 level, respectively. The mitral valve coaptation height (MVCht), anterior angle (Aα) and posterior angle (Pα) can be quantified. Ao: aorta, LCX: left circumflex coronary artery, LV: left ventricle, LVOT: left ventricular outflow tract, RA: right atrium.

MV function.[3,7] Its assessment should be an integral part of the evaluation of per-operative success of mitral repair. With the use of multiplanar reformation planes, 3D-echocardiography and MDCT permit accurate assessment of these parameters (Figure 5).[14]

Functionally, normal leaflet mobility throughout the cardiac cycle (1) protects from systolic backflow of blood towards the left atrium, (2) forms an essential component of the funnel shaped LV outflow tract during ejection and (3) enables diastolic blood flow towards the LV without a significant forward gradient.[7] A mitral valve area of 4-5 cm^2 is considered normal.[7,8] The assessment of mitral leaflet mobility is pivotal to define the mechanism of MV regurgitation according to the Carpentier classification: normal, excessive (prolapse or flail) or restricted (rheumatic or functional MV disease) leaflet mobility.[12]

Finally, spectral- and color-Doppler echocardiographic methods can identify the presence of regurgitation or stenosis and provide the cornerstone of quantitative functional MV assessment (Table 2). Alternatively, mitral regurgitation can be detected as low signal intensity (signal void) on bright-blood steady state free precession-cine images and subsequently quantified by blood flow imaging using velocity-encoded phase-contrast CMR.[27] Except for mitral valve planimetry, MDCT currently does not allow quantitative MV function assessment as it lacks blood flow data and suffers low temporal resolution. Quantification of MV function by

Table 3.2
Usefulness of multimodality imaging to study mitral valve anatomy and function. CMR: cardiac magnetic resonance, Echo: echocardiography, MDCT: multidetector computed tomography, 2D: two-dimensional, 3D: three-dimensional.

Mitral valve	2D-echo	3D-echo	MDCT	CMR
Anatomy				
Annulus	++	+++	++	++
Left atrium	++	++	++	++
Leaflets	+++	+++	+	+/-
Subvalvular apparatus	+++	+	+++	+/-
Left ventricle	+++	+++	+++	+++
Function				
Mitral regurgitation	+++	++	-	++
Mitral stenosis	+++	+++	+/-	++

different imaging modalities and applications will be extensively discussed in other articles included in this issue.

Subvalvular apparatus and left ventricle

The subvalvular apparatus consists of fibrous tendinous chords and the papillary muscles. The antero-lateral papillary muscle usually arises from the apico-lateral third of the LV and the postero-medial papillary muscle originates from the middle third of the LV inferior wall, avoiding the interventricular septum.[7,8] Both papillary muscles give rise to several dozens of tendinous chords that attach to the ipsilateral half of the anterior and posterior mitral leaflets. Commissural chords however originate only from the papillary muscle in closest proximity beneath.[7,8] Tendinous chords remain at the same length throughout the cardiac cycle and give rise to several branches of chords that can attach to the edges of the mitral leaflets (primary chords) or to the ventricular surface of the leaflet bodies (secondary chords). Few tertiary chords can be identified originating directly from the posterior LV wall to the posterior mitral leaflet only.[7,8]

With 2D transthoracic echocardiography, the basal and mid short-axis as well as long-axis bi-commissural views of the left ventricle allow systematic morphological evaluation of the subvalvular apparatus and end-diastolic measurement of the chordal length and various geometrical indices (Table 1).[8] Chordal elongation can be encountered in fibro-elastic deficiency and Marfan's disease for example.[33] The 90° (transgastric) 2-chamber view on TEE provides a clear view on the subvalvular apparatus.[13] Furthermore, MDCT has demonstrated the highly variable anatomy of the subvalvular apparatus.[3] While the antero-lateral papillary muscle usually has 1 or 2 heads and a single trabecularized insertion on the LV wall, the postero-medial papillary muscle has multiple anatomic variations with 1 to 3 heads and multiple trabecularized ventricular insertions.[3]

The normal geometric relations of the MV leaflets described above depend on the geometry of the subvalvular apparatus. The inter-papillary muscle distance refers to the distance in between the base or the heads of the papillary muscles in systolic short-axis mid-ventricular view or in a LV longitudinal view, respectively (Figure 5).[3,34] This parameter reflects the displacement of the papillary muscles in patients with dilated left ventricles. Similar to the mitral leaflets, the anterior and posterior angles and length between the tip of the papillary muscles and the mitral annulus can be quantified as a measure of mitral leaflet tethering. 3D-imaging techniques provide optimal assessment of all these geometrical indices. Acquisition of a full volume of the left ventricle with 3D-echocardiography and subsequent image post-processing displays best the entire subvalvular apparatus from the LV perspective.[13]

Functionally, the subvalvular apparatus ensures adequate leaflet mobility throughout the cardiac cycle by synchronous papillary muscle contraction in concert with ventricular contraction and relaxation in normal hearts.[7] These forces

are transmitted to the valvular leaflets by the primary chords to ensure leaflet coaptation. Secondary chordae permit limited bulging of the leaflet bodies, which reduces leaflet stress in concert with the 3D-shape of the mitral annulus. The secondary 'strut' chordae only attach to the anterior mitral leaflet and are part of a ventriculo-valvular fibrous loop, essential to suspend the aorto-mitral angle and maintain normal LV shape, geometry and function.[7] Normal LV shape (sphericity index, end-diastolic volume index, end-systolic volume-index) and systolic function (ejection fraction, (dys)synchrony) are major determinants of normal geometric relations and function of the subvalvular apparatus.[3]

CLINICAL IMPLICATIONS

Studies of the normal MV by different noninvasive cardiac imaging modalities contributed to a wealth of (patho)physiological insights and clinical applications in patients with MV dysfunction. Echocardiography remains the first-line imaging technique of choice for evaluation of MV dysfunction (Table 2). 3D-echocardiography provides additional information to study function and anatomy of the mitral annulus, quantify mitral valve dysfunction and evaluate MV morphology, given by the ease of segmental anatomy recognition. However, 3D-image quality depends on 2D-image quality and still the temporal and spatial resolution are lower than 2D-echocardiography.[13] MDCT is highly suited to study MV anatomy (morphology and geometry), given its optimal spatial resolution. Radiation exposure, use of iodinated contrast agents, limited temporal resolution and current lack of applications to quantify blood flow are current drawbacks to systematically apply MDCT for MV evaluation.[35] As MDCT-angiography is increasingly performed to evaluate coronary artery disease, the report should mention when abnormal mitral morphology or geometry is encountered. CMR is a valid alternative for quantitative functional evaluation of the MV in case of suboptimal acoustic window and contraindication for TEE, but lacks spatial resolution to optimally address MV anatomy.[28] The costs, availability and high technical expertise needed for appropriate imaging additionally hamper the wide clinical use of CMR to image the MV.

Current surgical and percutaneous techniques or devices rely on careful noninvasive cardiac imaging for patient selection, planning, guiding and evaluation of the intervention. Morphologic MV characteristics determine MV reparability in organic MV disease, while geometric indices of the leaflets and subvalvular apparatus have shown to determine severity of MV dysfunction, reparability and outcome after repair in functional mitral regurgitation.[12,31] The importance of geometrical indices in functional MV disease enforced the idea of targeting therapeutically

the subvalvular apparatus, resulting in different surgical possibilities such as LV remodeling techniques (Coapsys® system, external balloon patch, etc.), use of neo-chordae and translocation or reconstruction of papillary muscles.[10] MDCT may become useful to evaluate the subvalvular apparatus prior to abovementioned complex repair procedures.[3] Moreover, there is a growing interest in percutaneous techniques to treat mitral regurgitation. Devices for direct or indirect mitral annuloplasty (via coronary sinus approach), direct edge-to-edge leaflet repair and percutaneous mitral valve replacement have been introduced into clinical practice or are currently under development.[5] MDCT as well as CMR enable the study of the surrounding anatomy of the mitral annulus which is of major interest in the selection of candidates for percutaneous annuloplasty interventions via the coronary sinus, for example.[4-6]

CONCLUSION

The normal MV is a functional complex that relies on normal morphology, geometry and function of all its constituents. The role of 3D-imaging techniques to study the MV is increasingly recognized. Further development in this field of multimodality imaging will undoubtedly lead to novel (3D) applications and improved spatial and temporal resolution to study the (normal) mitral valve. This knowledge will ultimately refine our diagnostic performance, provide additional (patho)physiological insights and help to design new strategies for interventional or surgical treatment of diseased mitral valves.

REFERENCES

1. Nkomo VT, Gardin JM, Skelton TN et al. Burden of valvular heart diseases: a population-based study. *Lancet.* 2006; 368:1005-1011.
2. Iung B, Baron G, Butchart EG et al. A prospective survey of patients with valvular heart disease in Europe: The Euro Heart Survey on Valvular Heart Disease. *Eur Heart J.* 2003; 24:1231-1243.
3. Delgado V, Tops LF, Schuijf JD et al. Assessment of mitral valve anatomy and geometry with multislice computed tomography. *JACC Cardiovasc Imaging.* 2009; 2:556-565.
4. Van Mieghem NM, Piazza N, Anderson RH et al. Anatomy of the mitral valvular complex and its implications for transcatheter interventions for mitral regurgitation. *J Am Coll Cardiol.* 2010; 56:617-626.
5. Delgado V, Kapadia S, Marsan NA et al. Multimodality imaging before, during, and after percutaneous mitral valve repair. *Heart.* 2011; 97:1704-1714.
6. O'Gara P, Sugeng L, Lang R et al. The role of imaging in chronic degenerative mitral regurgitation. *JACC Cardiovasc Imaging.* 2008; 1:221-237.
7. Silbiger JJ, Bazaz R. Contemporary insights into the functional anatomy of the mitral valve. *Am Heart J.* 2009; 158:887-895.
8. Ho SY. Anatomy of the mitral valve. *Heart.* 2002; 88 Suppl 4:iv5-10.
9. Salcedo EE, Quaife RA, Seres T, Carroll JD. A framework for systematic characterization of the mitral valve by real-time three-dimensional transesophageal echocardiography. *J Am Soc Echocardiogr.* 2009; 22:1087-1099.
10. Silbiger JJ. Mechanistic Insights into Ischemic Mitral Regurgitation: Echocardiographic and Surgical Implications. *J Am Soc Echocardiogr.* 2011; 24:707-719.
11. Foster GP, Dunn AK, Abraham S et al. Accurate Measurement of Mitral Annular Dimensions by Echocardiography: Importance of Correctly Aligned Imaging Planes and Anatomic Landmarks. *J Am Soc Echocardiogr.* 2009; 22:458-463.
12. Lancellotti P, Moura L, Pierard LA et al. European Association of Echocardiography recommendations for the assessment of valvular regurgitation. Part 2: mitral and tricuspid regurgitation (native valve disease). *Eur J Echocardiogr.* 2010; 11:307-332.
13. Lang RM, Badano LP, Tsang W et al. EAE/ASE recommendations for image acquisition and display using three-dimensional echocardiography. *Eur Heart J Cardiovasc Imaging.* 2012; 13:1-46.
14. Shanks M, Delgado V, Ng AC et al. Mitral valve morphology assessment: three-dimensional transesophageal echocardiography versus computed tomography. *Ann Thorac Surg.* 2010; 90:1922-1929.
15. Veronesi F, Corsi C, Sugeng L et al. A study of functional anatomy of aortic-mitral valve coupling using 3D matrix transesophageal echocardiography. *Circ Cardiovasc Imaging.* 2009; 2:24-31.
16. Jensen MO, Jensen H, Levine RA et al. Saddle-shaped mitral valve annuloplasty rings improve leaflet coaptation geometry. *J Thorac Cardiovasc Surg.* 2011; 142:697-703.
17. Lansac E, Di Centa I, Al Attar N et al. Percutaneous mitral annuloplasty through the coronary sinus: an anatomic point of view. *J Thorac Cardiovasc Surg.* 2008; 135:376-381.
18. Tops LF, Van de Veire NR, Schuijf JD et al. Noninvasive evaluation of coronary sinus anatomy and its relation to the mitral valve annulus: implications for percutaneous mitral annuloplasty. *Circulation.* 2007; 115:1426-1432.

19. del Valle-Fernandez R, Jelnin V, Panagopoulos G, Ruiz CE. Insight into the dynamics of the coronary sinus/great cardiac vein and the mitral annulus: implications for percutaneous mitral annuloplasty techniques. *Circ Cardiovasc Interv*. 2009; 2:557-564.
20. Chiribiri A, Kelle S, Kohler U et al. Magnetic resonance cardiac vein imaging: relation to mitral valve annulus and left circumflex coronary artery. *JACC Cardiovasc Imaging*. 2008; 1:729-738.
21. Harnek J, Webb JG, Kuck KH et al. Transcatheter implantation of the MONARC coronary sinus device for mitral regurgitation: 1-year results from the EVOLUTION phase I study (Clinical Evaluation of the Edwards Lifesciences Percutaneous Mitral Annuloplasty System for the Treatment of Mitral Regurgitation). *JACC Cardiovasc Interv*. 2011; 4:115-122.
22. Quill JL, Hill AJ, Laske TG et al. Mitral leaflet anatomy revisited. *J Thorac Cardiovasc Surg*. 2009; 137:1077-1081.
23. Chan KM, Wage R, Symmonds K et al. Towards comprehensive assessment of mitral regurgitation using cardiovascular magnetic resonance. *J Cardiovasc Magn Reson.* 2008; 10:61.
24. Foster GP, Isselbacher EM, Rose GA et al. Accurate localization of mitral regurgitant defects using multiplane transesophageal echocardiography. *Ann Thorac Surg*. 1998; 65:1025-1031.
25. Tsang W, Weinert L, Sugeng L et al. The value of three-dimensional echocardiography derived mitral valve parametric maps and the role of experience in the diagnosis of pathology. *J Am Soc Echocardiogr*. 2011; 24:860-867.
26. Gabriel RS, Kerr AJ, Raffel OC et al. Mapping of mitral regurgitant defects by cardiovascular magnetic resonance in moderate or severe mitral regurgitation secondary 27. Han Y, Peters DC, Salton CJ et al. Cardiovascular magnetic resonance characterization of mitral valve prolapse. *JACC Cardiovasc Imaging*. 2008; 1:294-303.
27. Stork A, Franzen O, Ruschewski H et al. Assessment of functional anatomy of the mitral valve in patients with mitral regurgitation with cine magnetic resonance imaging: comparison with transesophageal echocardiography and surgical results. *Eur Radiol*. 2007; 17:3189-3198.
28. Gersh BJ, Maron BJ, Bonow RO et al. 2011 ACCF/AHA Guideline for the Diagnosis and Treatment of Hypertrophic Cardiomyopathy: a report of the American College of Cardiology Foundation/American Heart Association Task Force on Practice Guidelines. Developed in collaboration with the American Association for Thoracic Surgery, American Society of Echocardiography, American Society of Nuclear Cardiology, Heart Failure Society of America, Heart Rhythm Society, Society for Cardiovascular Angiography and Interventions, and Society of Thoracic Surgeons. *J Am Coll Cardiol*. 2011; 58:e212-260.
29. Di Mauro M, Gallina S, D'Amico MA et al. Functional mitral regurgitation From normal to pathological anatomy of mitral valve. *Int Journal Cardiol*. 2013; 10:242-248.
30. Ciarka A, Braun J, Delgado V et al. Predictors of mitral regurgitation recurrence in patients with heart failure undergoing mitral valve annuloplasty. *Am J Cardiol*. 2010; 106:395-401.
31. Lee AP, Acker M, Kubo SH et al. Mechanisms of recurrent functional mitral regurgitation after mitral valve repair in nonischemic dilated cardiomyopathy: importance of distal anterior leaflet tethering. *Circulation*. 2009; 119:2606-2614.
32. Adams DH, Rosenhek R, Falk V. Degenerative mitral valve regurgitation: best practice revolution. *Eur Heart J*. 2010; 31:1958-1966.
33. Sadeghpour A, Abtahi F, Kiavar M et al. Echocardiographic evaluation of mitral geometry in functional mitral regurgitation. *J Cardiothorac Surg*. 2008; 3:54.

34. Taylor AJ, Cerqueira M, Hodgson JM et al. ACCF/SCCT/ACR/AHA/ ASE/ASNC/NASCI/SCAI/ SCMR 2010 Appropriate Use Criteria for Cardiac Computed Tomography. A Report of the American College of Cardiology Foundation Appropriate Use Criteria Task Force, the Society of Cardiovascular Computed Tomography, the American College of Radiology, the American Heart Association, the American Society of Echocardiography, the American Society of Nuclear Cardiology, the North American Society for Cardiovascular Imaging, the Society for Cardiovascular Angiography and Interventions, and the Society for Cardiovascular Magnetic Resonance. *Circulation.* 2010; 122:e525-555.

Chapter 4

Leaflet remodeling in functional mitral valve regurgitation: characteristics, determinants and relation to regurgitation severity

Philippe Debonnaire, Ibtihal Al Amri, Darryl P Leong, Emer Joyce, Spyridon Katsanos, Vasilis Kamperidis, Martin J Schalij, Jeroen J Bax, Nina Ajmone Marsan, Victoria Delgado

Eur Heart J Cardiovasc Imaging, 2015 Mar 16(3):290-299.

ABSTRACT

Objectives

Recently it has been hypothesized that mitral leaflet remodeling may play a role in the pathophysiology of functional mitral regurgitation (FMR). We investigated the characteristics, determinants and relation of mitral leaflet remodeling to FMR severity.

Methods and Results

3-dimensional transesophageal echocardiographic data of the mitral valve (MV) were studied in 30 patients with FMR ≥grade 3 (≥3), 24 patients with FMR <grade 3 (<3) and 22 controls with normal MV. FMR <3 and ≥3 patients showed leaflet remodeling compared to control subjects with larger overall MV leaflet areas (11.47±3.16 and 9.58±1.99 vs. 7.30±1.57 cm^2/m^2, respectively; all $p<0.01$). Tenting volume ($r^2=0.55$), LV ejection fraction ($r^2=0.20$), annulus area ($r^2=0.87$) and LV sphericity index ($r^2=0.25$) were correlated with overall MV leaflet area (all $p<0.001$). Although these correlates were similar between FMR <3 and ≥3 patients (all $p>0.05$), the overall MV leaflet area was smaller in FMR ≥3 compared to FMR<3 patients ($p=0.01$), indicating less remodeling despite similar tethering degree. Particularly, coaptation/overall MV leaflet area ratio ≤0.24, reflecting insufficient leaflet remodeling, was associated with FMR ≥3 (area under ROC curve=0.93, sensitivity 90% and specificity 91%). This ratio was independently associated with FMR ≥3 (OR 61.3, 95%CI 9.4-399.9, $p<0.001$) and showed significant correlation with effective regurgitant orifice area ($r^2=0.38$, $p< 0.001$).

Conclusion

MV leaflet remodeling in FMR is common and relates to LV function, LV sphericity, MV tenting volume and annulus dilatation. Insufficient leaflet remodeling relative to the mitral annular and LV changes is independently associated with FMR severity.

INTRODUCTION

Functional mitral regurgitation (FMR) affects approximately 30% of patients with ischemic heart disease or dilated cardiomyopathy and yields a dismal prognosis.[1] FMR is a complex problem, comprising dysfunction of a structurally normal mitral valve (MV) secondary to local or global left ventricular (LV) dysfunction with distorted LV geometry.[2] Recent data, however, have challenged the idea of the MV being only an "innocent bystander" in FMR patients. In particular, it was shown that the MV in patients with end-stage heart failure exhibits extracellular matrix changes proportional to annular, atrial and ventricular dimensions and function, including increased fibrosis (collagen), deoxyribonucleic acid (DNA, cellularity) and glycosaminoglycan extent.[3] These alterations coincided with increased leaflet thickness and length, reflecting structural leaflet remodeling.[3] Animal studies have also shown an up-regulation of the extracellular matrix and mitral leaflet adaptation (increased area) as a compensatory response to LV dilatation or loading.[4, 5] More recent studies, using 3-dimensional (3D) echocardiography which is ideally suited for detailed evaluation of MV anatomy and morphology, have shown the presence of MV leaflet remodeling in patients with LV dysfunction and have suggested that inadequate leaflet remodeling may be related to the presence of significant FMR.[6-8] Data on characteristics, potential determinants and the relationship of MV leaflet remodeling to FMR severity are scarce, however. Therefore, the hypothesis of the present evaluation was to demonstrate whether inadequate leaflet remodeling on 3D echocardiography, expressed as lack of leaflet coaptation relative to annular or LV changes, relates to presence of significant FMR.

METHODS

Patients

Patients with FMR who underwent 3D transesophageal echocardiography were included. FMR was defined as MR due to local or global LV dysfunction and/or remodeling in the absence of macroscopic morphologic abnormalities of the mitral valve. Clinical reasons for transesophageal echocardiography in FMR patients comprised evaluation of severity of valvular dysfunction and specific underlying mechanism (n=35/54), screening for transcatheter mitral valve repair eligibility (n=17/54) or diagnostic work-up before ventricular tachyarrhytmia ablation (n=2/54). A control group included patients with macroscopically normal structural and functional MV who underwent clinically indicated 3D transesophageal echocardiography to exclude cardiac embolism source (n=19/22) or endocarditis (n=3/22). Patients

with aortic valve stenosis, MV stenosis, prior left-sided valve surgery, organic MV disease (prolapse, flail, cleft, rheumatic disease), congenital heart disease, active endocarditis, LV assist device or hypertrophic cardiomyopathy and patients with insufficient image quality were not included.

Clinical characteristics, medication use and heart failure etiology (ischemic versus non-ischemic, including location of prior myocardial infarction) were retrieved from the departmental Cardiology Information System (EPD-Vision®, Leiden University Medical Center, Leiden, the Netherlands). Patients with FMR were divided into two groups according to the mitral regurgitation grade (FMR<3 versus FMR≥3). MV apparatus geometry and mitral leaflet remodeling were evaluated and compared between groups.

The institutional ethical committee approved this evaluation and waived the need for patient written informed consent for retrospective analysis of clinically collected data.

2D echocardiography

All patients underwent 2-dimensional (2D) transthoracic echocardiography in the left lateral decubitus position using commercially available ultrasound machines (Vivid-5, Vivid-7 and E9, GE-Vingmed, Milwaukee, WI) equipped with 3.5 MHz and M5S transducers. 2D-gray-scale and Doppler images were acquired in cine-loop format with ECG-triggering. Off-line analysis of these images was performed on a workstation (EchoPAC 112.0.0, GE Medical Systems, Horten, Norway). LV and left atrial dimensions were assessed as recommended.[9] LV end-diastolic and end-systolic diameters were measured at the parasternal long-axis view. The Simpson's biplane method was applied to quantify LV volumes and to calculate LV ejection fraction. Left atrial volume was also measured according to the biplane method. All volumes were indexed to body surface area. LV sphericity index was defined as the ratio of end-diastolic mid-ventricular width to length of the LV. Early (E) and late (A) diastolic mitral inflow velocities as well as deceleration time were assessed by pulsed-wave Doppler, placing the sample volume at the tips of the mitral leaflets. Septal mitral annulus velocities (E`) were derived from tissue Doppler recordings and used to calculate the E/E` ratio. In line with current recommendations, integration of all available qualitative and (semi-)quantitative parameters assessed with 2D echocardiography, including vena contracta width and effective orifice area (EROA) by proximal isovelocity surface area method were evaluated to grade FMR as trivial (1), mild (2), moderate (3) or severe (4).[10, 11] A vena contracta width between 3-4 mm, 5-6 mm and ≥7 mm defined grade 2, 3 and 4 FMR, respectively. In addition, an EROA between 10.0-14.9 mm^2, 15.0-19.9 mm^2 and ≥20.0 mm^2 defined grade 2, 3 and 4 FMR, respectively.

3D echocardiography

Patients underwent 3D transoesophageal echocardiography using a Philips iE33 ultrasound machine (Philips Medical Systems). 3D datasets of the MV were acquired using full-volume or 3D-zoom mode, comprising a pyramidal volume of approximately 60º by 60º. In order to maximize frame rate, multi-beat (7-14 beats) full-volume acquisitions were performed during breath-hold whenever possible or 1-beat 3D-zoom acquisitions with the sector adjusted to include the MV if the patient could not hold the breath or when presenting with irregular heart rhythm such as atrial fibrillation.

3D mitral valve quantification

3D-volumetric datasets of the MV were studied off-line on a workstation (Qlab, Philips Medical Systems, version 9.0) using dedicated commercially available MV Quantification software (MVQ). To maximize spatial and temporal resolution, 3D-full volume acquisitions were preferred over 3D-zoomed acquisitions and mean frame rate was 26 frames/s. Stepwise reconstruction of a 3D-model of the MV was performed by a single experienced operator, blinded to FMR severity (Figure 1A). After selecting the end-systolic frame, multi-plane reformation (MPR) planes were automatically displayed and manually aligned to obtain a bicommisural, outflow tract and short-axis view of the MV. In addition, a 3D volume rendering of the MV is displayed and can be additionally used for identification of anatomic landmarks. The short-axis plane was set at the level of the mitral annulus. The antero-lateral and postero-medial mitral annulus were then indicated on the bi-commissural view whereas the anterior and posterior mitral annulus as well as the mitral leaflet coaptation point and the aortic annulus were set at the outflow tract view. An initial 3D-model containing an annular ring and mitral leaflets was then automatically displayed. The mitral annulus on the 3D-model was subsequently refined by indicating additionally 8 pairs of annulus points on sequential MPR rotational cross-sections in the long-axis views and the mitral leaflet commissural points were set on the short-axis MPR image. Subsequently, the mitral leaflets and the coaptation length were manually traced on multiple cross-sections (between 18 to 30) in the outflow tract view, orthogonal to the inter-commissural direction with a minimal distance of 0.17 cm between cross-sections. To correctly identify the coaptation point, the 3D-rendered volume of the MV (surgical en face view) was additionally used. Finally, the 3D model of the MV was displayed and several geometric measurements of the MV were automatically generated (Figure 1B). Lengths, areas and volumes were indexed to body surface area. In particular, the antero-posterior and inter-commissural annular diameter and circumferential annular area were assessed. In addition, the exposed leaflet area of the total MV and

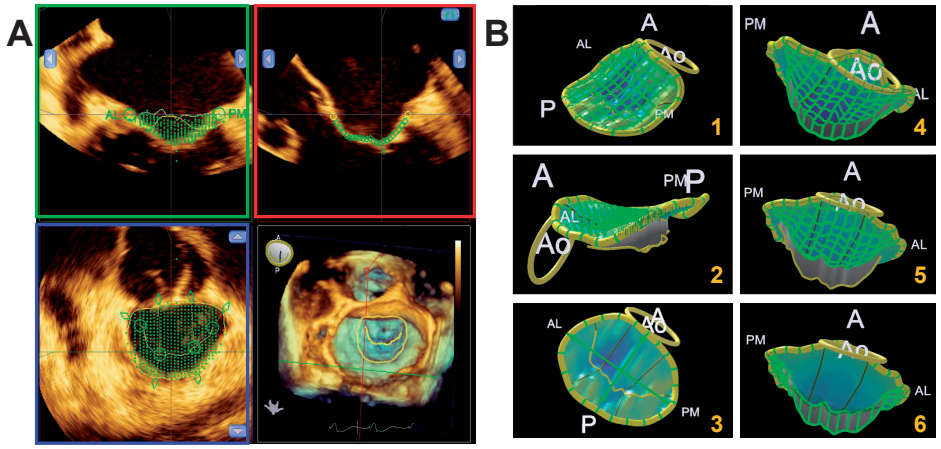

Figure 4.1
Mitral leaflet and annulus geometry by 3D transesophageal echocardiography. Panel A: A 3-dimensional (3D) model of the mitral valve is reconstructed after indicating mitral annulus landmarks, tracing leaflets and indicating the coaptation point on multi-plane reformation images that are manually aligned to obtain a bicommisural (green), outflow tract (red) and short-axis plane (blue) of the mitral valve. Panel B: Annulus area (1), tenting volume (2), annulus diameters (3), total valve area (4), exposed valve area (5) and coaptation area (6), calculated as total minus exposed leaflet area, are assessed on the derived 3D model. A: anterior, AL: anterolateral, Ao: aorta, P: posterior, PM: posteromedial.

the respective anterior and posterior leaflets, representing the surface exposed to the left atrium, were derived. The overall leaflet area, including the exposed area and coaptation area of each mitral leaflet was also computed. The *coaptation area* was calculated as the overall leaflet area minus the exposed leaflet area of the total MV.[8] Of note, the anatomic regurgitant orifice area is not excluded from the coaptation area as spatial resolution does not permit its adequate detection. The coaptation length at central level (A2-P2) and the tenting volume comprised between the leaflets and the annular surface area were also measured. Similar to prior reports, the ratio of overall total leaflet/annular area (*leaflet/annular area*) and coaptation/overall total leaflet area (*coaptation/leaflet area*) were assessed as measures of leaflet remodeling, relative to the mitral annulus and LV changes.[6-8]

Statistical analysis

Continuous variables are presented as mean ± SD and compared with the Student T-test or Mann-Whitney U-test, as appropriate. Categorical variables are presented as number and percentages and compared by Pearson chi-square test. Overall comparison among groups was performed by one-way ANOVA with Bonferroni post-hoc testing (for continuous variables with normal distribution), Kruskall-Wallis (for non-normally distributed continuous variables) or Pearson

chi-square (for categorical variables) tests. Correlates of overall total mitral leaflet area were explored with linear regression analysis. In addition binary logistic regression was performed to investigate the univariate associates of significant mitral leaflet remodeling (defined as ≥2 SD of the overall leaflet area of control subjects). A receiver operating characteristic (ROC) curve was subsequently constructed to evaluate the value of the coaptation/leaflet area to predict presence of FMR ≥3. Uni- and multivariate binary logistic regression analyses were in addition performed to identify independent correlates of FMR ≥3, using a backward elimination approach. Odds ratio (OR) and 95% confidence intervals (CI) were obtained. A significance level of $p<0.10$ qualified for entrance in the multivariate model. Finally the association between coaptation/leaflet area and FMR grade was further explored by linear regression analysis. Intra- and inter observer variability for overall and exposed mitral valve leaflet area was evaluated by intraclass correlation for 15 randomly selected patients (5 control subjects, 5 FMR<3 and 5 FMR≥3 patients). Statistical analyses were performed using the SPSS software version 20.0. (SPSS Inc., Chicago, Illinois). A two-sided p-value <0.05 was considered statistically significant.

RESULTS

Patients

Seventy-six patients were evaluated, including 22 controls (53±15 years old, 64% male), 24 patients with FMR<3 (61±16 years old, 50% male) and 30 patients with FMR≥3 (68±12 years old, 60% male). Characteristics of the control and FMR groups are outlined in Table 1. Control subjects were younger, more likely to be in sinus rhythm, had less diabetes mellitus and were using less cardiovascular medication. Patients with FMR≥3 had lower systolic and diastolic blood pressure and higher prevalence of ischemic heart failure etiology compared to patients with FMR<3. Location of myocardial infarction between patients with ischemic FMR<3 vs. FMR≥3 was however, similar. Cardiovascular medication use was comparable between both groups.

FMR patients had significantly larger LV diameters, LV volumes, LA volume and showed significantly worse LV systolic and diastolic function with higher systolic arterial pulmonary pressures compared to controls.

Mitral leaflet remodeling

Geometric and morphologic characteristics of the mitral annulus and leaflets are listed in Table 2. Patients with FMR had significantly larger annular diameters and

Table 4.1
Baseline patient characteristics.

	Controls n=22	FMR<3 n=24	FMR≥3 n=30	p value*	p value†
Men, n (%)	14 (64)	12 (50)	18 (60)	0.17	0.46
Age, years	53 ± 15	61 ± 16	68 ± 12	0.001	0.22
BSA, m²	1.95 ± 0.2	1.90 ± 0.2	2.03 ± 0.2	0.08	-
Sinus rhythm, n (%)	22 (100)	19 (79)	19 (63)	<0.001	0.21
Systolic BP, mmHg	130 ± 16	129 ± 26	112 ± 21	0.004	0.015
Diastolic BP, mmHg	75 ± 10	76 ± 15	65 ± 9	0.002	0.006
Arterial hypertension, n (%)	7 (32)	10 (42)	15 (50)	0.17	0.54
Diabetes mellitus, n (%)	1 (5)	4 (17)	11 (37)	<0.001	0.10
Active/ex-smoker, n (%)	9 (45)	11 (46)	16 (53)	0.82	0.58
Hypercholesterolemia, n (%)	13 (59)	13 (54)	15 (50)	0.49	0.76
Ischemic FMR, n (%)	-	12 (50)	25 (83)	-	0.009
Prior myocardial infarction					
Anterior, septal and/or apical	-	7/12 (58)	15/25 (60)		0.92
Inferior, posterior and/or lateral	-	6/12 (50)	11/25 (44)		0.73
β-blocker, n (%)	5 (24)	18 (75)	23 (77)	0.036	0.89
ACE-inhibitor, n (%)	3 (14)	12 (50)	13 (43)	0.036	0.52
ARB II, n %	3 (14)	6 (25)	10 (33)	<0.001	0.57
Diuretic, n (%)	2 (10)	17 (71)	28 (93)	0.014	0.09
Spironolactone, n (%)	1 (5)	6 (25)	11 (37)	<0.001	0.41
Statin, n (%)	15 (75)	13 (54)	22 (73)	0.002	0.20
LVEDD, mm	45 ± 6	60 ± 9	65 ± 9	<0.001	0.64
LVESD, mm	26 ± 5	47 ± 9	50 ± 10	<0.001	0.45
LVEDVI, mL/m²	48 ± 15	99 ± 56	99 ± 41	<0.001	1.00
LVESVI, mL/m²	17 ± 6	67 ± 47	67 ± 37	<0.001	1.00.
LVEF, %	66 ± 6	36 ± 10	36 ± 14	<0.001	1.00
LVED sphericity index	0.47 ± 0.1	0.61 ± 0.1	0.62 ± 0.1	<0.001	1.00
LAVI, mL/m²	25 ± 5	51 ± 18	55 ± 20	<0.001	1.00
E/A	1.0 ± 0.3	1.7 ± 0.8	2.6 ± 1.0	<0.001	0.001
E/E'	11 ± 5	30 ± 12	41 ± 23	<0.001	0.044
DecT, msec	206 ± 37	167 ± 48	146 ± 48	<0.001	0.29
MV mean gradient, mmHg	1.2 ± 0.4	1.8 ± 0.9	2.0 ± 1.1	0.008	1.00
MR grade, n (%)				0.003	<0.001
Grade 1	-	7 (29)	0 (0)		
Grade 2	-	17 (71)	0 (0)		
Grade 3	-	0 (0)	7 (23)		
Grade 4	-	0 (0)	23 (77)		
MR vena contracta, mm	-	3.8 ± 0.7	8.1 ± 1.7	-	<0.001
MR EROA (Pisa), cm²	-	0.12 ± 0.1	0.40 ± 0.1	-	<0.001
PAPsyst, mmHg	26 ± 5	37 ± 11	43 ± 14	<0.001	0.14

* for comparison between all patient groups
† for comparison of FMR <3 versus ≥3 patients
ACE: angiotensine converting enzyme, ARBII: angiotensine receptor bocker, BP: blood pressure, BSA: body surface area, DecT: deceleration time, ED: end-diatsolic, EDD: end-diastolic diameter, ESD: end-systolic diameter, EDVI: end-diastlic volume indexed to BSA, EF: ejection fraction, ESVI: end-systolic volume indexed to BSA, FMR: functional mitral regurgitation, LAVI: left atrial volume indexed to BSA, MV: mitral valve, MR: mitral regurgitation, PAPsyst: systolic arterial pulmonary pressure, Pisa: proximal isovelocity surface area

area compared with controls. The presence of leaflet remodeling was identified in both FMR groups showing larger overall leaflet area compared to controls. Patients with FMR <3 and ≥3 had a respective relative increase of overall total leaflet area of 57% and 31% compared to controls (both, p<0.001). Significant leaflet remodeling, defined as ≥2 SD overall total leaflet area of control subjects, was respectively observed in 67% (n=16/24) and 37% (n=11/30) of patients with FMR<3 and FMR≥3. The pattern of relative leaflet remodeling was symmetrical for the anterior and posterior mitral leaflets. In patients with FMR<3 the anterior and posterior mitral leaflet areas were increased by 53% and 62% whereas in patients with FMR≥3 these increments were of 31% and 32%, respectively. In addition, symmetrical leaflet remodeling was also noted in patients with infero-posterior myocardial infarction (n=17), showing a 35% and 39% relative increase of the posterior and anterior MV leaflet respectively.

Table 4.2
Mitral valve geometry and leaflet remodeling by 3D echocardiography.

	Controls n=22	FMR<3 n=24	FMR≥3 n=30	p value*	p value†
ANNULUS					
AP diameter, mm/m^2	14.3 ± 1.8	18.0 ± 2.5	16.9 ± 2.3	<0.001	0.18
IC diameter, mm/m^2	18.8 ± 2.8	21.1 ± 3.1	19.6 ± 2.0	<0.001	0.12
Annulus area, cm^2/m^2	4.6 ± 1.0	6.7 ± 1.6	6.1 ± 1.2	<0.001	0.21
LEAFLETS					
Exposed leaflet area, cm^2/m^2					
AMVL	3.12 ± 0.65	4.81 ± 1.15	4.37 ± 0.80	<0.001	0.23
PMVL	2.15 ± 0.52	3.62 ± 1.23	3.16 ± 0.84	<0.001	0.21
Total (AMVL + PMVL)	5.27 ± 1.12	8.42 ± 2.30	7.53 ± 1.54	<0.001	0.18
Overall leaflet area, cm^2/m^2					
AMVL	4.13 ± 0.86	6.33 ± 1.59	5.39 ± 1.03	<0.001	0.016
PMVL	3.17 ± 0.74	5.14 ± 1.62	4.18 ± 1.03	<0.001	0.013
Total (AMVL + PMVL)	7.30 ± 1.57	11.47 ± 3.16	9.58 ± 1.99	<0.001	0.012
Coaptation area, cm^2/m^2	2.03 ± 0.50	3.04 ± 0.97	2.04 ± 0.51	<0.001	<0.001
A2-P2 coaptation L, mm/m^2	2.8 ± 0.7	3.2 ± 0.9	2.1 ± 0.40	<0.001	<0.001
Leaflet /annular area	1.57 ± 0.09	1.70 ± 0.14	1.59 ± 0.17	0.004	0.013
Coaptation/ leaflet area	0.28 ± 0.02	0.26 ± 0.03	0.21 ± 0.02	<0.001	<0.001
Leaflet/exposed area	1.38 ± 0.05	1.36 ± 0.06	1.27 ± 0.03	<0.001	<0.001
Tenting volume, mL/m^2	0.74 ± 0.29	2.09 ± 1.13	1.87 ± 1.1	<0.001	1.00

* for comparison among all patient groups
† for comparison of FMR <3 versus ≥3 patients
AMVL: anterior mitral valve leaflet, AP: antero-posterior, A2: AMVL medial scallop, IC: inter-commissural, L: length, PMVL: posterior mitral valve leaflet, P2: PMVL medial scallop

Correlates of mitral leaflet remodeling

Potential determinants of mitral leaflet remodeling were explored by logistic and linear regression analysis. Larger MV tenting volume (OR 10.04, 95% CI 3.52-28.68, p<0.001), LV sphericity index ≥0.65 (OR 17.00, 95% CI 4.76-60.77, p<0.001) and increased mitral annulus area (OR 1.04, 95% CI 1.02-1.07, p<0.001), all reflecting increased tethering forces, significantly correlated with the presence of significant leaflet remodeling and overall mitral leaflet area (Figure 2). In addition LV ejection fraction was significantly and inversely associated with the presence of significant leaflet remodeling (OR 0.94, 95% CI 0.91-0.97, p<0.001) and overall MV leaflet area (Figure 2).

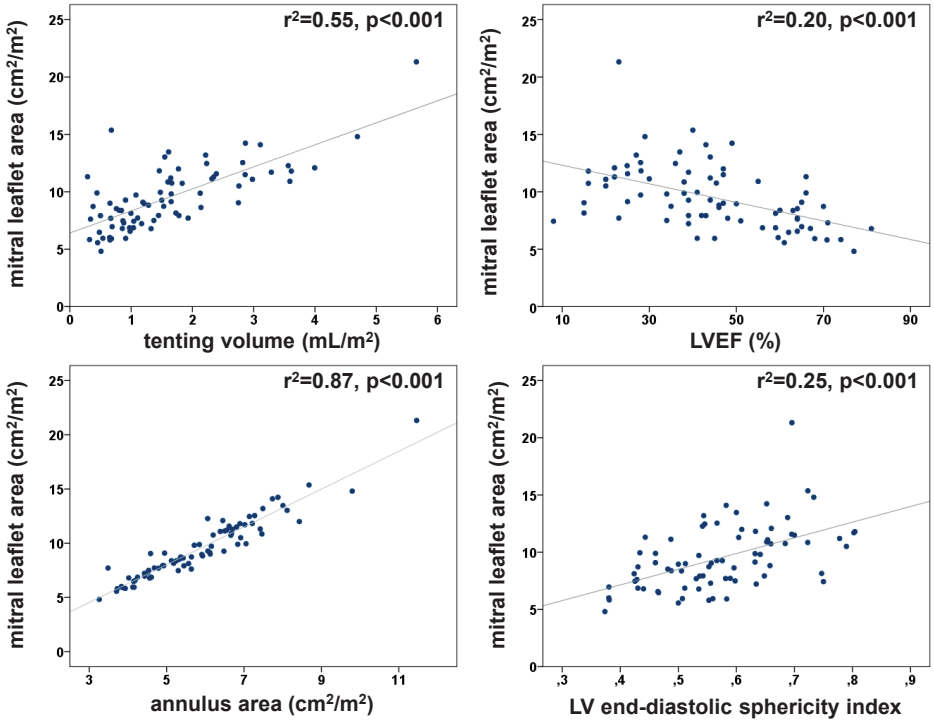

Figure 4.2
Correlates of total mitral valve leaflet area by linear correlation. LVEF: left ventricular ejection fraction.

Leaflet remodeling and mitral regurgitation severity

Significant mitral leaflet remodeling was present in both FMR groups. Importantly, a similar degree of tethering was noted in both groups, shown by comparable MV tenting volumes, annulus dilatation and LV size, shape and function (Table 1 and 2). Less extensive leaflet remodeling, however, was observed in patients with FMR≥3 vs. patients with FMR<3, as reflected by smaller overall total MV leaflet

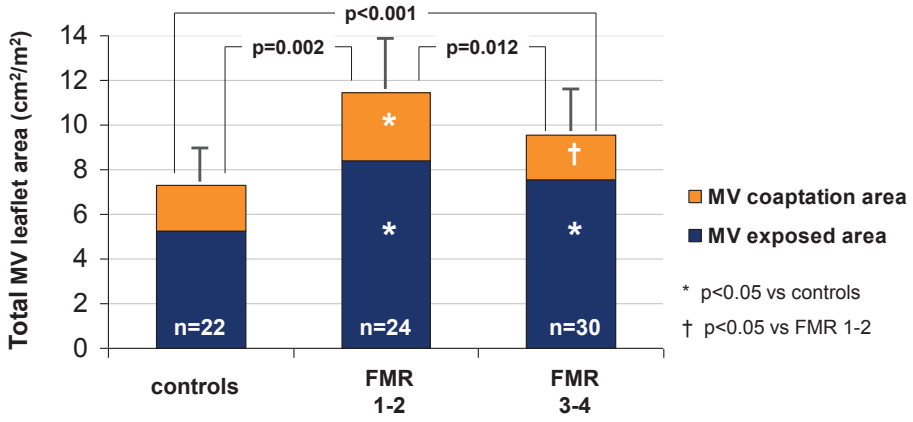

Figure 4.3
Mitral valve remodeling among different groups. Patients with functional mitral regurgitation (FMR) show larger total mitral leaflet area than control subjects (leaflet remodeling). Leaflet area in patients with FMR ≥3 versus <3, however, is smaller, mainly due to smaller coaptation area rather than exposed leaflet area. Insufficient leaflet remodeling resulting in lack of coaptation reserve might prohibit adequate systolic leaflet closure and facilitate occurrence of significant FMR. FMR: functional mitral regurgitation, MV: MV.

area (Table 2; Figure 3). This difference was mainly attributed to smaller coaptation area in patients with FMR≥3 compared with patients with FMR<3, as both groups had comparable exposed leaflet area. The coaptation/leaflet area was preserved (proportional to increased leaflet size) in patients with FMR<3, however, it was significantly decreased in patients with FMR≥3 compared with control patients, reflecting insufficient leaflet remodeling (lack of coaptation reserve) to compensate for the requirements of the dysfunctional dilated LV (Figure 4).

The ROC curve analysis showed that coaptation/leaflet area was an accurate predictor of the presence of FMR≥3 with AUC=0.925 (p<0.001) (Figure 5A). In particular a coaptation/leaflet area ≤0.24, indicating a coaptation area ≤24% of the overall total leaflet area, had a sensitivity and specificity of 90% and 91% to predict the presence of FMR≥3, respectively.

As shown in Table 3, the multivariate regression analysis demonstrated that coaptation/leaflet area ≤0.24 is strongly related to the presence of FMR≥3, independently of degree of LV tethering or infarct location in case of ischemic FMR. Coaptation/leaflet area showed a significant inverse correlation with FMR severity (r^2=0.38, p<0.001) (Figure 5B).

Additionally, the leaflet/annular area ratio of patients with FMR≥3 was significantly smaller than patients with FMR<3, suggesting insufficient leaflet remodeling to compensate for the increased annulus size.

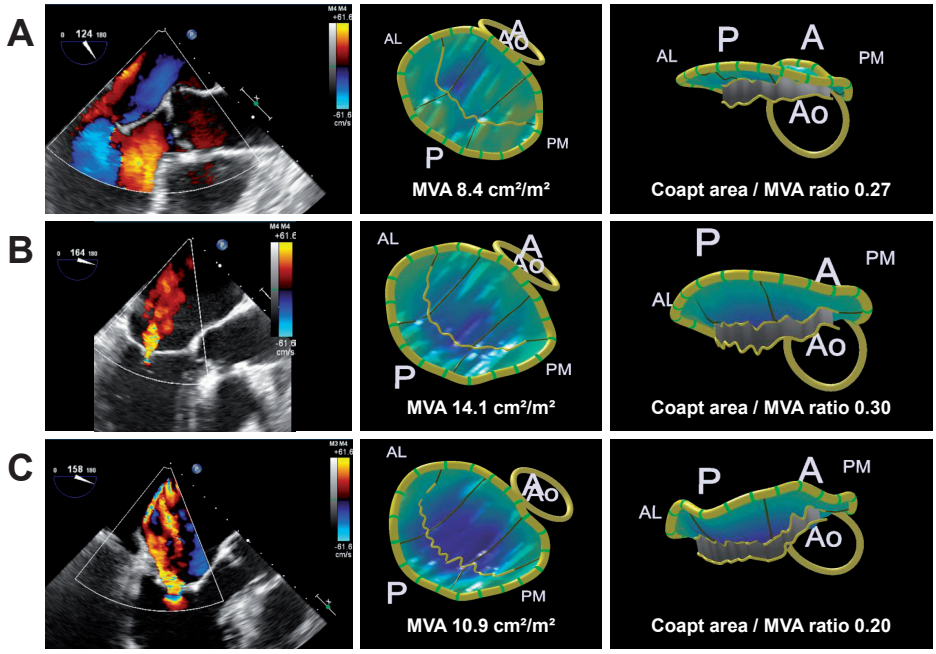

Figure 4.4

Examples of mitral valve leaflet remodeling in representative subjects. Panel A: control patient without functional mitral regurgitation (FMR). Patients with mild (Panel B) and severe FMR (Panel C), both secondary to inferior infarction. Note larger mitral valve area (MVA) and coaptation area to MVA ratio in patient with mild versus severe FMR. A: anterior, AL: anterolateral, Ao: aorta, P: posterior, PM: posteromedial.

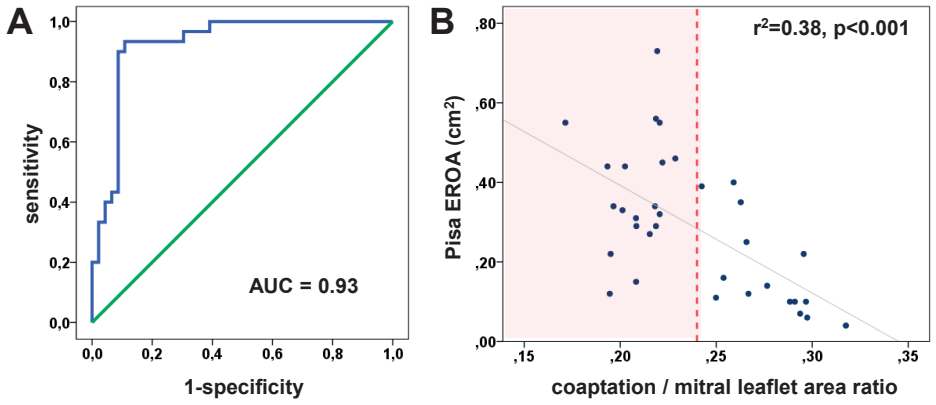

Figure 4.5

Relation of coaptation to mitral valve leaflet area and severity of functional mitral regurgitation. Panel A: ROC-curve analysis, coaptation/leaflet area ratio ≤0.24 predicts FMR ≥ grade 3 with sensitivity of 90% and specificity of 91%. Panel B: Reduced coaptation/mitral leaflet area ratio correlates linearly to FMR severity. Red dashed line indicates the ROC-curve derived cut-off point of ≤0.24. AUC: area under the curve, EROA: effective regurgitant orifice area, Pisa: proximal isovelocity surface area.

Table 4.3
Independent associates to functional mitral regurgitation ≥ grade 3.

	Univariate			Multivariate		
	OR	95% CI	p value	OR	95% CI	p value
Age, per year	1.06	1.02-1.10	0.004	1.01	0.93-1.08	0.96
Male gender	1.15	0.45-2.94	0.76			
Ischemic FMR	5.00	1.43-17.5	0.012	3.19	0.50-20.5	0.22
Infarct location						
Ant, sept and/or apical	1.07	0.26-4.34	0.92			
Inf, post and/or lateral	0.79	0.19-3.12	0.73			
LVEF, per %	0.95	0.92-0.98	0.001	0.98	0.91-1.06	0.61
LVED sphericity index ≥0.65	3.63	1.27-10.4	0.016	1.04	0.15-7.12	0.97
Annulus area, per mm^2/m^2	1.01	0.99-1.01	0.68			
Tenting volume, per mL/m^2	1.45	0.93-2.25	0.10			
Leaflet/annulus ratio	0.07	0.01-2.23	0.13			
Coaptation/leaflet ratio ≤0.24	93.3	17.5-496.6	<0.001	70.0	11.7-419.9	<0.001

CI: confidence interval, LVED: left ventricular end-diastolic, LVEF: left ventricular ejection fraction,MR: mitral regurgitation, OR: odds ratio

Reproducibility

Intraclass correlation coefficients for overall (total) leaflet area were 0.903 (intra-observer) and 0.947 (inter-observer). For exposed leaflet area measurements, the intraclass correlation coefficients were 0.955 and 0.947 for intra-observer and inter-observer reproducibility, respectively.

DISCUSSION

The present evaluation demonstrated that MV leaflet remodeling is common in FMR, showing a symmetrical involvement of both leaflets, and relates to MV tethering and closing forces. In addition, insufficient MV leaflet remodeling to compensate for annular and LV changes is strongly and independently associated with FMR severity, reflecting a potential therapeutic target for patients with functional MV disease.

Leaflet remodeling evidence

FMR results from an imbalance between valvular closing (LV dysfunction, LV and papillary muscle dyssynchrony and reduced annular contraction) and tethering forces (LV sphericity, papillary muscle displacement, annular dilatation and MV tenting).[2, 12] This imbalance causes relocation of the MV coaptation point more api-

cally and/or posteriorly, thereby restricting the leaflets movement with secondary loss of coaptation and FMR.[12] Therefore FMR is generally regarded as a ventricular problem leading to dysfunction of a structurally normal valve.[2] Differences in FMR severity despite similar tethering degree, however, have been observed.[6-8] For instance in patients with moderate to severe aortic regurgitation and significant LV remodeling, the prevalence of FMR is surprisingly low.[6] Such observations enforce the idea that the MV itself might develop compensatory adaptations to the chronic stress imposed by the annular and LV changes.[7, 13] Indeed, alterations in biochemical extracellular matrix and increased cellularity in mitral leaflets of humans with LV dysfunction have been reported.[3] This ultra-structural remodeling coincides with increased stiffness and reduced leaflet stretch abilities.[14] In addition, structural mitral leaflet remodeling, including increased mitral leaflet length, area and thickness in response to mitral annular and LV dilatation was observed in animal models of both ischemic and non-ischemic heart failure.[5, 13, 15] Evidence of prospective increase in mitral leaflet size >30% in response to imposed stress and as the result of an active biological process was recently provided by longitudinal animal model studies.[5, 15] The current evaluation also shows that patients with FMR have increased MV area of >30% compared to normal controls, indicating presence of leaflet remodeling. These findings are in line with previous reports on transthoracic or transesophageal 3D echocardiography of the MV, showing relative increases in mitral leaflet area of 23% to 35% .[6-8] This evidence suggests that in patients with FMR the MV shows structural remodeling and should, therefore, not be regarded as `normal`.

Characteristics and determinants of leaflet remodeling

The present evaluation indicates that significant leaflet remodeling (defined as ≥2 SD of the overall leaflet area of control subjects) is prevalent. In addition, a symmetrical pattern of relative enlargement of the posterior compared to the anterior MV leaflet was found, even in patients with ischemic cardiomyopathy with prior infero-posterior myocardial infarction. These findings are in line with a recent finite element analysis in a unique sheep model of the LV and MV after infero-posterior infarction, showing that both anterior and posterior mitral valve leaflets were subjected to similar extent of leaflet stress.[16] As the posterior and anterior MV leaflet have comparable surface areas, one could anticipate that the leaflets show similar extent of enlargement, as shown in current study.[17] Another study using an animal model of non-ischemic cardiomyopathy also reported similar relative increase of the anterior and posterior mitral leaflet area.[13] Other factors than leaflet stress alone, however, might also determine leaflet remodeling. In a recent sheep model with a perforation created in the anterior mitral leaflet, ultra-

structural leaflet remodeling at follow-up was identified, suggesting that isolated MR is able to cause leaflet remodeling of the MV.[18]

However, data on determinants of structural leaflet remodeling in humans are limited. Our findings suggest that both tethering (LV sphericity, annulus size and tenting volume) and closing forces (LV systolic function) are potential determinants of leaflet remodeling. A preserved or higher leaflet/annular ratio in FMR patients compared to controls confirms the idea that leaflet size increases relative to annular dilatation. Other reports have shown similar findings.[6-8] These results indicate that leaflet remodeling occurs as an adaptive response to annular and LV changes that pose specific requirements to the mitral leaflet size to ensure adequate surface and leaflet coaptation area to prevent from significant FMR.

Leaflet remodeling and regurgitation severity

Despite similar tethering and LV remodeling degree, patients with FMR≥3 compared to FMR<3 intriguingly showed less increase in MV area. These results point out that isolated LV remodeling fails to account for the observed FMR variability. The reported variability of FMR prevalence in ischemic patients may suggest that there are other associated pathophysiological factors than regional or global LV remodeling or dysfunction contributing to FMR.[19, 20] In the present study, although ischemic etiology was significantly more frequent among FMR≥3 patients than in FMR<3 patients, the location of myocardial infarction was not significantly different within the FMR≥3 group. In addition, there was significantly leaflet remodeling difference between groups that was attributed mainly to smaller coaptation area rather than exposed leaflet area. Hence, coaptation/leaflet area (coaptation index) was significantly smaller in FMR≥3 patients versus FMR<3 patients, similar to a prior report on 3D transesophageal echocardiography and comparable to two other studies that mentioned smaller leaflet/exposed (closure) area.[6-8] These data suggest that leaflet remodeling in FMR≥3 patients is insufficient to compensate for the changes in MV annular and LV dimensions. In particular, the lack of coaptation reserve defined by the ratio coaptation/leaflet area was an independent associate of significant FMR. The presence of limited coaptation reserve <24 % of total MV area was independently related to FMR severity. These findings are in line with the study by Chaput et al. reporting a cut-off value for leaflet/closure area ratio of <1.7 to predict the presence of significant FMR, which reflects <30 % coaptation reserve .[7] This absolute difference in cut-off value compared to our study might be due to the measurement of mitral valve area at a different time point during the cardiac cycle, to the use of different 3D quantification software and to the use of transthoracic 3D echocardiography characterized by lower spatial resolution, compared to transesophageal 3D echocardiography.[21]

Clinical significance

The current data show, in line with previous reports, that the presence of larger MV leaflets for the same LV tethering degree may protect from FMR.[6-8] These findings might have implications for the treatment of FMR patients, which remains a clinical challenge.[2]

First, elucidating the mechanisms including signaling pathways and triggers that are responsible for leaflet remodeling may help to explain the variability in leaflet remodeling observed in patients despite similar LV dilatation. This knowledge might lead to identification of patients with LV dysfunction that are prone to inadequate MV leaflet remodeling. These patients would represent ideal candidates to undergo biological modification with specific drugs developed to block adverse or stimulate beneficial remodeling of mitral leaflets to prevent from significant FMR.

Second, results of restrictive mitral annuloplasty for FMR overall have been relatively disappointing with high recurrence rates at medium to long-term follow up. In addition, no robust survival benefit has been shown so far for FMR surgery.[2] Current data lend support to the principle of surgical mitral leaflet augmentation plasty, which involves insertion of a pericardial bovine patch into the anterior or posterior MV leaflet in addition to restrictive annuloplasty.[22, 23] MV augmentation plasty increases MV leaflet area, reduces leaflet stress and increases coaptation reserve which might be of paramount importance as the underlying process of adverse LV remodeling potentially continues, imposing specific requirements to the MV area.[22, 24] Given the importance of coaptation reserve that should ideally exceed 24% of the total MV area, as indicated by the current study, this alternative surgical MV repair technique might warrant further study. Small series using posterior (n=44) and anterior (n=25) leaflet augmentation have shown promising results, but long-term results are lacking.[22, 23] The complexity of LV remodeling and FMR, however, probably precludes a single best option to treat FMR that rather requires a tailored approach to the individual patient and MV complex.[25]

Limitations

FMR severity assessment is prone to well-known limitations and challenges associated with the functional nature of the valvular regurgitation. Use of a multi-integrative approach, as recommended, partly accounts for these limitations. Mitral leaflet area was assessed at end-systole to ensure evaluation of leaflet coaptation. Therefore a contribution of acute stretch to the measured leaflet area, known to potentially increase leaflet size, can not be excluded.[26] Similar values for leaflet areas compared to our study measured during diastole, however have been reported.[6, 7] In addition, leaflet remodeling in FMR occurs also independently of acute leaflet stretching.[5] Furthermore, LV volumes were derived from 2D echocar-

diographic data. Due to retrospective analysis in a limited number of patients, the present study should be interpreted as hypothesis generating analysis.

CONCLUSION

Mitral leaflet remodeling in patients with FMR is highly prevalent, symmetrical and determined by MV closing and tethering forces. Insufficient leaflet remodeling relative to the annular and LV dilatation causes lack of coaptation reserve and is independently associated with FMR severity. MV leaflets in FMR should not be regarded as `normal` and might represent a biological or interventional therapeutic target.

REFERENCES

1. Trichon BH, Felker GM, Shaw LK et al. Relation of frequency and severity of mitral regurgitation to survival among patients with left ventricular systolic dysfunction and heart failure. *Am J Cardiol.* 2003; 91:538-543.
2. Joint Task Force on the Management of Valvular Heart Disease of the European Society of Cardiology, European Association for Cardio-Thoracic Surgeons, Vahanian A, Alfieri O, Andreotti F et al. Guidelines on the management of valvular heart disease (version 2012). *Eur Heart J.* 2012; 33:2451-2496.
3. Grande-Allen KJ, Borowski AG, Troughton RW et al. Apparently normal mitral valves in patients with heart failure demonstrate biochemical and structural derangements: an extracellular matrix and echocardiographic study. *J Am Coll Cardio.l* 2005; 45:54-61.
4. Willems IE, Havenith MG, Smits JF et al. Structural alterations in heart valves during left ventricular pressure overload in the rat. *Lab Invest.* 1994; 71:127-133.
5. Chaput M, Handschumacher MD, Guerrero JL et al. Mitral leaflet adaptation to ventricular remodeling: prospective changes in a model of ischemic mitral regurgitation. *Circulation.* 2009; 120:S99-103.
6. Beaudoin J, Handschumacher MD, Zeng X et al. Mitral valve enlargement in chronic aortic regurgitation as a compensatory mechanism to prevent functional mitral regurgitation in the dilated left ventricle. *J Am Coll Cardiol.* 2013; 61:1809-1816.
7. Chaput M, Handschumacher MD, Tournoux F et al. Mitral leaflet adaptation to ventricular remodeling: occurrence and adequacy in patients with functional mitral regurgitation. *Circulation.* 2008; 118:845-852.
8. Saito K, Okura H, Watanabe N et al. Influence of chronic tethering of the mitral valve on mitral leaflet size and coaptation in functional mitral regurgitation. *JACC Cardiovasc Imaging.* 2012; 5:337-345.
9. Lang RM, Bierig M, Devereux RB et al. Chamber Quantification Writing Group, American Society of Echocardiography's Guidelines, Standards Committee, European Association of Echocardiography. Recommendations for chamber quantification: a report from the American Society of Echocardiography's Guidelines and Standards Committee and the Chamber Quantification Writing Group, developed in conjunction with the European Association of Echocardiography, a branch of the European Society of Cardiology. *J Am Soc Echocardiogr.* 2005; 18:1440-1463.
10. Zoghbi WA, Enriquez-Sarano M, Foster E et al. American Society of Eechocardiography. Recommendations for evaluation of the severity of native valvular regurgitation with two-dimensional and Doppler echocardiography. *J Am Soc Echocardiogr.* 2003; 16:777-802.
11. Lancellotti P, Moura L, Pierard LA et al. European Association of Echocardiography recommendations for the assessment of valvular regurgitation. Part 2: mitral and tricuspid regurgitation (native valve disease). *Eur J Echocardiogr.* 2010; 11:307-332.
12. Marwick TH, Lancellotti P, Pierard L. Ischaemic mitral regurgitation: mechanisms and diagnosis. *Heart.* 2009; 95:1711-1718.
13. Timek TA, Lai DT, Dagum P et al. Mitral leaflet remodeling in dilated cardiomyopathy. *Circulation.* 2006; 114:I518-523.
14. Grande-Allen KJ, Barber JE, Klatka KM et al. Mitral valve stiffening in end-stage heart failure: evidence of an organic contribution to functional mitral regurgitation. *J Thorac Cardiovasc Surg.* 2005; 130:783-790.

15. Dal-Bianco JP, Aikawa E, Bischoff J et al. Active adaptation of the tethered mitral valve: insights into a compensatory mechanism for functional mitral regurgitation. *Circulation.* 2009; 120:334-342.
16. Wenk JF, Zhang Z, Cheng G et al. First finite element model of the left ventricle with mitral valve: insights into ischemic mitral regurgitation. *Ann Thorac Surg.* 2010; 89:1546-1553.
17. Debonnaire P, Palmen M, Marsan NA et al. *Curr Opin Cardiol* 2012; 27:455-64.
18. Stephens EH, Nguyen TC, Itoh A et al. The effects of mitral regurgitation alone are sufficient for leaflet remodeling. *Circulation.* 2008; 118:S243-249.
19. Bursi F, Enriquez-Sarano M, Nkomo VT et al. Heart failure and death after myocardial infarction in the community: the emerging role of mitral regurgitation. *Circulation.* 2005; 111:295-301.
20. Meris A, Amigoni M, Verma A et al. Valsartan in Acute Myocardial Infarction I. Mechanisms and predictors of mitral regurgitation after high-risk myocardial infarction. *J Am Soc Echocardiogr.* 2012; 25:535-542.
21. Lang RM, Tsang W, Weinert L et al. Valvular heart disease. The value of 3-dimensional echocardiography. *J Am Coll Cardio.l* 2011; 58:1933-1944.
22. de Varennes B, Chaturvedi R, Sidhu S et al. Initial results of posterior leaflet extension for severe type IIIb ischemic mitral regurgitation. *Circulation.* 2009; 119:2837-2843.
23. Kincaid EH, Riley RD, Hines MH et al. Anterior leaflet augmentation for ischemic mitral regurgitation. *Ann Thorac Surg.* 2004; 78:564-568.
24. Rahmani A, Rasmussen AQ, Honge JL et al. Mitral valve mechanics following posterior leaflet patch augmentation. *J Heart Valve Dis.* 2013; 22:28-35.
25. Di Salvo TG, Acker MA, Dec GW et al. Mitral valve surgery in advanced heart failure. *J Am Coll Cardiol.* 2010; 55:271-282.
26. Kunzelman KS, Cochran RP. Stress/strain characteristics of porcine mitral valve tissue: parallel versus perpendicular collagen orientation. *J Card Surg.* 1992; 7:71-78.

Chapter 5

Tools and techniques: 3D-transesophageal echocardiography for selecting and guiding in percutaneous mitral valve repair using MitraClip

Philippe Debonnaire, Victoria Delgado, Jeroen J Bax, Nina Ajmone Marsan

EuroIntervention, 2014 Nov 10(7): 884-886.

ABSTRACT

Objectives

This report provides an illustrative and practical approach for screening of patients with mitral regurgitation who are candidates for MitraClip® therapy and for procedural guidance using 3D-transesophageal echocardiography (3D-TOE), providing state-of-the-art practice for imagers (what and how to assess mitral valve with 3D-TOE) and interventionalists (how to interpret and translate 3D-TOE images for the intervention).

Summary

Superior anatomic performance and comprehensive evaluation of regurgitant jet characteristics represent cornerstones for eligibility assessment. Standardized mitral valve display, alternating 1-beat 3D full volume and bi-plane acquisitions, improves procedural guidance. Intensive communication between a skilled imager and a well-trained interventionalist with each understanding of 3D-TOE from a technical and practical point of view, respectively, are prerequisites to obtain high procedural success rates.

Conclusions

3D-TOE has become indispensable for optimal candidate selection and procedural guidance in patients treated with MitraClip® therapy.

INTRODUCTION

Mitral valve repair using the MitraClip® system (Abott Vascular) consists of a percutaneous approach to attach both leaflets of the mitral valve to each other by one or more cobalt-chromium clips where the regurgitant jet originates.[1] Thereby it resembles the surgical Alfieri-stitch technique, creating a double-orifice mitral valve.[2] This therapy has currently been adopted in over 15000 symptomatic patients with severe primary (organic) or secondary (functional) mitral regurgitation that are at high surgical risk or with contraindications for surgery. The EVEREST-II trial and large real-world registries have shown high feasibility (successful clip implantation achieved in >95%) and efficacy with reduction of mitral regurgitation to grade 2 or less (acute procedural success) in at least 80% of treated subjects.[1, 3-5] Adequate patient selection and procedural guidance is a prerequisite for procedural and clinical success of MitraClip® therapy. Although 2-dimensional transesophageal echocardiography (TOE) remains the reference standard to assess the anatomy of the mitral valve and the severity of mitral regurgitation of patients who are candidates for this therapy, 3-dimensional (3D) TOE has improved and standardized communication between interventionalists and imagers. This report provides a brief, illustrative and practical approach for screening of patients with mitral regurgitation who are candidates for MitraClip® therapy and for procedural guidance using 3D-TOE, providing state-of-the-art practice for imagers (what and how to assess mitral valve with 3D-TOE) and interventionalists (how to interpret and translate 3D-TOE images for the intervention), as summarized in Figure 1.

PATIENT SELECTION

Selection of patients who are candidates for MitraClip® therapy includes thorough analysis of the anatomy of the mitral valve and mechanism as well as severity of mitral regurgitation.[6] Evaluation of anatomy requires high spatial resolution whereas accurate quantification of mitral regurgitation relies on high temporal resolution (high frame rate data). Using 3D TOE, anatomical and functional data can be obtained with 3 different acquisition modes (Figure 2):

- 1-beat full volume: provides in one beat the 3D rendering of the mitral valve. The spatial resolution is high while avoiding stitching artifacts that may distort the anatomy.
- Multi-beat full volume: the 3D rendering of the mitral valve is created from several pyramidal subvolumes obtained during 2-7 beats. This mode provides high temporal and spatial resolution data. The patient, however, needs to hold

the breath to avoid stitching artifacts during compilation of the subvolumes. Similarly, the presence of irregular heart rhythms (atrial fibrillation) may create stitching artifacts that will limit the analysis and visualization.

- Bi-plane view: This mode provides simultaneous visualization of 2-dimensional orthogonal planes. Using the bicommissural plane as reference, the perpendicular (left ventricular outflow tract) view can be displayed at specific levels of the mitral valve (anterolateral, central and posteromedial). This acquisition mode provides high temporal resolution data.

3D color Doppler data can be obtained with any of the above acquisition methods. However, high temporal resolution must prevail over spatial resolution and therefore, multi-beat color Doppler 3D full-volume and bi-plane view will be the acquisition modes of choice.

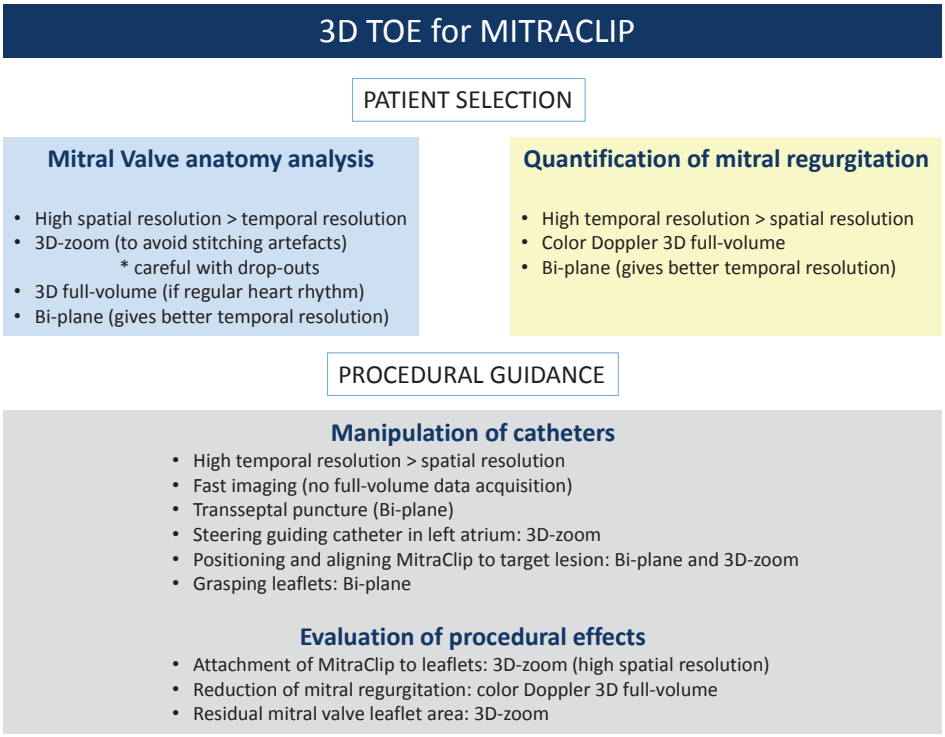

Figure 5.1
Summary of 3D transesophageal echocardiography (3D-TOE) for patient selection and procedural guidance for MitraClip® treatment.

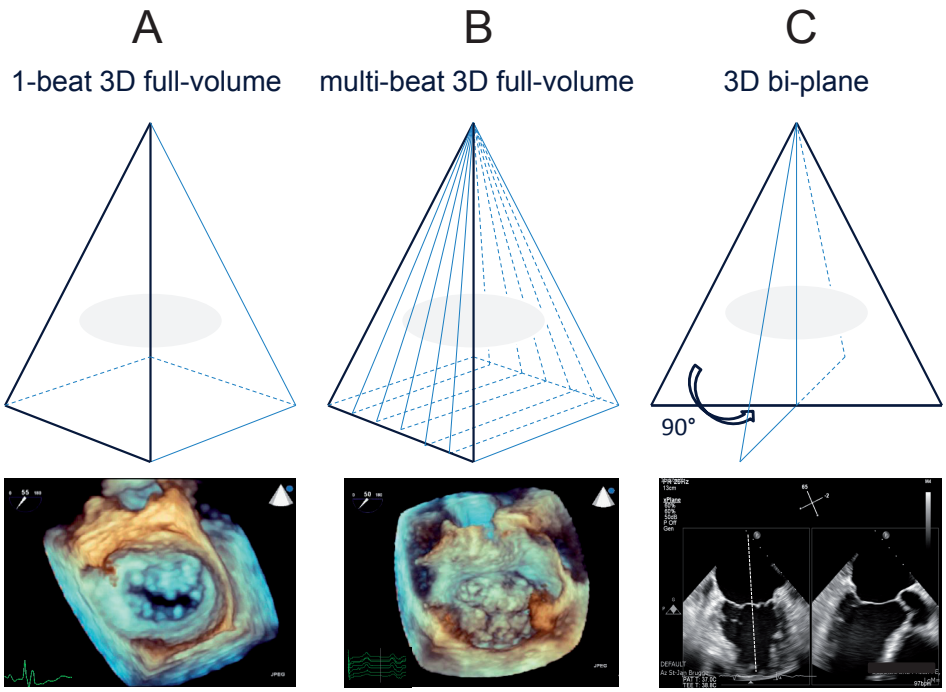

Figure 5.2
Principles of 3D (transesophageal) echocardiography. A: 1-beat 3D full volume acquires pyramidal volume in single beat. B: multibeat 3D full volume acquires pyramidal volume stitching sub-volumes together over multiple heart beats. C: 3D bi-plane shows a reference image (left) with corresponding 90 degrees perpendicular view (right).

Analysis of mitral anatomy

The mitral valve 'en face' or 'surgical view' comprises 3D-visualization of the entire mitral valve as seen from the left atrium, including mitral annulus, all anterior (A1-A2-A3) and posterior (P1-P2-P3) leaflet scallops as well as both anterolateral and posterolateral commissures (Figure 3). To orient the 3D volume rendering several anatomical landmarks need to be included: the left atrial appendage indicating the anterolateral region and the aorta indicating the anterior region of the mitral valve. By displaying the 3D volume rendering with the aortic valve at 12 o'clock position and left atrial appendage at lateral (left) side the communication between interventionalists and imagers may be facilitated. The mitral valve can be also analyzed using the bi-plane view using as reference the bicommissural mitral valve view, mostly found at about 60º, and bisecting each level of the mitral valve (from anterolateral – P1 scallop –, central – A2 scallop – and to posteromedial –P3 scallop) to display the simultaneous left ventricular outflow tract view with the anterior and posterior scallops of the mitral valve at each level (Figure 4).

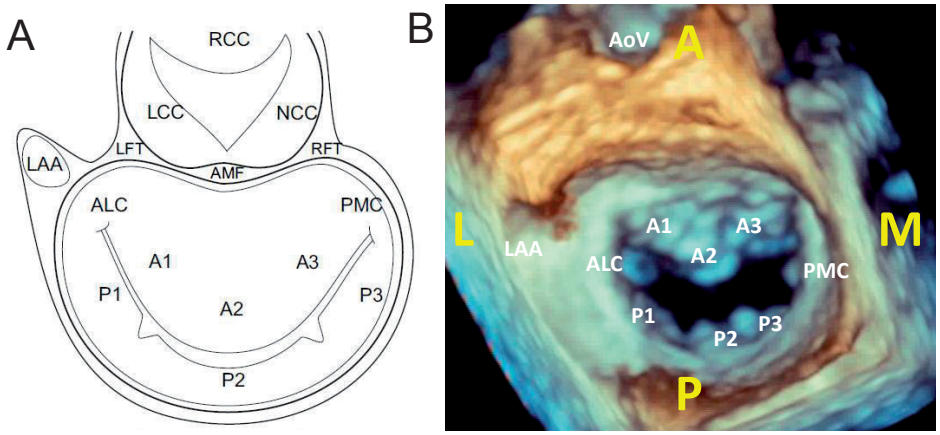

Figure 5.3
Mitral valve anatomy on 3D 'surgical' or en 'face view' of mitral valve. A: schematic mitral valve anatomy. B: Corresponding 1-beat 3D full volume view. A: anterior, ALC: antero-lateral commissure, anterior mitral valve leaflet with lateral (A1), middle (A2) and medial (A3) scallop, AMF: aortic-mitral fibrosa, AoV: aortic valve with left (LCC), right (RCC) and non coronary (NCC) cusp, L: lateral, LFT: left fibrous trigonum, M: medial, P: posterior, PMC: postero-medial commissure, posterior mitral valve leaflet with lateral (P1), middle (P2) and medial (P3) scallop, RFT: right fibrous trigonum. *Adapted with permission*[10].

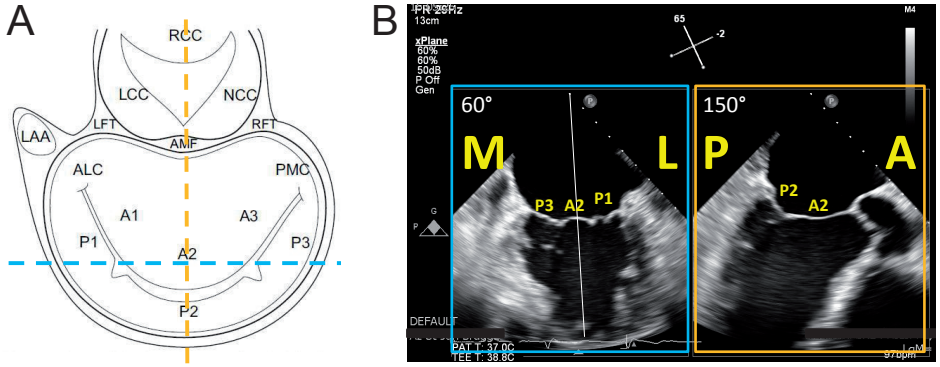

Figure 5.4
Mitral valve anatomy on 3D bi-plane view, at bi-commissural level. A: schematic mitral valve and B: bi-plane view. The blue dashed line corresponds to the bi-commissural view on bi-plane (left panel) and the orange dashed line corresponds to the 90 degrees perpendicular antero-posterior view on bi-plane (right panel). This bi-plane view allows for simultaneous orientation in latero-medial direction (L-M) as well as antero-posterior direction (A-P). See figure 2 for abbreviations.

Adherence to initial EVEREST-II criteria for technical feasibility (Table 1) yields high procedural success rates.[1] Based on the underlying pathophysiological mechanisms, mitral regurgitation can be classified as organic or primary, when the lesion affects the mitral valve leaflets, or functional or secondary, when the mitral leaflets are anatomically normal but left ventricular remodeling and dysfunction or atrial remodeling lead to dilatation of the mitral annulus, leaflet tethering and

restriction as well as coaptation failure. In patients with organic mitral regurgitation, the exact location of the lesions (prolapse/flail) and numbers of leaflet scallops involved should be assessed (Figure 5).

Table 5.1
Technical echocardiographic requirements for MitraClip® treatment, adapted from EVEREST-II trial.[1]

Mitral valve assessment	Measurements	3D acquisition
Anatomy		
organic: flail width	< 15 mm	full-volume
flail gap	< 10 mm	bi-plane
functional: coaptation depth	<11 mm	bi-plane
coaptation length	≥ 2 mm	bi-plane
excluding cleft, calcification in grasping area	-	full-volume, bi-plane
excluding asymmetrical leaflet thickness	≤ 5 mm	full-volume, bi-plane
area (cm²)	≥ 4.0 cm²	full-volume
mean gradient (mmHg)	< 5 mmHg	*(Continuous wave)*
mobile leaflet length at jet origin	≥ 8 mm	bi-plane
Regurgitation		
jet location	preferably A2-P2	color full-volume, bi-plane
severe functional, EROA	≥ 20 mm²	color full-volume
severe organic, EROA	≥ 40 mm²	color full-volume

EROA: effective regurgitant orifice area

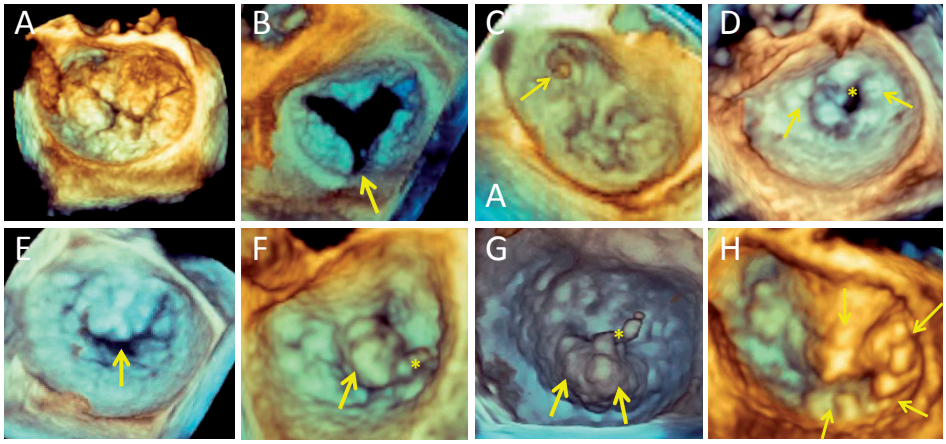

Figure 5.5
Additional value of 3D mitral valve echocardiography for anatomic and morphologic assessment in screening for MitraClip® therapy. All patients presented with severe mitral regurgitation but are anatomically not eligible for MitraClip® therapy. A: Complex Barlow degeneration involving prolapse of all mitral segments. B: Posterior leaflet cleft. C: Anterolateral commissural prolapse. D: Severe rheumatic stenosis (*) with diffuse calcifications and commissural fusion (arrows). E: Loss of central coaptation during systole. F: A2 flail with chordal rupture (*), flail width 17 mm. G: P2 flail with chordal rupture (*), flail width 22 mm. H: Complex Barlow with prolapse of A2, A3, posteromedial commissure and P3 scallops.

From 3D volume rendering, the type of lesion and number of valve segments involved are readily assessable. Using the multiplanar reformation planes, the 3D volume rendering can be analyzed and the flail width and gap can be measured. The flail width, comprising the width of the prolapsing segment(s), can be measured on the surgical view and should be ≤15 mm (Figure 6). The flail gap, reflecting the distance between both leaflet tips during mid-systole needs to be ≤10 mm (Figure 6). In patients with functional mitral regurgitation a coaptation length (apposition of both leaflets in systole) of ≥2 mm should be present at the level of the mitral regurgitant jet origin during mid-systole to allow for grasping of both leaflets (Figure 6). In addition the coaptation height between the leaflet tips and the annular plane, reflecting leaflet tethering severity, should be ≤11 mm to avoid excessive

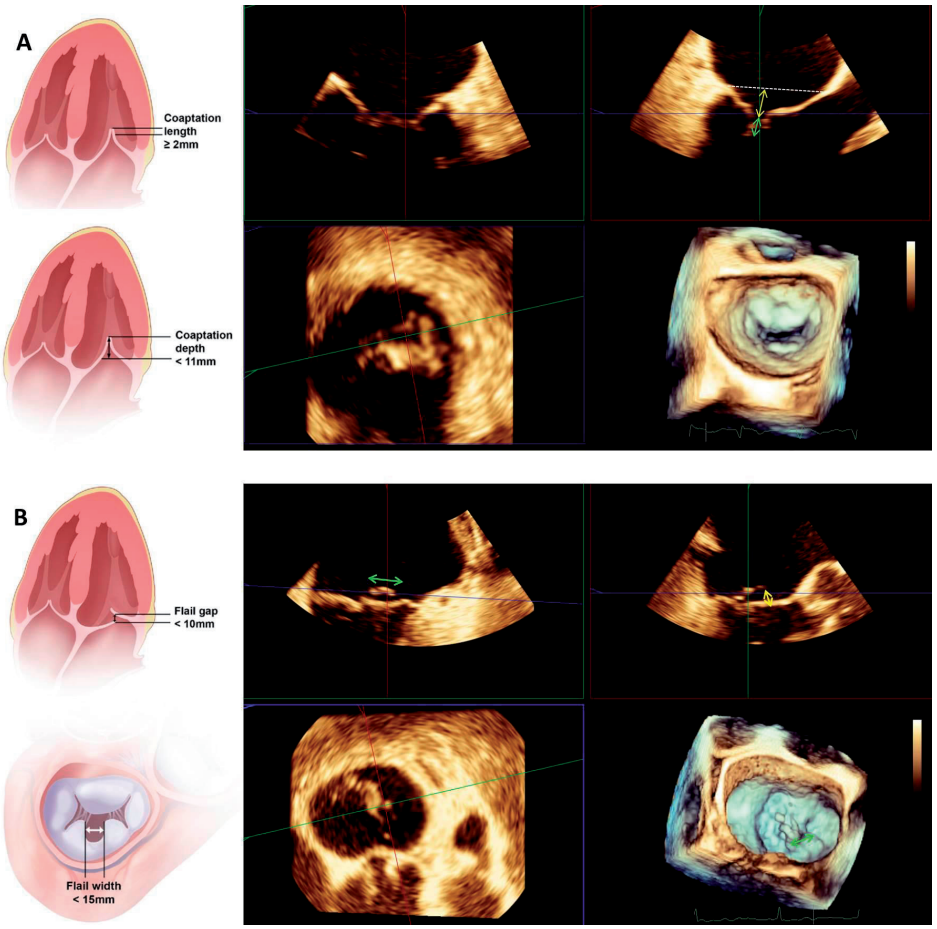

Figure 5.6
Mitral valve geometric measurements for evaluation of technical feasibility for MitraClip® therapy in patients with functional (A) or organic (B) mitral regurgitation. See text for details. *Adapted with permission.*[11]

tension in the system and mitral leaflets (Figure 6). Patients with rheumatic valve disease, calcification in the leaflet grasping area or cleft (congenital defect in or between leaflet scallops reaching the mitral annulus) are not ideal candidates for MitraClip® therapy (Figure 5). In addition, asymmetrical leaflet thickness at the origin of the regurgitant jet implies technical ineligibility due to risk of future clip detachment (Figure 7).

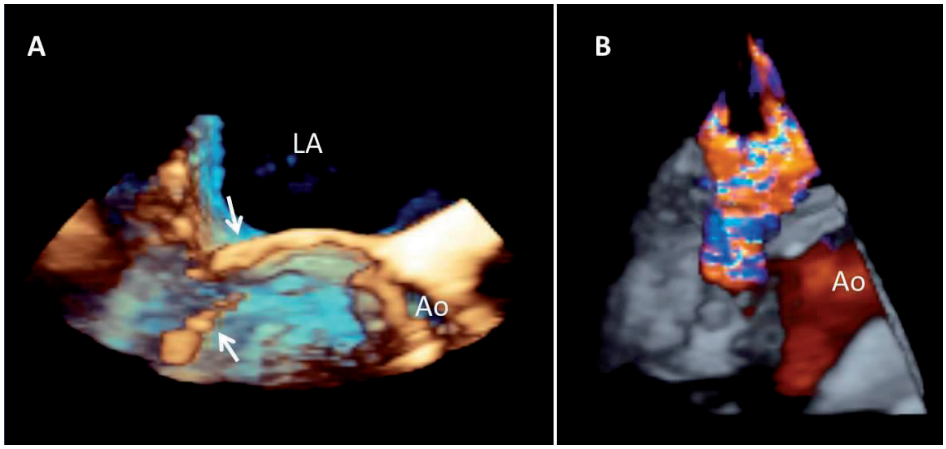

Figure 5.7
Mitral valve thickening. Panel A: Asymmetrical thickened A2 leaflet (arrow) with thickened subvalvular chordae (arrow) which challenges MitraClip® therapy. Panel B: 3D-color Doppler data showing severe mitral regurgitation.

Second, the mitral valve area should be evaluated. MitraClip® therapy reduces mitral valve area about 25 to 50% and therefore mitral valve area should be ≥4.0 cm² to avoid development of significant leaflet stenosis (Figure 8).[7] Apart from 2D-planimetry, mitral valve area can be assessed on 3D-planimetry at multi-plane reformation analysis at the maximal opening of the tip of the leaflets during systole. The mean valvular gradient should be <5 mmHg, assessed by tracing the diastolic mitral inflow on continuous wave Doppler acquisition.

Finally, the length of the mobile leaflet part of both anterior and posterior mitral leaflets at the origin of the regurgitant jet should be ≥8 mm to allow ability to grasp, to avoid inducing valvular stenosis and to prevent from later clip detachment.

Quantification of mitral regurgitation

Quantification of the regurgitant orifice area (EROA), most often by the proximal isovelocity surface area method (PISA), is the gold standard for quantifying regurgitation severity as it least depends on hemodynamic loading conditions.[8] An EROA of ≥40 mm² and ≥20 mm² defines severe mitral regurgitation for organic and

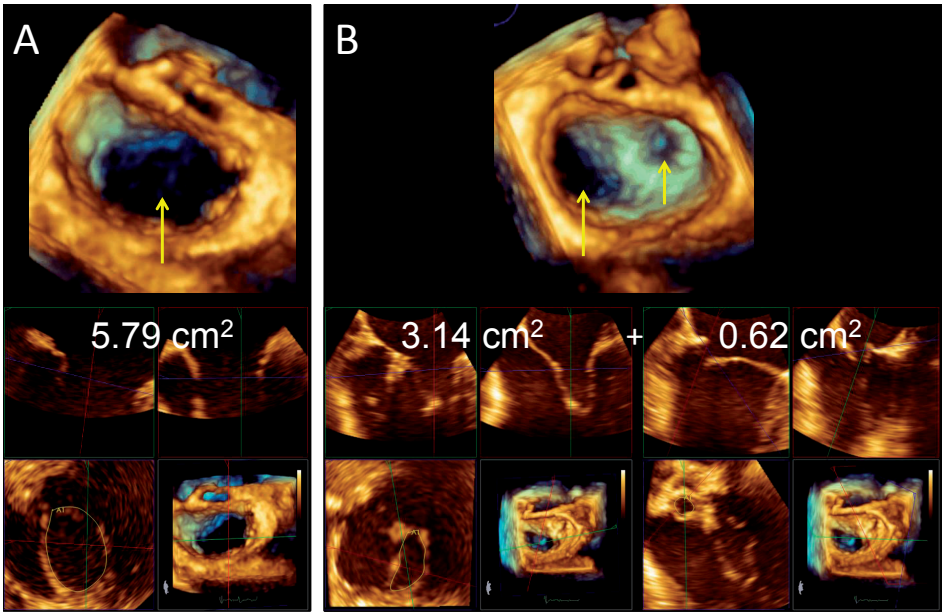

Figure 5.8
3D planimetry of mitral valve area before and after MitraClip® therapy. A: Mono-orifice valve before MitraClip® (upper panel) with valve area planimetry on multi-reformation planes (lower panel). B: Double-orifice valve after MitraClip (upper panel) with selective planimetry of lateral orifice (left lower panel) and medial orifice (right lower panel). Mitral valve area is reduced from 5.14 cm² to 3.76 cm², comprising mitral valve area reduction of 27% post MitraClip® therapy.

functional mitral regurgitation, respectively. The EROA of patients with functional mitral regurgitation, however, is often not circular as in organic mitral valve disease, explaining lower thresholds when applying the PISA method. Particularly for these subjects, 3D quantification of the vena contracta area can be performed, comprising direct anatomic measurement of the area of the vena contracta, namely the small neck of the regurgitant jet at the atrial level (Figure 9). This technique can also be applied in case of multiple jets by adding values obtained at the different jets (Figure 10).

Central regurgitant jet origin, at A2-P2 scallops, represents an ideal scenario for MitraClip® treatment. The origin, number and exact location of the regurgitant jet(s) is most easily evaluated on 3D-TOE, applying the 'en face view' as well as the bi-plane biplane mitral valve view (Figure 11). Building on experience by treatment of higher numbers of patients, more lateral or medial jet origins can be targeted, being the most challenging lesions those located at the commissures since they are associated with entangling into or rupturing of commissural mitral chords.

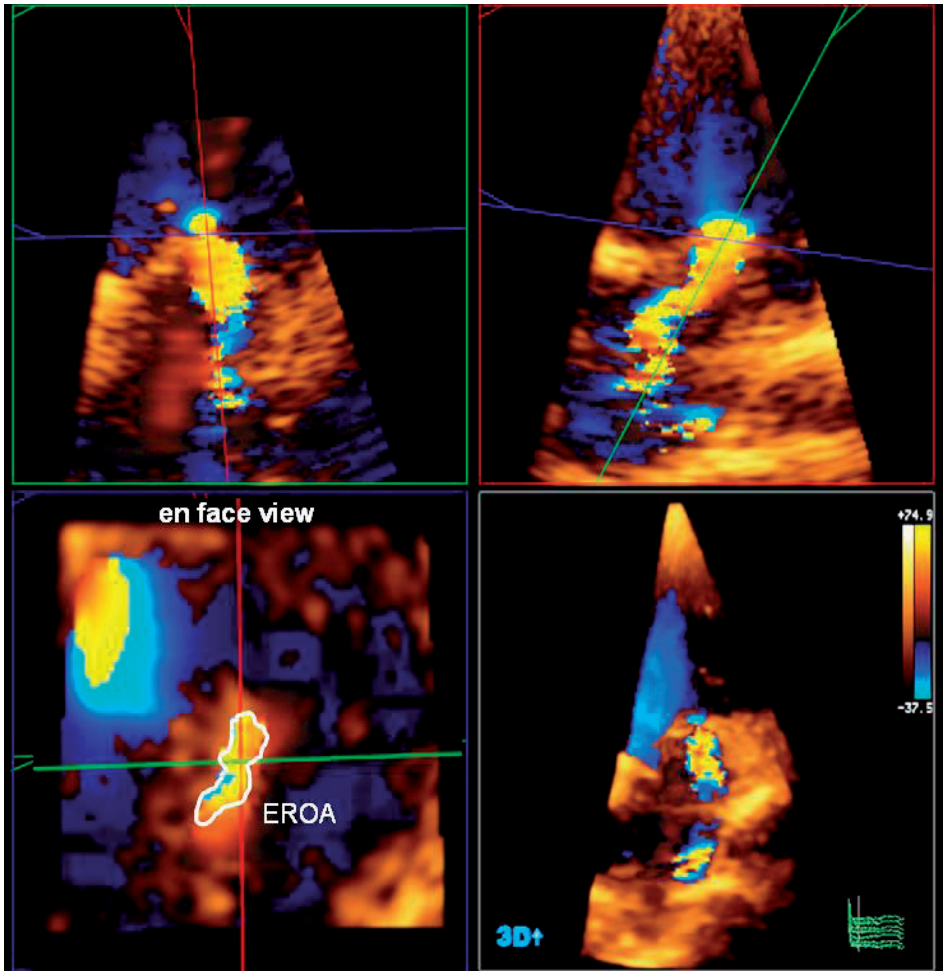

Figure 5.9
3D Vena contracta area assessment. After mid-systolic orthogonal alignment of the regurgitant jets on multi reformation planes (green and red planes) from a 3D color full-volume acquisition, the short axis plane (blue) is set at the level of the vena contracta. The non circular regurgitant orifice area of this functional mitral regurgitation is traced, measuring 45 mm², compatible with severe mitral regurgitation.

PROCEDURAL GUIDANCE

Comprehensive guiding of MitraClip® implantation procedure requires extensive use and switching between different 3D-TOE modalities; fluoroscopy guiding is limited since the non-calcified mitral valves are not well depicted. Catheter manipulation requires accurate visualization of the mitral valve and surrounding anatomical structures and high temporal resolution. One-beat 3D full volume and bi-plane acquisitions are the most common 3D modes of visualization (Figure 2).

Procedural results, reduction of mitral regurgitation severity and clip attachment, require high temporal and spatial resolution, respectively.

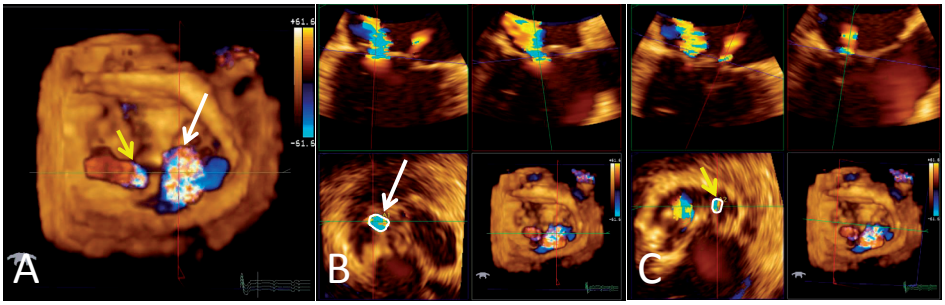

Figure 5.10
3D Vena contracta area assessment in multiple jets. A: Mitral regurgitation with a small centrolateral jet (yellow arrow) and large centromedial jet (white arrow). Selective assessment of the vena contracta area of the centromedial jet (B, 29 mm²) and of the centrolateral jet (C, 11 mm²). The total vena contracta area of the entire regurgitation measures 40 mm².

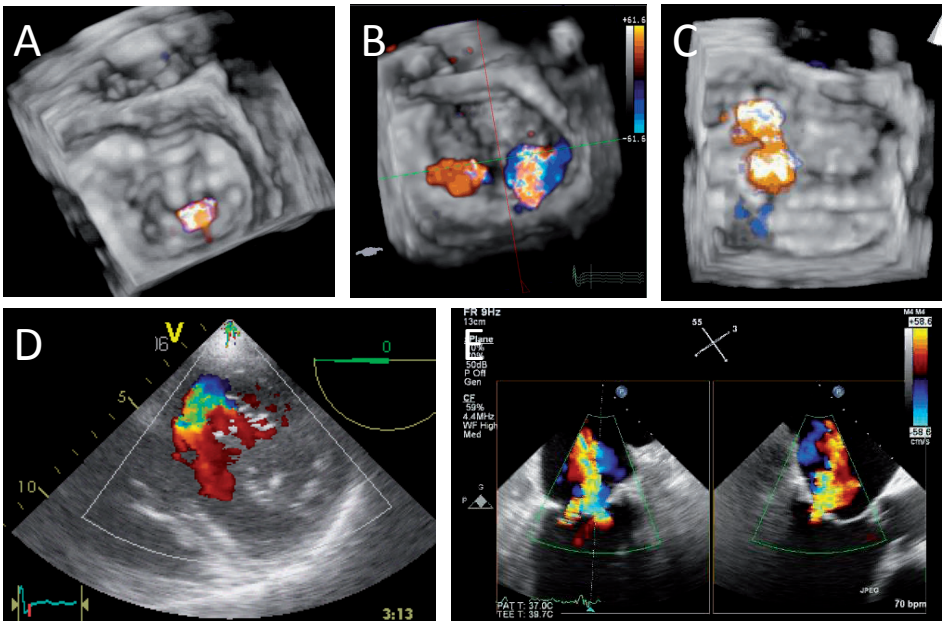

Figure 5.11
Assessment of regurgitant jet characteristics and location. A: central jet origin at A2-P2 level on en face mitral view. B: Double jet at centromedial (large) and centrolateral (small) level. C: Anterolateral commissural and lateral jet origin, unsuitable for MitraClip® therapy. D: Short axis transgastric 2D mitral view indicating posteromedial commissural jet origin, contra-indication for MitraClip® treatment. E: Bi-plane view at bicommissural level, displaying central jet origin at A2-P2 level, ideal target for MitraClip® therapy.

Manipulation of catheters

Transseptal puncture.

The location of the transseptal puncture is crucial as it determines further clip delivery system manipulations needed to obtain the optimal angle for subsequent alignment and grasping mitral valve leaflets. Ideally the puncture should target the middle to slightly superior part of the non-muscular part of the interatrial septum at a slightly posterior level (Figure 12). The bi-plane interatrial septal view allows for simultaneous posteroanterior and inferosuperior guiding on the short-axis aortic valve view and bicaval view respectively. By slightly pressing with the Brockenbrough or Verres needle on the targeted area, tenting of the interatrial septum can be observed which allows for subsequent measurement of puncture height from the mitral annular plane in 4-chamber TOE view. This height should ideally range between 3.5 and 4.0 cm (Figure 12). Of note, the maximal length of the

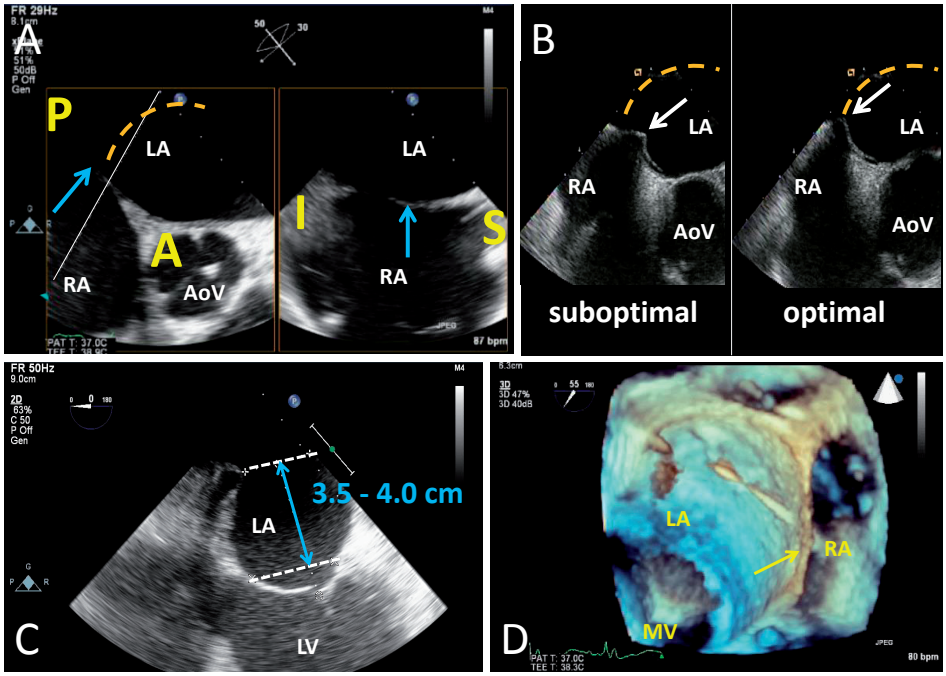

Figure 5.12

Ideal location and guiding transseptal puncture. A: bi-plane view of interatrial septum showing short axis aortic valve (left panel, anteroposterior direction) and bicaval view (right panel, inferosuperior direction). The dashed orange line indicates the location of mitral leaflet coaptation. The blue arrow points out the ideal puncture side: slightly posterior and mid-to-slightly-superior. B: suboptimal (too anterior) and optimal position seen by tenting of the needle (arrows). C: Measuring puncture height from tenting to mitral annular plane on 4-chamber view. D: 3D view of wire (black arrows) across interatrial septum (yellow arrow). A: anterior, AoV: aortic valve, I: inferior, LA: left atrium, LV: left ventricle, MV: mitral valve P: posterior, RA: right atrium, S: superior.

MitraClip® delivery system in the left atrium is limited to 5.0 cm and one should be aware that the clip needs to be advanced distally from the leaflet tips into the left ventricle to allow for proper leaflet grasping. Severe tenting in functional mitral regurgitation might lead to choose a slightly lower puncture site. Likewise, organic mitral regurgitation caused by prolapse or flail might benefit from a slightly higher puncture site. The puncture is guided on bi-plane interatrial septal view and subsequent advancement of the wire into the left atrium and secured into the left upper pulmonary vein can be visualized with 3D full volume views (Figure 12).

Steering the guiding catheter in left atrium.

Over the wire across the interatrial septum, a septal dilator is inserted. After dilatation, the guiding catheter is advanced into the left atrium, guided by alternating 1-beat 3D full volume and bi-plane imaging to accurately follow the advancement and avoiding perforation of the posterior atrial wall, aortic puncture and impingement of the left atrial appendage (Figure 13. Subsequently the clip is introduced into the left atrium through the guiding catheter. 3D-TOE is useful for catheter

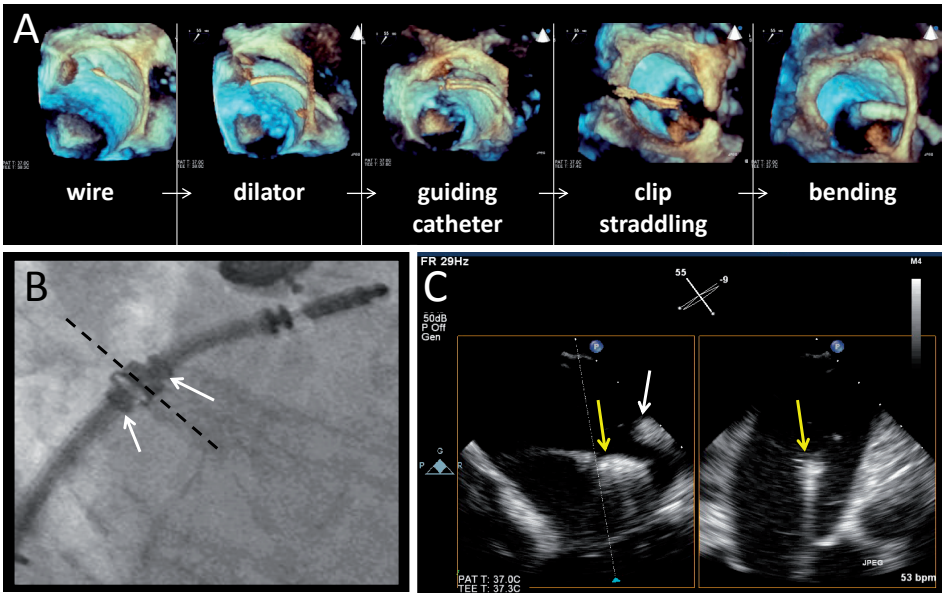

Figure 5.13

Steering guiding catheter in left atrium. A: Large 1-beat 3D full volume views of interatrial septum and mitral valve showing consecutive steps of introducing the guiding catheter into the left atrium and bending towards the mitral valve. This anatomic overview is used for orientation and to make sure no anatomic structures are damaged during manipulation. B: straddling position: sleeve markers (white arrows) are paired on the guide marker (black dashed line). C: bi-plane bicommissural central view showing clip (yellow arrow), avoiding to hook on the pulmonary vein ridge (white arrow).

manipulation avoiding any damage to left atrial structures or aorta, particularly since the clip system must be introduced further until straddling position is obtained (Figure 13). Following straddling, using 1-beat 3D full volume or bi-plane views, the clip is bended medially and inferiorly towards the mitral valve, avoiding damage of the pulmonary vein ridge.

Positioning and aligning MitraClip® to target lesion.

The clip system is manipulated into mediolateral and anteroposterior direction to obtain a position on top of the target lesion. Color Doppler and bi-plane views at the bicommissural level and 1-beat 3D full volume acquisitions are the most frequently used views to guide this step (Figures 3, 4 and 14). It is important to notice that when the target regurgitant lesion on the color Doppler bi-plane view is identified, the system should be steered to appear in this view without further adjustments of the image.

Once the clip is at the target region, slight advancing and retracting of the system towards and away from the mitral leaflets and left ventricle is repeatedly tested in order to verify the system follows the correct path and angle, remaining at the target lesion site. Then the clip is opened and oriented perpendicular to the line

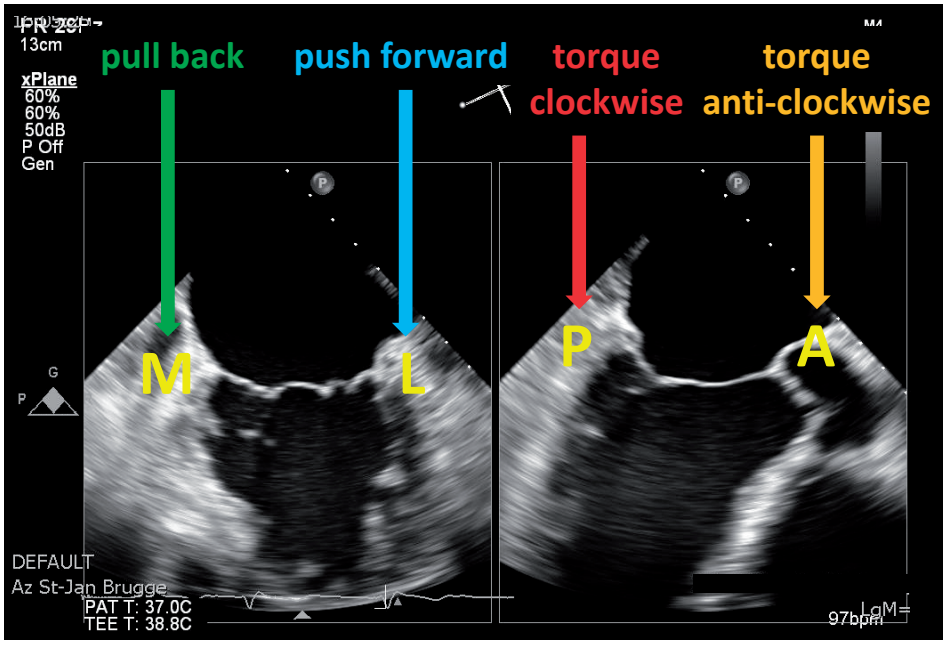

Figure 5.14

Device manipulations and resulting effects on bi-plane bicommissural view. Pulling back and pushing forward results in medial (M) and lateral (L) device orientation, respectively. Clockwise and anti-clockwise torque leads to posterior (P) and anterior (A) relocation, respectively.

of coaptation of the mitral valve leaflets. This step is crucial as non-perpendicular clip attachment yields a significant risk of future clip detachment or leaflet laceration. Bi-plane bicommisural view is used to adapt the clip orientation until perpendicularity is ascertained by absence of clip arm visualization on the bicommissural view, and symmetric appearance of both clip arms on the corresponding outflow tract view (Figure 15). Similarly, 1-beat 3D full volume acquisition allows for easy clip orientation (Figure 16). Once a satisfactory alignment is achieved, the clip is gently introduced into the left ventricle guided by bi-plane mode with simultaneous visualization of the bicommissural and long-axis views of the mitral valve, and maintenance of clip alignment should be vigorously checked as leaflet motion tends to affect clip arm alignment.

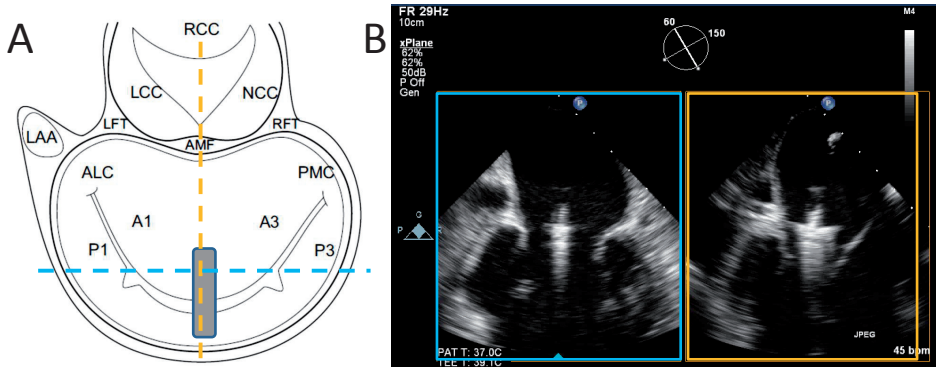

Figure 5.15
Clip orientation and alignment on bi-plane imaging. A: The clip (grey) should be perpendicular to the line of coaptation. B: Perpendicularity is ascertained when on bicommisural bi-plane view (blue) no clip arms are seen and when both clip arms appear symmetrically on the corresponding left ventricular outflow tract view (orange).

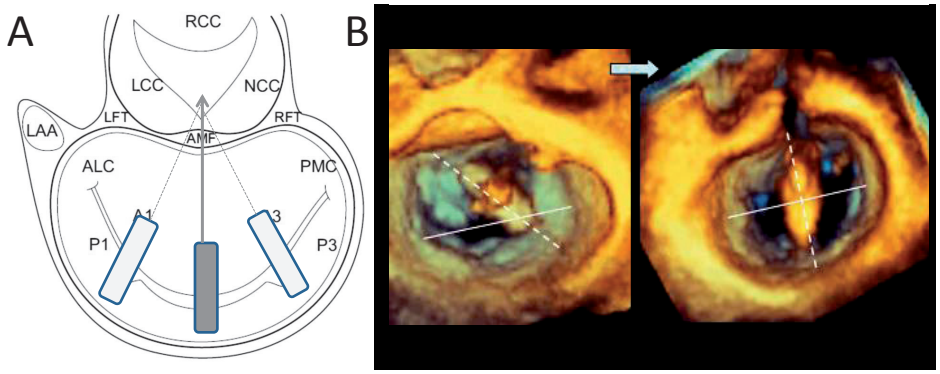

Figure 5.16
Clip orientation and alignment on 1-beat 3D full volume imaging. A: Perpendicularity to the line of coaptation is found when on the en face mitral view the clip points towards the center of the aortic valve. B: Left panel shows clip non-perpendicularity. After clockwise rotation of the clip, perpendicularity at central leaflet level is obtained, depicted on the right panel.

Mitral leaflet grasping.

In order to grasp both leaflets the clip system is pulled back gently with discrete manipulations by the interventionalist mainly in anteroposterior direction until both leaflets land on the clip arms, maintaining the perpendicular alignment and central position of the clip (Figure 17). Once both leaflets are on the clip arms, the grippers are lowered and the clip is closed (Figure 17). It is important to record this grasping procedure by a long cine run acquisition as a reference to re-evaluate in case of doubt about accurate grasping. Ideally both leaflets need to be in the clip for about 5 mm.

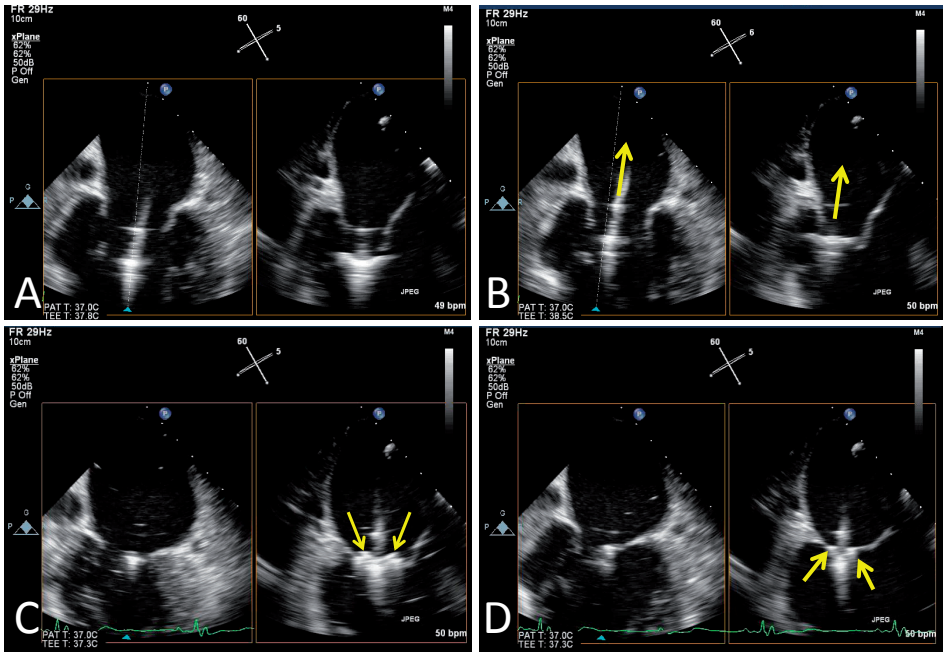

Figure 5.17
Leaflet grasping guided by bi-plane imaging. A: Clip in left ventricle with open arms, perpendicular orientation. B: Clip system is pulled back (arrows) with manipulations in anteroposterior direction to grasp both mitral leaflets. C: Grippers are lowered (arrows) when both mitral leaflets are on the clip arms. D: The clip is closed (arrows), approximating both the posterior and anterior mitral valve leaflet.

Evaluation of procedural effects

Mitral regurgitation reduction.

At first, reduction of mitral regurgitation should be evaluated. A double orifice mitral valve is created by MitraClip® therapy (Figure 19), often splitting the original jet into two small residual jets. Although qualitative interpretation of jet sever-

ity reduction can easily be assessed by evaluation of reduction in jet width and jet area, these measures inherently are load dependent (Figure 18). No specific method for quantification of acute regurgitation reduction after MitraClip® therapy has been validated so far. As pointed out in Figure 10, 3D vena contracta area assessment of a single or multiple residual jets can be performed as a quantitative approach. A 3D vena contracta area reduction of >50 % has been suggested as the best quantitative parameter relating to subsequent reverse left ventricular remodeling after MitraClip® therapy.[7] In addition semi-quantitative evaluation such as increased systolic forward pulmonary vein flow, increased left ventricular stroke volume and amelioration of pulmonary artery systolic pressures indirectly reflect adequate reduction of severity of mitral valve regurgitation (Figure 18). Acute procedural success is defined as reduction of mitral regurgitation ≤grade 2.

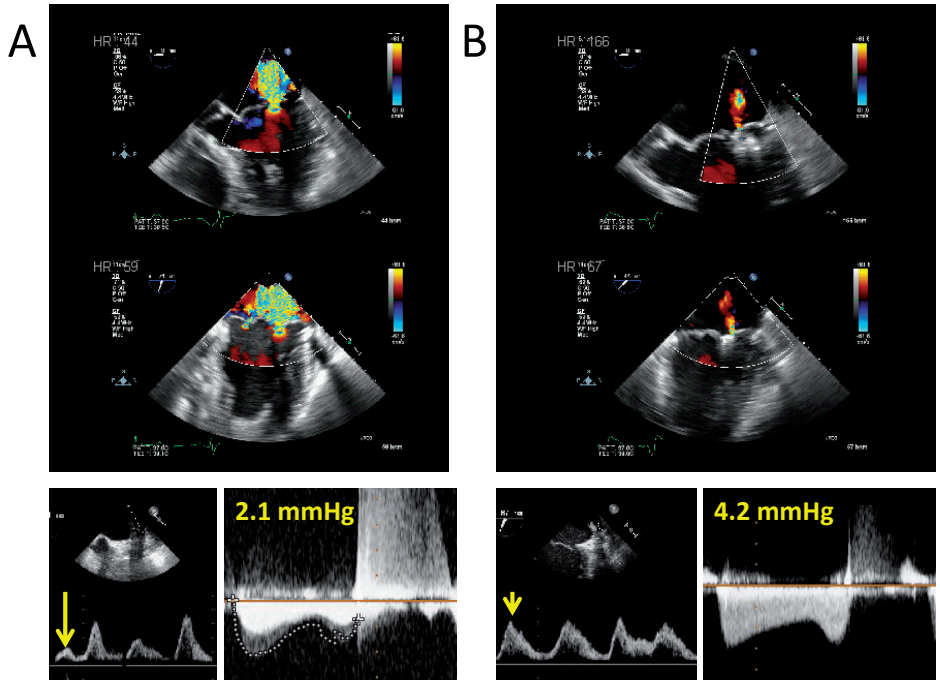

Figure 5.18
Acute procedural effect evaluation. A: Before MitraClip® therapy. B: After MitraClip® therapy. Significant reduction of mitral regurgitation based on reduced jet area and jet width is depicted. The blunted forward systolic pulmonary vein flow is significantly increased after the procedure (yellow arrows at left lower panels), indirectly reflecting adequate reduction of mitral regurgitation severity. No significant transmitral gradient developed after the intervention (right lower panel).

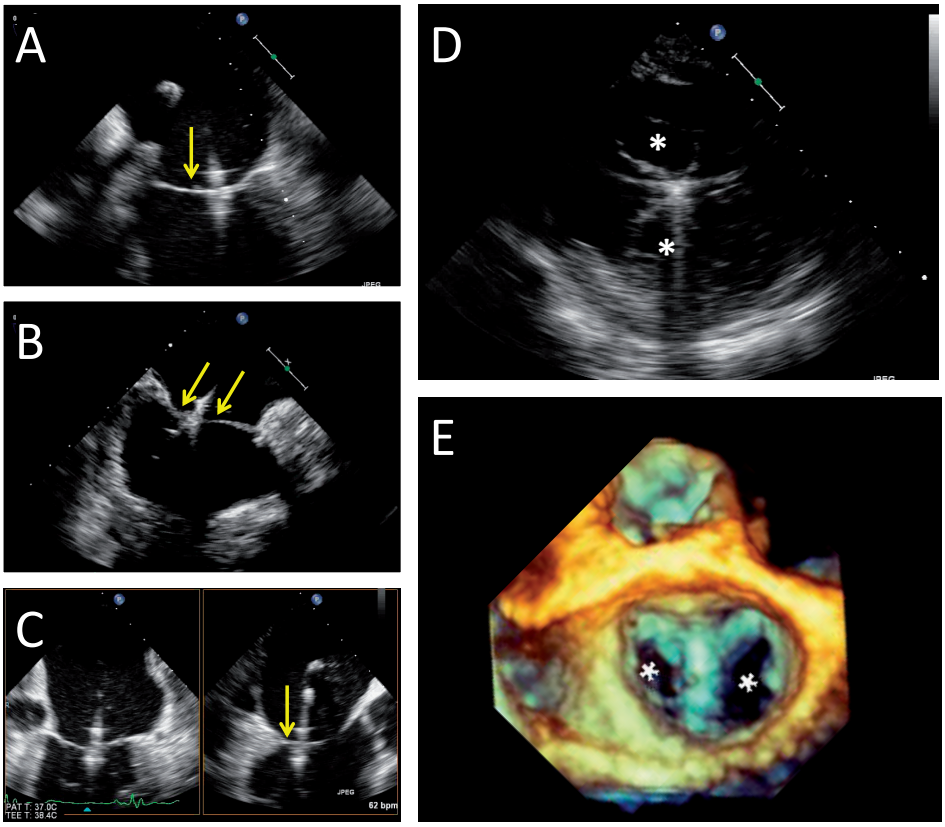

Figure 5.19
Mitral leaflet insertion evaluation. A: Anterior mitral leaflet (arrow) evaluation on 4 chamber view. B: Angel's view at bicommissural mitral valve level. C: Posterior mitral leaflet (arrow) evaluation at outflow tract view. D: Transgastric view showing dog-bone or figure eight pattern of double orifice (asterisks) mitral valve. E: 3D-zoom of double orifice (asterisks) mitral valve, indicating perpendicular clip alignment. See text for details.

Leaflet insertion.

Secondly, to avoid the risk of future clip detachment, it is essential to assure both leaflets are adequately captured and inserted between the grippers and both clip arms. Re-evaluation of the cine run of the grasping step can be particularly helpful. Anterior leaflet insertion is best seen on a 4-chamber mid-esophageal TOE view and the posterior leaflet insertion can adequately be visualized on the long-axis view. Both leaflets should be seen as going over the tip of both clip arms and at this point leaflet motion throughout the cardiac cycle needs to be restricted or absent to assure adequate leaflet insertion. The leaflet length inserted into the clip arms (ideally about 5 mm) can be assessed by subtracting the remaining mobile leaflet length from the preprocedual mobile leaflet length. At the bicommissural mitral valve level the clip should be visualized transecting the mid portion by the leaf-

lets. On short-axis transgastric view the double orifice can be appreciated, similar to a 1-beat 3D full volume view, resembling a figure eight or dog-bone pattern. Additionally, the 1-beat 3D full volume view is essential to confirm perpendicular alignment of the clip arms to the mitral coaptation line.

Mitral valve area reduction.
Finally transmitral gradient and mitral valve area are evaluated to ascertain no functional mitral stenosis is created by the MitraClip® intervention. Continuous wave Doppler through one of the orifices created by the clip permits measurement of the mean mitral valve gradient, which ideally remains below 5 mmHg (Figure 18). As the flow velocities across asymmetrical mitral orifices are equal, the choice of orifice for Doppler alignment is no issue.[9] Less load and flow dependent quantification is provided by summing mitral areas of the orifices by planimetry at the tips of both leaflets during mid diastole, which can easily be obtained on 3D-TOE post-processing on-line or off-line (Figure 8).

CONCLUSION

3D-TOE has become indispensable for optimal candidate selection and procedural guidance in patients treated with MitraClip® therapy. Superior anatomic performance and comprehensive evaluation of regurgitant jet characteristics represent cornerstones for eligibility assessment. Standardized mitral valve display, alternating 1-beat 3D full volume and bi-plane acquisitions, improves procedural guidance. Intensive communication between a skilled imager and a well-trained interventionalist with each understanding of 3D-TOE from a technical and practical point of view, respectively, are prerequisites to obtain high procedural success rates.

REFERENCES

1. Feldman T, Foster E, Glower DD et al. Percutaneous repair or surgery for mitral regurgitation. *N Engl J Med.* 2011; 364:1395-1406.
2. Maisano F, La Canna G, Colombo A et al. The evolution from surgery to percutaneous mitral valve interventions: the role of the edge-to-edge technique. *J Am Coll Cardiol.* 2011; 58:2174-2182.
3. Maisano F, Franzen O, Baldus S et al. Percutaneous mitral valve interventions in the real world: early and 1-year results from the ACCESS-EU, a prospective, multicenter, nonrandomized post-approval study of the MitraClip therapy in Europe. *J Am Coll Cardiol.* 2013; 62:1052-1061.
4. Baldus S, Schillinger W, Franzen O et al. MitraClip therapy in daily clinical practice: initial results from the German transcatheter mitral valve interventions (TRAMI) registry. *Eur J Heart Fail.* 2012; 14:1050-1055.
5. Whitlow PL, Feldman T, Pedersen WR et al. Acute and 12-month results with catheter-based mitral valve leaflet repair: the EVEREST II (Endovascular Valve Edge-to-Edge Repair) High Risk Study. *J Am Coll Cardiol.* 2012; 59:130-139.
6. Vahanian A, Alfieri O, Andreotti F et al. Guidelines on the management of valvular heart disease (version 2012): the Joint Task Force on the Management of Valvular Heart Disease of the European Society of Cardiology (ESC) and the European Association for Cardio-Thoracic Surgery (EACTS). *Eur J Cardiothorac Surg.* 2012; 42:S1-44.
7. Altiok E, Hamada S, Brehmer K et al. Analysis of procedural effects of percutaneous edge-to-edge mitral valve repair by 2D and 3D echocardiography. *Circ Cardiovasc Imaging.* 2012; 5:748-755.
8. Lancellotti P, Moura L, Pierard LA et al. European Association of Echocardiography recommendations for the assessment of valvular regurgitation. Part 2: mitral and tricuspid regurgitation (native valve disease). *Eur J Echocardiogr.* 2010; 11:307-332.
9. Maisano F, Redaelli A, Pennati G et al. The hemodynamic effects of double-orifice valve repair for mitral regurgitation: a 3D computational model. *Eur J Cardiothorac Surg.* 1999; 15:419-425.
10. Salcedo EE, Quaife RA, Seres T et al. A framework for systematic characterization of the mitral valve by real-time three-dimensional transesophageal echocardiography. *J Am Soc Echocardiogr.* 2009; 22:1087-1099.
11. Feldman T, Kar S, Rinaldi M et al. Percutaneous mitral repair with the MitraClip system: safety and midterm durability in the initial EVEREST (Endovascular Valve Edge-to-Edge REpair Study) cohort. *J Am Coll Cardiol.* 2009; 54:686-694.

Chapter 6

Acute effect of MitraClip on valve geometry in functional mitral regurgitation: insights from 3-dimensional transesophageal echocardiography

Philippe Debonnaire, Ibtihal Al Amri, Frank van der Kley,Martin J Schalij, Jeroen J Bax, Nina Ajmone Marsan, Victoria Delgado

EuroIntervention, 2015 Sep 11(5): in press.

ABSTRACT

Objectives

Our aim was to evaluate the acute effects of transcatheter edge-to-edge mitral valve repair using the MitraClip device on mitral valve geometry in patients with functional mitral regurgitation (FMR).

Methods and Results

Forty-two patients (age 73 years [IQ range 66.1-78.0], 55% men, 62% ischaemic FMR) with moderate-to-severe and severe FMR treated with the MitraClip were included. Three-dimensional transoesophageal echocardiography was performed prior to and immediately after MitraClip implantation. Acute changes of mitral annular and leaflet geometry were assessed with dedicated mitral modelling software. FMR less than moderate grade was achieved in 36 (86%) patients. After MitraClip implantation, the mitral annulus became more elliptical (ellipticity from 122±17% to 129±18%; p=0.04) with a non-significant reduction in anteroposterior diameter (33±6 to 32±5 mm, p=0.08). The coaptation area increased from 350 mm^2 (IQ range 289-493 mm^2) to 434 mm^2 (IQ range 328-523 mm^2, p=0.008). In particular, a larger part of the anterior mitral leaflet was included in the coaptation, leaving a smaller exposed anterior leaflet length of the A2 segment (from 27±6 mm to 25±5 mm, p<0.05) while the exposed length of the posterior leaflet (P2 level) remained unchanged (12±4 mm pre- vs. 13±4 mm post-repair, p=0.15). There was no change in total leaflet area (1,811±582 mm^2 pre- vs. 1,870±506 mm^2 post-repair, p=0.18). Annular height to intercommissural width ratio and tenting volume remained unchanged, suggesting no increase in leaflet stress.

Conclusions

The MitraClip device affects MV geometry in FMR patients by increasing mitral annular ellipticity and coaptation area.

INTRODUCTION

Functional mitral regurgitation (FMR) is common in heart failure patients and is associated with poor clinical outcomes.[1-4] Surgical mitral valve repair has proven to be beneficial, providing significant improvement in symptoms and left ventricular (LV) function.[5,6] However, many patients with significant FMR are not referred for or are denied surgical intervention due to a high operative risk, related to advanced age and the presence of associated comorbidities.[7] Several minimally invasive and transcatheter based mitral valve repair techniques provide feasible alternative treatment options to conventional valve surgery for patients with a high operative risk. The transcatheter edge-to-edge mitral valve repair technique using the MitraClip system (Abbott Vascular-Structural Heart, Menlo Park, CA, USA) is designed to grasp the mitral valve leaflets at the middle scallops, creating a double orifice valve during diastole and maintaining closer apposition of the leaflets during systole to reduce the regurgitant volume. With more than 17,000 patients treated worldwide, the MitraClip device has demonstrated to be a feasible and safe procedure, also in patients with FMR, and to improve symptoms.[8,9] The effect of the MitraClip device on the geometry and function of the mitral valve, however, remains largely unexplored. Three-dimensional transesophageal (TEE) echocardiography allows for accurate measurements of mitral valve geometry.[10] Accordingly, the present study aimed at evaluating the acute effects of transcatheter edge-to-edge repair on mitral annular geometry and leaflet coaptation zones of patients with FMR using 3-dimensional TEE.

METHODS

Patient population and data collection

A total of 59 patients were treated with the MitraClip device at the Leiden University Medical Centre between January 2012 and July 2014. Thorough clinical and echocardiographic evaluation was performed prior to the procedure by an interdisciplinary team of cardiac surgeons and cardiologists. Patients had symptomatic moderate-to-severe or severe mitral regurgitation and were at high risk for conventional surgical mitral valve repair, defined by a logistic EuroSCORE>20% or the presence of specific risk factors associated with excessive morbidity and mortality. Evaluation of clinical symptoms included assessment of functional capacity according to the New York Heart Association (NYHA) functional class and the 6-minute walked distance test. Furthermore, a quality of life assessment was performed using the Minnesota Living With Heart Failure® questionnaire.[11] Trans-

thoracic echocardiographic (TTE) and TEE assessment were routinely performed before the intervention to assess left ventricular (LV) dimensions and function, mitral valve morphology and mitral regurgitation grade and evaluation of factors that may contraindicate the procedure.[12] The procedure was guided with 3-dimensional TEE allowing acquisition of 3-dimensional data of the mitral valve. In the current analysis only patients with FMR and sufficient quality of peri-procedural 3-dimensional TEE data allowing for geometrical analysis of the mitral valve were included (n= 42).

Two-dimensional transthoracic echocardiographic evaluation

Pre-procedural TTE was performed using commercially available ultrasound systems (E9 or Vivid 7, GE Norway, Horten, Norway) equipped with an M5S transducer and 2-dimensional, M-mode and Doppler data were acquired with the patient in the left lateral decubitus position. LV dimensions and function were assessed according to the recommendations of the American Society of Echocardiography and the European Association of Echocardiography.[13] From the apical 4- and 2-chamber views the LV end-diastolic and end-systolic volumes and LV ejection fraction were measured according to the biplane Simpson's method. LV diameters were assessed at end-diastole and end-systole from the parasternal long-axis view or M-mode recordings. From the apical 2-, 3- and 4-chamber views, colour and continuous wave Doppler data of the mitral valve were acquired and mitral regurgitation was quantitatively determined by the proximal isovelocity surface area method and by measuring the vena contracta according to current guidelines.[14]

Three-dimensional transesophageal echocardiographic data acquisition and evaluation

TEE was performed during the procedure using a commercially available ultrasound system (iE33, Philips Medical Systems, Andover, MA, USA) equipped with a fully sampled matrix-array TEE transducer (X7-2t Live 3D-TEE transducer, iE33, Philips Medical Systems, Andover, MA, USA) capable of acquiring both 2- and 3-dimensional images to guide implantation of the MitraClip device and to assess acute procedural success. Three-dimensional images were acquired during the intervention before and directly after implantation of the MitraClip device, using multi-beat (7-14 beats) full-volume or 1-beat 3-dimensional-zoom acquisitions encompassing a pyramid volume. The multi-beat full-volume images were acquired during respiratory breath-hold whenever possible to avoid stitch artefacts. In patients with atrial fibrillation, 1-beat 3-dimensional-zoom acquisitions with the sector adjusted to include the MV were performed. Furthermore, special care was taken to stabilize the probe during 3-dimensional data acquisition. All images

were digitally stored for off-line analysis with the MVQ software (QLAB Cardiac 3DQ v.10.0; Philips Medical Systems, Andover, MA, USA), which allows semi-automated 3-dimensional quantification of the mitral valve geometry.[10] From 3-dimensional full-volume or zoomed datasets of the mitral valve, the software displays three orthogonal multiplanar reformation planes of the mitral valve. The planes are manually aligned across the mitral annulus in a selected end-systolic frame to obtain bicommissural, outflow tract and short-axis views of the mitral valve. The bicommissural view was used to indicate the antero-lateral and postero-medial points of the mitral annulus, whereas the outflow tract view was used to define the anterior and posterior points of the mitral annulus, the aortic annulus and the mitral leaflet coaptation point. The mitral leaflet commissural points were set on the short-axis plane and the mitral leaflets and coaptation length were traced on multiple cross-sections (18-30) in the outflow-tract view, orthogonal to the inter-commissural direction. The 3-dimensional rendered surgical en face view was used to correctly identify the coaptation point (Figure 1). Subsequently, the software automatically creates a 3-dimensional model of the mitral valve geometry and various measurements can be derived.

The measurements of the mitral valve performed with the MVQ software included anteroposterior and intercommissural annular diameters and area, and leaflet lengths, angles and areas. Mitral annular ellipsicity was calculated as the ratio between the anteroposterior annular diameter and the intercommisural diameter. Furthermore, to assess the effect of the MitraClip on mitral leaflet coaptation, the coaptation length at the middle scallops (A2P2) was measured and coaptation area was calculated by subtracting the exposed area of the anterior and posterior mitral leaflet (i.e. the area without the coapting part of the leaflets) from the total area of the anterior and posterior leaflet (i.e. the area including the coapting part of the leaflets). Moreover, the effect of the MitraClip on leaflet stress was analysed by assessing the annular-height-to-intercommissural-width ratio and the non-planarity angle. The non-planarity angle was determined as the angle between the two vectors from the anterior and posterior leaflet hinge points of the annulus to the centre of the intercommissural line. Additionally, tenting height at the A2P2 level, tenting volume and the angle between the mitral annulus and aortic annulus were measured. Three-dimensional TEE data were analysed by two experienced observers. An example of mitral geometry measurements performed before and after MitraClip implantation in a patient using MVQ software is displayed in Figure 2.

Procedural technique

The transcatheter edge-to-edge mitral valve intervention was performed as previously described using the MitraClip system and guided by fluoroscopy and 2- and

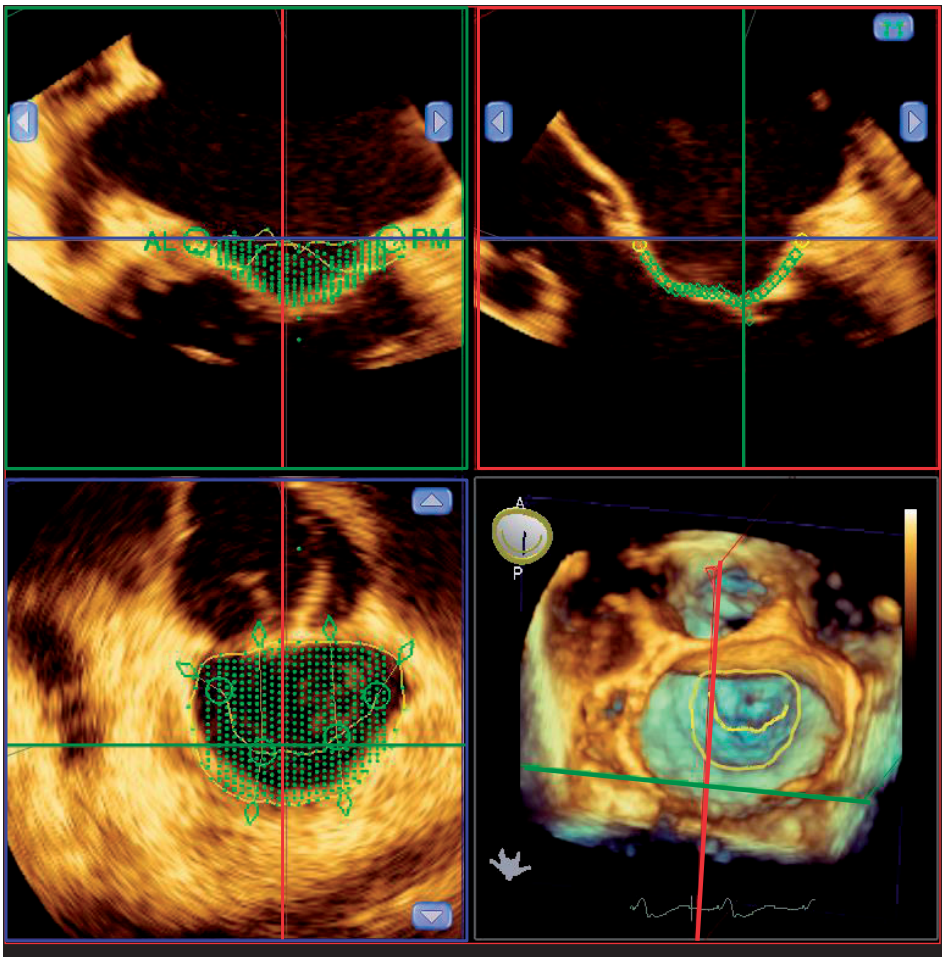

Figure 6.1
Identification of 3-dimensional landmarks on multiplanar reformation planes using Mitral Valve Quantification (MVQ) software. Using the multiplanar reformation planes, the MVQ software identifies the landmark points of the mitral annulus. The anterior, posterior, anterolateral and posteromedial points of the mitral annulus are identified on the 2- and 3-chamber views. The en face view provides the cross-sectional area of the mitral annulus and simultaneously the 3-dimensional full volume of the mitral valve can be visualised. Left upper panel: identification of leaflet insertion points, right upper panel: tracing the mitral leaflets and marking the leaflet coaptation point, left lower panel: tracing the coaptation line, right lower panel: 3-dimensional surgical view of the mitral valve with the manually traced lines visible.

3-dimensional TEE.[12,15] In brief, after transseptal punction, the clip delivery system was advanced into the left atrium and positioned above the mitral valve plane over the origin of the regurgitant jet. The device was oriented perpendicular to the line of coaptation and the system was advanced into the LV with the arms slightly opened. After ensuring good alignment of the device (just below the regurgitant orifice on the TEE bicommissural view of the mitral valve) and simultaneously visu-

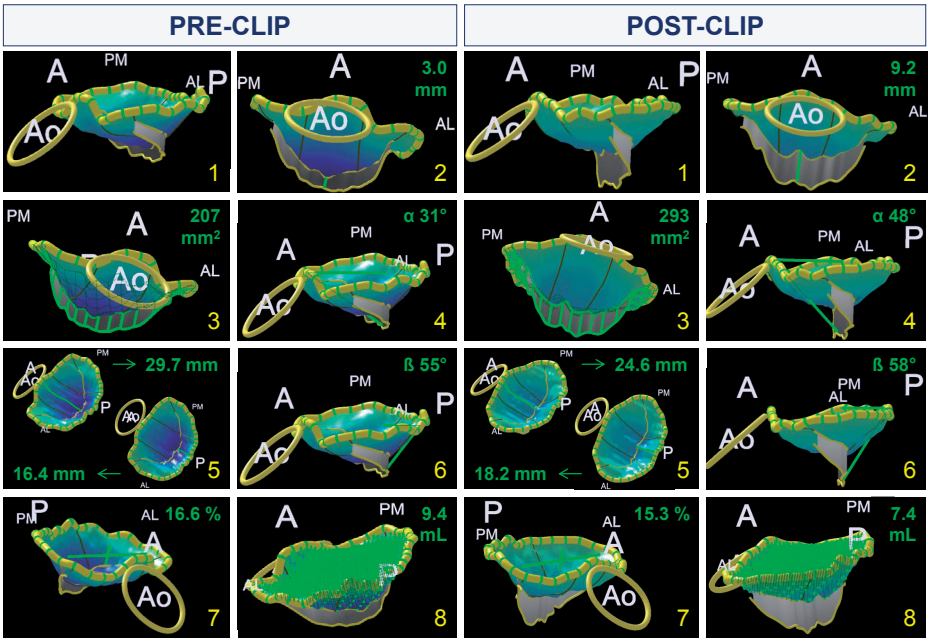

Figure 6.2
Example of changes in mitral valve geometry in a patient before and after MitraClip implantation with 3-dimensional model. 1: 3-dimensional model of the mitral valve, 2: Coaptation length at the A2P2 level pre- and post-MitraClip implantation, 3: Coaptation area pre- and post-MitraClip implantation, 4: Angle between anterior leaflet and mitral annulus aorta pre- and post-MitraClip implantation, 5: Length of the anterior (left) and posterior (right) leaflet at the A2 and P2 level respectively pre- and post-MitraClip implantation, 6: Angle between posterior leaflet and mitral annulus pre- and post-MitraClip implantation, 7: Ellipsicity pre- and post-MitraClip implantation, 8: Tenting volume pre- and post-MitraClip implantation. A = anterior, AL = anterolateral, Ao = Aorta, P = posterior, PM = posteromedial.

alizing the arms of the device opened in the perpendicular TEE view (120-150°, or LV outflow tract view) the system was pulled-back to grasp the mitral leaflets in the arms of the clip and create a double-orifice valve. The grade of MR was assessed during the procedure using color and continuous wave Doppler echocardiography. Procedural success was defined as reduction of MR to grade ≤ 2. If needed, a second clip was placed to ensure grade ≤ 2 MR without significant stenosis. The grade of residual MR was also evaluated at predischarge transthoracic echocardiogram using color flow Doppler and color flow jet area (MR jet area/ LA jet area).[16]

Statistical analysis

Distribution of the continuous data was tested by the Kolmogorov-Smirnov one-sample test and the Shapiro-Wilk test. Normally distributed continuous variables are presented as mean ± standard deviation, whereas non-normally distributed variables are presented as median and interquartile range. Categorical variables

Table 6.1
Baseline demographic, clinical and echocardiographic patient characteristics.

	n = 42
Male gender, n (%)	23 (55)
Age (years)	72.8 (IQ range 66.1-78.0)
Hypertension, n (%)	18 (43)
Hypercholesterolemia, n (%)	17 (42)
Positive family history of CVD, n (%)	8 (20)
(Ex-) smoker, n (%)	21 (50)
Diabetes Mellitus, n (%)	16 (38)
COPD, n (%)	6 (14)
Peripheral vascular disease, n (%)	11 (26)
Prior stroke, n (%)	5 (12)
Ischemic cardiomyopathy, n (%)	26 (62)
Prior myocardial infarction, n (%)	22 (52)
Location of myocardial infarction, n (%)	11 (50)
Anterior	6 (27)
Inferior	2 (9)
Anteroseptal	2 (9)
Posterolateral	1 (5)
Posterior	
NYHA class III-IV, n (%)	35 (83)
Logistic EuroSCORE (%)	17.7 (IQ range 10.9-27.4)
Glomerular filtration rate (ml/min/1.73m^2)	49.3 (IQ range 26.4-75.0)
Sinus rhythm, n (%)	14 (33)
CRT, n (%)	16 (38)
Medication, n (%)	
Betablockers	34 (81)
ACE-/ Angiotensin receptor II inhibitors	28 (78)
Diuretics	37 (88)
Digoxin	11 (26)
Statin	29 (69)
Calcium antagonist	4 (10)
Aspirin	13 (31)
Anticoagulants	40 (95)
LV end-diastolic diameter (mm)	63.2 ± 9.3
LV end-systolic diameter (mm)	52.7 ± 13.5
LV end-diastolic volume (ml)	176.5 (IQ range 133.8-243.8)
LV end-systolic volume (ml)	118.5 (IQ range 82.5-163.8)
LV ejection fraction (%)	33.7 ± 10.3
Mitral regurgitation	
Grade 3	20 (48)
Grade 4	22 (52)
Number of clips implanted	
1 clip	24 (57)
2 clips	15 (36)
3 clips	1 (2)
4 clips	2 (5)

ACE: Angiotensin Converting Enzyme, COPD: Chronic Obstructive Pulmonary Disease, CRT: Cardiac Resynchronization Therapy, CVD: cardiovascular disease; LV: left ventricular, NYHA: New York Heart Association functional class.

are expressed as numbers and percentages. Comparisons of MV geometry pre- and post-procedure were performed using the paired Student T-test for normally distributed variables and the Wilcoxon signed-rank test for non-normally distributed variables. All statistical tests were 2-tailed and a $p<0.05$ was considered statistically significant. Statistical analysis was performed using SPSS 20.0.0 for windows (SPSS Inc., Chicago IL, USA).

RESULTS

Baseline characteristics

Baseline demographic, clinical and echocardiographic characteristics of the patients are listed in Table 1. Moderate-to-severe FMR was observed in 48% of patients and severe FMR in 52%. Ischemic heart failure was the most frequent underlying etiology of heart failure (62%).

Changes in 3-dimensional mitral valve geometry after MitraClip

FMR reduction to ≤grade 2 was achieved in 36 (86%) patients (Figure 3). Changes in mitral valve geometry post-MitraClip implantation are presented in Table 2. After the procedure, the mitral annulus became more elliptical indicated by an increase in ellipsicity (from 122±17% to 129±17%, $p<0.05$), increase in both the anterior (from 27±7º to 34±8º, $p<0.001$) and posterior mitral leaflet angle (from 49±14º to 56±10º, $p=0.02$) and a decrease in the antero-posterior mitral annular diameter (from 33±6 mm to 32±5 mm, $p=0.08$). Furthermore, an increase in both coaptation length at the A2-P2 level (from 50±11 mm to 53±9 mm, $p<0.001$) and total coaptation area (from 215 mm^2 (IQ range 164-264) to 281 mm^2 (IQ range 238-386), $p=0.005$) were observed. In addition, the exposed length of the anterior mitral leaflet (i.e. excluding the coapting part of the leaflet) at the A2 level (from 27±6 mm to 25±5 mm, $p=0.03$) and the exposed anterior leaflet area (from 795±277 mm^2 to 730±222 mm^2, $p=0.04$) decreased while the posterior leaflet length at the P2 level and total leaflet area remained unchanged, indicating that the improvement in leaflet coaptation is due to a larger area of the anterior mitral leaflet involved in the coaptation (Figures 4 and 5). The annular height-to-intercommissural-width ratio, non-planarity angle and tenting volume remained unchanged after MitraClip therapy, suggesting no increase in leaflet stress.

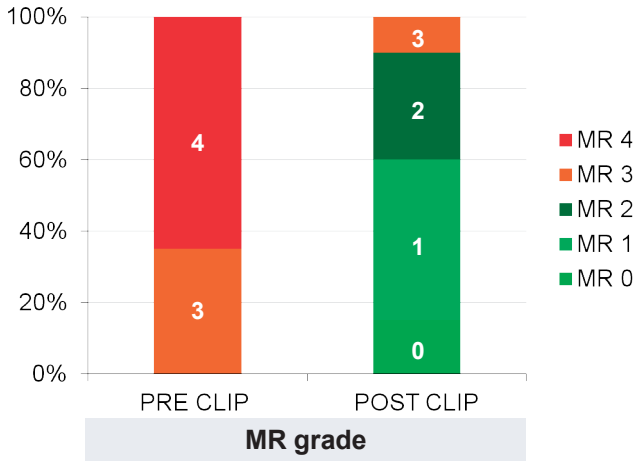

Figure 6.3
Mitral regurgitation grade reduction post-MitraClip implantation. MR: mitral regurgitation.

DISCUSSION

The results of this study demonstrate that the percutaneous edge-to-edge mitral valve repair procedure using the MitraClip device directly affects mitral valve geometry. By grasping the anterior and posterior leaflets, the coaptation length and area of the mitral leaflets significantly increase in end-systole. The contribution of the anterior mitral leaflet in the coaptation increases and the antero-posterior diameter of the mitral annulus is reduced leading to a more elliptical mitral annular shape.

Few studies have assessed the effect of surgical annuloplasty on mitral valve anatomy using 3D-TEE. Greenhouse *et al.* used intraoperative 3-dimensional TEE to examine the regional effects of surgical mitral annuloplasty on annular geometry and leaflet coaptation zones in patients with FMR.[17] A significant increase in mitral leaflet coaptation length after band annuloplasty was observed, particularly at the middle scallops of the anterior mitral leaflet (2.9±2.6mm at baseline vs 5.5±2.5mm post-surgery, $p<0.01$). The posterior annulus was displaced anteriorly leading to an increase of coaptation surface of the anterior leaflet and correction of the mitral regurgitation. Our findings are in agreement with this concept by showing that the exposed length and area of the anterior leaflet at the central scallop (i.e. the anterior leaflet length and area without the coapting part) decreased. These changes were not accompanied by changes in the total mitral leaflet area, indicating inclusion of a larger proportion of the anterior leaflet into the area of coaptation (Figure 4). Therefore, implantation of a MitraClip device seems to af-

Table 6.2
Echocardiographic mitral valve geometry parameters pre- and post- MitraClip implantation measured with 3-dimensional transesophageal echocardiography.

	Pre-MitraClip	Post-MitraClip	p-value
Annulus			
Anteroposterior diameter (mm)	33.2 ± 6.2	32.1 ± 5.3	0.08
Intercommissural diameter (mm)	39.9 ± 6.4	41.1 ± 6.5	0.15
Ellipsicity (%)	121.8 ± 17.3	129.4 ± 18.4	0.04
Circumference (mm)	124.5 ± 19	124.8 ± 17.4	0.88
Annular area (mm^2)	1178.0 ± 380.2	1170.7 ± 326.1	0.81
Annular height (mm)	5.5 ± 1.9	5.7 ± 1.9	0.62
Annular height to intercommissural width ratio (%)	20.2 ± 13.8	18.3 ± 6.3	0.41
Leaflets			
Anterior leaflet length exposed A2 segment (mm)*	27.2 ± 5.5	25.4 ± 5.0	0.03
Posterior leaflet length exposed P2 segment (mm)*	11.6 ± 4.1	12.5 ± 4.3	0.15
Anterior leaflet exposed area (mm^2)*	795.4 ± 277.0	729.8 ± 222.0	0.04
Posterior exposed leaflet area (mm^2)*	636.9 ± 257.0	666.3 ± 227.5	0.32
Total leaflet area (mm^2)	1811.2 ± 582.2	1870.3 ± 505.5	0.18
Anterior leaflet angle (°)	27.1 ± 7.4	33.6 ± 7.9	<0.001
Posterior leaflet angle (°)	49.0 ± 13.6	56.1 ± 10.3	0.02
Aortomitral angle (°)	134.8 ± 11.2	133.0 ± 11.3	0.39
Non-planarity angle (°)	122.6 ± 18.3	123.3 ± 18.4	0.82
Tenting height A2-P2 (mm)	8.1 ± 3.4	8.2 ± 3.0	0.65
Tenting volume (mL)	2.9 (IQ range 1.7-4.5)	3.3 (IQ range 2.5-4.5)	0.80
Coaptation			
Coaptation length A2P2 (mm)	5.0 ± 0.11	5.3 ± 0.87	<0.001
Coaptation area (mm^2)	349.6 (IQ range 289.0-492.8)	433.8 (IQ range 327.6-522.7)	0.008

*The exposed length and area of the leaflets does not include the coapting part of the leaflet.

fect mitral coaptation geometry similarly to surgical mitral annuloplasty, however, through a different mechanism.

In patients with FMR treated with the Mitraclip device, Schmidt *et al.*, reported significant reductions of the mitral annular area (mean difference 0.39±0.49cm^2, p<0.001) and antero-posterior annular diameter (mean difference 0.28±0.32cm, p<0.001) as well as a significant reduction in tenting area (mean difference 0.39±0.49cm^2, p<0.001).[18] The disparate results of the study by Schmidt et al and the present study may be explained by the different post-processing analysis. While Schmidt et al performed the measurements on the orthogonal multiplanar reformations of the 3-dimensional TEE volume set, in the present study the

measurements were performed on 3-dimensional models that permit better assessment of the saddle shape of the mitral annulus. The current analysis did however show a change in the shape of the mitral annulus with an increase in annular ellipsicity and a decrease in anteroposterior diameter which is consistent

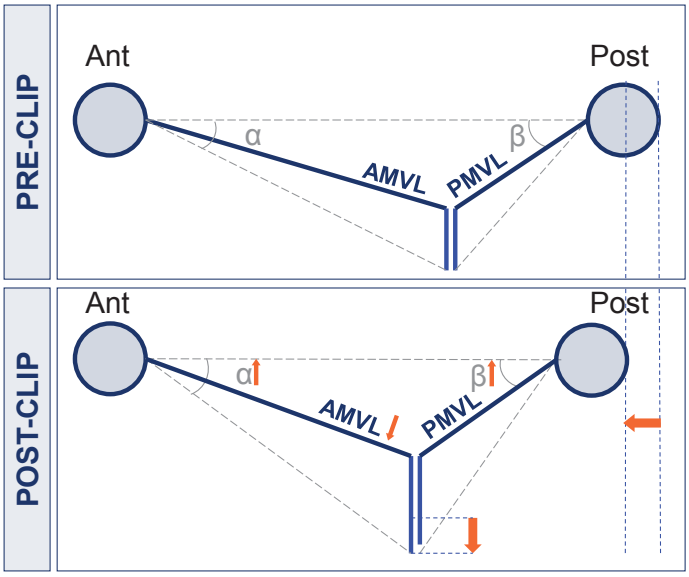

Figure 6.4
Schematic overview of acute effect of MitraClip device on mitral valve geometry. The MitraClip device leads to a decrease in exposed anterior leaflet length (AMVL) at the A2 level without change in overall mitral leaflet length and area, indicating a higher contribution of the AMVL into coaptation. Furthermore, the antero-posterior diameter tends to reduce with corresponding increases in the anterior and posterior mitral leaflet angle (α and β). AMVL = Anterior mitral valve leaflet, PMVL = Posterior mitral valve leaflet.

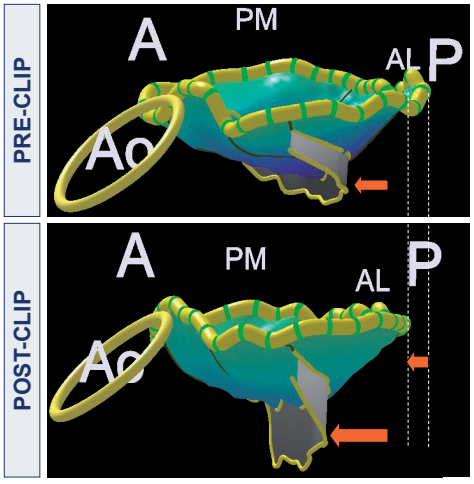

Figure 6.5
3-dimensional overview of acute effect of MitraClip therapy on mitral valve geometry showing an increase in coaptation area. The long-axis view of the 3-dimensional model is showed at baseline (upper panel) and after (bottom panel) MitraClip implantation with the arrow pointing the area of coaptation. A = anterior, AL = anterolateral, Ao = Aorta, P = posterior, PM = posteromedial.

with previous reports.[18-20] Recently, Schueler *et al.* showed that patients with FMR showed significant decreases in the anteroposterior diameter of the mitral annulus (from 4.0±0.6 cm to 3.6±0.6 cm, p<0.001), 3-dimensional mitral annulus area (from 14.4±3.9 cm^2 to 12.9±3.4 cm^2, p<0.001) and mitral valve sphericity index (from 0.9±0.1 to 0.8±0.1, p<0.001) whereas the intercommisural diameter remained unchanged.[20] Interestingly, these changes were not observed in patients with degenerative mitral regurgitation. Furthermore, patients in whom the antero-posterior diameter acutely reduced ≥6.4% had superior clinical response to MitraClip therapy after 6 months of follow-up compared with patients showing less acute annulus diameter reduction. However, an acute reduction in the anteroposterior diameter after MitraClip therapy would indicate significant traction on the mitral leaflets to reduce the distance between the anterior and posterior annulus. This high leaflet stress could affect the durability of the procedure. To assess leaflet stress, we analysed the annular-height to intercommissural-width ratio. In the present study, the annular-height to intercommissural-width ratio did not significantly reduce after MitraClip implantation, suggesting no acute increase in leaflet stress.[21] Understanding the effects of the MitraClip on the geometry of the mitral valve will eventually help to identify patients that will benefit most from this procedure.

Clinical implications

Evaluating the effects of MitraClip on 3-dimensional mitral valve geometry is important to understand its therapeutic efficacy and durability. The present study showed that MitraClip increases the coaptation length and area due to a larger contribution of the anterior mitral leaflet into the coaptation. Furthermore, the anteroposterior diameter tends to reduce with corresponding increases in the anterior and posterior mitral leaflet angles. Subsequent iterations of the device or development of newer systems may consider these findings to improve the efficacy of the repair. Although the effects of these geometrical changes on long-term durability were not evaluated in the present study, future investigations may shed light on this topic and help in the design of novel devices.

Limitations

There are several limitations inherent to this study. First, the study population was rather small. By recording both the pre- and postprocedural views during anaesthesia we aimed at creating a similar hemodynamic status for the pre- and postprocedural measurements of mitral annular geometry. However, the effects of the anaesthetics on patients' hemodynamic status must be considered. Furthermore, the clips caused shadowing artifacts and limited the evaluation of the

coaptation point. By tracing the coaptation point in the body of the MitraClip after the procedure, which is the point where the leaflets are grasped by the clip, we aimed at reducing the effect of the artifacts on the outcomes.

CONCLUSION

Percutaneous MitraClip therapy affects mitral valve geometry in FMR patients by increasing coaptation length and area mainly due to a larger contribution of the anterior mitral leaflet into coaptation after the procedure.

REFERENCES

1. Bursi F, Enriquez-Sarano M, Nkomo VT et al. Heart failure and death after myocardial infarction in the community: the emerging role of mitral regurgitation. *Circulation.* 2005;111(3):295-301.
2. Trichon BH, Felker GM, Shaw LK et al. Relation of frequency and severity of mitral regurgitation to survival among patients with left ventricular systolic dysfunction and heart failure. *Am J Cardiol.* 2003;91(5):538-543.
3. Bursi F, Barbieri A, Grigioni F et al. Prognostic implications of functional mitral regurgitation according to the severity of the underlying chronic heart failure: a long-term outcome study. *Eur J Heart Fail.* 2010;12(4):382-388.
4. Rossi A, Dini FL, Faggiano P et al. Independent prognostic value of functional mitral regurgitation in patients with heart failure. A quantitative analysis of 1256 patients with ischaemic and non-ischaemic dilated cardiomyopathy. *Heart.* 2011;97(20):1675-1680.
5. Bax JJ, Braun J, Somer ST et al. Restrictive annuloplasty and coronary revascularization in ischemic mitral regurgitation results in reverse left ventricular remodeling. *Circulation.* 2004;110(11 Suppl 1):II103-II108.
6. Westenberg JJ, van der Geest RJ, Lamb HJ et al. MRI to evaluate left atrial and ventricular reverse remodeling after restrictive mitral annuloplasty in dilated cardiomyopathy. *Circulation.* 2005;112(9 Suppl):I437-I442.
7. Mirabel M, Iung B, Baron G et al. What are the characteristics of patients with severe, symptomatic, mitral regurgitation who are denied surgery? *Eur Heart J.* 2007;28(11):1358-1365.
8. Whitlow PL, Feldman T, Pedersen Wret al. Acute and 12-month results with catheter-based mitral valve leaflet repair: the EVEREST II (Endovascular Valve Edge-to-Edge Repair) High Risk Study. *J Am Coll Cardiol.* 2012;59(2):130-139.
9. Feldman T, Kar S, Rinaldi M et al. Percutaneous mitral repair with the MitraClip system: safety and midterm durability in the initial EVEREST (Endovascular Valve Edge-to-Edge REpair Study) cohort. *J Am Coll Cardiol.* 2009;54(8):686-694.
10. Shanks M, Delgado V, Ng AC et al. Mitral valve morphology assessment: three-dimensional transesophageal echocardiography versus computed tomography. *Ann Thorac Surg.* 2010;90(6):1922-1929.
11. Rector TS, Kubo SH, Cohn J.N. Patients' self-assessment of their congestive heart failure. Part 2: Content, reliability and validity of a new measure, the Minnesota Living with Heart Failure questionnaire. *Heart Failure.* p. 198-209.
12. Mauri L, Garg P, Massaro JM et al. The EVEREST II Trial: design and rationale for a randomized study of the evalve mitraclip system compared with mitral valve surgery for mitral regurgitation. *Am Heart J.* 2010;160(1):23-29.
13. Lang RM, Bierig M, Devereux RB et al. Recommendations for chamber quantification: a report from the American Society of Echocardiography's Guidelines and Standards Committee and the Chamber Quantification Writing Group, developed in conjunction with the European Association of Echocardiography, a branch of the European Society of Cardiology. *J Am Soc Echocardiogr.* 2005;18(12):1440-1463.
14. Zoghbi WA, Enriquez-Sarano M, Foster E et al. Recommendations for evaluation of the severity of native valvular regurgitation with two-dimensional and Doppler echocardiography. *J Am Soc Echocardiogr.* 2003;16(7):777-802.

15. Delgado V, Kapadia S, Marsan NA et al. Multimodality imaging before, during, and after percutaneous mitral valve repair. *Heart.* 2011;97(20):1704-1714.
16. Foster E, Wasserman HS, Gray W et al. Quantitative assessment of severity of mitral regurgitation by serial echocardiography in a multicenter clinical trial of percutaneous mitral valve repair. *Am J Cardiol.* 2007;100(10):1577-1583.
17. Greenhouse DG, Dellis SL, Schwartz CF et al. Regional changes in coaptation geometry after reduction annuloplasty for functional mitral regurgitation. *Ann Thorac Surg.* 2012;93(6):1876-1880.
18. Schmidt FP, von Bardeleben RS, Nikolai P et al. Immediate effect of the MitraClip procedure on mitral ring geometry in primary and secondary mitral regurgitation. *Eur Heart J Cardiovasc Imaging.* 2013;14(9):851-857.
19. Altiok E, Hamada S, Brehmer K et al. Analysis of procedural effects of percutaneous edge-to-edge mitral valve repair by 2D and 3D echocardiography. *Circ Cardiovasc Imaging.* 2012;5(6):748-755.
20. Schueler R, Momcilovic D, Weber M et al. Acute changes of mitral valve geometry during interventional edge-to-edge repair with the MitraClip system are associated with midterm outcomes in patients with functional valve disease: preliminary results from a prospective single-center study. *Circ Cardiovasc Interv.* 2014;7(3):390-399.
21. Salgo IS, Gorman JH, III, Gorman RC et al. Effect of annular shape on leaflet curvature in reducing mitral leaflet stress. *Circulation.* 2002;106(6):711-717.

Part II

Echocardiographic deformation imaging

Chapter 7

Fragmented QRS and QTc duration relate to malignant ventricular tachyarrhythmias and sudden cardiac death in patients with hypertrophic cardiomyopathy

Philippe Debonnaire, Spyridon Katsanos, Emer Joyce,
Olivier VW van den Brink, Douwe E Atsma, Martin J Schalij, Jeroen J Bax,
Victoria Delgado, Nina Ajmone Marsan

J Cardiovasc Electrophysiol, 2015 May 26(5): 547-555.

ABSTRACT

Objectives

QRS fragmentation (fQRS) and prolonged QTc interval on surface ECG are prognostic in various cardiomyopathies, other than hypertrophic cardiomyopathy (HCM). The association between fQRS and prolonged QTc duration with occurrence of ventricular tachyarrhythmias or sudden cardiac death (VTA/SCD) in patients with HCM was explored.

Methods and Results

195 clinical HCM patients were studied. QTc duration was derived applying Bazett's formula; fQRS was defined as presence of various RSR' patterns, R or S notching and/or >1 additional R wave in any non-aVR lead in patients without pacing or (in) complete bundle branch block. The endpoints comprised SCD, ECG documented sustained VTA (tachycardia or fibrillation) or appropriate implantable cardioverter defibrillator (ICD) therapies [anti-tachycardia pacing (ATP) or shock] for VTA in ICD recipients [n=58 (30%)]. QT prolonging drugs recipients were excluded. After a median follow-up of 5.7 years (IQR 2.7-9.1), 26 (13%) patients experienced VTA or SCD. Patients with fQRS in ≥3 territories (inferior, lateral, septal and/or anterior) (p=0.004) or QTc ≥460 ms (p=0.009) had worse cumulative survival free of VTA/SCD than patients with fQRS in <3 territories or QTc <460 ms. fQRS in ≥3 territories (β 4.5, p=0.020, 95%CI 1.41-14.1) and QTc ≥460 ms (β 2.7, p=0.037, 95%CI 1.12-6.33) were independently associated with VTA/SCD. Likelihood ratio test indicated assessment of fQRS and QTc on top of conventional SCD risk factors provides incremental predictive value for VTA/SCD (p=0.035).

Conclusions

Both fQRS in ≥3 territories and QTc duration are associated with VTA/SCD in HCM patients, independently of and incremental to conventional SCD risk factors.

INTRODUCTION

Hypertrophic cardiomyopathy (HCM) is characterized by cellular hypertrophy, interstitial fibrosis and myofiber disarray that increase the risk of (arrhythmic) sudden cardiac death (SCD).[1] These ultra-structural alterations may account for abnormalities in left ventricular (LV) electrical activation, including depolarization and repolarization, reflected on surface electrocardiography (ECG).[1, 2] Abnormal ECG findings, although non-specific, are found in between 75% and 95% of HCM patients.[3] Recently the severity of ECG abnormalities in HCM patients were linked to the presence and extent of phenotypic expression as evaluated by cardiac magnetic resonance (CMR) imaging, including LV mass, hypertrophy and scarring (fibrosis).[4] However, whether ECG abnormalities might relate to electrical instability and be useful for stratification of HCM patients at risk for ventricular tachyarrhythmia (VTA) or SCD remains poorly explored.

Fragmentation of the QRS complex (fQRS) on surface ECG (comprising various RSR` patterns of QRS morphology) represents a depolarization abnormality that has been related to presence of myocardial fibrosis.[5-7] Moreover, the presence of fQRS is an independent predictor of VTA and/or mortality in patients with ischemic and non-ischemic cardiomyopathies, has been associated with reduced event-free survival in patients with Brugada syndrome and is a diagnostic marker in arrhythmogenic right ventricular dysplasia.[6, 8-10] Its potential clinical prognostic value in patients with HCM, however, is poorly studied.[11] In addition, congenital or acquired QT prolongation on ECG is a well-known repolarization abnormality implying increased risk of VTA and SCD.[12, 13] Heart rate corrected QT (QTc) prolongation is not infrequent in HCM patients, but limited data exist on its clinical significance.[14-20]

Therefore the aim of this study was to explore the association of both fQRS and QTc duration with the occurrence of malignant VTA or SCD in HCM patients.

METHODS

Patient population

Clinical HCM patients enrolled in an ongoing echocardiographic and clinical registry at our department were included in this analysis if ECG was present within one year before or after the baseline echocardiographic exam and subjects were ≥18 year-old (n=323). Clinical HCM was defined as a non-dilated LV with a maximal wall thickness of ≥15 mm on echocardiography in patients without systemic or alternative explanations for the magnitude of LV hypertrophy.[21] Patients with ventricular pacing (n=20) or (in)complete bundle branch block (BBB) at baseline ECG were

excluded. In particular, RSR' pattern in lead V1 and/or V2 with QRS duration ≥110 or ≥120 ms and S wave of greater duration than R wave or greater than 40 ms in leads I and V6 was defined as incomplete right BBB (n=11) and complete right BBB (n=19), respectively.[22] Left BBB (n= 12) was defined as a QRS duration ≥120 ms with RSR' pattern in leads I, aVL, V5 and V6.[22] In addition, patients taking QTc prolonging medications were excluded (n=20). Finally, patients without clinical follow-up within the last 3 years (n=46) were also excluded from further analysis.

Extensive baseline evaluation including medical history, demographics, medications, ECG and echocardiography was performed in all patients and data were prospectively collected at the departmental Cardiology Information System (EPD-Vision®, Leiden University Medical Center, Leiden, the Netherlands) and retrospectively analyzed. According to guidelines, the SCD risk profile of the patients was determined based on the following clinical and echocardiographic parameters [21]: secondary prevention implantable cardioverter defibrillator (ICD) indication, maximal LV wall thickness ≥30 mm, family history of SCD (≥ one 1st to 3th degree relative), unexplained syncope and, as additional risk factor, documented non-sustained ventricular tachycardia (≥3 beats at ≥120 bpm) prior to device implantation. Blood pressure response during exercise testing was not systematically available and therefore not included as a conventional SCD risk factor.

Patients were followed-up at the out-patient clinic or through contact with the general practitioners in order to evaluate the occurrence of cardiac events. The Ethical Committee of the Leiden University Medical Center approved this retrospective study and waived the need for written informed consent.

ECG analysis

Routine 12-lead ECG (settings: 0.05-300 Hz filter range, AC filter 50 Hz, paper speed 25 mm/s and voltage 10 mm/mV) was performed and stored digitally for off-line analysis, using a dedicated software (Siemens/Dräger Mega Care ECG Management System). QT interval and heart rate were automatically provided by the software. Heart rate corrected QT (QTc) duration was calculated applying Bazett's formula [QTc=QT/√(60/heart rate)]. Detection of fQRS was performed manually. As shown in Figure 1, QRS fragmentation comprises presence of various RSR' patterns, notching in the R or S wave or presence of >1 additional R in ≥2 beats of a non-aVR lead. fQRS was allocated to a territory when present in ≥2 contiguous leads of the inferior (II, III, aVF), lateral (I, aVL, V6), septal (V1,V2) or anterior (V3,V4,V5) regions.[5] Assessment of fQRS required consensus of 2 independent observers, blinded for the study endpoint.

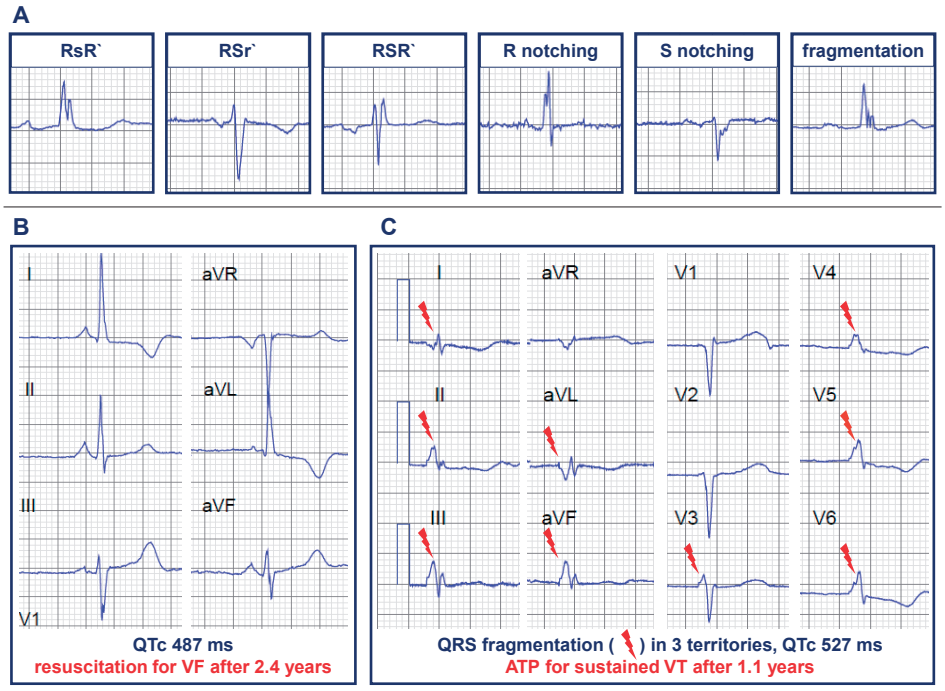

Figure 7.1
Baseline electrocardiographic abnormalities: QRS fragmentation and QTc prolongation. Panel A: QRS fragmentation includes various RSR` patterns, notched R wave, notched S wave or presence of >1 additional R wave (fragmentation) in ≥2 beats per lead. (In)complete bundle branch block patients are excluded (see text for details). Panel B: Hypertrophic cardiomyopathy (HCM) patient with QTc prolongation. Of note, QRS fragmentation is also present in lead III (S notching). Panel C: QTc prolongation and extensive QRS fragmentation in the inferior (II,III,aVF), lateral (I,V6,aVL) and anterior (V3,V4,V5) territories in a HCM patient. ATP: antitachycardia pacing, QTc: heart rate corrected QT duration, VF: ventricular fibrillation, VT: ventricular tachycardia.

Echocardiography

Standard 2-dimensional transthoracic echocardiography was performed with the patient in left lateral decubitus position using commercially available ultrasound machines (System-5, Vivid-7 and E9, GE-Vingmed, Milwaukee, WI) equipped with a 3.5 MHz transducer. ECG-triggered standard 2-dimensional gray-scale and color-Doppler images were acquired in cine-loop format and transferred to a workstation for off-line analysis (EchoPAC version 112, GE Medical Systems, Horten, Norway). Cardiac chamber quantification was performed in accordance with current recommendations.[23] Maximal LV wall thickness was assessed at end-diastole on the basal, mid or apical short-axis LV view. Simpson`s biplane method was applied to assess LV volumes that were indexed to body surface area and additionally used to calculate LV ejection fraction. Systolic anterior mitral leaflet motion was evaluated on M-mode acquisition in parasternal long-axis LV view. Mitral regurgitation was

semi-quantitatively graded as trivial (grade 1), mild (grade 2), moderate (grade 3) or severe (grade 4), according to current recommendations.[24] Finally, presence of intraventricular or LV outflow tract gradient at rest was evaluated by pulsed-wave Doppler on the apical long-axis view and peak gradient was measured on continuous wave Doppler recordings.

ICD implantation and settings

Transvenous approach was used for implantation of all defibrillator devices (Boston Scientific [Natick, MA, USA, formerly CPI, Guidant (St Paul, MN, USA)], Biotronik (Berlin, Germany), St Jude Medical/Ventritex (St Paul, MN, USA) and Medtronic (Minneapolis, MN, USA). The antitachycardia modus was set in all devices using 3 consecutive zones with slightly varying limits per manufacturer: a monitor zone (150-155 to 185-190 bpm), an antitachycardia pacing (ATP) shock zone (185-190 to 205-210 bpm), and an initial shock zone (≥205-210 bpm). In the monitor zone no therapy was programmed, unless during follow-up VTA was detected. An initial attempt to terminate arrhythmias by two ATP bursts was programmed in the ATP-shock zone, however, defibrillator shocks were fired if arrhythmia persisted. Shocks were the initial therapy for VTA with higher rate than the ATP shock zone. ICD device interrogation was regularly performed every 3 to 6 months after implantation.

Study endpoint

The primary endpoint of the study included occurrence of malignant VTA or SCD, whichever occurred first. VTA was defined as sustained ventricular tachycardia or fibrillation documented on ECG or by appropriate ICD therapies (shock/ATP) for VTA in patients with an ICD. SCD was defined as (unexpected) death of a HCM patient inside or outside a hospital due to any cardiac cause within 1 hour of onset of symptoms (if documented).[25] Deaths and cause of death were assessed by evaluating the official Dutch National Survival Registry, patients` clinical files and by direct communication with general practitioners.

Statistical analysis

According to distribution, continuous data were expressed as mean ± standard deviation or median ± interquartile range and compared between groups by Student-T test and Mann-Whitney U test, respectively. Categorical data were presented as percentages and compared with χ^2 or Fisher-exact test, as appropriate. A receiver operating curve (ROC) was constructed to derive a cut-off value for QTc with cut-point maximizing sum of sensitivity and specificity for prediction of the study endpoint. The cumulative survival free of VTA/SCD was evaluated

with Kaplan-Meier curve analysis. Patients were dichotomized according to the QTc duration cut-off and presence of fQRS in <3 vs ≥3 territories, and compared by log-rank test. Sensitivity, specificity, positive and negative predictive value for the study endpoint of these dichotomized ECG criteria were calculated. Among the various clinical, ECG and echocardiographic variables, the independent correlates of VTA/SCD were evaluated with multivariate Cox proportional hazard ratios. Variables showing a p-value <0.05 in univariate analysis were entered in multivariate Cox regression analysis. Finally, the likelihood ratio test was applied to explore the incremental value of QTc duration and fQRS on top of conventional SCD risk factors to predict the occurrence of VTA/SCD. Statistical analysis was performed using SPSS version 20.0. (SPSS Inc., Chicago, Illinois). All tests were two-sided and a p-value of <0.05 was considered statistically significant.

RESULTS

Patient population

A total of 195 HCM patients (mean age 52 ± 13 years, 61% male) were included. Baseline clinical, echocardiograhic characteristics and SCD risk profile are summarized in Table 1. The overall HCM population had a median LV wall thickness of 21 mm (IQR: 18-24 mm), small ventricular cavity and preserved LV ejection fraction. Only a minority of patients (n=58, 30%) had an ICD at baseline, of which 13 (22%) were for secondary prevention reasons (survived sustained VTA).

Primary prevention ICD implantation was performed, in accordance to current guidelines, if ≥1 conventional SCD risk factor(s) was present (n=43).[21] ICD implantation in patients without SCD risk factors was performed in one patient with total atrio-ventricular conduction block and in one patient due to induction of ventricular fibrillation during electrophysiological study. Few patients (n=16) had prior septal alcohol ablation for symptomatic drug refractory LV obstruction.

Study endpoint

A total of 26 out of 195 patients (13.3%) experienced VTA/SCD after a median follow-up of 5.7 years (IQR 2.7-9.1). In particular 10 out of 137 patients without ICD (7%) reached the endpoint, consisting of sustained ventricular tachycardia (n=4), ventricular fibrillation (n=2) and SCD (n=4). Of note, at that time point these patients did not fulfill criteria for primary prevention ICD implantation. Additionally in 16 out of 58 baseline ICD recipients (28%) appropriate ICD therapy occurred with a total of 9 ATP and 7 shocks.

Table 7.1
Baseline clinical and echocardiographic characteristics of the overall patient population and divided according to the study endpoint.

	Overall cohort (n 195)	No VTA/SCD (n 169)	VTA/SCD (n 26)	p value*
Clinical				
Age, years	52 ± 13	52 ± 13	50 ± 10	0.51
BSA, m^2	2.02 ± 0.2	2.02 ± 0.2	2.01 ± 0.2	0.91
Male, n (%)	119 (61)	99 (59)	20 (77)	0.07
Sinus rhythm, n (%)	171 (88)	147 (87)	24 (92)	0.44
Heart rate, bpm	69 ± 14	69 ± 14	72 ± 14	0.32
Arterial hypertension, n (%)	69 (35)	63 (37)	6 (23)	0.09
β-blocker use, n (%)	69 (35)	59 (35)	10 (38)	0.91
Previous MI, n (%)	8 (5)	7 (4)	1 (4)	1.00
Echocardiography				
Max wall thickness, mm	21 (18-24)	21 (18-24)	23 (20-26)	0.15
LVEDVI, ml/m^2	50 (41-59)	49 (39-59)	53 (44-65)	0.28
LVESVI, ml/m^2	16 (11-20)	16 (11-20)	19 (14-25)	0.28
LVEF, %	69 (63-73)	69 (63-73)	66 (55-71)	0.05
SAM of mitral valve, n (%)	75 (38)	66 (39)	9 (35)	0.63
MR grade, (0-4/4)	1.11 ± 0.7	1.07 ± 0.8	1.15 ± 0.7	0.74
IVPG rest ≥30 mmHg, n (%)	37 (19)	33 (20)	4 (15)	1.00
HCM risk profile				
Max wall thickness ≥ 30 mm, n (%)	20 (10)	19 (11)	1 (4)	0.48
Family Hx SCD, n (%/175)	91 (52)	78 (51)	13 (59)	0.48
Non-sustained VT, n (%/189)	52 (28)	39 (24)	13 (50)	0.006
Unexplained syncope, n (%/193)	17 (9)	9 (5)	8 (31)	<0.001
ICD at baseline, n (%)	58 (30)	42 (25)	16 (62)	<0.001
Secondary prevention ICD, n (%/58)	13 (22)	10 (24)	3 (19)	1.00
Prior septal alcohol ablation, n (%)	16 (8)	14 (8)	2 (8)	1.00

BSA: body surface area (Mosteller formula), EDVI, end-diastolic volume indexed to BSA, EF: ejection fraction, ESVI: end-systolic volume indexed to BSA, Hx: history, ICD: implantable cardioverter defibrillator, IVPG: intra ventricular pressure gradient, LV: left ventricular, Max: maximal, MI: myocardial infarction, SAM: systolic anterior movement, SCD: sudden cardiac death, VT: ventricular tachycardia, VTA: ventricular tachyarrhythmia, *: for comparison of VTA/SCD versus no VTA/SCD group

QTc and fQRS

Data on fQRS and for QTc duration on ECG are listed in Table 2. Mean QTc duration in the overall study population was 427 ± 28 ms. QTc duration ≥460 ms comprised highest sum of sensitivity (31%) and specificity (89%) for prediction of the study endpoint (area under curve 0.61 on ROC analysis). Significant QTc prolongation ≥460 ms was noted in a total of 26 out of 195 HCM patients (13%). The vast majority of HCM patients (n=181, 93%) displayed a fQRS in at least one ECG

lead with a median of 4 leads affected per patient. A total of 145 patients (75%) exhibited a fQRS in ≥1 ECG territory. Leads III, aVF and aVL were the most affected in 69%, 62% and 52% of cases, respectively. Leads V4, V3 and V1 were the least affected in only 13%, 16% and 21% of patients, respectively. fQRS was most commonly observed in the inferior territory (61%), followed by the lateral (31%), anterior (13%) and septal territories (11%). Presence of fQRS in ≥3 territories was noted in 15 out of 195 (8%) of patients.

Table 7.2
Baseline electrocardiographic characteristics of the overall patient population and divided according to the study endpoint.

QRS	Overall (n 195)	No VTA/SCD (n 169)	VTA/SCD (n 26)	p value*
Duration, ms	97 ± 12	97 ± 12	99 ± 13	0.30
Fragmentation, n (%)				
≥ 1 lead	181 (93)	156 (92)	25 (96)	0.70
Inferior territory	118 (61)	101 (60)	17 (65)	0.56
Lead II	85 (44)	73 (43)	12 (46)	0.78
Lead III	135 (69)	114 (67)	21 (81)	0.17
Lead aVF	121 (62)	105 (62)	16 (62)	0.95
Lateral territory	60 (31)	48 (28)	12 (46)	0.07
Lead I	50 (26)	40 (24)	10 (38)	0.11
Lead aVL	102 (52)	86 (51)	16 (62)	0.31
Lead V6	55 (28)	47 (28)	8 (31)	0.76
Septal territory	22 (11)	17 (10)	5 (19)	0.17
Lead V1	41 (21)	85 (21)	6 (23)	0.78
Lead V2	42 (25)	36 (21)	6 (23)	0.84
Anterior territory	22 (13)	16 (9)	6 (23)	0.04
Lead V3	32 (16)	28 (17)	4 (15)	1.00
Lead V4	26 (13)	21 (12)	5 (19)	0.34
Lead V5	42 (25)	33 (20)	9 (35)	0.08
Number of leads	4 (2-5)	4 (2-5)	4 (3-6)	0.53
≥ 3 territories	15 (8)	10 (6)	5 (19)	0.02
QTc				
Duration, ms	427 ± 28	425 ± 25	440 ± 34	0.01
≥460 ms, n (%)	26 (13)	18 (11)	8 (31)	0.01

QTc: heart rate corrected QT duration, SCD: sudden cardiac death, VTA: ventricular tachyarrhythmia, * p value for comparison of no VTA/SCD versus VTA/SCD group.

HCM patients with versus without study endpoint

The patient population was dichotomized based on the occurrence (n=26, 13.3%) or absence (n=169, 86.7%) of the study endpoint (VTA/SCD). These 2 groups showed similar clinical and conventional echocardiographic characteristics, as summarized in Table 1. Patients with VTA/SCD, however, showed higher baseline HCM SCD risk profile, evidenced by higher prevalence of non-sustained ventricular tachycardia (50% versus 24%, p=0.006) and prior unexplained syncope (31% versus 5%, p<0.001).

Concerning baseline ECG characteristics (Table 2), mean QTc duration was longer in patients with VTA/SCD versus patients without (440 ± 34 ms versus 425 ± 25 ms, p=0.01) and a higher percentage of patients with VTA/SCD showed a QTc duration ≥460 ms as compared to their counterparts (31% versus 11%, p=0.01; Figure 2). No significant difference between patients with versus without VTA/SCD was observed for the presence of fQRS in any individual lead, the median number of leads with fQRS, nor the territory affected by fQRS, except for the anterior territory (23% versus 9%, p=0.04). Interestingly, the prevalence of fQRS in ≥3 territories was higher in subjects with VTA/SCD (19% versus 6%, p=0.03; Figure 2).

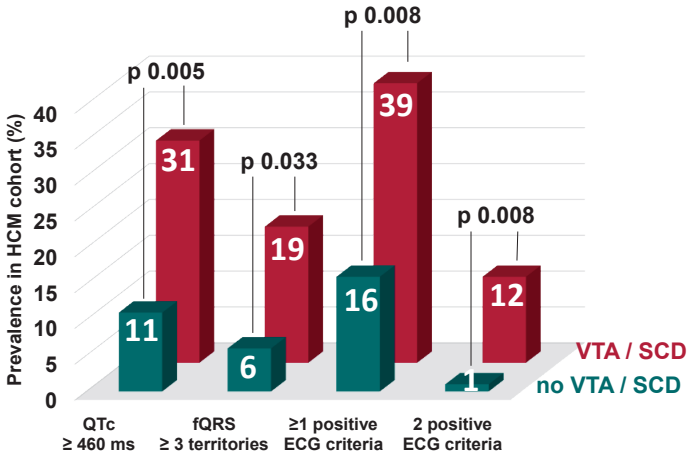

Figure 7.2
Prevalence of novel electrocardiographic criteria in relation to the study endpoint. HCM: hypertrophic cardiomyopathy, fQRS: presence of QRS fragmentation, QTc: heart rate corrected QT duration, SCD: sudden cardiac death, VTA: ventricular tachyarrhytmia. Positive criteria: presence of QTc ≥460 ms, fQRS ≥3 territories.

QTc duration, fQRS and the study endpoint

The cumulative survival free of VTA/SCD was worse in patients with a QTc duration ≥460 vs <460 ms (p=0.009) or fQRS in ≥3 vs <3 territories (p=0.004). (Figure 3). As shown in Table 3, presence of QTc ≥460 ms has a positive predictive value for

occurrence of VTA/SCD of 31%, comparable to 33% if presence of fQRS ≥3 territories. When both ECG criteria co-exist in one patient, a high positive predictive value of 75% is noted, yielding low sensitivity, however. As shown in Table 4, QTc duration ≥460 ms, fQRS in ≥3 territories, non-sustained ventricular tachycardia and unexplained syncope were univariate correlates of VTA/SCD. Of note, other conventional SCD risk factors, secondary prevention ICD indication and prior septal alcohol ablation were not significantly associated with the study endpoint. In the multivariate analysis, both QTc duration ≥460 ms and fQRS in ≥3 territories remained independently related to VTA/SCD, in addition to non-sustained ventricular tachycardia and unexplained syncope (Table 4).

Moreover, excluding secondary prevention ICD recipients (n=13), likelihood ratio test indicated that assessment of both ECG parameters, QTc duration ≥460 ms and fQRS in ≥3 territories, provided incremental value over conventional SCD risk factors to predict occurrence of VTA/SCD (p=0.035; Figure 4).

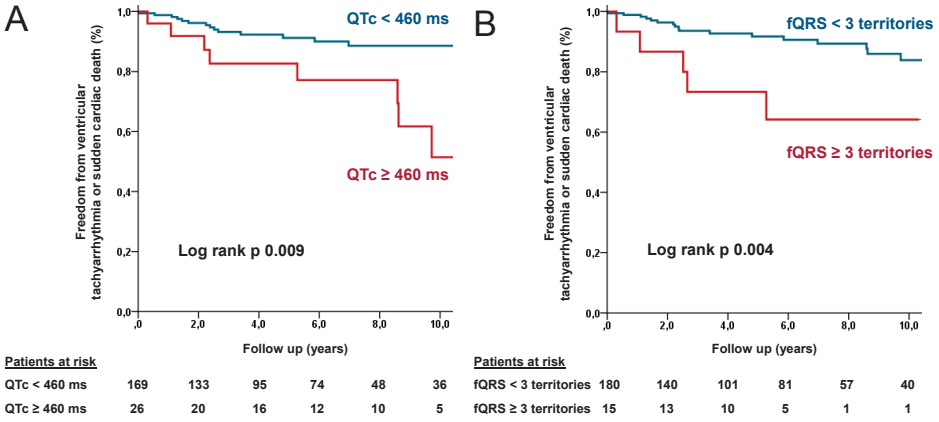

Figure 7.3
Cumulative survival free of ventricular tachyarrhythmia or sudden cardiac death according to novel electrocardiographic criteria. fQRS: presence of QRS fragmentation, QTc: heart rate corrected QT duration.

Table 7.3
Sensitivity, specificity, positive and negative predictive value of novel ECG criteria for prediction of ventricular tachyarrhythmia or sudden cardiac death.

	Sensitivity %	Specificity %	NPV %	PPV %
QTc ≥460 ms	31	89	89	31
fQRS ≥3 territories	19	94	88	33
QTc ≥460 ms AND fQRS ≥3 territories	12	99	80	75

fQRS: presence of QRS fragmentation, NPV: negative predictive value, PPV: positive predictive value

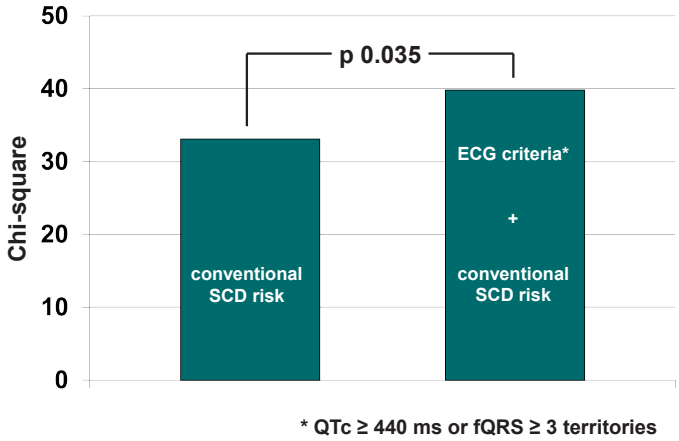

Figure 7.4
Likelihood ratio test to predict occurence of ventricular tachyarrhythmia or sudden cardiac death. Excluding secondary prevention ICD recipients (n=13), assessment of the novel electrocardiographic (ECG) criteria on top of conventional sudden cardiac death (SCD) risk factors (see main text for details) in the remaining HCM patients yields incremental value to predict occurrence of ventricular tachyarrhythmia or sudden cardiac death. fQRS: QRS fragmentation, QTc: heart rate corrected QT duration.

Table 7.4
Univariate and multivariate Cox regression analysis for the study endpoint.

	univariate			multivariate		
	HR	p value	95% CI	HR	p value	95% CI
Age, years	1.0	0.638	0.98-1.04			
Male gender	2.0	0.140	0.80-4.96			
β-blocker use	1.1	0.807	0.49-2.50			
LVEF, per %	0.96	0.081	0.93-1.01			
Max wall thickness ≥ 30 mm	3.6	0.209	0.49-26.6			
Family Hx SCD	1.4	0.397	0.62-3.40			
Non-sustained VT	2.5	0.019	1.16-5.45	3.3	0.005	1.42-7.48
Unexplained syncope	5.6	<0.001	2.41-13.5	4.7	0.002	1.95-11.7
Secondary prevention ICD	1.7	0.217	0.73-4.00			
fQRS ≥3 territories	4.0	0.008	1.44-10.9	4.5	0.020	1.41-14.1
QTc ≥460 ms	2.9	0.013	1.25-6.62	2.7	0.037	1.12-6.33

CI: confidence interval, fQRS: presence of QRS fragmentation, HR: hazard ratio, other abbreviations: see table 1 and 2

DISCUSSION

The main findings of this study are 1) fQRS in ≥3 territories and QTc prolongation ≥460 ms are easily identifiable surface ECG markers which are prevalent in 8% and 13% respectively of clinical HCM patients without (in)complete bundle branch

block and 2) both parameters are independently associated with VTA and SCD in this HCM population (with almost 50% at relatively low-risk), showing incremental predictive value over conventional SCD risk factors for primary prevention.

Most HCM patients have a benign course reflected by a 1% annual risk of presumed arrhythmic SCD in non-selected cases.[1] Identification of the subset of HCM patients at high-risk for SCD, however, remains a clinical challenge. Various SCD risk factors, including personal history of cardiac arrest, massive LV hypertrophy, family history of SCD, presence of non-sustained ventricular tachycardia and unexplained syncope have been identified.[21] Although ICD therapy in HCM patients at high risk for SCD based on these risk factors undoubtly remains a treatment cornerstone, the robustness of evidence supporting these risk factors is variable and in particular risk factors for primary prevention are limited by low positive predictive value (between 10% and 20%).[21, 26] Therefore improvement of risk prediction in HCM remains an unmet clinical need.[27] Although the vast majority of HCM patients show abnormal ECG findings, no specific ECG abnormality has been validated for risk stratification so far.[3, 28, 29] This study indicated that the presence of fQRS in ≥3 territories or QTc ≥460 ms on baseline ECG were independently associated with VTA or SCD.

fQRS in HCM

In ischemic and non-ischemic dilated cardiomyopathy patients, fQRS has been related to fibrosis and represents a strong prognostic marker for VTA and/or mortality.[6-8, 30]

Th e origin of fQRS on ECG in HCM patients is poorly studied. Recently, in a study including 82 HCM patients, detection of fQRS was reported to predict presence of fibrosis identified on DE-CMR, yielding a positive and negative predictive value of 86% and 68% respectively.[31] In addition, the ECG lead territory displaying fQRS correlated with the myocardial region where fibrosis was detected. In this study 75% of HCM patients displayed fQRS in ≥1 ECG territory, with the inferior territory most often affected. These findings are in line with previous reports, indicating presence of fibrosis on DE-CMR in up to 80% of HCM patients, with small amounts of fibrosis often detected in the inferior region at the conjunction with the right ventricle.[32, 33] However, apart from local fibrosis (scar), it should be considered that fQRS in HCM may also stem from tissue heterogeneity such as myofiber disarray, interstitial (diffuse) fibrosis or functional rather than structural (scar) modulation of conduction, as suggested in other channelopathies (such as Brugada syndrome).[9] Therefore fQRS in HCM patients may not necessarily relate focal fibrosis, as assessed by DE-CMR imaging.

The potential clinical value of fQRS on ECG in HCM to predict malignant VTA or SCD was suggested previously.[34] Recently, a study involving 179 HCM subjects showed that presence of paced ventricular ECG fractionation during electrophysiologic testing was predictive of SCD.[35] Only one study so far by Kang et al., comprising 167 relatively low-risk HCM patients without BBB (no ICD recipients, but presence of ≥1 conventional SCD risk factors in 42%), reported that presence of fQRS (in particular in the inferior leads) on surface ECG independently of conventional SCD risk factors related to occurrence of VTA/SCD during follow-up.[11] The present study demonstrated that fQRS in ≥3 territories in HCM was independently associated with a nearly 5-fold increased risk for VTA or SCD, suggesting that the extent of fibrosis rather than its presence is related to adverse cardiac outcome, in line with previous reports in HCM patients using delayed-enhancement CMR (DE-CMR) to identify fibrosis.[33, 36] The fact that presence of ≥3 territories was required to relate to VTA/SCD in our study compared to ≥1 territory (in particular the inferior territory) in the report of Kang et al., might also be attributed to the use of more sensitive ECG settings by default in our centre, which allows for more sensitive detection of fQRS (0.05-300 Hz vs. 0.15-100 Hz filter range).[11] Similar to our report, Kang et al. also pointed out higher predictive value for VTA/SCD when adding fQRS to conventional SCD risk factors.[11]

fQRS in HCM patients, likely representing (local or diffuse) fibrosis and/or tissue heterogeneity, may reflect the vulnerable structural substrate that is a prerequisite for occurrence of re-entry VTA that occurs if appropriate triggers coincide.

QTc in HCM

The QT interval, comprising the interval between QRS onset and end of the T wave, mainly reflects myocardial repolarization. QTc prolongation in HCM patients is consistently reported.[14, 15, 19, 20] In our large cohort of 195 HCM subjects, QTc prolongation defined as a duration ≥460 ms had a prevalence of 13%. In HCM patients QTc prolongation has been, although weakly, related to extent of LV maximal wall thickness, LV outflow tract obstruction, underlying causative mutation (potentially affecting sodium or potassium ion channels related to depolarization and repolarization) and even sympathetic tone differences.[4, 14, 15, 20, 37] Furthermore, the presence of fibrosis, myofiber disarray and/or (microvascular) ischemia might be other determinants of QTc in this patient population.

QTc duration has prognostic value in predicting occurrence of VTA or SCD in patients with congenital or acquired long QT.[12, 13] In the present study a QTc duration ≥460 ms was significantly associated with a nearly 3-fold increased risk for VTA or SCD. QTc duration ≥460 ms was independently associated with VTA/SCD and was incremental to conventional SCD risk factors in predicting its occurrence.[21]

Recently Gray et al., in a group of 164 high-risk HCM patients, all ICD recipients, showed that QTc duration ≥439 ms independently of presence of conventional risk factors predicts appropriate ICD therapies, yielding a more than 3-fold risk increase.[20] QTc prolongation, comparable to numbers reported in our lower risk profile HCM patients, was 2 times more frequent in patients that received versus did not experience appropriate ICD therapy, up to 79% versus 40% respectively.[20] Longer QTc duration in patients with history of SCD or SCD during follow-up was also noted in a study by Baranowski et al., including a group of 26 HCM subjects.[18] Sherrid et al. in a study involving 330 HCM ICD recipients did not find a significant difference in QTc duration between subjects with appropriate versus no ICD discharge.[29] However, this study did not exclude QTc duration confounders such as intake of QTc prolonging drugs or bundle branch block, had shorter follow-up time compared to our study and to that of Gray et al., and focused on high-risk HCM patients with ICD only.[20] A QTc duration ≥480 ms in a subgroup analysis of 90 out of 479 HCM patients was not able to discriminate between subjects with and without appropriate ICD discharge, but again involved exclusively high-risk HCM patients without excluding patients with BBB.[14]

The exact mechanism of VTA or SCD in HCM patients with prolonged QTc remains speculative, but may involve early after depolarizations due to prolonged ventricular repolarization which can lead to re-entry and provoke torsades de pointes. Another potential mechanism is depolarization abnormality, including fQRS, offering a substrate for maintaining the re-entry circuit after initiation of torsades de pointes.[38]

Clinical implications

The current study suggests that surface ECG may be of clinical value for management and decision-making in selected HCM patients. Conventional SCD risk factors have only moderate PPV about 10 to 20%, particularly when applied for primary prevention.[39] We indicated that PPV of both novel ECG criteria for VTA/SCD is above 30% and is of incremental predictive value when applied in primary prevention HCM patients. Therefore presence of fQRS or QTc prolongation in fact might serve as an easy to obtain additional SCD risk marker on top of conventional risk parameters and help to optimize selection of candidates for prophylactic ICD implantation. Nevertheless, appropriate ICD therapy does not entirely correspond to SCD events and thus further prospective validation in larger HCM patient cohorts is needed to confirm these findings. In addition, given the prognostic impact of QTc duration in HCM patients, the current study underlines the clinical importance of measuring QTc duration in HCM patients and suggests a restrictive approach when considering administration of drugs that may prolong QTc duration

or careful monitoring of QTc duration if drug initiation is deemed to be necessary in this population.

Limitations

Some limitations to this study need consideration. First, high ECG filter settings allow high sensitivity to detect ECG abnormalities but imply a risk of over-diagnosing fQRS which cannot be excluded in the current study. Second, although a potential mechanistic link between fQRS and myocardial fibrosis (as assessed by DE-CMR) has been previously suggested in HCM patients, this evaluation was not performed in this study cohort due to absence of systematic CMR data at the time of ECG. Although validation of equating true fractionation with a local conduction abnormality such as r-prime is lacking, the definition of QRS fragmentation applied in present analysis is similar to the study of Das et al, demonstrating the link between scar due to myocardial infarction and fQRS in patients with coronary artery disease.[5] Third, our findings were observed in a relatively low-risk HCM population (only 30% ICD recipients and 48% without family history of SCD) in the absence of BBB or QTc prolonging drugs and therefore can-not be extrapolated to other subsets of HCM patients. Four, appropriate ICD therapy should not be regarded as a full surrogate of SCD as it tends to overestimate historical mortality in HCM. Fifth, the absolute number of events was typically low despite a moderately sized HCM study cohort. Finally, as ICD recipients have continued rhythm monitoring, the occurrence of VTA events is potentially biased in favor of these patients. Due to these limitations, this study should be regarded as hypothesis generating.

CONCLUSION

Extensive QRS fragmentation and QTc prolongation in clinical HCM patients are independently associated with VTA and/or SCD in this cohort of HCM patients (48% at relatively low-risk). Both parameters are incremental to conventional SCD risk factors. These findings suggest that baseline ECG, widely available at low cost, might be valuable for risk-stratification and management of HCM patients.

REFERENCES

1. Maron BJ, Maron MS. Hypertrophic cardiomyopathy. *Lancet.* 2012;381:242-255.
2. Dumont CA, Monserrat L, Soler R et al. Interpretation of electrocardiographic abnormalities in hypertrophic cardiomyopathy with cardiac magnetic resonance. *Eur Heart J.* 2006; 27:1725-1731.
3. Maron BJ. Hypertrophic cardiomyopathy: a systematic review. *JAMA.* 2002; 287:1308-1320.
4. Delcre SD, Di Donna P, Leuzzi S et al. Relationship of ECG findings to phenotypic expression in patients with hypertrophic cardiomyopathy: a cardiac magnetic resonance study. *Int J Cardiol.* 2013; 167:1038-1045.
5. Das MK, Khan B, Jacob S et al. Significance of a fragmented QRS complex versus a Q wave in patients with coronary artery disease. *Circulation.* 2006; 113:2495-2501.
6. Das MK, Suradi H, Maskoun W et al. Fragmented wide QRS on a 12-lead ECG: a sign of myocardial scar and poor prognosis. *Circ Arrhythm Electrophysiol.* 2008; 1:258-268.
7. Basaran Y, Tigen K, Karaahmet T et al. Fragmented QRS complexes are associated with cardiac fibrosis and significant intraventricular systolic dyssynchrony in nonischemic dilated cardiomyopathy patients with a narrow QRS interval. *Echocardiography.* 2011; 28:62-68.
8. Das MK, Maskoun W, Shen C et al. Fragmented QRS on twelve-lead electrocardiogram predicts arrhythmic events in patients with ischemic and nonischemic cardiomyopathy. *Heart Rhythm.* 2010; 7:74-80.
9. Morita H, Kusano KF, Miura D et al. Fragmented QRS as a marker of conduction abnormality and a predictor of prognosis of Brugada syndrome. *Circulation.* 2008; 118:1697-1704.
10. Peters S, Trummel M, Koehler B. QRS fragmentation in standard ECG as a diagnostic marker of arrhythmogenic right ventricular dysplasia-cardiomyopathy. *Heart Rhythm.* 2008; 5:1417-1421.
11. Kang KW, Janardhan AH, Jung KT et al. Fragmented QRS as a candidate marker for high-risk assessment in hypertrophic cardiomyopathy. *Heart Rhythm.* 2014 Aug 11(8): 1433-1440.
12. Goldenberg I, Moss AJ. Long QT syndrome. *J Am Coll Cardiol.* 2008; 51:2291-2300.
13. Straus SM, Kors JA, De Bruin ML et al. Prolonged QTc interval and risk of sudden cardiac death in a population of older adults. *J Am Coll Cardiol.* 2006; 47:362-367.
14. Johnson JN, Grifoni C, Bos JM et al. Prevalence and clinical correlates of QT prolongation in patients with hypertrophic cardiomyopathy. *Eur Heart J.* 2011; 32:1114-1120.
15. Jouven X, Hagege A, Charron P et al. Relation between QT duration and maximal wall thickness in familial hypertrophic cardiomyopathy. *Heart.* 2002; 88:153-157.
16. Martin AB, Garson A, Jr., Perry JC. Prolonged QT interval in hypertrophic and dilated cardiomyopathy in children. *Am Heart J.* 1994; 127:64-70.
17. Yetman AT, Hamilton RM, Benson LN et al. Long-term outcome and prognostic determinants in children with hypertrophic cardiomyopathy. *J Am Coll Cardiol.* 1998; 32:1943-1950.
18. Baranowski R, Chojnowska L, Michalak E et al. Analysis of the corrected QT before the onset of nonsustained ventricular tachycardia in patients with hypertrophic cardiomyopathy. *Pacing Clin Electrophysiol.* 2003; 26:387-389.
19. Yi G, Elliott P, McKenna WJ, Prasad K et al. QT dispersion and risk factors for sudden cardiac death in patients with hypertrophic cardiomyopathy. *Am J Cardiol.* 1998; 82:1514-1519.
20. Gray B, Ingles J, Medi C, Semsarian C. Prolongation of the QTc Interval Predicts Appropriate Implantable Cardioverter-Defibrillator Therapies in Hypertrophic Cardiomyopathy. *JACC Heart Fail.* 2013; 1:149-155.

21. Gersh BJ, Maron BJ, Bonow RO et al. 2011 ACCF/AHA Guideline for the Diagnosis and Treatment of Hypertrophic Cardiomyopathy: a report of the American College of Cardiology Foundation/American Heart Association Task Force on Practice Guidelines. *J Am Coll Cardiol*. 2011; 58:e212-260.
22. Surawicz B, Childers R, Deal BJ et al. AHA/ACCF/HRS recommendations for the standardization and interpretation of the electrocardiogram: part III: intraventricular conduction disturbances: a scientific statement from the American Heart Association Electrocardiography and Arrhythmias Committee, Council on Clinical Cardiology; the American College of Cardiology Foundation; and the Heart Rhythm Society. Endorsed by the International Society for Computerized Electrocardiology. *J Am Coll Cardiol*. 2009; 53:976-981.
23. Lang RM, Bierig M, Devereux RB et al. Chamber Quantification Writing Group, American Society of Echocardiography's Guidelines, Standards Committee, European Association of Echocardiography. Recommendations for chamber quantification: a report from the American Society of Echocardiography's Guidelines and Standards Committee and the Chamber Quantification Writing Group, developed in conjunction with the European Association of Echocardiography, a branch of the European Society of Cardiology. *J Am Soc Echocardiogr*. 2005; 18:1440-1463.
24. Zoghbi WA, Enriquez-Sarano M, Foster E et al. American Society of Echocardiography. Recommendations for evaluation of the severity of native valvular regurgitation with two-dimensional and Doppler echocardiography. *J Am Soc Echocardiogr*. 2003; 16:777-802.
25. Goldberger JJ, Cain ME, Hohnloser SH et al. AHA/ACCF/HRS scientific statement on noninvasive risk stratification techniques for identifying patients at risk for sudden cardiac death: a scientific statement from the American Heart Association Council on Clinical Cardiology Committee on Electrocardiography and Arrhythmias and Council on Epidemiology and Prevention. *Circulation*. 2008; 118:1497-1518.
26. Maron BJ, Spirito P, Shen WK et al. Implantable cardioverter-defibrillators and prevention of sudden cardiac death in hypertrophic cardiomyopathy. *JAMA*. 2007; 298:405-412.
27. O'Mahony C, Jichi F, Pavlou M et al. A novel clinical risk prediction model for sudden cardiac death in hypertrophic cardiomyopathy (HCM Risk-SCD). *Eur Heart J*. 2014; 35:2010-2020.
28. Bongioanni S, Bianchi F, Migliardi A et al. Relation of QRS duration to mortality in a community-based cohort with hypertrophic cardiomyopathy. *Am J Cardiol*. 2007; 100:503-506.
29. Sherrid MV, Cotiga D, Hart D et al. Relation of 12-lead electrocardiogram patterns to implanted defibrillator-terminated ventricular tachyarrhythmias in hypertrophic cardiomyopathy. *Am J Cardiol*. 2009; 104:1722-1726.
30. Das MK, Saha C, El Masry H et al. Fragmented QRS on a 12-lead ECG: a predictor of mortality and cardiac events in patients with coronary artery disease. *Heart Rhythm*. 2007; 4:1385-1392.
31. Sheikh N, Papadakis M, Bastiaenen R et al. Fragmented QRS: a predictor of myocardial fibrosis in hypertrophic cardiomyopathy. *J Am Coll Cardiol*. 2012; 59: E1584-E1584.
32. Choudhury L, Mahrholdt H, Wagner A et al. Myocardial scarring in asymptomatic or mildly symptomatic patients with hypertrophic cardiomyopathy. *J Am Coll Cardiol*. 2002; 40:2156-2164.
33. Moon JC, McKenna WJ, McCrohon JA et al. Toward clinical risk assessment in hypertrophic cardiomyopathy with gadolinium cardiovascular magnetic resonance. *J Am Coll Cardiol*. 2003; 41:1561-1567.

34. Femenia F, Arce M, Arrieta M et al. Surface fragmented QRS in a patient with hypertrophic cardiomyopathy and malignant arrhythmias: Is there an association? *J Cardiovasc Dis Res.* 2012; 3:32-35.
35. Saumarez RC, Pytkowski M, Sterlinski M et al. Paced ventricular electrogram fractionation predicts sudden cardiac death in hypertrophic cardiomyopathy. *Eur Heart J.* 2008; 29:1653-1661.
36. O'Hanlon R, Grasso A, Roughton M et al. Prognostic significance of myocardial fibrosis in hypertrophic cardiomyopathy. *J Am Coll Cardiol.* 2010; 56:867-874.
37. Yanagisawa-Miwa A, Inoue H, Sugimoto T. Diurnal change in QT intervals in dilated cardiomyopathy and hypertrophic cardiomyopathy. *Am J Cardiol.* 1991; 67:1428-1430.
38. Haraoka K, Morita H, Saito Y et al. Fragmented QRS is associated with torsades de pointes in patients with acquired long QT syndrome. *Heart Rhythm.* 2010; 7:1808-1814.
39. Gersh BJ, Maron BJ, Bonow RO et al. 2011 ACCF/AHA guideline for the diagnosis and treatment of hypertrophic cardiomyopathy: a report of the American College of Cardiology Foundation/American Heart Association Task Force on Practice Guidelines. *Circulation.* 2011; 124:e783-831.

Chapter 8

Potential role of fibrosis imaging in severe valvular heart disease

Philippe Debonnaire, Jeroen J Bax, Victoria Delgado

Heart, 2015 Mar 101(5): 397-407.

ABSTRACT

The increasing burden of valvular heart disease (predominantly aortic stenosis and mitral regurgitation) parallels the ageing of the population. Timing of surgery in asymptomatic patients is controversial, and is currently considered in the presence of variables (such as reduced left ventricular ejection fraction, left ventricular dilatation, pulmonary hypertension, reduced exercise capacity, increased plasma levels of biomarkers and arrhythmias) that occur relatively late in the disease progression, with suboptimal outcome after surgery. Accordingly, early markers to guide therapeutic management are needed. In both aortic stenosis and mitral regurgitation, left ventricular fibrosis can be detected in the early stage of the disease and the extent of LV fibrosis may provide an early marker for disease severity. Currently, new non-invasive imaging technology is being developed that may permit direct or indirect assessment of left ventricular fibrosis; indirect assessment of left ventricular fibrosis refers mainly to sophisticated quantification of left ventricular function (which indirectly reflects left ventricular fibrosis extent). An overview of these non-invasive imaging techniques is provided in this article, and the potential role of early detection of left ventricular fibrosis in patients with aortic stenosis or mitral regurgitation is discussed.

KEY POINTS

1. In left-sided valvular heart disease, pressure overload (aortic stenosis) is more pro-fibrotic than volume overload (mitral regurgitation)
2. Fibrosis causes adverse left ventricular remodeling, functional impairment and is associated with poor clinical outcome
3. Non-invasive imaging techniques to assess direct left ventricular fibrosis include:
   - o Contrast-enhanced cardiac magnetic resonance:
     - § Focal (replacement) fibrosis
   - o T1-weighted cardiac magnetic resonance:
     - § Diffuse fibrosis: T1-mapping, extracellular volume (ECV)
   - o Echocardiographic calibrated integrated backscatter
   - o Molecular imaging:
     - § Collagen-targeted agents with cardiac magnetic resonance
     - § Radiolabelled angiotensin converting enzyme inhibitors and angiotensin receptors antagonists with single photon emission computed tomography or positron emission tomography
4. Non-invasive imaging techniques to assess indirect left ventricular fibrosis include:
   - o Strain and strain rate imaging:
     - § Tissue Doppler imaging
     - § Speckle tracking echocardiography
     - § Tagged cardiac magnetic resonance
   - o Perfusable tissue fraction and index with positron emission tomography

INTRODUCTION

Currently, the most encountered valve diseases include aortic stenosis (AS) and mitral regurgitation (MR); data from population-based studies showed that approximately 9% of individuals aged 65 years or more have either MR or AS.[1,w1] While indications for surgery are well-defined in symptomatic patients, the optimal timing of surgery in asymptomatic severe AS or MR remains controversial. Currently, surgical intervention is considered in the presence of reduced left ventricular ejection fraction (LVEF), left ventricular (LV) dilatation, pulmonary hypertension, reduced exercise capacity, increased plasma levels of biomarkers (e.g. NT-proBNP) and arrhythmias (e.g. atrial fibrillation), since all these variables are associated with worse prognosis if treated medically.[w2-w3] However, most of these variables are encountered only once AS or MR have progressed significantly, leading to suboptimal clinical outcomes after surgery.[w2-w3]

Accordingly, markers that could identify early structural and functional abnormalities of the LV are needed to potentially facilitate the decision for timing of surgery thereby improving clinical outcomes. In both AS and MR, ultra-structural changes of the LV with expansion of the extracellular matrix and fibrosis formation may occur due to pressure and volume overload, respectively.[w4-w5] Fibrosis causes increased LV stiffness, leading to diastolic dysfunction and subtle worsening of systolic function, whereas overt LV systolic dysfunction (reduced LVEF) will occur later in the course of AS and MR.

Focal fibrosis reflects scar tissue formation by replacement of dead myocardial cells by collagen, which is observed after myocardial infarction, for example. In valvular heart disease however, pressure or volume overload predominantly cause diffuse interstitial fibrosis, a distinct type of fibrosis.[w4-w6] This type of fibrosis increases the interstitial collagen without notable cell loss and therefore it may be (partially) reversible.[w6]

Recently, a rapid development in non-invasive imaging technology has occurred which may permit direct or indirect assessment of LV fibrosis. Particularly new cardiac magnetic resonance (CMR) techniques (with or without contrast agents) permit direct assessment of LV fibrosis, whereas strain imaging with advanced echocardiographic techniques or CMR can be used to detect subtle systolic LV dysfunction (while LVEF is still normal), which provides an indirect reflection of LV fibrosis. This article provides an overview of these non-invasive imaging techniques and the potential role for early detection of structural and functional LV abnormalities in patients with AS or MR. In Table 1, a summary is provided of direct and indirect imaging techniques for quantitative or qualitative fibrosis evaluation.[2] In the paragraphs below the different imaging techniques for fibrosis detection are discussed.

Table 1.
Non-invasive imaging modalities and techniques for left ventricular fibrosis assessment. Adapted with permission from Jellis et al. *J Am Coll Cardiol* 2010;56:89-97.

		Availability	Fibrosis specificity	Limitations	Experience in AS	Experience in MR
Echocardiography	IBS	++	+++	Modest reproducibility,	+	-
	TDI	++++	+	Angle dependent	++	++
	2D speckle tracking	++++	+	Vendor variability, Low frame rate	++++	++++
Cardiac Magnetic Resonance	Delayed- enhanced (replacement fibrosis)	++++	++	Focal fibrosis only	++++	-
	T1 weighted imaging (diffuse fibrosis)	++	+++	Many confounders, expertise, standardization	++	-
	Tissue tagging	+	+	Expertise	+	+
	Collagen-specific contrast	±	+++	Experimental	-	-
Nuclear Imaging	PET perfusable water index	++	+++	Radiation, expertise	-	-
	PET molecular imaging	±	+++	Radiation, expertise, experimental	-	-
	SPECT molecular imaging	±	+++	Radiation, expertise, experimental	-	-

AS: aortic stenosis, ECV: extracellular volume, IBS: integrated backscatter, PET: positron emission tomography, MR: mitral regurgitation, SPECT: single photon emission computed tomography, TDI: tissue Doppler imaging.

IMAGING TECHNIQUES FOR DIRECT ASSESSMENT OF LV FIBROSIS

1. Delayed contrast-enhanced cardiac magnetic resonance

Delayed contrast-enhanced cardiac magnetic resonance (CMR) has become the gold standard imaging technique to assess and quantify focal fibrosis in the left ventricle. Gadolinium chelates are extracellular contrast media that do not penetrate intact cell membranes and accumulate in the myocardial extracellular space. Several minutes after intravenous administration, the contrast agent is trapped into the expanded extracellular space and (after nullifying the signal of the myocardium), is visualized as increased signal intensity (white) compared to normal myocardium (black) (Figure 1).[3] However, detection of diffuse LV fibrosis with delayed contrast-enhanced CMR standard techniques may be difficult since this technique relies on relative signal differences between normal myocardium and interstitial collagen.

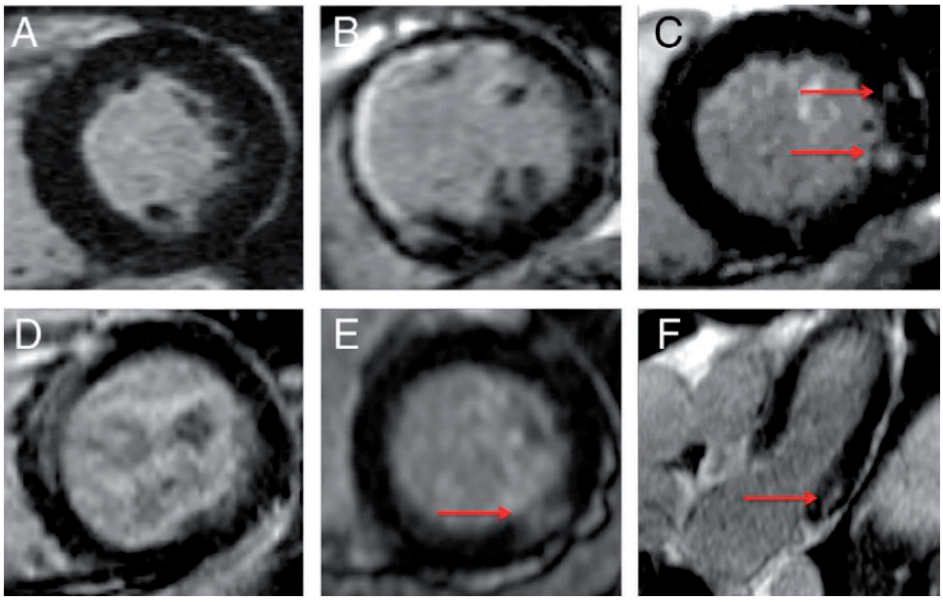

Figure 8.1
Delayed contrast-enhanced cardiac magnetic resonance patterns that can be observed in patients with severe aortic stenosis (AS). A. Absence of delayed enhancement. B. Anterior and septal sub-endocardial contrast-enhancement, similar to that noted in infarcted myocardium. C. Focal spots of contrast-enhancement in the lateral midwall (arrows). D. Linear septal midwall contrast-enhancement. E and F: Midwall contrast-enhancement of the lateral wall (arrows). With permission from Dweck et al. *J Am Coll Cardiol* 2011;58:1271-9.

2. T1 weighted cardiac magnetic resonance

For assessment of diffuse LV fibrosis, where there is no clear differentiation between normal and diseased myocardium, T1 weighted CMR imaging techniques are increasingly applied. T1 weighted techniques are based on the energy released by the tissue (protons) after applying radiofrequency pulses. This relaxation process follows an exponential formula that includes a time constant, the so-called T1 time. The shorter the T1 time constant is, the faster the relaxation process. T1 time can be assessed prior to (native T1) or after (post-contrast T1) contrast administration using a variety of possible techniques with multiple or single breath-holds (Figures 2 and 3).[4]

Normal native T1 values range between 900 and 1100 ms and increase in circumstances of increased density of protons (water content or edema).[4] The

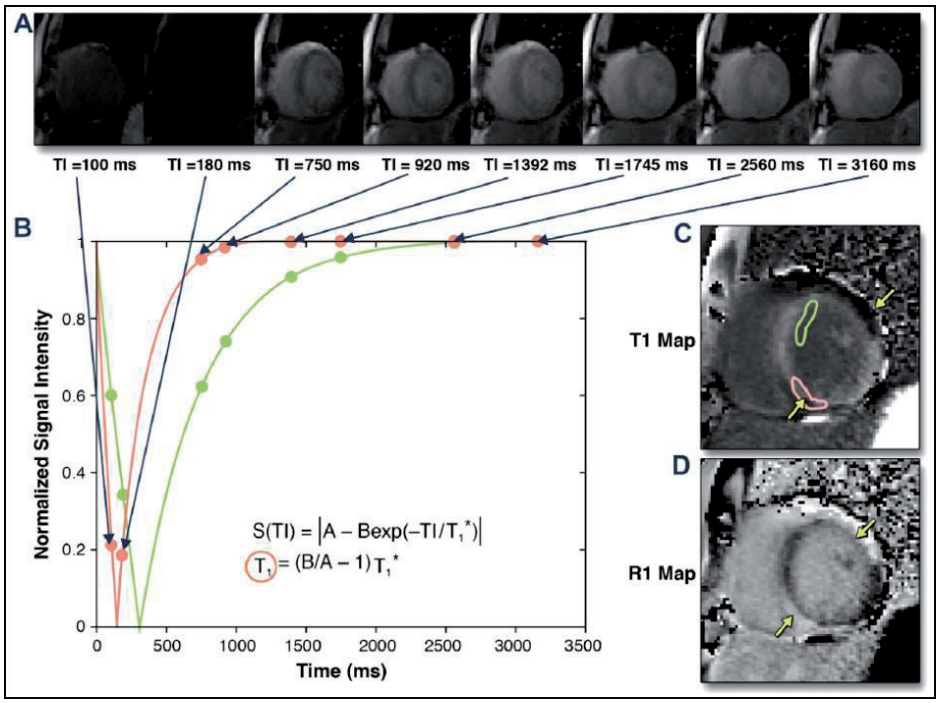

Figure 8.2

T1 relaxation time assessment by cardiac magnetic resonance. A. Sequential images at the same cardiac phase of different heartbeats are acquired after an inversion pulse, thereby obtaining a multitude of different inversion times. T1 recovers secondary to longitudinal magnetization paralleled by inversion time increment. B. T1 relaxation curves are constructed after data sorting by inversion time. Post-contrast shorter T1 relaxation time is seen in areas of myocardium with increased interstitium (fibrosis, inflammation) (red curve) versus normal myocardium (green curve). C. Epicardial inflammation is seen on the T1 map (red region and yellow arrows). D. By inverting the pixel values, an R1 map (1/T1) can be generated providing visualization of regions of fibrosis similar to conventional LGE images (bright). With permission from Salerno et al. *JACC Cardiovasc Imaging* 2013;6:806-22.

measurement of native T1 time is also highly dependent on the magnetic field strength and acquisition techniques.[5,w7]

Post-contrast T1 weighted techniques have been used more frequently to assess diffuse LV fibrosis. After continuous or bolus gadolinium contrast administration, the volume distribution of contrast media is higher within the interstitium or fibrotic myocardium than in normal myocardium, resulting in a shortened T1 time.[4,w7] The relative shortening in T1 time is related to the extent of myocardial fibrosis. Renal clearance, acquisition protocol, contrast dose, body composition and hematocrit may significantly affect the absolute post-contrast T1 value.[5] To partially overcome these limitations, quantification of extracellular volume (ECV) has been developed.[4,w7] The ECV is estimated by calculating the volume distribution of gadolinium in the extracellular myocardial space relative to the blood in a dynamic steady state. In the myocardial tissue, the contrast exchange rate with the blood is higher than the net clearance of the contrast from the blood, which defines the dynamic steady state. This dynamic steady state can be achieved with continuous intravenous infusion of gadolinium (until the T1 in the myocardium and blood pool are constant) or following an intravenous bolus of gadolinium (assuming equilibrium between the concentration of contrast in blood pool and

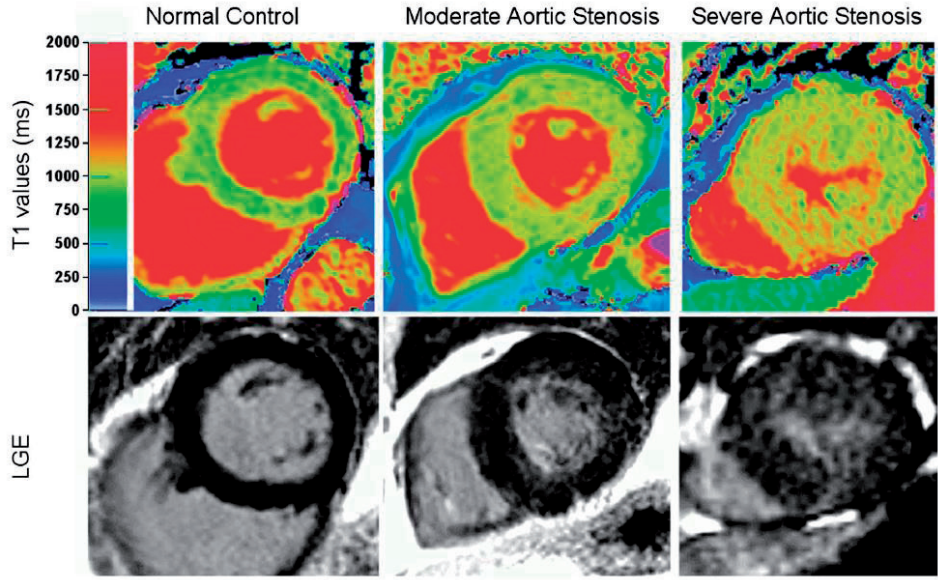

Figure 8.3
Native T1 relaxation mapping in aortic stenosis. Mid-ventricular short-axis color-coded T1 maps (upper row) and corresponding delayed contrast-enhanced cardiac magnetic resonance images. Examples (from left to right) of a normal individual (T1=944 ms), a patient with moderate AS and moderate left ventricular hypertrophy (T1=951 ms), and a patients with severe AS and severe hypertrophy (T1=1020 ms). With permission from Bull et al. *Heart* 2013;99:932-7.

myocardium at each time point after the bolus).[4, 5] The T1 time is then calculated according to the formula: *(1-Hematocrit) x (post 1/T1$_{myocardium}$ - pre 1/T1$_{myocardium}$) / (post 1/T1$_{blood}$ - pre 1/T1$_{blood}$)* where the factor *(1-Hematocrit)* represents the volume distribution of gadolinium in blood pool.[5] Normal ECV values range between 24% and 28% of the myocardium.[4] Both myocardial T1 and ECV can be visually represented by color-coded maps of the left ventricle. ECV represents a very promising biomarker of diffuse myocardial fibrosis closely correlated with collagen extent. However, its assessment is technically challenging and needs further standardization to allow accurate and reproducible measurements during single-breath-hold without confounding effects of heart-rate and through-plane motion.[4] To optimize T1 scan planning and acquisition, and to standardize analysis, a recent expert consensus document has been produced.[6]

3. Calibrated integrated backscatter with echocardiography

Collagen and water content affect myocardial tissue reflectivity of ultrasound waves. Dedicated off-line cardiac ultrasound software permits evaluation of tissue reflectivity amplitudes, sampled at the pericardium and the LV myocardium at different locations. Subsequently, calibrated integrated backscatter (IBS) is calculated by subtraction of mean backscatter intensity of the pericardium from the LV myocardium (Figure 4).[2] Higher IBS values (less negative) suggest larger diffuse fibrosis burden, as validated by in vivo biopsy specimens.[w8] Echocardiographic IBS offers relatively easy and fast assessment of LV fibrosis, but the main limitations include reduced inter- and intra-observer reproducibility due to noise, confounding effects of the location of the sample volume, artefacts and dependence on the settings of the ultrasound systems.[7]

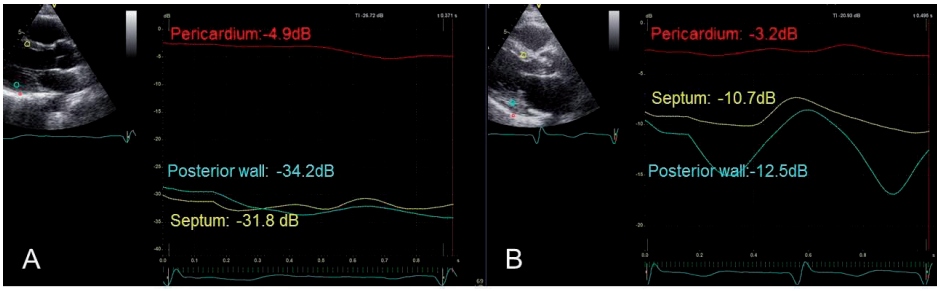

Figure 8.4
Calibrated integrated backscatter (IBS) in aortic stenosis. A. Normal subject: with values of calibrated IBS of the septum and posterior wall of -26.9 dB and -29.3 dB, respectively (after subtracting the value of the pericardium, in red). B. Patient with severe aortic stenosis shows increased calibrated IBS (less negative) of the septum (-7.5 dB) and posterior wall (-9.3 dB), suggestive of diffuse fibrosis.

4. Molecular imaging

Molecular imaging of fibrosis comprises direct visualization and quantification of radionuclide tracers that bind to specific molecular or cellular compounds involved in the pathogenesis of myocardial fibrosis. Integrins, matrix metalloproteinases, angiotensin converting enzyme (ACE) inhibitors, angiotensin II receptor antagonist, factor XIII and collagen constitute the main targeted agents for molecular imaging of fibrosis.[w6] So far, the studies evaluating the role of molecular imaging to assess fibrosis have focused on animal models of myocardial infarction and ischemic heart failure and there are no data on fibrosis associated to valvular heart disease.[w6,w9] The use of integrins, matrix metalloproteinases and factor XIII as targeted agents permits assessment of early inflammatory response and wound healing process of the infarcted tissue and therefore may predict LV remodeling. In contrast, collagen-targeted CMR contrast agents or radiolabeled ACE-inhibitors or angiotensin receptor antagonists have been developed to characterize postinfarction myocardial fibrosis and LV remodeling. In mouse models of chronic myocardial infarction, the use of gadolinium-based collagen-targeted contrast agent (EP-3533) for in vivo CMR imaging of myocardial fibrosis has shown feasible.[w10] On dynamic T1-weighted CMR data, the washout time constants of the targeted agent (EP-3533) was significantly longer than those for gadolinium alone in the regions of scar (194.8±116.8 min vs 25.5±4.2 min and 45.4±16.7 min vs 25.1±9.7 min, respectively, $p<0.05$ for both) which suggest improvement in visualization and characterization of scar.[w10] The cardiac renin-angiotensin system is enhanced in cardiac hypertrophy and fibrosis and the development of targeted radiolabeled agents have permitted in vivo imaging of angiotensin converting enzyme activity in the myocardium with positron emission tomography (PET) and single photon emission computed tomography (SPECT).[8] By using a high-affinity analog of lisinopril radiolabelled with ^{99m}Technetium, the tissue upregulation of angiotensin converting enzyme in heart failure may be visualized with SPECT-CT. This molecular imaging may help to identify the patients at high risk to develop overt heart failure in whom a more aggressive therapeutic strategy may be needed to improve the prognosis. However, molecular imaging of fibrosis is currently restricted to research and further histological validation is needed.

IMAGING TECHNIQUES FOR INDIRECT ASSESSMENT OF LV FIBROSIS

1. Strain and strain rate imaging with echocardiography and cardiac magnetic resonance

Deformation imaging comprises quantitative assessment of the magnitude of myocardial fiber contraction and relaxation (myocardial mechanics).[9] Strain refers to the relative change of myocardial fiber length over time and is expressed as a percentage with positive and negative values reflecting myocardial shortening or thickening and lengthening or thinning, respectively. Strain rate refers to change of strain per unit of time. Deformation imaging is highly sensitive to detect subtle changes in systolic LV function, even before LVEF becomes reduced (Figure 5) or LV dilatation occurs.[10,11]

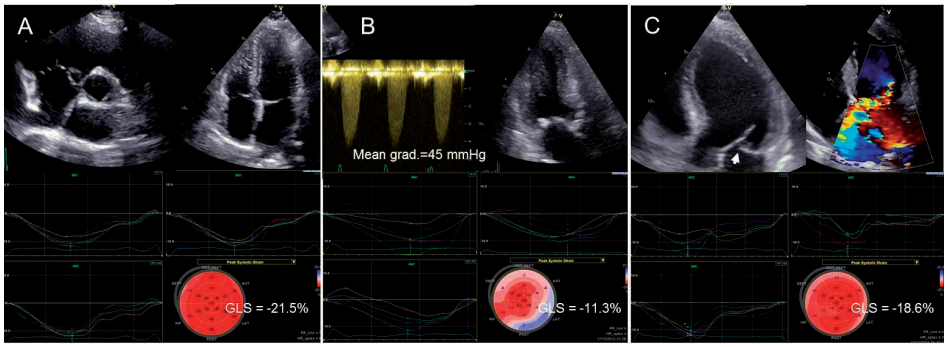

Figure 8.5
Differences in left ventricular strain in patients with normal ejection fraction. A. Normal subject with normal global longitudinal strain (GLS, -21.5%) and left ventricular ejection fraction (LVEF 65%). B. Patient with severe aortic stenosis, LV hypertrophy and subclinical LV dysfunction shown by reduced GLS (-11.3%) despite preserved LVEF (62%). C. Impaired GLS (-18.6%) in a patient with LV dilatation, due to severe organic mitral regurgitation, despite high normal LVEF (67%).

Early loss of longitudinal deformation is observed in the majority of cardiac disorders and is inversely associated to the presence and extent of fibrosis (reduced elasticity) in both ischemic and non-ischemic cardiomyopathies. Intrinsic contractility, loading conditions as well as chamber geometry influence myocardial deformation.[12] Accordingly, deformation imaging represents an indirect and non-specific measure of fibrosis.[2]

Quantitative deformation analysis can be performed with echocardiographic imaging techniques such as tissue Doppler imaging (TDI) or 2-dimensional speckle tracking echocardiography (STE), but also with CMR using tissue tagging. TDI assesses myocardial tissue velocities to calculate strain (rate). However (as with any Doppler technique), TDI-derived strain is dependent on the insonation angle and

strain can only be assessed accurately in those LV segments which are properly aligned along the ultrasound beam.[7] STE, developed more recently, assesses myocardial displacement to calculate deformation, based on 2-dimensional (or even 3-dimensional) spatial tracking of 'speckles' (natural acoustic markers present in bimodal echocardiographic images) throughout the cardiac cycle. This technique operates at lower frame rates and is angle-independent. Therefore comprehensive function analysis including longitudinal, circumferential and radial function as well as rotational mechanics can be studied for all myocardial segments. Recent advances also allow differentiation between epicardial and endocardial layers. High quality grey-scale images are required for proper tracking and definition of the region of interest confined to the LV myocardium. Absolute values might differ between software vendors due to different speckle tracking algorithms.[7, 9]

CMR tissue tagging is a complex technique of spatial modulation of cardiac tissue magnetization. Specific magnetic field gradients and time series of radiofrequency pulses 'taggs' the myocardium, creating a dark line grid that can be followed during subsequent acquisitions throughout the cardiac cycle. This permits assessment of LV displacement and strain (rate) calculation. Similar to STE, it allows comprehensive analysis of longitudinal, circumferential and rotational mechanics of the LV myocardium.[w11] The technique is not widely available, requires expertise and is currently restricted for research.

2. Perfusable tissue fraction and index with positron emission tomography

Focal or diffuse myocardial fibrosis can be also detected with PET using ^{15}O-labeled water and carbon monoxide ($C^{15}O$) as radiotracers and quantifying the perfusable tissue fraction and index of the LV. The perfusable tissue fraction is defined as the fraction of tissue capable to exchange ^{15}O-labeled water within a region of interest while the perfusable tissue index is the proportion of ^{15}O-labeled water-perfusable tissue within the anatomic tissue derived from the transmission scan. Increased myocardial fibrosis diminishes exchangeability of water leading to a low perfusable tissue index.[2] A reduction in the perfusable tissue index has been correlated with increasing extent of LV fibrosis after myocardial infarction.[w12] In addition, compared with healthy volunteers, patients with hypertrophic cardiomyopathy show a decreased perfusable tissue index in the non-hypertrophied lateral wall suggesting the presence of diffuse fibrosis.[w13] In light of these observations, it would be expected that patients with severe AS and LV hypertrophy for example could also show reduced perfusable tissue index, although currently no such data are available.

RELEVANCE OF FIBROSIS IMAGING IN AORTIC STENOSIS

In AS, the increased wall stress due to pressure overload is initially compensated by concentric LV hypertrophy to maintain normal cardiac output. This structural remodeling often coincides with development of predominantly reactive (diffuse interstitial) and later replacement (focal) fibrosis as a result of a complex interplay, mainly determined by up-regulation of the renin-angiotensin-aldosterone system, transforming growth-factor β and tissue inhibitors of matrix metalloproteinases. [w4,w14-w15] Interestingly, the fibrotic response (similar to the extent of LV hypertrophy) may vary substantially between patients despite similar AS severity, indicating multi-factorial pathophysiology.[3] While calcification is established as the main determinant of progressive valve narrowing, fibrosis initiates transition from compensating LV hypertrophy towards adverse LV remodeling, functional impairment and poor outcome in patients with severe AS (Table 2).[w4,w14-w15] The pathophysiological mechanism relating myocardial fibrosis to adverse prognosis in patients with AS is debated but probably involves deterioration of diastolic and systolic LV function as well as substrate formation for atrial/ventricular tachy-arrhythmias. [w14] Hence, fibrosis could be a strong biomarker of early cardiac dysfunction in severe AS implying increased mortality risk and may prove useful to select optimal timing for aortic valve replacement. Currently symptomatic status or LVEF<50% is considered a class I indication for valve replacement in patients with severe AS.[w3] However, most patients are asymptomatic and have normal LVEF. Moreover, few non-randomized studies demonstrated significant survival benefit with earlier intervention.[w16-w17] These findings point out the clinical need for additional markers in patients with severe AS to optimize timing of intervention. A non-invasive imaging technique that detects and quantifies fibrosis, and correlates to outcome may be of use.

Experience with fibrosis imaging in aortic stenosis

Focal fibrosis is detected in 30% to 60% of patients with severe AS using delayed contrast-enhanced CMR and comprises between 3% and 7% of the LV myocardium, depending on the population.[3,13,14,15,w18-w19] Often, the distribution of fibrosis is patchy, multifocal and restricted to (often basal) subendocardial or mid-wall myocardial layers (Figure 1).[3,13,w18] Excessive activation of the cardiac renin-angiotensin system, direct mechanical forces and ischemia due to an imbalance between the increased myocardial mass and the relatively reduced capillary flow reserve are proposed pathophysiological mechanisms for this replacement fibrosis. [3,13,w18] A positive correlation between fibrosis degree on the one hand, and both LV mass and valvuloarterial impedance on the other hand, partly explains the

Table 8.2
Correlations between the extent and severity of left ventricular fibrosis on non-invasive imaging and clinically relevant parameters in patients with aortic stenosis.

Parameters	Positive correlation with LV fibrosis	Negative correlation with LV fibrosis
Valve hemodynamics	Mean aortic valve pressure gradient	
	Peak aortic valve pressure	
	Valvuloarterial impedance	
Remodeling	LV mass (index)	
	LV volume	
	LA volume	
LV systolic function		LVEF
		LV stroke volume
		Longitudinal strain (rate)
		Systolic mitral annulus displacement (TDI or M-mode)
	LV end systolic pressure	
LV diastolic function	LV end diastolic pressure	
	E/E'	
Biomarkers	NT-proBNP	
Baseline clinical variables	NYHA class	
Variables after aortic valve replacement		NYHA class improvement
		Reverse LV remodeling
		Improvement LV systolic function

AVR: aortic valve replacement, LA: left atrial, EF: ejection fraction, LV: left ventricle, NYHA: New York Heart Association, TDI: Tissue Doppler Imaging

higher fibrotic burden in the LV demonstrated in low-gradient severe AS patients, irrespective of LVEF.[w20] More extensive fibrosis on delayed contrast-enhanced CMR in AS patients is associated with heart failure symptoms and increased NT-proBNP levels.[15] In 58 patients with symptomatic severe AS, Weidemann et al. observed that patients without fibrosis significantly improved in New York Heart Association (NYHA) functional class, LVEF and showed LV reverse remodeling after surgical valve replacement, contrary to patients who showed focal fibrosis in ≥2 LV segments.[15] Focal fibrosis remained unchanged for all patient groups postoperatively, indicating irreversible myocardial damage (macroscopic scar formation).[15] A more recent study (including 28 symptomatic AS patients) extended these results showing that the degree of fibrosis was independently associated with survival (irrespective of age), LVEF and symptomatic status.[w18] This independent relation was confirmed by Dweck et al. in 143 patients with moderate (40%) and severe (60%) AS.[3] Those patients with mid-wall hyperenhancement had 5-fold increased

all-cause mortality (HR 5.35; 95% CI 1.16-24.56). Patients with mid-wall enhancement who underwent aortic valve surgery had better survival than those treated conservatively but worse compared to surgically treated patients without fibrosis. Interestingly, almost half of the deaths occurred in patients with only moderate AS and mid-wall fibrosis, underscoring the prognostic relevance of focal fibrosis.[3]

Focal fibrosis, however, occurs at later disease stages, while diffuse fibrosis is the predominant pattern in AS patients. Higher septal IBS values, correlating with diffuse fibrosis histology, were shown in 35 severe AS patients (Figure 4).[w21] The presence of significant LV fibrosis, defined as a value of end-diastolic IBS of the septum indexed to the pericardial IBS >56.6%, permitted identification of patients with LV dysfunction. In addition, significant LV fibrosis assessed with calibrated IBS was associated with lack of LVEF improvement after valve replacement.[w21] A reduction of IBS values after surgical replacement suggests at least partial reversibility of diffuse fibrosis (or reduced water content due to cell volume reduction) in AS patients and could predict LV reverse remodeling.[w22] Recent development of T1 mapping techniques has renewed interest on diffuse fibrosis imaging in this group of patients. Various studies have correlated several parameters derived from native and post-contrast T1 mapping CMR techniques. In 18 patients with severe AS the correlation between contrast-enhanced T1 weighted CMR derived ECV and histological quantification of myocardial fibrosis was assessed.[w23] ECV showed a strong linear correlation with histological collagen volume fraction (r^2 = 0.86), suggesting the potential of T1 weighted CMR for fibrosis assessment.[w23] However, using native T1 mapping, Bull et al. showed a modest correlation between native T1 values and histological collagen volume fraction in 19 patients with severe AS undergoing aortic valve replacement (Figure 3).[16] These findings suggest a significant variability among the different methodologies to assess diffuse myocardial fibrosis (Table 3).[16,17,w18,w21,w23] Independently of the T1 mapping CMR technique used, all studies showed that patients with AS have increased diffuse myocardial fibrosis.[16,w23] Bull et al. reported higher native T1 values in symptomatic (1014±38 ms) versus asymptomatic (972±33 ms) AS patients.[16] In addition, Flett et al. showed higher ECV (18.1±8.1 versus 13.4±6.5 %, p<0.05) in 63 patients with AS as compared to 30 control patients and this parameter was an important predictor of 6-minute walking distance.[14] After valve surgery ECV (as a measure of diffuse fibrosis) remained unchanged and 80% of patients who died within the first 6 months were within the upper ECV tertile.[14] However, the considerable overlap of the T1 mapping results between the patients with AS versus control individuals as well as reproducibility issues may currently limit the use of this technique for individual patients.[14] In addition to direct fibrosis assessment, reduction in LV function has been used as indirect marker for LV fibrosis. Impaired LVEF in patients with AS

Table 8.3
Correlations of non-invasive imaging versus histology based fibrosis assessment in valvular heart disease patients (all p<0.05).

Study	Imaging technique	Nr patients, type of valve disease	Correlation
Di Bello et al[w21]	Calibrated integrated backscatter	35, AS	r = 0.74
Camelli et al[17]	Longitudinal left atrial strain	46, MR	r = - 0.82*
Azevedo et al[w18]	Delayed contrast-enhancement	28, AS	r = 0.69
Bull et al[16]	Native T1 relaxation time	19, AS	r = 0.66
Flett et al[w23]	T1 based extracellular volume	18, AS	r^2 = 0.86

* Correlated to left atrial biopsy.

is inversely correlated to extensive histological fibrosis (r = -0.57).[w15] However, the vast majority of patients with AS have preserved LVEF, since LVEF mainly reflects radial function, which is preserved in hypertrophied hearts until end-stage of the disease.[w24-w25]

In patients with AS however, fibrosis mainly affects subendocardial to mid-wall layers of the myocardium that determine longitudinal LV function. Weidemann et al. showed an inverse relationship between the extent of fibrosis and LV longitudinal strain (rate) in patients with severe AS.[15] Many patients with severe AS and preserved LVEF present with impaired longitudinal deformation.[11] In more advanced disease stages, impaired LV radial and circumferential strain, corresponding to more transmural myocardial fibrosis, have been reported.[11] The main determinants of global LV longitudinal strain in AS patients are stenosis valve severity, global afterload (valvulo-arterial impedance), LV mass, fibrosis and con tractility.[11,12,15,w20,w26-w27] Since all these determinants show a significant relation with outcome in patients with AS, detection of subtle LV dysfunction by strain imaging may improve risk stratification (and therapeutic decision making). Indeed, reduced LV longitudinal function relates to exercise intolerance and was the single independent predictor of mortality or heart failure hospitalization after valve replacement in symptomatic patients with severe AS.[w27-w28] Importantly, LV longitudinal deformation was an independent predictor of death or symptom-driven valve replacement in asymptomatic patients with severe AS and preserved LVEF. In particular, a global LV longitudinal strain value >-15% indicated worse event-free survival.[w29]

RELEVANCE OF FIBROSIS IMAGING IN MITRAL REGURGITATION

Assessment of myocardial fibrosis in patients with organic MR is of interest since early detection of associated LV and left atrial (LA) structural changes may help to

identify patients who may benefit from surgical valve repair while still asymptomatic. In contrast, in functional (ischemic) MR, there is often extensive focal fibrosis with severe structural LV changes due to scar formation after previous infarction, and therefore detection of diffuse fibrosis may not help in the timing of surgery.

Organic MR comprises primary abnormalities of the mitral valve morphology and causes volume overload of both the LV and the LA, leading to chamber dilatation and eccentric LV hypertrophy. In contrast to concentric pressure overload LV hypertrophy (as noted with AS), the eccentric LV hypertrophy caused by chronic volume overload associated with organic MR is less pro-fibrotic.[w30] A recent study involving rat surgical models of pressure and volume overload attempted to explain this phenomenon.[w31] Compared with pressure overload models, volume overload models showed less myocardial ischemia and replacement fibrosis.[w31] In addition, proteolytic activity in large animal models of MR, has been related to reduced support and content of extracellular matrix in eccentric hypertrophy, thereby facilitating LV dilatation.[w31-w32] Although MR is less pro-fibrotic than AS, increased interstitial tissue in the LV on biopsies obtained in patients undergoing mitral valve repair/replacement is suggested to contribute to development of cardiac failure.[w33] Moreover, histology revealed a larger content of subendocardial diffuse LV interstitial fibrosis in patients with MR as compared to patients without MR (18% versus 4%, $p<0.05$).[w34] Similar to AS, compelling evidence points out that LV fibrosis in MR relates to LV dilatation, functional impairment and adverse outcome. These findings may impact on timing of surgery in patients with severe organic MR. Development of symptoms or LV dysfunction (LVEF ≤60% or LV end-systolic diameter ≥40-45 mm) are class I indications for mitral valve surgery in patients with severe organic MR.[w3] However, these indications should probably not be awaited for, as surgical outcome seems better in absence of these characteristics.[18,w35-w36] Additional risk stratification is therefore warranted and (indirect) fibrosis imaging may be of importance.

Experience with fibrosis imaging in organic mitral regurgitation

In organic MR, indirect myocardial fibrosis assessment has been obtained using strain imaging. In contrast, CMR, IBS or molecular imaging studies in patients with MR are scarce. Similar to patients with AS, most MR patients have preserved LVEF. Of note, in significant MR supra-normal LVEF values defines normal systolic function due to coincidence of increased preload and reduced afterload during the initial compensated phase. Subclinical LV dysfunction despite preserved LVEF, assessed by impaired LV longitudinal strain, however, is often encountered in asymptomatic patients with severe MR (Figure 5).[10] More advanced disease stages are associated with impaired LV circumferential and radial strain.[w37] The main determinants

of LV longitudinal strain in MR are regurgitant volume, LV geometry (dilatation) and intrinsic contractility, related to myocardial fibrosis.[10,w38-w39] Reduced strain in MR patients may therefore parallel LV geometric changes (dilatation) rather than contractility impairment, and therefore, some authors have advocated to correct the LV strain values for LV dimensions.[10,12]

In a large series of 233 patients with moderate-severe MR and overall preserved LVEF, Witkowski et al. showed that impaired longitudinal LV strain together with LV end-systolic dimension predict postoperative LV dysfunction (LVEF <50%), independently of baseline LVEF ≤60%, symptoms and atrial fibrillation.[19] In particular, a global LV longitudinal strain value ≥-19.9% predicted long-term LV dysfunction after mitral valve repair with a sensitivity and specificity of 90% and 79%, respectively.[19] Additionally, impaired recruitment of longitudinal contractility by strain imaging during exercise was also associated with post-operative LV dysfunction in patients with preserved LVEF undergoing surgery for severe MR.[w40] Pre-operative high-normal LVEF may be misleading and mask latent LV dysfunction that is only observed post-operatively when acute preload reduction leads to LVEF decrease below normal values.[19,w41] Whether impaired LV longitudinal strain also predicts worse survival after valve intervention remains to be demonstrated.

Not only the LV, but also the LA has been the subject of research. Recently, a close inverse correlation between left atrial global (reservoir) strain and histological interstitial fibrosis in patients with severe organic MR (r = -0.82) was shown (Figure 6).[17] The potential clinical relevance of such findings was explored in another study involving 121 patients with severe MR.[20] Impaired global LA longitudinal (reservoir) strain was related to long-term mortality after mitral valve surgery, incremental to guideline based indications for mitral surgery and LA size.[20, w3] LA strain could potentially predict post-operative survival in patients with severe MR, without guidelines-based risk factors (Figure 7).[20] Apart from myocardial deformation, both delayed contrast-enhancement CMR and, more recently, T1 weighted imaging of the LA have shown correlation to LA fibrosis.[w42-w43] However, no data exist on assessment of LA fibrosis with CMR techniques in patients with severe MR.

UNRESOLVED ISSUES

Based on these experimental and clinical studies, the question remains whether fibrosis may help in the decision when to intervene in asymptomatic AS patients with preserved LVEF. Various other issues need further study to define the precise role of LV fibrosis for risk stratification and decision-making strategies. For example, is fibrosis independent from and superior to other risk factors currently

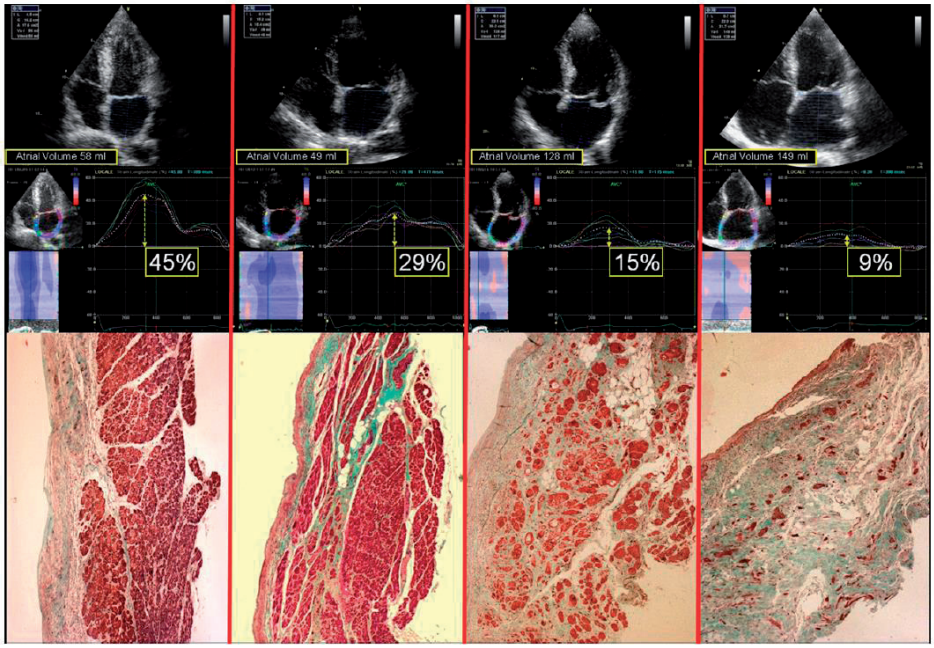

Figure 8.6
Relation between extent of left atrial fibrosis and left atrial reservoir strain in patients with severe mitral regurgitation. Four patients operated on for severe mitral regurgitation with (from left to right) progressive left atrial dilatation corresponding to more impaired left atrial function (reservoir strain, decreasing from 45% to 9%) and larger extent of fibrosis on histology of the left atrial free wall (hematoxylin-eosin and Masson's trichrome staining). With permission from Cameli et al. *Am J Cardiol* 2013;111:595-601.

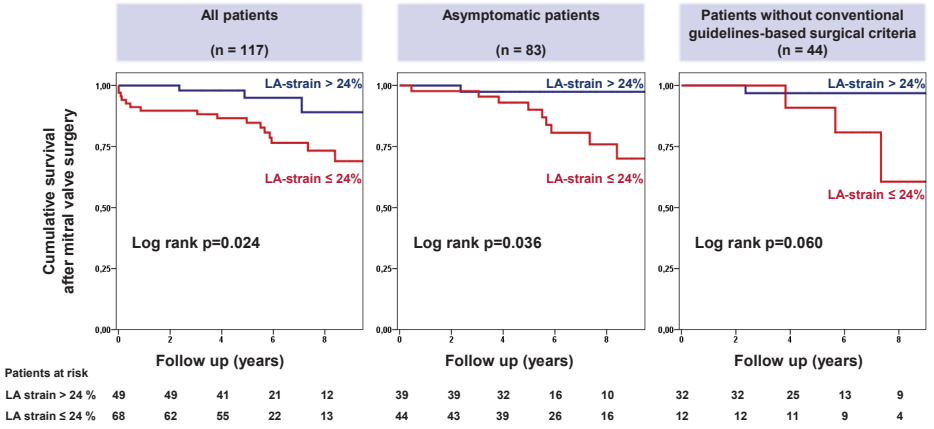

Figure 8.7
Prognostic value of LA strain in patients undergoing mitral valve surgery for severe organic mitral regurgitation. Dichotomizing the population based on a cut-off value of LA strain of 24%, patients with an LA strain >24% had better cumulative survival compared with patients with an LA strain ≤24%, independently of symptoms or the presence of guidelines-based surgical criteria. With permission from Debonnaire et al. *J Am Soc Echocardiogr* 2013;26:1053-62.

used, such as NT-proBNP? In addition, for risk estimation, should LV fibrosis be considered as a continuum or should a threshold be applied (if more than a certain percentage fibrosis is present in the LV, then surgical intervention should be considered)? which fibrosis needs to be detected: focal or diffuse fibrosis? And which non-invasive imaging technique is optimal for assessment and quantification of LV fibrosis? And what will be the precise role of indirect fibrosis assessment using LV strain? Moreover, it is not clear whether a potential relation between fibrosis and outcome can be extrapolated to patients with different AS severity. And finally, does infarct related LV fibrosis alter predictive value in AS patients?

Similarly, for asymptomatic patients with severe organic MR, the key issue is whether strain imaging is specific enough for risk stratification of individual patients and to justify early intervention in asymptomatic patients with preserved LVEF. In addition, would LV or LA strain provide the optimal risk stratification and therapy guidance in these patients? And will strain imaging be independent and superior to other risk factors, including NT-proBNP? And, if considered for risk stratification and therapy guidance, will a threshold of LV and/or LA strain be used or a continuum? Moreover, the value of imaging techniques such as contrast-enhanced CMR or T1 mapping in MR should be explored both for the LV and the LA.

Importantly, apart from fibrosis (extracellular matrix alterations), other factors such as cell death, impaired excitation-contraction coupling due to altered calcium homeostasis and mismatch between cardiomyocyte and vascular growth contribute to transition of compensated hypertrophy towards heart failure.[w31] Molecular imaging of specific signaling pathways involved in these factors may therefore provide novel insights and ultimately contribute to risk stratification in patients with valvular heart disease.

CONCLUSION

If successfully performed prior to complications arise, surgical correction of AS or MR may reverse patients to normal life expectancy. Timing of surgery in asymptomatic patients is currently considered in the presence of reduced LVEF, LV dilatation, pulmonary hypertension, reduced exercise capacity, increased plasma levels of biomarkers or atrial fibrillation. These markers however, occur relatively late in the disease progression, and outcome after surgery is suboptimal. LV fibrosis occurs earlier, and may be a future marker to improve therapeutic decision making. Novel non-invasive imaging techniques have been developed to detect fibrosis directly or to assess subtle changes in LV systolic dysfunction (while LVEF is still preserved), secondary to LV fibrosis. Future research is needed to determine

whether LV fibrosis assessment with these imaging techniques may further refine the timing of surgery in severe AS or MR, and whether this will improve outcome after surgery.

REFERENCES

1 Go AS, Mozaffarian D, Roger VL, et al. Heart disease and stroke statistics--2013 update: a report from the American Heart Association. *Circulation.* 2013;127:e6-e245.

2 Jellis C, Martin J, Narula J, et al. Assessment of nonischemic myocardial fibrosis. *J Am Coll Cardiol.* 2010;56:89-97.

3 Dweck MR, Joshi S, Murigu T, et al. Midwall fibrosis is an independent predictor of mortality in patients with aortic stenosis. *J Am Coll Cardiol.* 2011;58:1271-1279.

4 Salerno M, Kramer CM. Advances in parametric mapping with CMR imaging. *JACC Cardiovasc Imaging.* 2013;6:806-822.

5 Kellman P, Wilson JR, Xue H, et al. Extracellular volume fraction mapping in the myocardium, part 1: evaluation of an automated method. *J Cardiovasc Magn Reson.* 2012;14:63.

6 Moon JC, Messroghli DR, Kellman P, et al. Myocardial T1 mapping and extracellular volume quantification: a Society for Cardiovascular Magnetic Resonance (SCMR) and CMR Working Group of the European Society of Cardiology consensus statement. *J Cardiovasc Magn Reson.* 2013;15:92.

7 Mor-Avi V, Lang RM, Badano LP, et al. Current and evolving echocardiographic techniques for the quantitative evaluation of cardiac mechanics: ASE/EAE consensus statement on methodology and indications endorsed by the Japanese Society of Echocardiography. *J Am Soc Echocardiogr.* 2011;24:277-313.

8 Dilsizian V, Zynda TK, Petrov A, et al. Molecular imaging of human ACE-1 expression in transgenic rats. *JACC Cardiovasc Imaging.* 2012;5:409-418.

9 Blessberger H, Binder T. Non-invasive imaging: Two dimensional speckle tracking echocardiography: basic principles. *Heart.* 2010;96:716-722.

10 Marciniak A, Claus P, Sutherland GR, et al. Changes in systolic left ventricular function in isolated mitral regurgitation. A strain rate imaging study. *Eur Heart J.* 2007;28:2627-2636.

11 Ng AC, Delgado V, Bertini M, et al. Alterations in multidirectional myocardial functions in patients with aortic stenosis and preserved ejection fraction: a two-dimensional speckle tracking analysis. *Eur Heart J.* 2011;32:1542-1550.

12 Bijnens BH, Cikes M, Claus P, et al. Velocity and deformation imaging for the assessment of myocardial dysfunction. *Eur J Echocardiogr.* 2009;10:216-226.

13 Debl K, Djavidani B, Buchner S, et al. Delayed hyperenhancement in magnetic resonance imaging of left ventricular hypertrophy caused by aortic stenosis and hypertrophic cardiomyopathy: visualisation of focal fibrosis. *Heart.* 2006;92:1447-1451.

14 Flett AS, Sado DM, Quarta G, et al. Diffuse myocardial fibrosis in severe aortic stenosis: an equilibrium contrast cardiovascular magnetic resonance study. *Eur Heart J Cardiovasc Imaging.* 2012;13:819-826.

15 Weidemann F, Herrmann S, Stork S, et al. Impact of myocardial fibrosis in patients with symptomatic severe aortic stenosis. *Circulation.* 2009;120:577-584.

16 Bull S, White SK, Piechnik SK, et al. Human non-contrast T1 values and correlation with histology in diffuse fibrosis. *Heart.* 2013;99:932-937.

17 Cameli M, Lisi M, Righini FM, et al. Usefulness of atrial deformation analysis to predict left atrial fibrosis and endocardial thickness in patients undergoing mitral valve operations for severe mitral regurgitation secondary to mitral valve prolapse. *Am J Cardiol.* 2013;111:595-601.

18 Suri RM, Enriquez-Sarano M. Association between early surgical intervention vs watchful waiting and outcomes for mitral regurgitation due to flail mitral valve leaflets. *JAMA.* 2013;310:609-616.
19 Witkowski TG, Thomas JD, Debonnaire PJ, et al. Global longitudinal strain predicts left ventricular dysfunction after mitral valve repair. *Eur Heart J Cardiovasc Imaging.* 2013;14:69-76.
20 Debonnaire P, Leong DP, Witkowski TG, et al. Left atrial function by two-dimensional speckle-tracking echocardiography in patients with severe organic mitral regurgitation: association with guidelines-based surgical indication and postoperative (long-term) survival. *J Am Soc Echocardiogr.* 2013;26:1053-1062.

REFERENCES (ON LINE)

w1 Nkomo VT, Gardin JM, Skelton TN, et al. Burden of valvular heart diseases: a population-based study. *Lancet.* 2006;368:1005-1011.
w2 Nishimura RA, Otto CM, Bonow RO, et al. 2014 AHA/ACC Guideline for the Management of Patients With Valvular Heart Disease: A Report of the American College of Cardiology/American Heart Association Task Force on Practice Guidelines. *Circulation.* 2014; 129:521-643.
w3 Vahanian A, Alfieri O, Andreotti F, et al. Guidelines on the management of valvular heart disease (version 2012). *Eur Heart J.* 2012;33:2451-2496.
w4 Heymans S, Schroen B, Vermeersch P, et al. Increased cardiac expression of tissue inhibitor of metalloproteinase-1 and tissue inhibitor of metalloproteinase-2 is related to cardiac fibrosis and dysfunction in the chronic pressure-overloaded human heart. *Circulation.* 2005;112:1136-1144.
w5 Verheule S, Wilson E, Everett T, et al. Alterations in atrial electrophysiology and tissue structure in a canine model of chronic atrial dilatation due to mitral regurgitation. *Circulation.* 2003;107:2615-2622.
w6 Won S, Davies-Venn C, Liu S, et al. Noninvasive imaging of myocardial extracellular matrix for assessment of fibrosis. *Curr Opin Cardiol.* 2013;28:282-289.
w7 Moon JC, Treibel TA, Schelbert EB. T1 mapping for diffuse myocardial fibrosis: a key biomarker in cardiac disease? *J Am Coll Cardiol.* 2013;62:1288-1299.
w8 Picano E, Pelosi G, Marzilli M, et al. In vivo quantitative ultrasonic evaluation of myocardial fibrosis in humans. *Circulation.* 1990;81:58-64.
w9 Nahrendorf M, Sosnovik DE, French BA, et al. Multimodality cardiovascular molecular imaging, Part II. *Circ Cardiovasc Imaging.* 2009;2:56-70.
w10 Helm PA, Caravan P, French BA, et al. Postinfarction myocardial scarring in mice: molecular MR imaging with use of a collagen-targeting contrast agent. *Radiology.* 2008;247:788-796.
w11 Fernandes VR, Edvardsen T, Rosen BD, et al. The influence of left ventricular size and global function on regional myocardial contraction and relaxation in an adult population free of cardiovascular disease: a tagged CMR study of the MESA cohort. *J Cardiovasc Magn Reson.* 2007;9:921-930.
w12 Iida H, Tamura Y, Kitamura K, et al. Histochemical correlates of (15)O-water-perfusable tissue fraction in experimental canine studies of old myocardial infarction. *J Nucl Med.* 2000;41:1737-1745.

w13 Knaapen P, van Dockum WG, Bondarenko O, et al. Delayed contrast enhancement and perfusable tissue index in hypertrophic cardiomyopathy: comparison between cardiac MRI and PET. *J Nucl Med.* 2005;46:923-929.
w14 Dweck MR, Boon NA, Newby DE. Calcific aortic stenosis: a disease of the valve and the myocardium. *J Am Coll Cardiol.* 2012;60:1854-1863.
w15 Hein S, Arnon E, Kostin S, et al. Progression from compensated hypertrophy to failure in the pressure-overloaded human heart: structural deterioration and compensatory mechanisms. *Circulation.* 2003;107:984-991.
w16 Brown ML, Pellikka PA, Schaff HV, et al. The benefits of early valve replacement in asymptomatic patients with severe aortic stenosis. *J Thorac Cardiovasc Surg.* 2008;135:308-315.
w17 Kang DH, Park SJ, Rim JH, et al. Early surgery versus conventional treatment in asymptomatic very severe aortic stenosis. *Circulation.* 2010;121:1502-1509.
w18 Azevedo CF, Nigri M, Higuchi ML, et al. Prognostic significance of myocardial fibrosis quantification by histopathology and magnetic resonance imaging in patients with severe aortic valve disease. *J Am Coll Cardiol.* 2010;56:278-287.
w19 Rudolph A, Abdel-Aty H, Bohl S, et al. Noninvasive detection of fibrosis applying contrast-enhanced cardiac magnetic resonance in different forms of left ventricular hypertrophy relation to remodeling. *J Am Coll Cardiol.* 2009;53:284-291.
w20 Herrmann S, Stork S, Niemann M, et al. Low-gradient aortic valve stenosis myocardial fibrosis and its influence on function and outcome. *J Am Coll Cardiol.* 2011;58:402-412.
w21 Di Bello, V, Giorgi D, Viacava P, et al. Severe aortic stenosis and myocardial function: diagnostic and prognostic usefulness of ultrasonic integrated backscatter analysis. *Circulation.* 2004;110:849-855.
w22 Fijalkowski M, Koprowski A, Galaska R, et al. Improvement of ultrasonic myocardial properties after aortic valve replacement for pure severe aortic stenosis: the predictive value of ultrasonic tissue characterization for left ventricle reverse remodeling. *J Am Soc Echocardiogr.* 2010;23:1060-1066.
w23 Flett AS, Hayward MP, Ashworth MT, et al. Equilibrium contrast cardiovascular magnetic resonance for the measurement of diffuse myocardial fibrosis: preliminary validation in humans. *Circulation.* 2010;122:138-144.
w24 Lancellotti P, Donal E, Magne J, et al. Impact of global left ventricular afterload on left ventricular function in asymptomatic severe aortic stenosis: a two-dimensional speckle-tracking study. *Eur J Echocardiogr.* 2010;11:537-543.
w25 Ozkan A, Kapadia S, Tuzcu M, et al. Assessment of left ventricular function in aortic stenosis. *Nat Rev Cardiol.* 2011;8:494-501.
w26 Cramariuc D, Gerdts E, Davidsen ES, et al. Myocardial deformation in aortic valve stenosis: relation to left ventricular geometry. *Heart.* 2010;96:106-112.
w27 Dahl JS, Videbaek L, Poulsen MK, et al. Global strain in severe aortic valve stenosis: relation to clinical outcome after aortic valve replacement. *Circ Cardiovasc Imaging.* 2012;5:613-620.
w28 Lafitte S, Perlant M, Reant P, et al. Impact of impaired myocardial deformations on exercise tolerance and prognosis in patients with asymptomatic aortic stenosis. *Eur J Echocardiogr.* 2009;10:414-149.
w29 Yingchoncharoen T, Gibby C, Rodriguez LL, et al. Association of myocardial deformation with outcome in asymptomatic aortic stenosis with normal ejection fraction. *Circ Cardiovasc Imaging.* 2012;5:719-725.

w30 Kehat I, Molkentin JD. Molecular pathways underlying cardiac remodeling during pathophysiological stimulation. *Circulation.* 2010;122:2727-2735.
w31 Chemaly ER, Kang S, Zhang S, et al. Differential patterns of replacement and reactive fibrosis in pressure and volume overload are related to the propensity for ischaemia and involve resistin. *J Physiol.* 2013;591:5337-5355.
w32 Spinale FG. Myocardial matrix remodeling and the matrix metalloproteinases: influence on cardiac form and function. *Physiol Rev.* 2007;87:1285-1342.
w33 Fuster V, Danielson MA, Robb RA, et al. Quantitation of left ventricular myocardial fiber hypertrophy and interstitial tissue in human hearts with chronically increased volume and pressure overload. *Circulation.* 1977;55:504-508.
w34 Lopes MM, Ribeiro GC, Tornatore TF, et al. Increased expression and phosphorylation of focal adhesion kinase correlates with dysfunction in the volume-overloaded human heart. *Clin Sci (Lond).* 2007;113:195-204.
w35 Enriquez-Sarano M, Tajik AJ, Schaff HV, et al. Echocardiographic prediction of survival after surgical correction of organic mitral regurgitation. *Circulation.* 1994;90:830-837.
w36 Tribouilloy C, Grigioni F, Avierinos JF, et al. Survival implication of left ventricular end-systolic diameter in mitral regurgitation due to flail leaflets a long-term follow-up multicenter study. *J Am Coll Cardiol.* 2009;54:1961-1968.
w37 Kim MS, Kim YJ, Kim HK, et al. Evaluation of left ventricular short- and long-axis function in severe mitral regurgitation using 2-dimensional strain echocardiography. *Am Heart J.* 2009;157:345-351.
w38 Lancellotti P, Magne J. Stress echocardiography in regurgitant valve disease. *Circ Cardiovasc Imaging.* 2013;6:840-849.
w39 Yurdakul S, Tayyareci Y, Yildirimturk O, et al. Subclinical left ventricular dysfunction in asymptomatic chronic mitral regurgitation patients with normal ejection fraction: a combined tissue Doppler and velocity vector imaging-based study. *Echocardiography.* 2011;28:877-885.
w40 Lancellotti P, Cosyns B, Zacharakis D, et al. Importance of left ventricular longitudinal function and functional reserve in patients with degenerative mitral regurgitation: assessment by two-dimensional speckle tracking. *J Am Soc Echocardiogr.* 2008;21:1331-1336.
w41 Starling MR, Kirsh MM, Montgomery DG, et al. Impaired left ventricular contractile function in patients with long-term mitral regurgitation and normal ejection fraction. *J Am Coll Cardiol.* 1993;22:239-250.
w42 Beinart R, Khurram IM, Liu S, et al. Cardiac magnetic resonance T1 mapping of left atrial myocardium. *Heart Rhythm.* 2013;10:1325-1331.
w43 Kuppahally SS, Akoum N, Burgon NS, et al. Left atrial strain and strain rate in patients with paroxysmal and persistent atrial fibrillation: relationship to left atrial structural remodeling detected by delayed-enhancement MRI. *Circ Cardiovasc Imaging.* 2010;3:231-239.

Chapter 9

Left atrial function by two-dimensional speckle tracking echocardiography in patients with severe organic mitral regurgitation: association with guidelines-based surgical indication and postoperative (long-term) survival

Philippe Debonnaire, Darryl P Leong, Tomasz G Witkowski, Ibtihal Al Amri, Emer Joyce, Spyridon Katsanos, Martin J Schalij, Jeroen J Bax, Victoria Delgado, Nina Ajmone Marsan

J Am Soc Echocardiogr, 2013 Sep 26(9): 1053-1062.

ABSTRACT

Objectives

Left atrial (LA) mechanics in patients with severe mitral regurgitation (MR) remain largely unexplored. The present evaluation assessed the effect of severe mitral regurgitation (MR) on left atrial (LA) function, its potential relation with conventional surgery indications and long-term postoperative survival.

Methods and Results

2D-speckle tracking strain and volumetric indices of LA reservoir, conduit and contractile function were assessed in 121 severe MR patients and 70 controls. Patients were divided according to presence (n=46) or absence (n=75) of ≥1 guidelines-based criteria for mitral surgery (symptoms, left ventricular (LV) ejection fraction ≤60%, LV end-systolic diameter ≥40mm, atrial fibrillation or systolic pulmonary arterial pressure >50mmHg).

In patients with severe MR, as compared to controls, significant LA reservoir and contractile dysfunction was observed, which was more pronounced in patients with mitral surgery indication (all $p<0.05$ for strain and volumetric indices). Of all LA function indices, LA reservoir strain was an independent predictor (OR=0.88, 95%CI 0.82-0.94, $p<0.001$) and had the highest accuracy to identify patients with indication for mitral surgery (area under ROC curve=0.8, 95%CI 0.72-0.87). A total of 117 patients underwent mitral valve surgery. Patients with LA reservoir strain ≤24% showed worse survival at a median of 6.4 years (4.7-8.7 years) after mitral surgery ($p=0.02$), regardless the symptomatic status prior to surgery. LA reservoir strain, on top of mitral surgery indications, provided incremental predictive value for postoperative survival.

Conclusion

Impaired LA reservoir strain in patients with severe organic MR relates to long-term survival after mitral valve surgery, independently of and incremental to current guidelines-based indications for mitral surgery.

INTRODUCTION

Severe chronic mitral regurgitation (MR) causes a significant left atrial (LA) volume overload, leading to LA dilatation as compensatory mechanism to maintain LA pressure homeostasis and prevent pulmonary congestion.[1] Measures of LA remodeling, such as LA diameter and LA volume index, have been shown to predict outcome in patients with severe organic MR, and are helpful for risk stratification and clinical decision-making in these patients.[2-4] However, chronic MR may induce significant LA ultra-structural changes, potentially affecting LA myocardial contractility and relaxation before LA dilatation occurs.[3,5-8] Therefore, assessment of LA function, rather than dimension, might be of significant value to guide therapy in patients with severe MR. However, data on the effect of severe MR on LA function are scarce and the potential incremental value of LA function assessment to predict timing for surgery is unexplored.[9-12]

Different LA functions can be evaluated, including reservoir (storage of pulmonary venous inflow during ventricular systole), conduit (passive emptying during early diastole) and contractile (active emptying at late diastole) functions. These sequential LA functions play a crucial role in cardiac performance by optimizing left ventricular (LV) filling,[13,14] and can be measured with conventional 2-dimensional (2D) echocardiography by detecting the phasic changes of LA volume during the cardiac cycle. More recently, 2D speckle tracking longitudinal deformation (strain and strain rate) imaging also showed accurate characterization of all phases of LA function.[14-18]

Therefore, the aim of this study was 1) to characterize LA reservoir, conduit and contractile function using 2D-speckle tracking deformation imaging in patients with chronic severe organic MR, 2) to determine its clinical relation to the presence of guidelines-based conventional indications for mitral surgery and 3) to explore its association with long-term survival after mitral valve surgery.[2,19]

METHODS

Patient population

The patient population consisted of patients presenting with chronic severe organic MR, who were referred to our centre within the last decade. Clinical and echocardiographic data were prospectively collected in the departmental Cardiology Information System (EPD-Vision®, Leiden University Medical Center, Leiden, and the Netherlands) and retrospectively analyzed.

Clinical assessment included demographics, medications, identification of co-morbidities and symptoms according to the New York Heart Association (NYHA) functional class. Echocardiographic evaluation included conventional measurements and speckle tracking analysis for LA deformation analysis. Patients with prior cardiac surgery or myocardial infarction, congenital heart disease, concomitant mitral stenosis exceeding mild severity (mean gradient ≥5 mmHg) or significant aortic valve disease were excluded. In addition, in order to avoid confounders for increased pulmonary pressure, patients with significant pulmonary disease were excluded.

Patients were further dichotomized based on the presence of ≥1 conventional criterion for mitral surgery indication, according to current guidelines: NYHA class 3 to 4 symptoms, LV ejection fraction (EF) ≤60 %, LV end-systolic diameter ≥40 mm, atrial fibrillation or systolic pulmonary arterial pressure at rest >50 mmHg.[2] Accordingly, phasic LA functions were evaluated in both patient groups.

In addition, 70 individuals with similar age, body surface area and gender distribution served as a control group. These subjects underwent clinically indicated echocardiography for evaluation of potential cardiac symptoms, murmur or increased cardiovascular risk profile, but all showed absence of significant structural or functional abnormalities.

A total of 117 (97%) patients underwent mitral valve surgery at a mean of 85 ± 19 days after the baseline echocardiographic exam. This practice is in line with current guidelines, advocating that early mitral valve surgery may be performed in experienced valve centers with high repair rate for patients presenting with severe organic mitral regurgitation, despite absence of symptoms or LV dysfunction.[2] All-cause mortality was assessed in all operated patients by reviewing patients' medical files and by evaluation of the official Dutch National Survival Registry for patients that were followed by the referring center postoperatively.

Echocardiography

Transthoracic 2D-echocardiography was performed in left lateral decubitus position using commercially available ultrasound systems (System-5, Vivid-7 and E9, GE-Vingmed, Milwaukee, WI) equipped with a 3.5 MHz transducer. ECG-triggered standard 2D gray-scale and color-Doppler images were acquired in cine-loop format and transferred to a workstation for off-line analysis (EchoPAC 110.0.0, GE Medical Systems, Horten, Norway). Chamber quantification was performed conform to current recommendations.[20] Left atrial anteroposterior linear diameter was measured on 2D left parasternal long axis view. LV and LA volumes were assessed using Simpson biplane method and were indexed to body surface area.[20] LVEF was calculated from LV volumes as recommended. In accordance with recent

guidelines, a multi-parametric integrative approach was used to assess MR severity (additional transesophageal images were used when available).[21] In particular, an effective regurgitant orifice area ≥40 mm² or regurgitant volume ≥60 ml, using the proximal isovelocity surface area method (PISA), as well as the presence of flail mitral leaflet or ruptured papillary muscle defined severe mitral regurgitation. If none of these factors were present or PISA was not feasible (due to excentricity of regurgitant jet), presence of vena contracta width ≥7 mm in combination with ≥1 qualitative (large central jet, severe coanda effect, large flow convergence radius, dense mitral envelope at continuous wave Doppler) and/or semi-quantitative (pulmonary Doppler systolic venous flow reversal, E wave dominance ≥1.5 m/s) variable(s) defined severe mitral regurgitation.[21] MR etiology was categorized as flail (free mitral leaflet edge reversing into the LA), prolapse (mitral leaflet coaptation line behind annular plane without edge reversing into LA) or degenerative (degenerative mitral valve abnormalities without flail or prolapse).[20] All Doppler measurements represented the average of 3 beats and 5 beats if atrial fibrillation was present. Mitral inflow was analyzed to assess early flow (E wave), deceleration time and mitral valve pressure gradient.[22] Early diastolic peak velocity (E`) was derived from the lateral wall on the apical four-chamber view color tissue Doppler acquisition. Systolic pulmonary arterial pressure at rest was calculated using the maximal tricuspid regurgitant jet velocity and right atrial pressure estimation, based on diameter and respiratory variation of the inferior caval vein.[20]

Left atrial function: volumetric indices

LA volumes were assessed just before mitral valve opening (maximal LA volume, Vol_{max}), at mitral valve closure (minimal LA volume, Vol_{min}) and at P-wave onset on ECG just before atrial contraction, if sinus rhythm (pre-A LA volume, Vol_P). As previously reported, LA reservoir function was calculated as LA expansion index (Vol_{max} - Vol_{min} / Vol_{min} x 100), LA conduit function as LA passive emptying fraction (Vol_{max} - Vol_P / Vol_{max} x 100) and LA contractile function as LA active emptying fraction (Vol_P - Vol_{min} / Vol_P x 100).[14,17] In patients with atrial fibrillation, LA contractile function could not be calculated.

Left atrial function: deformation indices

LA longitudinal strain and strain rate was assessed with 2D-speckle tracking analysis with QRS onset as the reference point, applying a commercially available LV strain software package on the LA (EchoPAC 110.0.0).[23] In summary, the region of interest was adjusted to include the LA myocardium in both the four-chamber and two-chamber apical views that included both the LA and LV. Manual correction was performed to optimize tracking results if needed. The values of LA strain and strain

rate were calculated as the average value of the four-chamber and two-chamber view, as described in Figure 1. As previously reported, LA reservoir function was calculated as peak systolic LA strain (LA reservoir strain), while LA contractile function was measured as the LA strain value at P-wave onset on ECG, if sinus rhythm (LA contractile strain). Finally, LA conduit function was assessed as the difference between LA reservoir and contractile strain (LA conduit strain).[15] In addition**,** LA reservoir strain rate was measured as peak systolic positive value, LA conduit strain rate as the early diastolic negative peak and LA contractile strain rate as the late diastolic negative peak (if in sinus rhythm) (Figure 1). In patients with atrial fibrillation, LA contractile strain (rate) could not be calculated.

Fifteen subjects were randomly selected to perform a blinded inter- and intra-observer (one week after the first observation) agreement test for LA strain measurements.

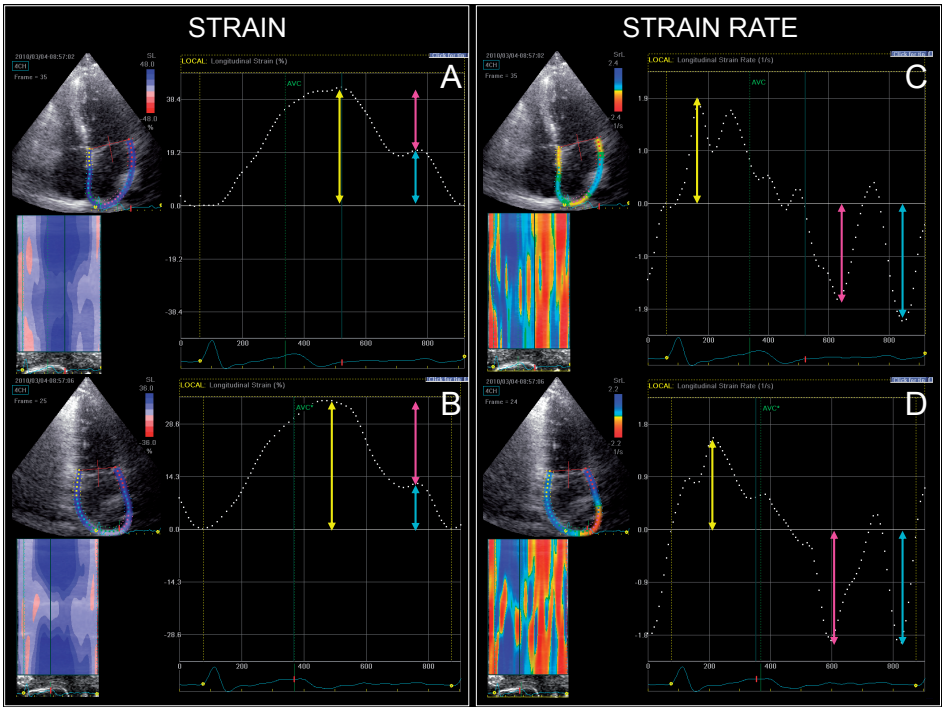

Figure 9.1
Assessment of left atrial phasic function by 2D-speckle tracking echocardiography in a control subject. Panel A: four-chamber longitudinal strain, panel B: two-chamber longitudinal strain, panel C: four-chamber longitudinal strain rate, panel D: two-chamber longitudinal strain rate. The white dotted line represents the mean value of the tracked left atrial segments. Reservoir, conduit and contractile phase are represented by color-coded arrows (yellow, pink and blue respectively). Measurements are averaged over the four-chamber and two-chamber views. In this subject, reservoir, conduit, and contractile strain and strain rate were 38.6%, -22.1%, -16.5% and 1.75 s^{-1}, -1.8 s^{-1}, -2.0 s^{-1} respectively.

For simplicity reasons, the absolute deformation values were reported as positive numbers.

Statistical analysis

Continuous variables were presented as mean ± standard deviation and compared with independent Student-t test and Mann-Whitney or Kruskal-Wallis tests if not normally distributed. Percentages were used for categorical values and compared by χ^2-test. Multiple group comparisons were performed with one-way ANOVA test with post hoc Bonferroni test. Receiver-operating characteristic (ROC) analysis was performed to assess the accuracy of various deformation and volumetric indices of LA function to predict presence of conventional indications for mitral surgery. The optimal cut-off value was obtained by maximizing the sum of sensitivity and specificity. Subsequently, multiple logistic regression analysis identified independent predictors of the presence of mitral surgery indications. Covariates with a significance $p<0.05$ at univariate level were included in the multivariate logistic regression analysis, which was performed using a backward elimination approach. In addition, Cox regression analysis including conventional guidelines-based criteria for mitral surgery and LA reservoir strain was performed to identify the independent determinants of long-term mortality after mitral surgery. To maximize the possibility to detect any relationship of this clinical model with post-operative mortality, covariates with univariate significance of $p<0.10$ were introduced in the multivariate analysis. Kaplan-Meier curves were constructed to explore differences in long-term survival after mitral valve surgery in different patient subgroups that were stratified according to LA reservoir strain, using the previously mentioned ROC curve-based cut-off value and compared by log-rank test. The incremental value of successive conventional guidelines-based criteria for mitral surgery and LA reservoir strain to predict postoperative mortality was assessed with the likelihood ratio test: the model containing the covariate of interest was tested against the nested model not containing the covariate. Finally, linear regression analysis was performed to explore the correlation between LA reservoir strain, LA diameter and LA volume indexed to body surface area (LAVI) respectively. Statistical analysis was performed using SPSS version 17.0. (SPSS Inc., Chicago, Illinois) and STATA version 12.1 (STATA Corp., College Station, Texas) software. All tests were two-sided and a p-value of <0.05 was considered statistically significant.

RESULTS

Patient population

A total of 160 patients with chronic severe organic MR who underwent complete clinical and echocardiographic examination were included. Thirty-nine patients (24%) with poor acoustic window were excluded. Mean frame rate for echocardiographic exams performed within the first half of the last decade did not significantly differ from those performed during the most recent half (56.4 frames/s versus 59.4 frames/s, respectively, p=0.31). Clinical and echocardiographic characteristics of the remaining 121 patients (mean age 63 ± 13 years, 77% men) are summarized in Table 1. Overall, a preserved LV systolic function was observed, with mild LV dilatation and severe LA dilatation. Severe mitral regurgitation was documented with a mean mitral vena contracta width of 8 ± 0.9 mm, E wave 1.3 ± 0.2 m/s and PISA radius of 11 ± 2 mm. Forty-six patients did not have any conventional criterion for mitral surgery indication whereas 75 patients had ≥1 criterion. In particular, symptoms were present in 34 (28%) patients, LVEF ≤60 % in 19 (16%) patients, LV end-systolic diameter ≥40 mm in 27 (22%) patients, atrial fibrillation in 26 (21%) patients and systolic pulmonary arterial pressure at rest >50 mmHg in 29 (24%) patients. Of note, no patients presented with LVEF ≤30 %. By definition, presence of atrial fibrillation, NYHA class III and IV, LV end-systolic diameter, LVEF and pulmonary arterial pressure significantly differed between patients with conventional criteria for mitral surgery versus patients without (Table 1). In addition, age, use of β-blockers, use of diuretics, LAVI, MR vena contracta width, E wave and deceleration time were significantly different between both groups (all $p<0.05$).

Left atrial function in severe mitral regurgitation

Patients with severe organic MR showed significantly impaired LA reservoir function as compared to control subjects, assessed both by volumetric expansion index or strain and strain rate (all $p<0.001$), as indicated in Table 2. In addition, LA conduit function assessed with volumetric passive emptying fraction (p=0.20) or LA strain rate (p=0.57) did not differ significantly between patients with severe organic MR and controls, whereas LA strain was significantly impaired only in patients with severe organic MR (p=0.01). In 95 (79%) patients who were in sinus rhythm during echocardiography, LA contractile function was reduced when measured by volumetric active emptying function, LA strain and strain rate (all $p<0.001$).

Table 9.1
Baseline characteristics of controls and the overall study population with dichotomization according to presence or absence of mitral surgery indication.

Variable	Controls (n=70)	All Patients (n=121)	No surgical indication (n=46)	Surgical indication (n=75)	p *
Clinical characteristics					
Age, years	63 ± 12	63 ± 13	59 ± 14	66 ± 11	0.008
Men, n (%)	47 (67)	77 (64)	32 (70)	45 (60)	0.30
BSA, kg/m²	1.9 ± 0.21	1.9 ± 0.20	1.9 ± 0.21	1.9 ± 0.20	0.80
AF, n (%)	0 (0)	26 (21)	0 (0)	26 (35)	< 0.001
NYHA class, n (%)					< 0.001
I	70 (100)	38 (32)	20 (43)	18 (24)	
II	0 (0)	49 (40)	26 (57)	23 (31)	
III	0 (0)	30 (25)	0 (0)	30 (40)	
IV	0 (0)	4 (3)	0 (0)	4 (5)	
Hypertension, n (%)	31 (45)	11 (10)	4 (10)	7 (11)	1.00
Hypercholesterolemia, n (%)	20 (29)	11 (10)	4 (10)	7 (11)	1.00
Diabetes, n (%)	9 (13)	4 (3)	0 (0)	4 (5)	0.30
Smoking history, n (%)	25 (43)	21 (21)	7 (18)	14 (23)	0.20
Medication use, n (%)					
β-Blocker	8 (12)	41 (34)	8 (17)	33 (44)	0.003
Diuretic	9 (13)	36 (30)	7 (15)	29 (39)	0.006
ACE-I/ARB	22 (32)	54 (45)	17 (37)	37 (49)	0.20
Statin	21 (31)	20 (17)	5 (11)	15 (20)	0.20
MR etiology					0.13
Degenerative	-	7 (6)	1 (2)	6 (8)	
Flail	-	40 (33)	12 (26)	28 (37)	
Prolapse	-	74 (61)	33 (72)	41 (55)	
Echocardiographic data					
LVESD, mm	25.2 ± 4.1	34.8 ± 6.4	31.9 ± 4.5	36.6 ± 6.7	< 0.001
LVEDVI, mL/m²	55 ± 11	85 ± 21	84 ± 18	87 ± 23	0.70
LVESVI, mL/m²	20 ± 6	28 ± 11	25 ± 7	30 ± 13	0.20
LVEF, %	64 ± 6	68 ± 8	70 ± 5	66 ± 9	0.047
LA diameter, mm	35 ± 4	49 ± 8	46 ± 6	50 ± 8	0.001
LAVI, mL/m²	31 ± 8	76 ± 33	64 ± 23	83 ± 36	0.002
Vena contracta, mm	1.7 ± 1.25	8.0 ± 0.92	7.6 ± 0.81	8.2 ± 0.91	<0.001
E wave, m/s	0.6 ± 0.2	1.3 ± 0.2	1.2 ± 0.2	1.4 ± 0.2	<0.001
E'	7.3 ± 2.0	8.5 ± 2.1	8.5 ± 1.6	8.6 ± 2.4	0.9
DT, ms	218 ± 49	180 ± 43	189 ± 34	174 ± 47	0.01
PAPsys at rest, mmHg	26 ± 5	43 ± 16	32 ± 8	49 ± 17	<0.001

ACE-I/ARB: angiotensin-converting enzyme / angiotensin receptor blocker, AF: atrial fibrillation, BSA: body surface area, DT: deceleration time, EDVI: end-diastolic volume indexed to BSA, EF: ejection fraction, ESD: end-systolic diameter, ESVI: end-systolic volume indexed to BSA, LAVI: left atrial volume indexed to BSA, LV: left ventricle, MR: mitral regurgitation, NYHA: New York Heart Association, PAPsys: systolic pulmonary artery pressure, *: for comparison between patient group with versus without mitral surgery indication

Table 9.2
Phasic left atrial function indices of controls and the overall study population with dichotomization according to presence or absence of mitral surgery indication.

Left atrial function variable	Controls (n=70)	All patients (n=121)	No surgical indication (n=46)	Surgical indication (n=75)	p *
Reservoir function					
Strain (%)†	31 ± 6.1†	22 ± 8.4 †	27 ± 6.6 †	19 ± 7.7 †	<0.001†
Strain rate (s^{-1}) †	1.25 ± 0.28†	0.95 ± 0.32 †	1.12 ± 0.27	0.85 ± 0.31 †	<0.001†
Expansion index (%)†	191 ± 61†	111 ± 64 †	150 ± 70 †	87 ± 46 †	<0.001†
Conduit function					
Strain (%)†	17 ± 5.1†	15 ± 5.0 †	17 ± 4.7†	13 ± 4.7 †	<0.001†
Strain rate (s^{-1}) †	1.08 ± 0.38†	1.0 ± 0.32†	1.14 ± 0.34†	0.98 ± 0.32 †	0.04†
Passive emptying fraction (%)†	35 ± 9.9†	34 ± 9.6†	37 ± 9.9†	33 ± 9.1 †	<0.001†
Contractile function ‡					
Strain (%)†	14 ± 3.0†	9.2 ± 3.5 †	10 ± 3.5 †	8 ± 3.4 †	0.03†
Strain rate (s^{-1}) †	1.65 ± 0.55†	1.04 ± 0.39 †	1.15 ± 0.4 †	0.94 ± 0.35 †	0.06†
Active emptying fraction (%)†	44 ± 9.4†	28 ± 11 †	32 ± 12 †	24 ± 10 †	0.001†

All deformation indices are presented as positive absolute numbers. *: p-value for comparison between patient group without versus with mitral surgery indication, †: p<0.05 for comparison with controls, ‡: patients in sinus rhythm only

Left atrial function to predict surgical indication

As summarized in Table 2, LA dysfunction was more pronounced in patients with mitral surgery indications versus patients without and all phases of LA function (reservoir, conduit and contractile) were affected, either assessed by volumetric or deformation parameters. Patients without mitral surgery indications showed impairment of LA reservoir and contractile function but preserved conduit function.

Subsequently, ROC analysis was performed to determine the value of all different deformation and volumetric indices of phasic LA function to predict the presence of guidelines-based mitral surgery indications (Table 3). This analysis showed that LA reservoir strain had the highest predictive value among all LA function indices, evidenced by an area under the curve of 0.80 (CI 95% 0.72-0.87, Figure 2A). In particular, a value of LA reservoir strain ≤24 % predicted the presence of mitral surgery indications with a sensitivity and specificity of 76% and 72%, respectively (Figure 2B).

LA reservoir strain was therefore implemented into further analysis to explore the independent predictive value of LA function for the presence of mitral surgery indications in patients with severe organic MR. Univariate logistic regression analysis showed that age (OR 1.04, 95% CI 1.01-1.07, p=0.01), use of β-blockers (OR 3.7, 95% CI 1.5-9.1, p=0.004), use of diuretics (OR 3.5, 95% CI 1.4-8.9, p=0.008),

Table 9.3
Receiver operating characteristic analysis to assess predictive value for presence of conventional guidelines-based mitral surgical indication(s).

Parameter	ROC AUC	95% CI
Reservoir function		
Strain (%)	0.80	0.72-0.87
Strain rate (s^{-1})	0.75	0.66-0.84
Expansion index (%)	0.79	0.71-0.87
Conduit function		
Strain (%)	0.73	0.64-0.82
Strain rate (s^{-1})	0.66	0.56-0.76
Passive emptying fraction (%)	0.60	0.49-0.71
Contractile function*		
Strain (%)	0.65	0.54-0.76
Strain rate (s^{-1})	0.66	0.55-0.77
Active emptying fraction (%)	0.70	0.59-0.81

Positive absolute numbers for all deformation indices were used. AUC: area under curve, CI: confidence interval, ROC: receiver operating characteristic, *: measured only in 95 out of 121 patients in sinus rhythm.

LAVI (OR 1.02, 95% CI 1.01-1.04, p=0.003), MR vena contracta width (OR 2.29, 95% CI 1.43-3.66, p=0.001) and LA reservoir strain (OR 0.86 95% CI 0.81-0.92, p<0.001) were significantly related to the presence of mitral surgery indications in patients with severe MR. Multivariate logistic regression analysis subsequently identified LA reservoir strain as an independent predictor of the presence of mitral surgery indication (OR 0.88, 95% CI 0.82-0.94, p<0.001), together with MR vena contracta width (OR 2.04, 95% CI 1.21-3.47, p=0.008) and use of β-blocker (OR 3.2, 95% CI 1.2-8.7, p=0.03). Each 1% decrease in LA reservoir strain increased the risk of having an indication for mitral surgery by 12%.

Left atrial strain and long-term survival after mitral valve surgery

After a median follow-up of 6.4 years (interquartile range 4.7-8.7 years) after mitral valve surgery, all-cause mortality occurred in 20 out of the 117 operated patients (17%). Cox regression analysis, restricted to LA function (reservoir strain) and remodeling parameters (LA diameter and LAVI), together with conventional criteria for mitral surgery, indicated that LA reservoir strain, using the ≤24 % cut off value (HR 3.8, p=0.04, CI 1.10-12.93), and symptoms (HR 2.3, p=0.07, CI 0.94-5.71) were related to long-term mortality after mitral valve surgery. In addition, LA diameter ≥55 m or LAVI ≥60 mL/m^2 did not show significant relation with postoperative mortality.[3,4] At multivariate level, only LA reservoir strain (HR 3.5, p=0.045, CI 1.03-12.20) showed to be independently related to mortality (Table

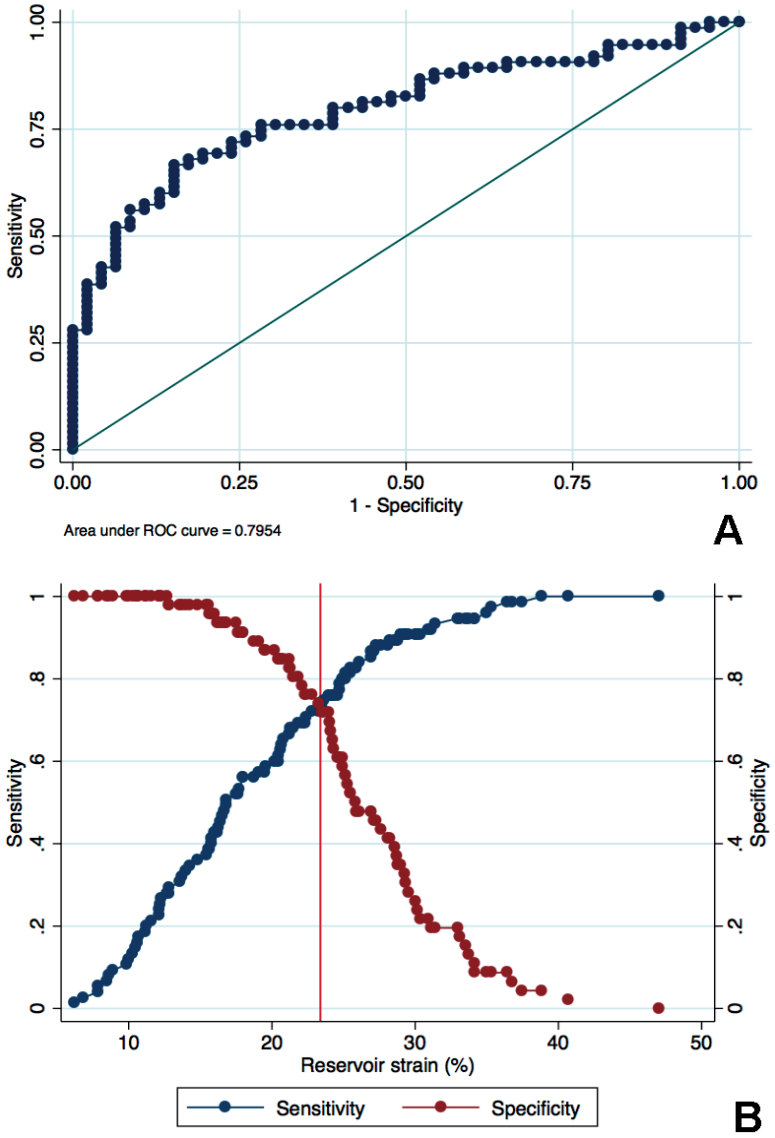

Figure 9.2
Left atrial reservoir strain to predict the presence of mitral surgery indication in patients with severe mitral regurgitation. Panel A: receiver operating characteristic curve. Panel B: sensitivity-specificity curve with vertical line indicating a reservoir strain cut-off value of ≤24 % to predict presence of surgical indication with sensitivity of 76 % and specificity of 72 %.

4). In addition, likelihood ratio test indicated that assessment of LA reservoir strain, using the cut-off value, on top of assessment of conventional guidelines-based indications for mitral surgery provides significant incremental value to predict long-term postoperative mortality (p=0.03). (Figure 3)

Table 9.4
Cox regression analysis for postoperative all-cause mortality. The relation of currently recommended clinical and echocardiographic variables for decision-making in severe organic mitral regurgitation with long-term postoperative mortality is explored.

	Univariate			Multivariate		
Variables	HR	(95% CI)	p	HR	(95% CI)	p
Symptoms (NYHA 3 or 4)	2.3	0.94-5.71	0.07	2.1	0.86-5.26	0.10
LVEF ≤60 %	1.1	0.31-3.63	0.93			
LVESD ≥40 mm	2.0	0.77-4.96	0.16			
Atrial fibrillation	1.8	0.70-4.87	0.21			
PAPsys at rest >50 mmhg	1.2	0.46-3.20	0.67			
LA diameter ≥55 mm	2.5	0.57-10.8	0.23			
LA volume index ≥60 mL/m2	1.8	0.58-5.35	0.32			
LA reservoir strain ≤24 %	3.8	1.10-12.93	0.04	3.5	1.03-12.20	0.045

CI: confidence interval, HR: hazard ratio, LA: left atrial, LVEF: left ventricular ejection fraction, LVESD: left ventricular end-systolic diameter, NYHA: New York Heart Association, PAPsys: systolic arterial pulmonary artery pressure.

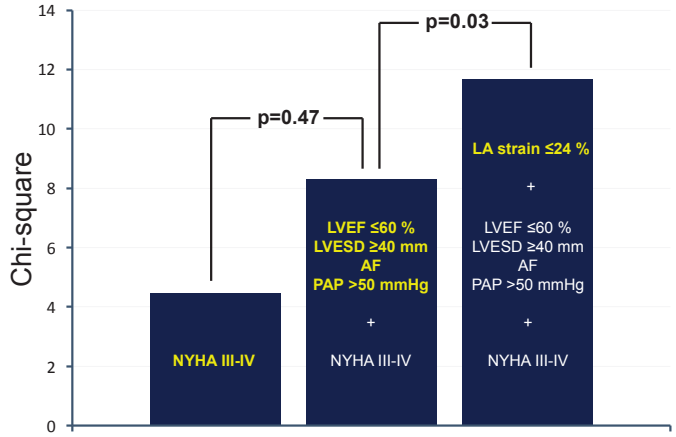

Figure 9.3
Likelihood ratio test for prediction of long-term mortality after mitral valve surgery. Left atrial reservoir strain shows incremental value to predict long-term postoperative mortality in severe organic mitral regurgitation when assessed on top of conventional guidelines-based indications for surgery. AF: atrial fibrillation, LVEF: left ventricular ejection fraction, LVESD: left ventricular end-systolic diameter, NYHA: New York Heart Association, PAP: systolic pulmonary artery pressure at rest.

Kaplan Meier survival analysis showed that patients with baseline LA reservoir strain values ≤24 % had worse long-term survival compared with patients with LA reservoir strain >24 % (log rank p=0.02) (Figure 3). This association was observed also among asymptomatic patients before mitral surgery (n= 83/117, log rank p=0.04) (Figure 3). Interestingly, a significant trend towards worse survival was observed in 44 out of 117 patients with baseline LA reservoir strain ≤24 % who

underwent early mitral valve surgery despite absence of any conventional surgical indication compared to patients with LA reservoir strain >24 % (log rank p=0.06) (Figure 4).

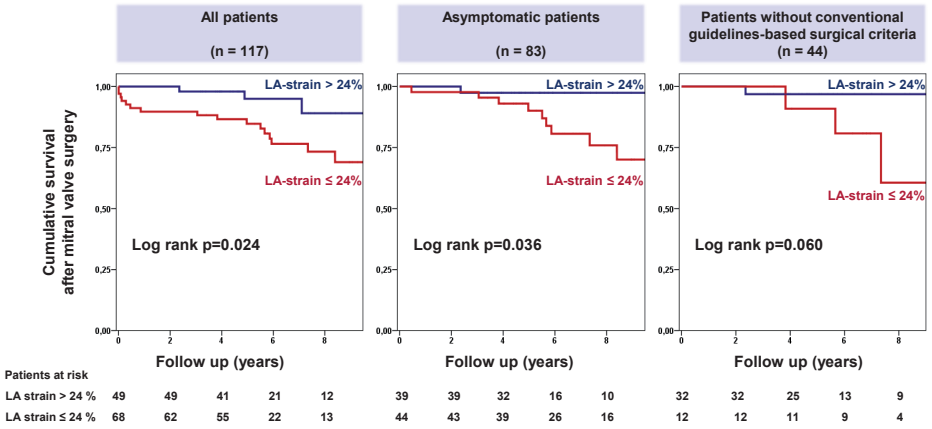

Figure 9.4

Kaplan-Meier survival after mitral valve surgery according to left atrial reservoir strain. Conventional surgical criteria: symptoms, left ventricular (LV) ejection fraction ≤60 %, LV end-systolic diameter ≤40 mm, atrial fibrillation and/or systolic arterial pulmonary pressure at rest >50 mmHg. LA: left atrial.

Left atrial reservoir strain versus diameter and volume

LA reservoir strain showed significant linear correlation with LA diameter (R -0.57, R^2 0.33, p<0.001, 95% CI -0.79 to -0.46) and LAVI (R -0.57, R^2 0.32, p<0.001, 95% CI -0.18 to -0.11) (Figure 5). However, 47 out of 98 patients (48%) with LA diameter <55 mm and 15 out of 44 patients (34%) with LAVI <60 mL/m^2 had LA reservoir strain ≤24 % (Figure 5).

Observer variability

Bland-Altman analysis showed an intra-observer bias of 1.1% (95% CI -4.2 to 6.4%), -0.02% (95% CI -5,1 to 5.0%) and -1.1% (95% CI -4.5 to 2.3%) for LA reservoir, conduit and contractile strain assessment, respectively. Similarly, respective inter-observer biases of -1.3% (95% CI -6.6 to 3.9%), 1.2% (95% CI -2.8 to 5.1%) and 0.1% (95% CI -4.1 to 4.3%) were noted.

DISCUSSION

The main findings of current study can be summarized as follows: 1) patients with chronic severe organic MR are characterized by overall impaired LA reser-

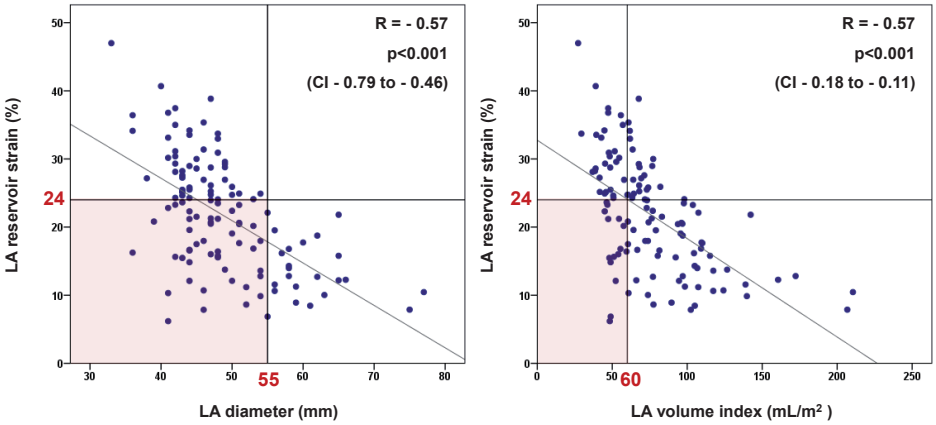

Figure 9.5

Correlation between left atrial reservoir strain, diameter and indexed volume. LA reservoir strain ≤24 % (associated with worse survival after mitral valve surgery) is present in 48% and 34% of patients despite LA diameter <55 mm and LAVI <60 mL/m^2, respectively (purple squares).

voir, conduit and contractile function, 2) LA reservoir strain is an accurate and independent predictor of the presence of conventional guidelines-based mitral surgery indications and 3) LA reservoir strain relates to long-term survival after mitral valve surgery, independently of and incremental to current conventional guidelines-based mitral surgery indications.

Phasic LA function in severe MR

LA reservoir function

During LV systole, pulmonary venous inflow distends the LA, which acts as a reservoir by storing energy under the form of pressure.[14] LA reservoir function is mainly determined by LA compliance (stiffness) and LV systolic function (systolic apical motion of the LV base, facilitating LA filling), and to a lesser extent by right ventricular systole (pulmonary venous inflow). [13,14,24] While increased LA reservoir function has been reported in mild MR, due to an initial increase in LA compliance,[1,9,10] decreased LA reservoir function has been described in patients with severe MR, as assessed with several imaging techniques. [9,10,12] Similarly, the current study showed that severe MR is associated with a significant reduction in LA reservoir function.

Reduced LV systolic function may lead to impaired LA reservoir function as previously demonstrated.[24] However, in the present study LV ejection fraction was preserved in the majority of the patients and therefore this factor may not explain per se the impairment of LA reservoir function.

Furthermore, significant ultra-structural changes of the LA myocardium, including presence of interstitial fibrosis, myocyte hypertrophy, chronic inflammatory changes and decreased capillary density have been reported in patients with severe MR and might cause the reduction in LA reservoir function.[5-7,25] In particular, a recent study on 46 severe MR patients that underwent mitral valve surgery showed a strong negative correlation between histological LA fibrosis and LA reservoir strain.[26] Ultra-structural changes are due to the chronic volume overload and increased LV filling pressures and significantly affect LA myocardial wall properties, such as relaxation and compliance (stiffness), ultimately leading to the observed reduction in LA reservoir function.[3]

LA conduit function

Following the reservoir phase, the LA functions as a conduit during early diastole, allowing for a passive transfer of blood from the pulmonary veins towards the LV. LA conduit function is mainly determined by LA elasticity (recoil) and afterload (LV relaxation and early LV filling pressure).[13,14] In the current study, reduced LA conduit function was observed in patients with severe MR and mitral surgery indication. Increased early diastolic LV filling pressures have been reported in subjects with MR, due to increased atrio-ventricular pressure gradient, increased LV stiffness and decreased LA recoil, and might therefore be an explanation of impaired LA conduit function in these patients.[9,25,27] In addition, ultra-structural changes of the LA wall may cause impaired LA elasticity, reducing LA recoil and affecting LA conduit function.[3,12]

LA contractile function

In patients in sinus rhythm, active LA contraction finalizes LV filling during late diastole and depends on LA afterload (LV compliance and end-diastolic filling pressure) and LA intrinsic contractility, following Starling's law.[13,14,28] Improved LA contractile function has been reported in patients with mild MR and may be explained by the fact that LA myocardial wall operates higher on the Frank-Starling curve (larger LA volumes leads to higher contractility).[9,10,28] In the current study, including severe organic MR patients, impaired LA contractile function assessed with speckle tracking echocardiography was observed. This finding may be related to the presence of a decreased LA contractility, due to exhaustion of the Frank-Starling mechanism by severe volume overload and to ultra-structural alterations of the atrial myocardium. Moreover, increased LA afterload may have also contributed to the impairment of LA contractile function, since increased LV end-diastolic filling pressures have been observed in the presence of severe MR.[28]

LA reservoir strain and mitral surgical indication

Optimal timing of surgical treatment of severe organic MR is crucial, particularly in asymptomatic patients.[2] Current guidelines recommend mitral valve surgery based on the presence of symptoms, LV systolic dysfunction, atrial fibrillation or pulmonary hypertension, which reflect MR severity and its impact on cardiac performance and symptomatic status.[2,19] However, severe MR primarily affects the LA causing significant LA dysfunction and remodeling, which implies that LA characteristics may indicate the hemodynamic implications of severe MR at an earlier stage than conventional criteria for surgical indication.[30] The predictive value of LA reservoir strain observed in the present evaluation might be explained by the fact that reduced LA compliance, and therefore impaired LA reservoir function, is directly related to the duration and severity of MR and represents an important substrate for the occurrence of symptoms, atrial fibrillation or the development of pulmonary hypertension. In fact, decreased atrial compliance due to increased LA stiffness may cause inadequate LA pressure homeostasis. Therefore small increases in LA volume may lead to significant increases of LA and pulmonary artery pressures, which can be associated with the development of pulmonary hypertension and symptoms during exercise.[13] This has been demonstrated in other clinical conditions, for example in patients with diastolic heart failure.[29] Reduced LA reservoir strain, and not LA volume, was shown to be associated with the presence of symptoms and was directly related to atrial stiffness.[29] In addition, LA reservoir strain was demonstrated to be inversely related to LA wall fibrosis (affecting atrial compliance), and to be associated to a higher burden of atrial fibrillation[14]. Finally, at more advanced stages, severe MR may cause LV systolic dysfunction which can decrease LA reservoir function by reduced systolic apical motion of the LV base.[24]

LA reservoir strain and mortality after mitral valve surgery

The present evaluation showed that LA reservoir strain is related to long-term survival in patients operated for severe organic MR, independently of conventional indications for mitral surgery, including symptoms, LV dysfunction, atrial fibrillation and significant pulmonary hypertension. In particular, LA reservoir strain ≤24 % was associated with increased risk for postoperative mortality. In addition to conventional mitral surgery indications, LA diameter ≥55 mm or LAVI ≥ 60 mL/m² have been recently proposed as additional criteria for indication to mitral surgery as they yield increased mortality under conservative management, but not after mitral valve surgery. We indicated, however, that LA reservoir might be a more sensitive approach than LA diameter or LAVI to detect the impact of MR on cardiac performance, as previously shown in diabetic and hypertensive patients.[8] A significant proportion of patients in fact showed LA reservoir strain <24 %, implying

increased mortality risk after mitral valve surgery, despite LA diameter <55 mm or LAVI <60 mL/m².

Limitations

Some limitations to the current study should be acknowledged: 1) no invasive assessment of LA mechanical properties or afterload was performed to prove the determinants of reduced LA function, which must be the focus of further specific studies; 2) Limited impairment of LA function in the control group of current study can not be excluded, due to a fairly high proportion of subjects with cardiovascular risk factors such as diabetes and hypertension. This population, however, represents a real-life population without presence of overt structural or functional disease and more stringent selection of patients without any risk factors most likely would have only amplified significance of differences in LA function found between controls and severe MR patients. 3) To firmly establish the predictive value of LA reservoir strain independent of conventional indications for mitral surgery, our findings need validation in larger patient cohorts.

CONCLUSION

Severe MR is associated with significant LA dysfunction that strongly relates to presence of conventional indications for mitral surgery and, more important, is associated with long-term postoperative survival. LA dysfunction, measured as reservoir strain, may be a valuable clinical marker for follow-up and decision-making in patients with severe organic MR, irrespective of conventional mitral surgery indications and more sensitive than LA diameter and volume.

REFERENCES

1. Kihara Y, Sasayama S, Miyazaki S et al. Role of the left atrium in adaptation of the heart to chronic mitral regurgitation in conscious dogs. *Circ Res.* 1988;62:543-553.
2. Bonow RO, Carabello BA, Chatterjee K et al. 2008 Focused update incorporated into the ACC/AHA 2006 guidelines for the management of patients with valvular heart disease: a report of the American College of Cardiology/American Heart Association Task Force on Practice Guidelines (Writing Committee to Revise the 1998 Guidelines for the Management of Patients With Valvular Heart Disease): endorsed by the Society of Cardiovascular Anesthesiologists, Society for Cardiovascular Angiography and Interventions, and Society of Thoracic Surgeons. *Circulation.* 2008;118:e523-661.
3. Le Tourneau T, Messika-Zeitoun D, Russo A et al. Impact of left atrial volume on clinical outcome in organic mitral regurgitation. *J Am Coll Cardiol.* 2010;56:570-578.
4. Rusinaru D, Tribouilloy C, Grigioni F et al. Left atrial size is a potent predictor of mortality in mitral regurgitation due to flail leaflets: results from a large international multicenter study. *Circ Cardiovasc Imaging.* 2011;4:473-481.
5. Anne W, Willems R, Roskams T et al. Matrix metalloproteinases and atrial remodeling in patients with mitral valve disease and atrial fibrillation. *Cardiovasc Res.* 2005;67:655-666.
6. Corradi D, Callegari S, Maestri R et al. Differential structural remodeling of the left-atrial posterior wall in patients affected by mitral regurgitation with or without persistent atrial fibrillation: a morphological and molecular study. *J Cardiovasc Electrophysiol.* 2012;23:271-279.
7. Verheule S, Wilson E, Everett Tt et al. Alterations in atrial electrophysiology and tissue structure in a canine model of chronic atrial dilatation due to mitral regurgitation. *Circulation.* 2003;107:2615-2622.
8. Mondillo S, Cameli M, Caputo ML et al. Early detection of left atrial strain abnormalities by speckle-tracking in hypertensive and diabetic patients with normal left atrial size. *J Am Soc Echocardiogr.* 2011;24:898-908.
9. Borg AN, Pearce KA, Williams SG et al. Left atrial function and deformation in chronic primary mitral regurgitation. *Eur J Echocardiogr.* 2009;10:833-840.
10. Cameli M, Lisi M, Giacomin E et al. Chronic mitral regurgitation: left atrial deformation analysis by two-dimensional speckle tracking echocardiography. *Echocardiography.* 2011;28:327-334.
11. Cameli M, Lisi M, Righini FM et al. Left atrial speckle tracking analysis in patients with mitral insufficiency and history of paroxysmal atrial fibrillation. *Int J Cardiovasc Imaging.* 2012;28:1663-1667.
12. Moustafa SE, Alharthi M, Kansal M et al. Global left atrial dysfunction and regional heterogeneity in primary chronic mitral insufficiency. *Eur J Echocardiogr.* 2011;12:384-393.
13. Pagel PS, Kehl F, Gare M et al. Mechanical function of the left atrium: new insights based on analysis of pressure-volume relations and Doppler echocardiography. *Anesthesiology.* 2003;98:975-994.
14. Rosca M, Lancellotti P, Popescu BA et al. Left atrial function: pathophysiology, echocardiographic assessment, and clinical applications. *Heart.* 2011;97:1982-1989.
15. Kim DG, Lee KJ, Lee S et al. Feasibility of two-dimensional global longitudinal strain and strain rate imaging for the assessment of left atrial function: a study in subjects with a

low probability of cardiovascular disease and normal exercise capacity. *Echocardiography*. 2009;26:1179-1187.
16. Saraiva RM, Demirkol S, Buakhamsri A et al. Left atrial strain measured by two-dimensional speckle tracking represents a new tool to evaluate left atrial function. *J Am Soc Echocardiogr.* 2010;23:172-180.
17. Vianna-Pinton R, Moreno CA, Baxter CM et al. Two-dimensional speckle-tracking echocardiography of the left atrium: feasibility and regional contraction and relaxation differences in normal subjects. *J Am Soc Echocardiogr*. 2009;22:299-305.
18. Motoki H, Dahiya A, Bhargava M et al. Assessment of left atrial mechanics in patients with atrial fibrillation: comparison between two-dimensional speckle-based strain and velocity vector imaging. *J Am Soc Echocardiogr*. 2012;25:428-435.
19. Joint Task Force on the Management of Valvular Heart Disease of the European Society of Cardiology, European Association for Cardio-Thoracic Surgeons, Vahanian A, Alfieri O, Andreotti F et al. Guidelines on the management of valvular heart disease (version 2012). *Eur Heart J.* 2012;33:2451-2496.
20. Lang RM, Bierig M, Devereux RB et al. Recommendations for chamber quantification: a report from the American Society of Echocardiography's Guidelines and Standards Committee and the Chamber Quantification Writing Group, developed in conjunction with the European Association of Echocardiography, a branch of the European Society of Cardiology. *J Am Soc Echocardiogr*. 2005;18:1440-1463.
21. Lancellotti P, Moura L, Pierard LA et al. European Association of Echocardiography recommendations for the assessment of valvular regurgitation. Part 2: mitral and tricuspid regurgitation (native valve disease). *Eur J Echocardiogr.* 2010;11:307-332.
22. Nagueh SF, Appleton CP, Gillebert TC et al. Recommendations for the evaluation of left ventricular diastolic function by echocardiography. *J Am Soc Echocardiogr*. 2009;22:107-133.
23. Mor-Avi V, Lang RM, Badano LP et al. Current and evolving echocardiographic techniques for the quantitative evaluation of cardiac mechanics: ASE/EAE consensus statement on methodology and indications endorsed by the Japanese Society of Echocardiography. *J Am Soc Echocardiogr*. 2011;24:277-313.
24. Barbier P, Solomon SB, Schiller NB et al. Left atrial relaxation and left ventricular systolic function determine left atrial reservoir function. *Circulation*. 1999;100:427-436.
25. Zile MR, Tomita M, Nakano K et al. Effects of left ventricular volume overload produced by mitral regurgitation on diastolic function. *Am J Physiol*. 1991;261:H1471-1480.
26. Cameli M, Lisi M, Righini FM et al. Usefulness of atrial deformation analysis to predict left atrial fibrosis and endocardial thickness in patients undergoing mitral valve operations for severe mitral regurgitation secondary to mitral valve prolapse. A*m J Cardiol*. 2013;111:595-601.
27. Katayama K, Tajimi T, Guth BD et al. Early diastolic filling dynamics during experimental mitral regurgitation in the conscious dog. *Circulation*. 1988;78:390-400.
28. Sasayama S, Takahashi M, Osakada G et al. Dynamic geometry of the left atrium and left ventricle in acute mitral regurgitation. *Circulation*. 1979;60:177-186.
29. Kurt M, Wang J, Torre-Amione G et al. Left atrial function in diastolic heart failure. *Circ Cardiovasc Imaging* 2009;2:10-15.
30. Messika-Zeitoun D, Bellamy M, Avierinos JF et al. Left atrial remodelling in mitral regurgitation--methodologic approach, physiological determinants, and outcome implications:

a prospective quantitative Doppler-echocardiographic and electron beam-computed tomographic study. *Eur Heart J*. 2007;28:1773-1781.

Chapter 10

Global longitudinal strain and left atrial volume index improve prediction of appropriate implantable cardioverter defibrillator therapy in hypertrophic cardiomyopathy patients

Philippe Debonnaire, Joep Thijssen, Darryl P Leong, Emer Joyce, Spyridon Katsanos, Georgette E Hoogslag, Martin J Schalij, Douwe E Atsma, Jeroen J Bax, Victoria Delgado, Nina Ajmone Marsan

Int J Cardiovasc Imaging, 2014 Mar 30(3): 549-558.

ABSTRACT

Objectives

Accurate predictors of appropriate implantable cardioverter defibrillator (ICD) therapy in hypertrophic cardiomyopathy (HCM) patients are lacking. Both left atrial volume index (LAVI) and global longitudinal strain (GLS) have been proposed as prognostic markers in HCM patients. The specific value of LAVI and GLS to predict appropriate ICD therapy in high-risk HCM patients was studied.

Methods and Results

LAVI and 2-dimensional speckle tracking-derived GLS were assessed in 92 HCM patients undergoing ICD implantation (69% men, mean age 50±14 years). During long-term follow-up, appropriate ICD therapies, defined as antitachycardia pacing and/or shock for ventricular arrhythmia, were recorded.

Appropriate ICD therapy occurred in 21 patients (23%) during a median follow-up of 4.7 (2.2-8.2) years. Multivariate analysis revealed LAVI (p=0.03) and GLS (p=0.04) to be independent predictors of appropriate ICD therapy. Both LAVI and GLS showed higher accuracy to predict appropriate ICD therapy compared to presence of ≥1 conventional sudden cardiac death (SCD) risk factor(s) [area under the curve 0.76 (95%CI:0.65-0.87) and 0.65 (95%CI:0.54-0.77) versus 0.52 (95%CI:0.43-0.58) respectively, p<0.001]. No patient with both LAVI <34mL/m^2 and GLS<-14% experienced appropriate ICD therapy. Assessment of both LAVI and GLS on top of conventional SCD risk factors provided incremental clinical predictive value for appropriate ICD therapy, as shown by likelihood ratio test (p<0.001) and integrated discrimination improvement index (0.17, p<0.001).

Conclusion

LAVI and GLS provide high negative predictive value for appropriate ICD therapy in high-risk HCM patients. Additionally to conventional SCD risk factors, both parameters may be useful to optimize criteria and timing for ICD implantation in these patients.

INTRODUCTION

Implantable cardioverter defibrillator (ICD) is currently recommended in patients with hypertrophic cardiomyopathy (HCM) at high risk for sudden cardiac death.[1] In particular, ICD implantation is a class I indication for secondary prevention in HCM patients who survive cardiac arrest or present with sustained ventricular tachycardia. In addition, the presence of one or more sudden cardiac death (SCD) risk factors, including family history of SCD, left ventricular (LV) hypertrophy ≥30 mm, non-sustained ventricular tachycardia (nsVT), recent unexplained syncope and/or abnormal blood pressure response during exercise testing qualifies patients for ICD implantation as primary prevention.[2] Although appropriate ICD therapy in this high-risk population occurs at a yearly rate of 3.3%, inappropriate ICD therapy or other device-related complications are seen in 4.8% and 3.4% of patients per year, respectively.[3] Hence, weighting risk-benefit of ICD implantation in HCM patients is of paramount importance and has created a currently unmet clinical need for accurate predictors of appropriate ICD therapy that may optimize candidate selection and timing criteria for ICD implantation.[2, 4]

Impaired myocardial mechanics are commonly observed in HCM patients, despite normal LV ejection fraction.[5, 6] Global longitudinal strain (GLS), which reflects the active deformation of all LV myocardial segments, has been proposed as a sensitive marker of LV systolic function and can be currently quantified by speckle tracking echocardiography.[7] In addition, HCM patients are often characterized by abnormal myocardial relaxation and significant LV diastolic dysfunction, ultimately resulting in increased left atrial volume index (LAVI).[8] Both GLS and LAVI, as a sensitive marker of LV systolic function and a specific marker of LV diastolic function respectively, have therefore been identified as prognostic factors in HCM patients.[9-14] However, their potential role to predict appropriate ICD therapy is unexplored. Therefore, the aim of our study was 1) to evaluate the value of SCD risk factors, GLS and LAVI to predict appropriate ICD therapy in high-risk HCM patients and 2) to explore whether LAVI and GLS assessment provide incremental prognostic value over SCD risk factors.

METHODS

Patient population

HCM patients who underwent ICD implantation for primary or secondary prevention in our centre during the last decade were evaluated. HCM was defined as presence of a non-dilated and hypertrophic LV with wall thickness ≥15 mm in

the absence of any other cardiac or systemic disease that could account for the magnitude of LV hypertrophy.[2] All patients underwent extensive clinical, electrocardiographic and echocardiographic evaluation before implantation and patients' data were prospectively collected in the departmental Cardiology Information System (EPD-Vision®, Leiden University Medical Center, Leiden, the Netherlands) and retrospectively analyzed. Patients were excluded from the analysis if 2-dimensional (2D) echocardiography was not available prior to ICD implantation. Patients with severe mitral regurgitation or prior extensive myocardial infarction were also excluded.

Clinical data included demographics, medications and identification of comorbidities. Echocardiographic evaluation consisted of conventional measurements and included 2D-speckle tracking echocardiography for LV deformation analysis. The SCD risk profile of HCM patients was determined based on clinical and echocardiographic parameters, according to current guidelines.[2] In particular, conventional SCD risk factors were defined as secondary prevention ICD indication, family history of SCD (≥ one 1st or 2nd degree relative), maximal LV wall thickness ≥30 mm, unexplained syncope or documented nsVT (≥3 beats at ≥120 bpm) prior to ICD implantation. Blood pressure response during exercise testing was not included as it was not part of clinical routine in the early years of our study period. In addition LV resting gradient ≥30 mmHg was determined.

The patient population was dichotomized based on occurrence or absence of appropriate ICD therapy at follow-up and the incremental prognostic value of LAVI and GLS was evaluated over conventional SCD risk factors.

ICD implantation and settings

All defibrillator systems used were implanted via transvenous approach. During the implant procedure, sensing and pacing threshold was determined and defibrillation threshold testing was performed. Used systems were manufactured by Biotronik (Berlin, Germany), Boston Scientific [Natick, MA, USA, formerly CPI, Guidant (St Paul, MN, USA)], Medtronic (Minneapolis, MN, USA), and St Jude Medical/Ventritex (St Paul, MN, USA). The antitachycardia settings in all devices were programmed with three consecutive zones with limits varying slightly per manufacturer: a monitor zone (lower limit between 150-155 bpm; upper limit between 185-190 bpm), an antitachycardia pacing (ATP) shock zone (lower limit between 185-190 bpm; upper limit between 205-210 bpm), and an initial shock zone (≥205-210 bpm). In the monitor zone, no therapy was programmed unless ventricular arrhythmia was detected during follow-up. In the ATP-shock zone, two bursts of ATP were administered and, if arrhythmia continued, defibrillator shocks were used. In case

of ventricular arrhythmia faster than the ATP shock zone, device shocks were the initial therapy. Therapy settings were adapted only when clinically indicated.

Echocardiography

Transthoracic 2D-echocardiography was performed with the patient in left lateral decubitus position using commercially available ultrasound machines (Vivid-5, Vivid-7 and E9, GE-Vingmed, Milwaukee, WI) equipped with a 3.5 MHz transducer. ECG-triggered standard 2D gray-scale and color-Doppler images were acquired in cine-loop format and transferred to a workstation for off-line analysis (EchoPAC 110.0.0, GE Medical Systems, Horten, Norway). Chamber quantification was performed conform to current recommendations.[15] Maximal LV end diastolic wall thickness was assessed by LV evaluation in short axis view at basal, mid and apical level. LV volumes were assessed by Simpson biplane method, indexed to body surface area and used to calculate LV ejection fraction.

Assessment of LV GLS was performed as previously described.[16] In summary, a region of interest covering the LV myocardium in a two-, four- and apical long-axis view was selected to perform automated frame-by-frame 2D-speckle tracking throughout the cardiac cycle. Manual correction was performed to optimize tracking results when appropriate. GLS was calculated as the average peak longitudinal strain value of the two-, four- and apical long-axis view (Figure 1). Mean frame rate for deformation analysis was 61 frames/s.

In addition, end-systolic LA volume was measured using Simpson biplane method and indexed to body surface area. LV diastolic function was analyzed assessing mitral inflow peak E (early diastolic) velocity, peak A (late diastolic) velocity, E/A ratio and deceleration time.[17] In addition, E prime was derived from the lateral wall on a four-chamber color tissue-Doppler acquisition. The presence of a systolic anterior movement of the mitral valve was also evaluated by M-mode imaging at the level of the mitral leaflets in a parasternal long-axis view. Mitral regurgitation severity was semi-quantitatively assessed, based on conventional spectral and color-Doppler echocardiography as recommended.[18] Screening for presence of an intraventricular or LV outflow tract gradient at rest was systematically performed using pulsed wave Doppler and peak gradient was measured by continuous wave Doppler.

Endpoints

Occurrence of appropriate ICD therapy, defined as ATP and/or shock for ventricular tachycardia and/or ventricular fibrillation, was the main endpoint of this study. Inappropriate ICD therapy was noted when ATP and/or shock occurred despite absence of ventricular tachycardia and/or ventricular fibrillation. ICD device in-

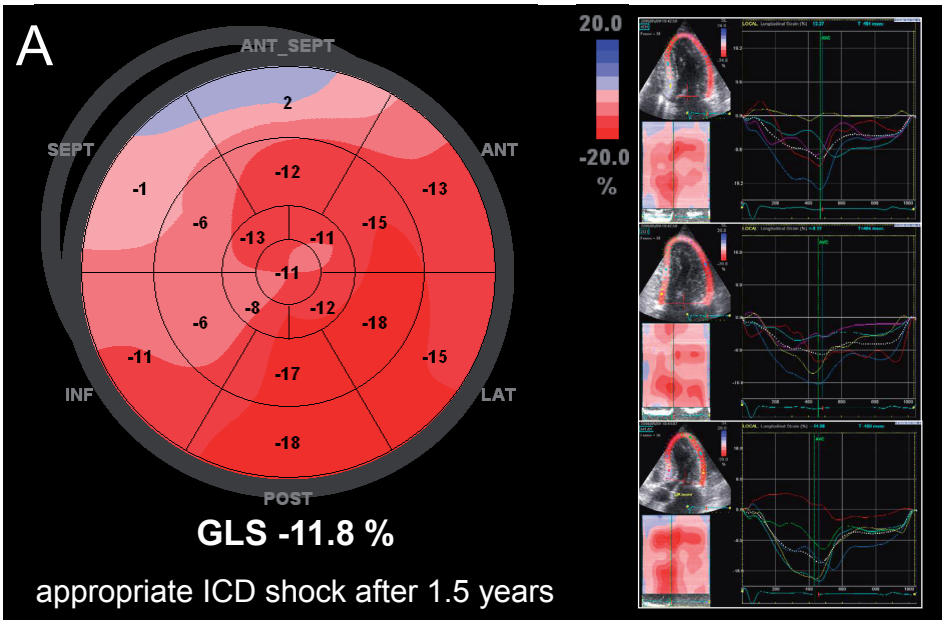

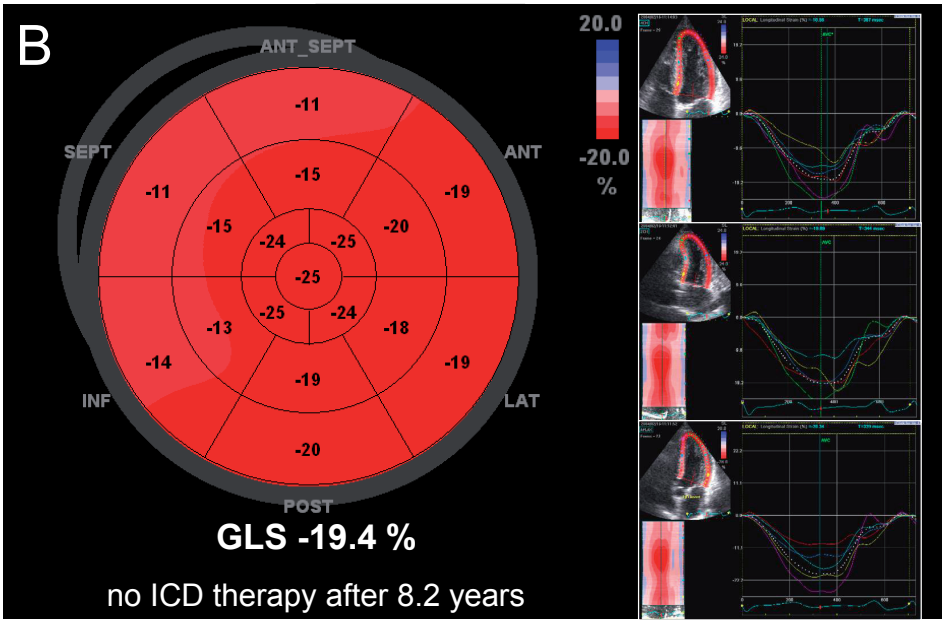

Figure 10.1
Assessment of 2D-speckle tracking global longitudinal strain. Left ventricular (LV) global longitudinal strain (GLS) is calculated as the average of the peak longitudinal strain values obtained in the 3 apical echocardiographic views. The bull's eye view is a color-coded representation of longitudinal strain values of all tracked LV segments (deep red reflects normal strain, light red and blue reduced and severely reduced strain, respectively). Panel A: Impaired GLS in a patient with hypertrophic cardiomyopathy that experienced appropriate implantable cardioverter defibrillator (ICD) therapy. Panel B: Preserved GLS in a patient without appropriate ICD therapy.

terrogation was scheduled every 3-6 months after implantation and data were included until occurrence of the study end point or until last date of ICD check-up during the last year (between February 2011 and March 2012) for patients that did not experience the study endpoint.

Statistics

Continuous variables are presented as mean ± standard deviation when normal and as median with inter-quartile ranges when not normally distributed. Categorical variables are given as absolute numbers and percentages. Baseline characteristics between groups with and without appropriate ICD therapy were evaluated by Student-t test, Kruskall-Wallis or χ^2-test, when appropriate. In order to evaluate the association between SCD risk factors and appropriate ICD therapy, only patients with primary prevention indication were considered, for which incidence rates of appropriate ICD therapy were calculated and expressed per 100-patient years. Difference in incidence rates according to the number of SCD risk factors were tested by Poisson regression, and expressed as incidence rate ratios.

In order to identify parameters potentially associated with appropriate ICD therapy, assessment of independent predictors of appropriate ICD therapy was initially performed using a staged multivariable Cox proportional-hazards regression analysis to avoid model over-fit, given the relatively low incidence of the end point. Significant univariable predictors at a threshold $p<0.2$ were entered in a first multivariable analysis that used a backward elimination approach to identify predictors of appropriate ICD therapy. Variables with $p<0.05$ in the first multivariable model were entered in a second multivariable model, now containing the variables of interest, LAVI and GLS. Second, the predictive value of LAVI and GLS and conventional SCD risk factors was evaluated by receiver operating characteristic (ROC) analysis and comparison of respective areas under the curve (AUC).[19] To define cut-offs from ROC analysis, a high sensitivity (>85%) was stipulated to ensure identification of patients who would experience the endpoint. These cut-offs were used for subsequent analysis. Sensitivity, specificity, negative and positive predictive values for appropriate ICD therapy were calculated for LAVI and GLS, as well as conventional SCD risk factors, assuming a realistic 20% 5-year incidence of appropriate ICD therapy. Kaplan-Meier curves were constructed for LAVI and GLS for survival free of appropriate ICD therapy, and compared by log-rank test. Additionally, the potential incremental value of LAVI and GLS over SCD risk factors to predict appropriate ICD therapy was evaluated by likelihood ratio testing and assessment of integrated discrimination improvement index (IDI). Absolute IDI is a reclassification statistic that studies a new model`s discriminatory improvement to predict the outcome variable (appropriate ICD therapy), calculated by summing

the IDI components (net true predictive probabilities) of cases (patients experiencing appropriate ICD therapy) and controls (patients without appropriate ICD therapy).[20] Finally, a similar explorative analysis was performed to test the relation of both LAVI and GLS with occurrence of inappropriate ICD therapy.

Statistical analysis was performed using SPSS version 17.0. (SPSS Inc., Chicago, Illinois) and STATA version 12 (STATA Corp., College Station, Texas) software. All tests were two-sided and a p-value of <0.05 was considered statistically significant.

RESULTS

Patient population

A total of 92 HCM patients (69% men, mean age 50 ± 14 years) who underwent ICD implantation were included. Baseline characteristics of the study population are summarized in Table 1. Peri-procedural echocardiography was performed at a median of 11 days before ICD implantation and all patients were in sinus rhythm at the time of echocardiographic evaluation. Despite normal LV volumes and preserved LV ejection fraction, mean GLS was impaired in the HCM patients (-13.3 ± 3.5%). In addition, an enlarged LA volume (LAVI) was observed in these patients [39 (31-49) mL/m^2]. A total of 22 patients (24%) that survived prior cardiac arrest, sustained ventricular tachycardia or ventricular fibrillation received an ICD for secondary prevention. The remaining 70 patients (76%) had a primary prevention indication for ICD implantation, based on the presence of ≥1 conventional SCD risk factors (n=63), or on additional factors such as complete heart block (n=1), LV systolic dysfunction (n=1), inducibility of ventricular fibrillation during electrophysiological study (n=3) or abnormal blood pressure response during exercise testing (n=2).

Long-term ICD end points

A total of 21 patients (23%) experienced an appropriate ICD therapy during a median follow-up of 4.7 (2.2-8.2) years (shock only n=6, shock after unsuccessful ATP n=3, ATP only n=12). According to ICD interrogation, appropriate ICD therapy was given for ventricular fibrillation (n=5), fast ventricular tachycardia in the programmed ventricular fibrillation zone (n=12) or ventricular tachycardia in the programmed ventricular tachycardia zone (n=4).

As shown in Table 1, patients presenting with versus without appropriate ICD therapy were more likely to be men (p=0.02) and were characterized by more impaired GLS (p=0.03) and increased LAVI (p<0.001). The overall HCM risk profile did not differ significantly between both groups (all p>0.05), although there was a

Table 10.1
Baseline characteristics of the patient population.

	overall group (n = 92)	No ICD therapy (n = 71)	ICD therapy (n = 21)	p value*
Clinical characteristics				
Age, years	50 ± 14	49 ± 14	53 ± 12	0.2
Men, n (%)	63 (69)	44 (62)	19 (91)	0.02
BSA kg/m^2	2.0 ± 0.24	2.0 ± 0.25	2.1 ± 0.19	0.3
Systolic BP, mmHg	133 ± 21	133 ± 20	133 ± 24	1.0
Diastolic BP, mmHg	77 ± 11	77 ± 11	77 ± 10	0.9
Medication use, n (%)				
β-blockers	51 (59)	36 (55)	15 (71)	0.2
Calcium-antagonists	23 (26)	17 (26)	6 (29)	0.8
Diuretics	11 (13)	8 (12)	3 (14)	0.7
Echocardiography				
IVS, mm	22 (18-26)	22 (18-26)	22 (21-26)	0.3
PW, mm	11 (10-13)	11 (10-13)	12 (11-14)	0.3
LV EDD, mm	44 ± 7	44 ± 6	45 ± 7	0.3
LV EDVI, mL/m^2	48 (35-60)	47 (39-59)	59 (40-69)	0.1
LV ESVI, mL/m^2	14 (10-19)	14 (10-18)	15 (11-26)	0.1
LV EF, %	70 (64-76)	71 (65-77)	68 (52-76)	0.3
GLS, %	-13.3 ± 3.5	-13.8 ± 3.6	-11.9 ± 2.5	0.03
LAVI, mL/m^2	39 (31-47)	36 (29-43)	47 (41-58)	< 0.001
E/A	1.0 (0.8-1.6)	0.96 (0.8-1.7)	1.2 (0.9-1.5)	0.66
E/E`	11 (8-14)	11 (8-14)	12 (7-15)	0.9
DT, ms	197 ± 53	192 ± 51	211 ± 56	0.14
Systolic anterior movement, n (%)	32 (35)	25 (36)	7 (33)	0.8
MR ≥grade 3, n (%)	2 (2)	2 (2)	0 (0)	1.0
HCM risk profile				
Primary prevention ICD, n (%)	70 (76)	54 (76)	16 (76)	1.0
LVH, mm	24.1 ± 4.9	23.6 ± 5.3	25.9 ± 3.0	0.1
LVH ≥30 mm, n (%)	10 (11)	9 (13)	1 (5)	0.5
Family SCD, n (%)	47 (57)	38 (59)	9 (50)	0.4
Family HCM, n (%)	54 (65)	44 (68)	10 (56)	0.3
Unexplained syncope, n (%)	19 (21)	12 (18)	7 (33)	0.1
nsVT, n (%)	34 (38)	23 (34)	11 (52)	0.1
Resting gradient ≥30 mmHg, n (%)	17 (19)	13 (18)	4 (19)	0.9

BP: blood pressure, BSA: body surface area, DT: deceleration time, EDD: end diastolic diameter, EDVI: end diastolic volume indexed to BSA, EF: ejection fraction, ESVI: end systolic volume indexed to BSA, GLS: global longitudinal strain, ICD: implantable cardioverter defibrillator, IVS: interventricular septum, HCM: hypertrophic cardiomyopathy, LAVI: left atrial volume indexed to BSA, LV: left ventricle, LVH: left ventricular hypertrophy, MR: mitral regurgitation, nsVT: non-sustained ventricular tachycardia, PW: posterior wall, SCD: sudden cardiac death. *: p value for comparison of group of patients with versus without appropriate ICD therapy

trend towards higher maximal LV wall thickness and increased prevalence of nsVT and syncope prior to ICD implantation in the group of patients with appropriate ICD therapy. Of note, incidence of appropriate ICD therapy did not differ between primary and secondary ICD indication patients (p=1.0), nor was it significantly related to the number of conventional SCD risk factors in primary prevention ICD recipients. In particular, compared with primary prevention ICD recipients with 1 SCD risk factor, patients with 2 SCD risk factors had an incidence rate ratio of appropriate ICD therapy of 1.5 (95%CI 0.93-2.6) and patients with 3 SCD risk factors had an incidence rate ratio of 2.0 (95%CI 0.60-6.4, p for trend=0.06) (Figure 2).

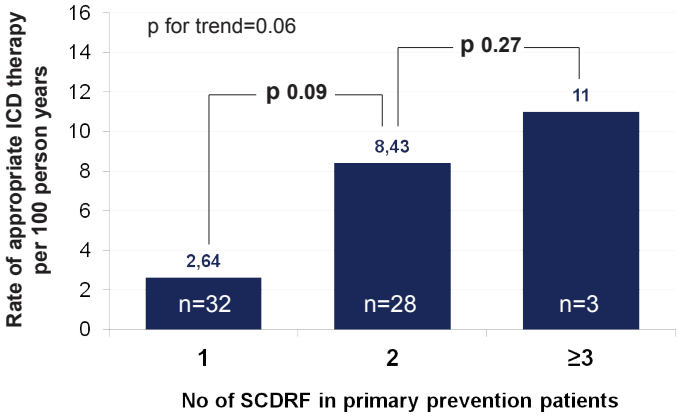

Figure 10.2
Appropriate ICD therapy in primary prevention patients according to number of sudden cardiac death risk factors (SCDRF). ICD: implantable cardioverter defibrillator.

Predictors of appropriate ICD therapy

Univariable Cox proportional-hazards regression analysis revealed LAVI, GLS, male gender, presence of nsVT and unexplained syncope prior to ICD implantation as predictors of appropriate ICD therapy (all p<0.2) (Table 2). Staged multivariable analysis showed that LAVI and GLS, and not any SCD risk factors, were independent predictors of appropriate ICD therapy (all p<0.05). A resting LV gradient of ≥30 mmHg was not related to appropriate ICD therapy in this patient cohort.

ROC curve analysis indicated that the presence of ≥1 SCD risk factors had limited value to predict appropriate ICD therapy when compared to both LAVI and GLS [AUC 0.52, 95% confidence interval (CI): 0.43-0.58 versus AUC 0.76, 95% CI 0.65-0.87 and AUC 0.65, 95% CI: 0.54-0.77, respectively] (p<0.001). LAVI ≥34 mL/m² and GLS ≥-14% provided high sensitivity of 95% and 86% respectively to predict appropriate ICD therapy, reaching up to 100% if at least one of both was present (Table 3). However, the same approach showed a modest positive predictive value

Table 10.2
Uni- and multivariable cox proportional-hazards regression analysis to identify predictors of appropriate implantable cardioverter defibrillator therapy.

	Univariable		Multivariable	
Parameter	HR (95% CI)	p-value	HR (95% CI)	p-value
Male gender	4.4 (1.0-19)	0.046	4.2 (0.99-18)	0.05
GLS, %	1.16 (1.02-1.31)	0.02	1.15 (1.02-1.30)	0.03
LAVI, mL/m^2	1.02 (1.01-1.03)	0.004	1.01 (1.00-1.03)	0.02
E/E'	0.98 (0.92-1.1)	0.7		
MR grade	1.1 (0.57-2.0)	0.9		
Secondary prevention ICD indication	1.1 (0.41-3.0)	0.8		
LVH ≥30 mm	0.36 (0.047-2.6)	0.3		
Family SCD	0.86 (0.34-2.2)	0.7		
Unexplained syncope	2.2 (0.88-5.6)	0.09	2.6 (0.99-6.7)	0.05
nsVT	2.36 (0.999-5.59)	0.05	2.38 (0.976-5.78)	0.06
Resting gradient ≥30 mmHg	1.3 (0.44-4.0)	0.6		

CI: confidence interval, GLS: global longitudinal strain, HR: hazard ratio, ICD: implantable cardioverter defibrillator, LAVI: left atrial volume indexed to body surface area, LVH: left ventricular hypertrophy, nsVT: non-sustained ventricular tachycardia, SCD: SCD.

Table 10.3
Predictors of appropriate implantable cardiac defibrillator therapy characteristics.

Variable	ROC AUC	95% CI	Sens* (%)	Spec* (%)	NPV* (%)	PPV* (%)
LAVI and GLS						
LAVI, ml/m²	0.76	0.65 - 0.87	-	-	-	-
LAVI ≥34 ml/ m²	-	-	95	45	97	30
GLS, %	0.65	0.54 - 0.77	-	-	-	-
GLS ≥-14%	-	-	86	45	93	28
GLS ≥-14% or LAVI ≥34 ml/m²	-	-	100	24	100	24
SCD risk factors						
Secondary prevention ICD indication	0.52	0.41-0.63	24	76	80	20
Primary prevention ICD indication:						
LVH ≥30 mm†	0.48	0.42 - 0.55	5	87	79	9
Family history of SCD†	0.45	0.32 - 0.59	50	41	77	17
Prior nsVT†	0.58	0.45 - 0.71	52	66	85	28
Prior unexplained syncope†	0.58	0.46 - 0.70	33	82	83	32

AUC: area under the curve, CI: confidence interval, FHSCD: family history of SCD, GLS: global longitudinal strain, HR: hazard ratio, ICD: implantable cardiac defibrillator, LAVI: left atrial volume indexed to body surface area, LVH: left ventricular hypertrophy, NPV: negative predictive value, nsVT: non-sustained ventricular tachycardia, PPV: positive predictive value, ROC: receiver operating characteristic analysis, SCD: SCD, SCD risk factors: SCD risk factor, sens: sensitivity, spec: specificity, *: calculation based on 20% prevalence of appropriate ICD therapy, †: one of SCD risk factors

of 24%. More importantly, the combined presence of LAVI <34 mL/m^2 and GLS <-14% adequately ruled out likelihood of appropriate ICD therapy, reflected by a negative predictive value of 100%.

Finally, the Kaplan-Meier survival curves for LAVI and GLS revealed a significant difference in time to survival free of appropriate ICD therapy for both LAVI ≥34 mL/ m^2 versus <34 mL/ m^2 (p<0.001) and GLS ≥-14% versus <-14% (p=0.003) (Figure 3). In particular, after a median follow-up of 1, 3 and 5 years a respective 12%, 24% and 32% of patients with LAVI ≥34 mL/m^2 reached the endpoint, whereas their counterparts showed significantly lower cumulative event rates (0%, 4% and 4%, respectively). HCM patients with GLS ≥-14% experienced appropriate ICD therapy in 9%, 23% and 32% after 1,3 and 5 years, respectively, while patients with GLS <-14% showed lower cumulative event rates of 6%, 9% and 9%.

Incremental value of LAVI and GLS to predict appropriate ICD therapy

The addition LAVI ≥34 mL/m² to a baseline model which included the presence of ≥1 SCD risk factor(s) provided incremental value to predict appropriate ICD therapy as indicated by the likelihood ratio test (p<0.001) and an IDI of 0.13 (p<0.001) (Figure 4). Sequential addition of GLS further improved prediction of appropriate ICD therapy (likelihood ratio test p=0.02 and IDI 0.04 with p=0.02). Therefore, adding both LAVI and GLS on top of presence of ≥1 SCD risk factors provided the best calibration for appropriate ICD therapy prediction, reflected by the likelihood ratio test p<0.001 and IDI 0.17 with p<0.001. Importantly, the same results were observed (IDI 0.19, p<0.001) when only considering IDI in primary prevention indication ICD recipients (n=70), which is of particular clinical interest as ICD implantation is unlikely to be withheld in secondary prevention indication HCM patients. Importantly, assessing both LAVI and GLS on top of conventional SCD risk factors in primary prevention patients results in reclassification of about 1 out of 5 primary prevention ICD recipients into a very low-risk group, who experienced no appropriate ICD therapy during follow-up [12/70 pts (17%) have both LAVI and GLS below the pre-specified cut-off values with presence of 0, 1 and 2 SCD risk factors in 3 (25%), 6 (50%) and 3 (25%) patients respectively].

LAVI, GLS and inappropriate ICD therapy

During the median follow-up of 4.7 (2.2-8.2) years 19 patients (21%) experienced at least one inappropriate ICD therapy event. Patients with versus without inappropriate ICD therapy had similar LAVI [37.4 (33.8-45.1) versus 39.3 (31.0-48.8) ml/m², p=0.806] and GLS (-13.8±3.23 versus -13.2±3.56 %, p=0.579) at baseline, respectively. In addition, at univariable Cox regression analysis LAVI did not relate to occurrence of inappropriate ICD therapy [HR 1.00 (95% CI 0.98-1.03), p=0.800],

nor did GLS [HR 0.99 (0.88-1.13), p=0.970]. Survival free of inappropriate ICD therapy during the follow-up period was similar between patients with baseline

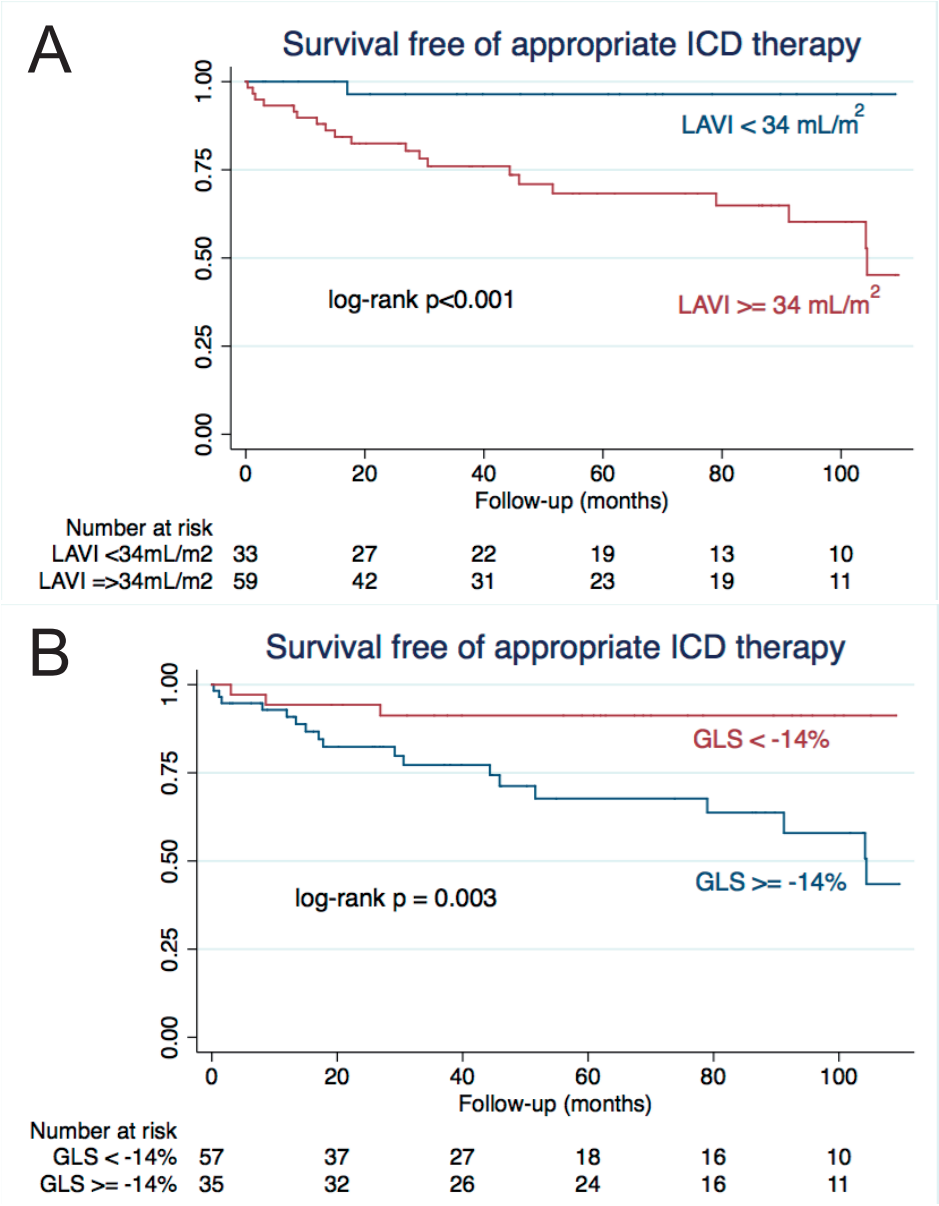

Figure 10.3
Kaplan-Meier analysis to evaluate survival free of appropriate ICD therapy in 92 HCM patients. Panel A: left atrial volume indexed to body surface area (LAVI). Panel B: left ventricular global longitudinal strain (GLS). ICD: implantable cardioverter defibrillator.

LAVI ≥34 versus <34 ml/m² (log rank p=0.330) as well as for patients with baseline GLS ≥-14 versus <-14 % (log rank p=0.670).

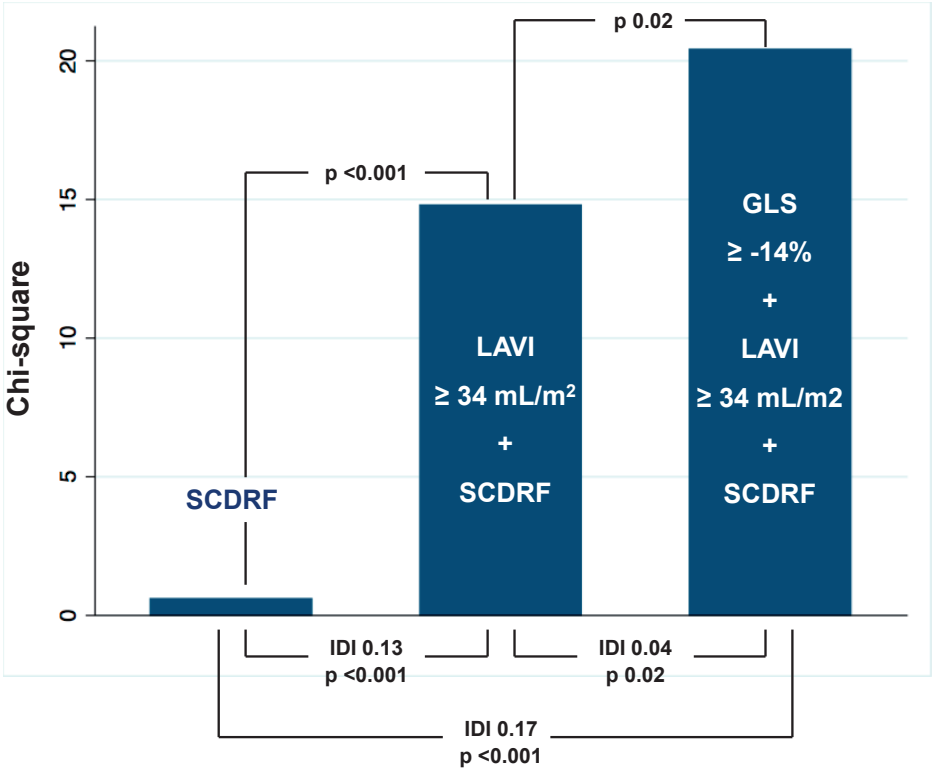

Figure 10.4
Likelihood ratio test bar graph. This test shows incremental value of sequential assessment of left atrial volume indexed to body surface area (LAVI) and left ventricular global longitudinal strain (GLS) over conventional sudden cardiac death risk factors (SCDRF) to predict appropriate implantable cardioverter defibrillator therapy. IDI: integrated discrimination improvement.

DISCUSSION

The main findings of the current study can be summarized as follows: 1) the value of conventional SCD risk factors to predict appropriate ICD therapy in high-risk HCM patients was limited, however, 2) LAVI and GLS were shown to be independent predictors of appropriate ICD therapy in this population and 3) assessment of both parameters provided significant incremental predictive value over conventional SCD risk factors, particularly to identify patients at very low risk of appropriate ICD therapy (100% negative predictive value).

SCD risk factors and appropriate ICD therapy

Although conventional SCD risk factors are established criteria to recommend ICD implantation in HCM patients, no strong evidence is currently available that these factors can also accurately predict the occurrence of appropriate ICD therapy.[2] The largest multi-center HCM registry so far, which included 506 unrelated HCM patients who underwent ICD implantation, observed in fact that no single conventional SCD risk factor, nor the number of SCD risk factors, was associated with appropriate ICD therapy.[1] A recent observational study in 1606 HCM patients (of which 19% with an ICD) also suggested that no single SCD risk factor could increase the risk of SCD or appropriate ICD shock, although aggregation of multiple SCD risk factors did increase this risk, however, with limited power to discriminate high versus low risk subjects.[21] Similar findings were also observed in smaller single-center series.[22-24] Only one study, evaluating 104 HCM patients, identified the presence of nsVT as an independent predictor of appropriate ICD therapy, although with wide confidence limits [HR 10.3 (95%CI 1.13-92.99)] and modest positive predictive value (22%).[25] Although the independent predictive value of secondary prevention indication for appropriate ICD therapy has not been shown unequivocally, appropriate ICD therapy is highly prevalent amongst secondary prevention ICD recipients and recently showed a significant association to appropriate ICD therapy on a univariable level.[1, 23, 26]

The results of the current evaluation are in line with previous studies, indicating rather limited predictive value of conventional SCD risk factors for appropriate ICD therapy.[1] Although conventional SCD risk factors remain mainstay to refer HCM patients for ICD implantation, additional markers are clinically needed to optimize candidate selection and allow accurate risk-benefit weighting of ICD implantation in these patients.

GLS and LAVI in HCM

HCM is a cardiomyopathy characterized by LV hypertrophy, myocardial fiber disarray and interstitial fibrosis.[4, 28, 29] These structural alterations are responsible for significant LV systolic dysfunction, which is often difficult to detect with conventional echocardiographic measures such as LV ejection fraction. Echocardiographic speckle tracking deformation imaging has been proposed as a highly sensitive technique which is able to accurately measure myocardial strain in a specific segment or in the overall LV.[7] With the use of this technique, a significant impairment of GLS was demonstrated in HCM patients, despite the presence of preserved LV ejection fraction.[5, 9, 10] In addition, impaired GLS in HCM patients has also been associated with occurrence of nsVT and adverse cardiac outcome.[10]

The above-mentioned HCM structural alterations are also responsible for a significant LV diastolic dysfunction, due to impaired myocardial relaxation, and increased LV filling pressures. In addition to these factors, intra-ventricular gradients and mitral regurgitation severity are main determinants of increased LA size, a characteristic finding in many HCM patients.[13, 30] Increased LA size is therefore considered a marker of HCM disease severity and showed to be an independent predictor of adverse outcome in this population.[11, 13] Increased LA diameter has shown to be a strong mortality predictor in a study including 1491 HCM patients.[31] Most recently, O'Mahony et al reported on a large series of 3675 relatively low-risk HCM patients (only 41 had baseline ICD, 1%), showing LA diameter independently related to SCD or appropriate ICD shock.[32] Asymmetric LA remodeling, however, may occur and therefore LAVI is currently recommended as the preferred parameter of LA size, as large variation in LA volume may coincide with little variation in LA diameter.[11, 15, 33]

Studies in HCM patients evaluating ICD recordings prior to appropriate ICD discharge have shown that the vast majority of patients suffered from sustained monomorphic ventricular tachycardia or ventricular fibrillation, often preceded by increased heart rate due to sinus tachycardia and atrial fibrillation or late-coupled premature ventricular complexes, respectively.[34, 35] These findings indicate that coincidence of arrhythmogenic substrate (allowing for uni-directional conduction block and re-entry) as well as adequate modulators (including electrolyte disturbances, maladaptive autonomic responses affecting heart rate, intra-ventricular gradients or ischemia) are prerequisites for ventricular tachyarrhytmias in these patients.[34, 35] We hypothesize that both GLS and LAVI may indirectly reflect the underlying arrhythmogenic substrate, if not modulators, in HCM patients, including fibrosis and fiber disarray. These findings may contribute to the rationale for the independent and incremental value of both LAVI and GLS over SCD risk factors to predict appropriate ICD therapy in this population, as shown in current study.

Clinical implications

The present findings suggest that assessment of *both* LAVI and GLS on top of conventional SCD risk factors may optimize referral criteria and timing of ICD implantation in HCM patients at increased risk for SCD. All patients that experienced appropriate ICD therapy were identified by presence of LAVI *or* GLS above the cut-off value of ≥34 mL/m^2 or ≥-14% respectively (sensitivity 100%). This strategy, however, showed a rather modest positive predictive value of 24%, indicating that, although patients who may benefit from ICD are identified applying this approach, still a large number of ICD's would be implanted in patients who will not experience any appropriate ICD therapy.

More importantly, when both LAVI *and* GLS were below the pre-specified cut-off values, a low-risk patient for appropriate ICD therapy was identified with a negative predictive value of 100%. When applying this strategy, no single patient experienced appropriate ICD therapy during a median period of approximately 5 years. In particular, about 1 out of 5 patients (19%) could be re-classified according to this approach as at low-risk and therefore eventually reassured that appropriate ICD therapy will not occur. These findings might therefore suggest considering the use of these parameters to delay ICD implantation in some HCM patients, with careful follow-up. This option might prevent these patients from exposure to potential adverse ICD-related events such as inappropriate therapy or device-related complications that might significantly impact on the quality of life or outcome of the ICD recipients.

Limitations

Several limitations to this study should be mentioned. The present evaluation most likely was underpowered to prove the absence of relationship between number of SCD risk factors and occurrence of appropriate ICD therapy, although our findings are in line with the largest HCM-ICD registry to date.[1] The specificity and negative predictive values of SCD risk factors to predict appropriate ICD therapy reported in the present evaluation should be interpreted with caution, as only an absolute minority of our patients presented without presence of conventional SCD risk factors. In addition, it should be emphasized that SCD risk factors are established markers and remain the cornerstone for a decision on ICD implantation in HCM patients.[2] The present results may not be generalizable to low-risk HCM patients for SCD. Therefore, given its retrospective observational single-center nature, this report should be considered as hypothesis generating and requires prospective validation in a larger HCM patient cohort.

CONCLUSION

Albeit conventional SCD risk factors are the cornerstone for clinical decision-making to implant ICD in HCM patients, these factors yield limited value to predict subsequent appropriate ICD therapy. Both LAVI and GLS are independent predictors of appropriate ICD therapy showing incremental benefit over conventional SCD risk factors, mainly attributed to high negative predictive value. Therefore, in addition to conventional SCD risk factors, assessment of both parameters may be clinically useful to optimize candidate selection and timing of ICD implantation, particularly to identify HCM patients at low risk for appropriate ICD therapy.

REFERENCES

1. Maron BJ, Spirito P, Shen WK et al. Implantable cardioverter-defibrillators and prevention of sudden cardiac death in hypertrophic cardiomyopathy. *JAMA.* 2007, 298:405-412.
2. Gersh BJ, Maron BJ, Bonow RO et al. 2011 ACCF/AHA guideline for the diagnosis and treatment of hypertrophic cardiomyopathy: a report of the American College of Cardiology Foundation/American Heart Association Task Force on Practice Guidelines. *Circulation.* 2011, 124:e783-831.
3. Schinkel AF, Vriesendorp PA, Sijbrands EJ et al. Outcome and complications after implantable cardioverter defibrillator therapy in hypertrophic cardiomyopathy: systematic review and meta-analysis. *Circ Heart Fail.* 2012, 5:552-559.
4. Maron BJ. Contemporary insights and strategies for risk stratification and prevention of sudden death in hypertrophic cardiomyopathy. *Circulation.* 2010, 121:445-456.
5. Serri K, Reant P, Lafitte M et al. Global and regional myocardial function quantification by two-dimensional strain: application in hypertrophic cardiomyopathy. *J Am Coll Cardiol.* 2006, 47:1175-1181.
6. Kato TS, Noda A, Izawa H et al. Discrimination of nonobstructive hypertrophic cardiomyopathy from hypertensive left ventricular hypertrophy on the basis of strain rate imaging by tissue Doppler ultrasonography. *Circulation.* 2004, 110:3808-3814.
7. Mor-Avi V, Lang RM, Badano LP et al. Current and evolving echocardiographic techniques for the quantitative evaluation of cardiac mechanics: ASE/EAE consensus statement on methodology and indications endorsed by the Japanese Society of Echocardiography. *J Am Soc Echocardiogr.* 2011, 24:277-313.
8. Maron BJ, Maron MS. Hypertrophic cardiomyopathy. *Lancet.* 2012, 381:242-55.
9. Paraskevaidis IA, Farmakis D, Papadopoulos C et al. Two-dimensional strain analysis in patients with hypertrophic cardiomyopathy and normal systolic function: a 12-month follow-up study. *Am Heart J.* 2009, 158:444-450.
10. Saito M, Okayama H, Yoshii T et al. Clinical significance of global two-dimensional strain as a surrogate parameter of myocardial fibrosis and cardiac events in patients with hypertrophic cardiomyopathy. *Eur Heart J Cardiovasc Imaging.* 2012, 13:617-623.
11. Losi MA, Betocchi S, Barbati G et al. Prognostic significance of left atrial volume dilatation in patients with hypertrophic cardiomyopathy. *J Am Soc Echocardiogr.* 2009, 22:76-81.
12. Tani T, Yagi T, Kitai T et al. Left atrial volume predicts adverse cardiac and cerebrovascular events in patients with hypertrophic cardiomyopathy. *Cardiovasc Ultrasound.* 2011; 9:34.
13. Yang H, Woo A, Monakier D et al. Enlarged left atrial volume in hypertrophic cardiomyopathy: a marker for disease severity. *J Am Soc Echocardiogr.* 2005, 18:1074-1082.
14. Yang WI, Shim CY, Kim YJ et al. Left atrial volume index: a predictor of adverse outcome in patients with hypertrophic cardiomyopathy. *J Am Soc Echocardiogr.* 2009, 22:1338-1343.
15. Lang RM, Bierig M, Devereux RB et al. Recommendations for chamber quantification: a report from the American Society of Echocardiography's Guidelines and Standards Committee and the Chamber Quantification Writing Group, developed in conjunction with the European Association of Echocardiography, a branch of the European Society of Cardiology. *J Am Soc Echocardiogr.* 2005, 18:1440-1463.
16. Antoni ML, Mollema SA, Delgado V et al. Prognostic importance of strain and strain rate after acute myocardial infarction. *Eur Heart J.* 2010; 31:1640-1647.

17. Nagueh SF, Appleton CP, Gillebert TC et al. Recommendations for the evaluation of left ventricular diastolic function by echocardiography. *J Am Soc Echocardiogr.* 2009, 22:107-133.
18. Zoghbi WA, Enriquez-Sarano M, Foster E et al. Recommendations for evaluation of the severity of native valvular regurgitation with two-dimensional and Doppler echocardiography. *J Am Soc Echocardiogr.* 2003, 16:777-802.
19. DeLong ER, DeLong DM, Clarke-Pearson DL. Comparing the areas under two or more correlated receiver operating characteristic curves: a nonparametric approach. *Biometrics.* 1988, 44:837-845.
20. Pencina MJ, D'Agostino RB, Sr., D'Agostino RB et al. Evaluating the added predictive ability of a new marker: from area under the ROC curve to reclassification and beyond. *Stat Med.* 2008, 27:157-172; discussion 207-112.
21. O'Mahony C, Tome-Esteban M, Lambiase PD et al. A validation study of the 2003 American College of Cardiology/European Society of Cardiology and 2011 American College of Cardiology Foundation/American Heart Association risk stratification and treatment algorithms for sudden cardiac death in patients with hypertrophic cardiomyopathy. *Heart.* 2013, 99:534-541.
22. Bos JM, Maron BJ, Ackerman MJ et al. Role of family history of sudden death in risk stratification and prevention of sudden death with implantable defibrillators in hypertrophic cardiomyopathy. *Am J Cardiol.* 2010, 106:1481-1486.
23. O'Mahony C, Lambiase PD, Quarta G et al. The long-term survival and the risks and benefits of implantable cardioverter defibrillators in patients with hypertrophic cardiomyopathy. *Heart.* 2012, 98:116-125.
24. Prinz C, Vogt J, Bitter T et al. Incidence of adequate ICD interventions in patients with hypertrophic cardiomyopathy supposed to be at high risk for sudden cardiac death. *Acta Cardiol.* 2010, 65:521-525.
25. Syska P, Przybylski A, Chojnowska L et al. Implantable cardioverter-defibrillator in patients with hypertrophic cardiomyopathy: efficacy and complications of the therapy in long-term follow-up. *J Cardiovasc Electrophysiol.* 2010, 21:883-889.
26. Vriesendorp PA, Schinkel AF, Van Cleemput J et al. Implantable cardioverter-defibrillators in hypertrophic cardiomyopathy: patient outcomes, rate of appropriate and inappropriate interventions, and complications. *Am Heart J.* 2013, 166:496-502.
27. Woo A, Monakier D, Harris L et al. Determinants of implantable defibrillator discharges in high-risk patients with hypertrophic cardiomyopathy. *Heart.* 2007, 93:1044-1045.
28. Bruder O, Wagner A, Jensen CJ et al. Myocardial scar visualized by cardiovascular magnetic resonance imaging predicts major adverse events in patients with hypertrophic cardiomyopathy. *J Am Coll Cardiol.* 2010, 56:875-887.
29. O'Hanlon R, Grasso A, Roughton M et al. Prognostic significance of myocardial fibrosis in hypertrophic cardiomyopathy. *J Am Coll Cardiol.* 2010, 56:867-874.
30. Bauer F, Shiota T, White RD et al. Determinant of left atrial dilation in patients with hypertrophic cardiomyopathy: a real-time 3-dimensional echocardiographic study. *J Am Soc Echocardiogr.* 2004, 17:968-975.
31. Nistri S, Olivotto I, Betocchi S et al. Prognostic significance of left atrial size in patients with hypertrophic cardiomyopathy (from the Italian Registry for Hypertrophic Cardiomyopathy). *Am J Cardiol.* 2006, 98:960-965.

32. O'Mahony C, Jichi F, Pavlou M et al. A novel clinical risk prediction model for sudden cardiac death in hypertrophic cardiomyopathy (HCM Risk-SCD). *Eur Heart J.* 2014, 35(30):2010-2020.
33. Tsang TS, Abhayaratna WP, Barnes ME et al. Prediction of cardiovascular outcomes with left atrial size: is volume superior to area or diameter? *J Am Coll Cardiol.* 2006, 47:1018-1023.
34. Cha YM, Gersh BJ, Maron BJ et al. Electrophysiologic manifestations of ventricular tachyarrhythmias provoking appropriate defibrillator interventions in high-risk patients with hypertrophic cardiomyopathy. *J Cardiovasc Electrophysiol.* 2007, 18:483-487.
35. O'Mahony C, Lambiase PD, Rahman SM et al. The relation of ventricular arrhythmia electrophysiological characteristics to cardiac phenotype and circadian patterns in hypertrophic cardiomyopathy. *Europace.* 2012, 14:724-733.

Chapter 11

Left atrial size and function in hypertrophic cardiomyopathy patients and risk of new onset atrial fibrillation

Philippe Debonnaire, Emer Joyce, Douwe E Atsma, Martin J Schalij, Jeroen J Bax, Victoria Delgado, Nina Ajmone Marsan

Submitted, 2016.

ABSTRACT

Objectives

Atrial fibrillation (AF) in hypertrophic cardiomyopathy (HCM) patients is highly prevalent, implies dismal prognosis, rendering risk stratification a priority. Whether LA volume and LA strain yield incremental value over LA diameter to risk stratify HCM patients for AF is unknown. The value of LA diameter, volume and strain to risk stratify HCM patients for new onset AF was explored.

Methods and results

A total of 243 HCM patients without AF history were retrospectively evaluated by (speckle tracking) echocardiography to assess LA diameter, volume and strain. New onset AF comprised the primary endpoint. During mean follow-up of 4.8±3.7 years, 40 patients (16%) developed AF. Multivariable analysis showed LA diameter (HR=1.07, 95%CI 1.02-1.13, p=0.011), LA volume (HR=1.03, 95%CI 1.01-1.06, p=0.007) and LA strain (HR=0.91, 95%CI 0.86-0.96, p<0.001) as independent AF correlates. Importantly, 58% (n=23) of AF events occurred despite a baseline LA diameter <45mm, observed in 186 patients. In this patient subset, LA strain (AUC 0.73, p<0.001) and LA volume (AUC 0.70, p=0.004) showed good predictive value for new onset AF. Furthermore, patients with LA volume <36 versus ≥36mL/m² (median value) and LA strain >23.4 versus ≤23.4% (median value) had superior 5-year AF-free survival of 92% versus 80% (p=0.013) and 98% versus 74% (p=0.001), respectively. Importantly, LA volume <36mL/m² and strain >23.4% yielded high negative predictive value (93% and 94%, respectively) for new onset AF. Likelihood ratio test indicated incremental value of LA volume assessment (p<0.001) on top of LA diameter to predict new onset AF in HCM patients with LA diameter <45mm, which further increased by addition of LA strain (p=0.042).

Conclusion

LA diameter, volume and strain all independently relate to new onset AF in HCM patients. In patients with normal LA size, however, both LA volume and strain further refine risk stratification for new onset AF.

INTRODUCTION

Primary hypertrophic cardiomyopathy (HCM), caused by sarcomeric gene mutation(s), encompasses increased risk for arrhythmia, heart failure and (sudden) cardiac death.[1,2] Atrial fibrillation is more prevalent than in the general population, typically affecting about 20% of HCM patients at an annual incidence of over 2%.[3-5] Importantly, one third of patients are diagnosed before the age of 50 years old.[3] HCM patients who develop atrial fibrillation are vulnerable to symptoms, impaired exercise tolerance, hospitalization for heart failure and, importantly, are prone to dismal prognosis.[3,4] Atrial fibrillation increases by 4-fold the risk of mortality independent of other known mortality risk factors, mainly due to heart failure and stroke related death.[3,4,6] In addition atrial fibrillation is associated with an 8-fold increased risk of thromboembolism in HCM patients, occurring at an annual incidence of 3.75%.[5,6] Early mortality or persistent neurologic disability are common in these patients, even more if onset of atrial fibrillation occurs at younger age.[3] Therefore accurate risk stratification for new onset atrial fibrillation in HCM patients should be a priority and may have an impact on follow-up and management strategies.

Left atrial (LA) diameter has consistently been identified as a strong predictor of atrial fibrillation development in HCM patients.[3,5] It has been suggested that the extent of atrial remodeling and therefore risk for atrial fibrillation, might be better reflected by 2-dimensional assessed LA volume rather than uni-dimensional LA diameter.[7,8] Two-dimensional (2-D) speckle tracking echocardiography is a novel method for accurate assessment of LA function, expressed as reservoir strain, more sensitive than LA size or volume. To date only one small study in HCM patients linked impaired LA strain to atrial fibrillation requiring hospitalization.[9] We hypothesized that LA volume and/or LA strain may yield incremental value over LA diameter to risk stratify HCM patients for new onset atrial fibrillation. The aim of current study is to explore the clinical value of all three LA parameters in relation to new onset atrial fibrillation in a large HCM population.

METHODS

Patient population

Patients ≥18 years with a clinical diagnosis of HCM based on otherwise unexplained ventricular hypertrophy, comprising a LV wall thickness of ≥15 mm were selected from an ongoing echocardiographic and clinical database. Patients with a history of atrial fibrillation before or at the moment of echocardiography, no

additional clinical follow-up visit after baseline echocardiography and insufficient image quality to allow LA strain assessment were excluded.

Baseline characteristics including age, gender, cardiovascular risk factors, medication use, presence of implantable cardioverter defibrillator (ICD) and results of sarcomere mutation testing, if performed, were extracted from the departmental electronic patient information system (EPD-Vision®, Leiden University Medical Center, Leiden, the Netherlands). In addition, at baseline all HCM patients had 12-lead electrocardiography (ECG) and 24-hour ambulatory electrocardiography (Holter) registration.

As recommended, patients were followed-up on a yearly basis at our and/or the referring institution, comprising a clinical visit and 12-lead ECG.[1,2] Repeated ECG or Holter recordings were performed at the discretion of the treating physician based on symptoms, presence of enlarged LA or for sudden cardiac death risk stratification. Device interrogation was performed every 3 to 6 months in ICD recipients.

The study was approved by the internal review board that waived the need for written informed consent for retrospective evaluation of prospectively collected clinical data.

Echocardiographic analysis

Comprehensive 2-D transthoracic echocardiography was performed in all patients in the left lateral decubitus using commercially available ultrasound systems (System-5, Vivid-7 and E9, GE-Vingmed, Milwaukee, WI) equipped with a 3.5 MHz or M5S transducers. Conventional ECG-triggered 2-D B-mode, M-mode, pulsed wave, continuous wave and color-Doppler images were acquired in still or cine-loop format and analyzed off-line (EchoPAC version 112, GE Medical Systems, Horten, Norway). From a short-axis view at basal, mid and apical level the maximal LV end-diastolic wall thickness was assessed. Septal LV wall thickness and LV diameters were calculated from parasternal long-axis views, as recommended.[10] Simpson's biplane method was used for evaluation of LV volumes and to calculate LV ejection fraction. Diastolic parameters, including E/A and E/e' were assessed using pulsed wave Doppler at the tips of the mitral leaflets and from tissue Doppler imaging at the level of the lateral annulus, respectively. A multi-integrative approach was used to grade presence of mitral regurgitation as grade 1 (trivial), 2 (mild), 3 (moderate) or 4 (severe), as recommended.[11] In addition systolic anterior movement of the anterior mitral leaflets was evaluated from M-mode parasternal acquisition. Presence of LV resting intraventricular or outflow tract gradient was systematically explored by pulsed wave Doppler and quantified by continuous wave Doppler.

LA analysis

LA diameter was derived from parasternal long axis B-mode view and LA volume was measured at end-systole with the Simpson's biplane rule. All volumes were indexed to body surface area. LA 2-D speckle tracking longitudinal strain was measured as peak systolic reservoir strain, as previously reported.[12] The smallest region of interest was set to include the thin atrial wall. The average value of both the apical 2-chamber and 4-chamber views was used. Mean frame rate for LA strain analysis was 57 frames per second. The intra- and interobserver variability for LA strain analysis in our department has been previously reported.[12]

Endpoint

New onset atrial fibrillation at out-patient or emergency room visit, defined as an irregular heart rhythm without distinct P-waves documented on ECG, Holter registration (if duration ≥30 seconds) or after expert analysis from device recordings in patients with ICD, comprised the study endpoint.[13]

Statistical analysis

Normally distributed and skewed continuous data are presented as mean ± standard deviation and median ± interquartile range, respectively, while percentages are used for categorical data. Comparison between groups was based on Student-T, Mann-Whitney U, Fisher exact or χ^2-test, when appropriate. Receiver Operator Characteristic (ROC) curve analysis was performed to test all 3 LA parameters (diameter, volume and strain) for prediction of the study endpoint. The study population was stratified based on LA diameter < or ≥45 mm, a cut-off value proposed by most recent HCM guidelines.[2] Stratification based on LA volume and strain was performed by their median value, given current lack of generally accepted cut-off in this patient population. Kaplan-Meier cumulative survival curves free of atrial fibrillation were constructed for all LA parameters, stratified according to their cut-off values, and compared by log-rank test. In addition sensitivity, specificity, positive and negative predictive values for the study endpoint prediction were calculated. Subsequently Cox proportional hazards regression analysis was performed to identify associates of new onset atrial fibrillation. Parameters at a significance threshold of $p<0.1$ at univariable level were entered into the multivariable analysis using a backward elimination approach. Multivariable testing was performed for each LA parameter of interest separately (diameter, volume and strain). Finally, similar statistical analysis was performed, restricting the study population to patients with LA diameter <45 mm, generally regarded as being at low risk for new onset atrial fibrillation.[2] In addition, likelihood ratio test was used to explore the potential incremental value of adding LA volume and strain on top

of LA diameter in relation to the study endpoint for this patient subset. SPSS version 20.0. (SPSS Inc., Chicago, Illinois) was used for statistical analysis. A p-value of <0.05 was considered statistically significant, all tests being two-sided.

RESULTS

Patient population

A total of 243 HCM patients comprised the final population after excluding patients for age <18 years old (n=18), history of atrial fibrillation (n=43), no follow-up visit (n=4) and insufficient image quality for LA strain assessment (n=54, 15%). Baseline demographic, clinical and echocardiographic characteristics of these patients (65% male, mean age 53±13 years) are provided in Table 1. The patient population showed typical characteristics of HCM such as increased wall thickness (median 21 mm), small LV cavities and preserved LV function (ejection fraction 68±8 %). In addition the presence of systolic anterior movement of the mitral valve or a significant LV outflow tract obstruction (≥30 mmHg) were noted in one third of the patients. Median LA size was slightly or moderately increased, when expressed as diameter [40 mm (36-44)] or volume [36 mL/m² (28-46)], respectively.[10] Median LA reservoir function measured with speckle tracking was 23.4% (16.9-29.1). By definition all patients were in sinus rhythm at baseline.

Study endpoint

During a mean follow-up of 4.8±3.7 years (range 1.7-7.1) 40 out of 243 patients (16%) experienced new onset atrial fibrillation. Particularly, more than half of these events (23/40, 58%) occurred in the sub-group of 186 HCM patients with a baseline LA diameter of <45 mm.

Atrial fibrillation in the overall population

Patients with versus without new onset atrial fibrillation had a larger LA size (diameter and volume) and more impaired LA function (strain), as shown in Table 2 (all p<0.001). ROC curve analysis, indicated a moderately higher predictive value for LA volume and LA strain than for LA diameter, to predict the occurrence of new onset atrial fibrillation (Table 2, all p<001).

Survival free from new onset atrial fibrillation was higher in patients with an LA diameter <45 versus ≥45 mm yielding a 5-year atrial fibrillation free survival of 88% versus 74%, respectively (p=0.005) (Figure 1). Similarly, survival free from new onset atrial fibrillation was higher in patients with an LA volume <36 versus ≥36 mL/m² (5-year survival 92% versus 78% respectively, p=0.001) and LA strain

Table 11.1
Baseline characteristics.

	Study population (n = 243)	LA <45 mm (n=186)	LA ≥45 mm (n=57)	p-value
Clinical characteristics				
Age, years	53 ± 13	53 ± 13	52 ± 14	0.544
Men, n (%)	157 (65)	108 (58)	49 (86)	<0.001
Systolic BP, mmHg	139 ± 23	138 ± 23	142 ± 21	0.432
Diastolic BP, mmHg	81 ± 11	81 ± 10	80 ± 11	0.512
Hypertension, n (%)	94 (39)	73 (39)	21 (37)	0.624
Diabetes, n (%)	20 (8)	17 (9)	3 (6)	0.773
Smoking history, n (%)	65 (27)	51 (27)	14 (24)	0.212
Hyperlipidemia, n (%)	73 (30)	60 (32)	13 (23)	0.325
ICD, n (%)	20 (8)	14 (8)	6 (10)	0.581
For primary prevention	14 (6)	10 (5)	4 (7)	-
For secondary prevention	6 (2)	4 (2)	2 (4)	-
Echocardiography				
IVS, mm	20 ± 5	19 ± 5	22 ± 6	<0.001
Maximal LVH, mm	21 (18-24)	20 (17-23)	24 (21-26)	<0.001
LVEDD, mm	43 ± 6	42 ± 6	47 ± 6	<0.001
LVESD, mm	24 ± 6	23 ± 6	26 ± 7	0.001
LV EDVI, mL/m^2	51 ± 16	49 ± 14	57 ± 18	0.001
LV ESVI, mL/m^2	16 ± 7	15 ± 6	19 ± 9	0.001
LV EF, %	68 ± 8	69 ± 8	67 ± 8	0.171
LA diameter, mm	40 ± 6	38 ± 5	48 ± 3	<0.001
LA volume, mL/m^2	38 ± 14	35 ± 12	50 ± 15	<0.001
LA strain, %	23.2 ± 8.0	24.6 ± 7.6	18.7 ± 7.4	<0.001
E/A	1.0 (0.7-1.4)	0.9 (0.7-1.4)	1.2 (0.9-1.6)	0.018
E/e'	10 (8-15)	10 (8-15)	13 (10-17)	0.011
Systolic anterior motion of MV, n (%)	90 (37)	62 (33)	28 (49)	0.041
MR grade	1.02 ± 0.71	0.98 ± 0.74	1.18 ± 0.69	0.075
Resting LV outflow gradient, mmHg	9 (6-20)	9 (6-17)	10 (7-55)	0.051
Resting LV outflow gradient >30 mmHg, n (%)	39 (16)	24 (13)	15 (26)	0.021
Sarcomeric mutation (n=119 tested), n (%)	61 (51)	43 (48)	18 (56)	0.541

BP: blood pressure, EDD: end-diastolic diameter, EDVI: end-diastolic volume index, EF: ejection fraction, ESD: end-systolic diameter, ESVI: end-systolic volume index, ICD: implantable cardioverter defibrillator, IVS: interventricular septum, LA: left atrium, LV: left ventricle, LVH: left ventricular hypertrophy, MR: mitral regurgitation, MV: mitral valve

>23.4 vs ≤23.4 % (5-year survival of 94% versus 75%, respectively, p<0.001). Table 2 shows the higher sensitivity at cost of lower specificity of LA volume and strain compared to LA diameter to predict new onset atrial fibrillation. Cox regres-

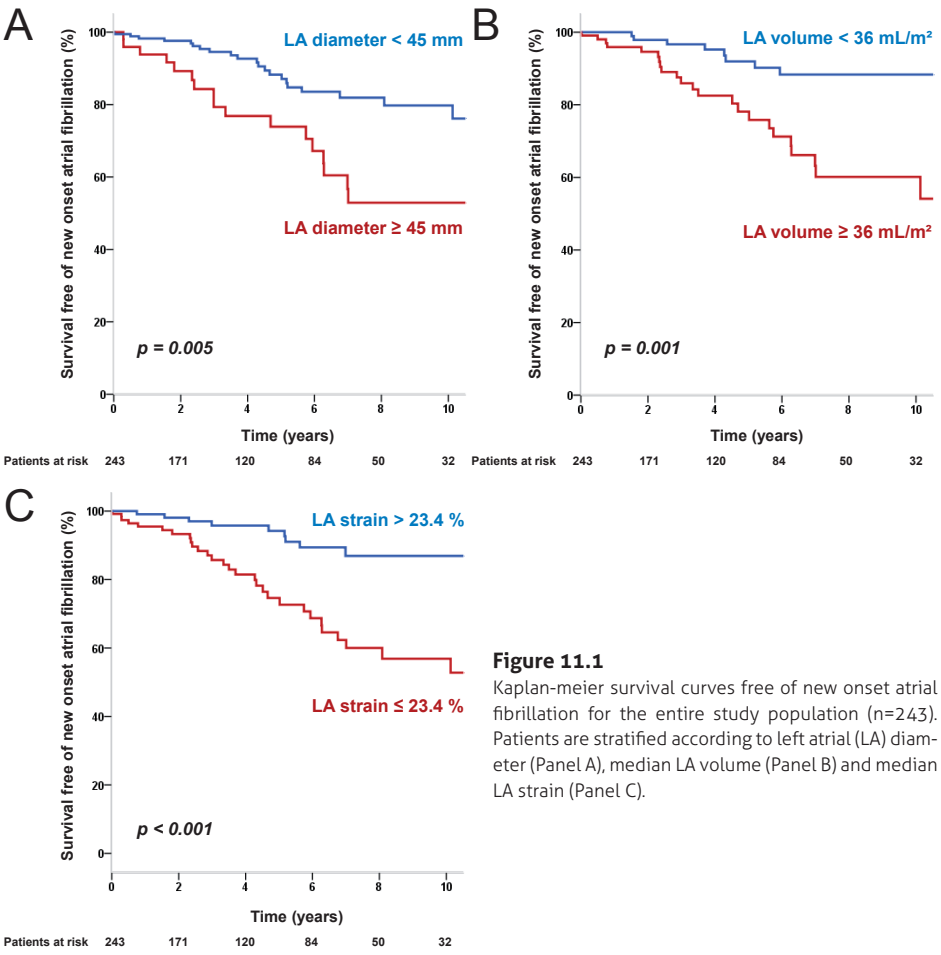

Figure 11.1
Kaplan-meier survival curves free of new onset atrial fibrillation for the entire study population (n=243). Patients are stratified according to left atrial (LA) diameter (Panel A), median LA volume (Panel B) and median LA strain (Panel C).

sion analysis identified age, diabetes, E/e', mitral regurgitation grade and all LA parameters (diameter, volume and strain) as univariate associates of new onset atrial fibrillation (all p<0.10) (Table 3). Moreover, multivariable analysis showed that all LA parameters were independently associated with the study endpoint: LA diameter (HR 1.07, 95% CI 1.02-1.13, p=0.011), LA volume (HR 1.03, 95% CI 1.01-1.06, p=0.007) and LA strain (HR 0.91, 95% CI 0.86-0.96, p<0.001) (Table 4).

Atrial fibrillation in patients with left atrial diameter <45 mm

Although HCM patients with LA diameter <45 mm are generally considered to be at relatively low risk for new onset atrial fibrillation, 58% (23 out of 40) of these events occurred in this subset of 186 patients (Figure 2), implicating a prevalence

Table 11.2

Left atrial parameters for prediction of new onset atrial fibrillation using the pre-specified cut-off values. Note superior sensitivity of LA volume and strain versus diameter to predict atrial fibrillation in entire study population. In the patient sub-group with preserved LA diameter (<45 mm, 186 patients), comprising 58% (n=23/40) of the atrial fibrillation events, both LA volume and LA strain show high negative predictive value.

Entire study population (n=243)	No AF (n=203)	AF (n=40)	p-value	AUC ROC	Cut-off	Sens %	Spec %	PPV %	NPV %
LA diameter, mm	40 ± 6	44 ± 6	<0.001	0.68	≥ 45	43	80	30	88
LA volume, mL/m²	36 ± 13	48 ± 16	<0.001	0.72	≥36	73	54	22	92
LA strain, %	24.1 ± 7.8	18.4 ± 7.3	<0.001	0.71	≤23.4	75	55	25	85
Patients with LA diameter <45 mm (n=186)	**No AF (n=163)**	**AF (n=23)**	**p-value**	**AUC ROC**	**Cut-off**	**Sens %**	**Spec %**	**PPV %**	**NPV %**
LA volume, mL/m²	34 ± 11	44 ± 16	<0.001	0.70	≥36	63	62	17	93
LA strain, %	25.4 ± 7.3	18.9 ± 7.5	<0.001	0.74	≤23.4	74	61	21	94

Abbreviations, see Table 1. AF: atrial fibrillation. AUC: area under the curve, NPV: negative predictive value, PPV: positive predictive value, ROC: receiver operating curve analysis, Sens: sensitivity, Spec: specificity

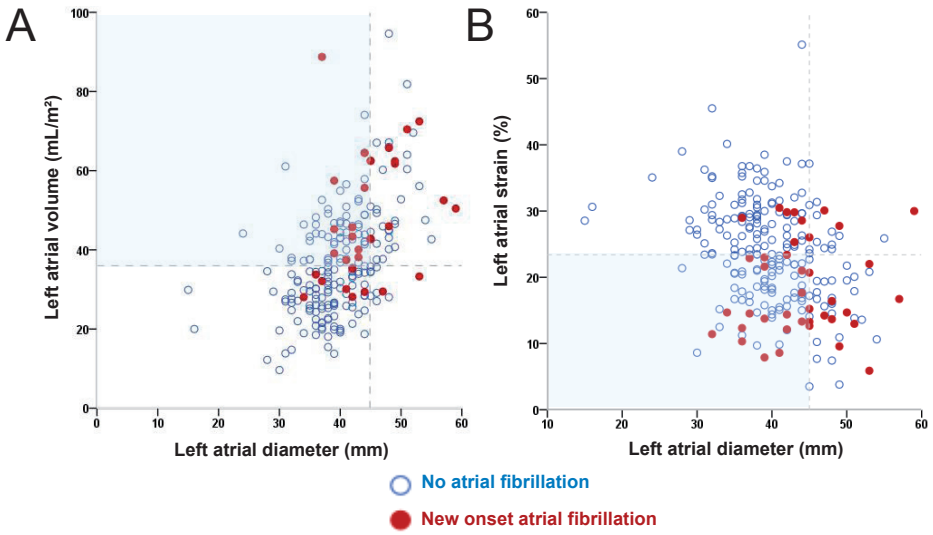

Figure 11.2

New onset atrial fibrillation according to left atrial size and function. Left atrial (LA) diameter versus volume (Panel A) and versus strain (panel B). Dashed vertical line represents the 45 mm LA diameter cut-off. The dashed horizontal line represents the 36 mL/m² and 23.4% cut-off for LA volume (panel A) and strain (panel B), respectively. A significant proportion of new onset atrial fibrillation events occurs despite 'normal' LA diameter (<45 mm) of which a significant part is detected based on the cut-offs set for enlarged LA volume and impaired LA strain (light blue area), explaining higher overall sensitivity. Relative few events occur in patients with preserved LA diameter without enlarged LA volume or preserved LA strain, explaining the high negative predictive value of the latter two parameters.

Table 11.3
Univariable Cox regression analysis to predict new onset atrial fibrillation. Abbreviations, see Table 1. LVOT: left ventricular outflow tract.

	Univariable	
	HR (95% CI)	p-value
Age, per year	1.04 (1.01-1.07)	0.002
Male gender	0.70 (0.37-1.31)	0.266
Systolic BP, per mmHg	1.00 (0.98-1.02)	0.808
Diastolic BP, per mmHg	1.02 (0.98-1.05)	0.409
Hypertension	1.42 (0.73-2.74)	0.300
Diabetes	2.66 (1.09-6.46)	0.031
Smoking history	0.79 (0.36-1.77)	0.577
Hypercholesterolemia	0.94 (0.47-1.89)	0.855
Maximal LVH, per mm	1.02 (0.97-1.07)	0.383
E/e'	1.04 (1.02-1.07)	0.003
MR grade	2.09 (1.38-3.15)	<0.001
Resting LV(OT)gradient, per mmHg	1.01 (1.00-1.02)	0.130
Resting LV(OT)gradient >30 mmHg	1.34 (0.61-2.91)	0.464
LVEDD, per mm	0.98 (0.93-1.03)	0.389
LVESD, per mm	1.01 (0.96-1.07)	0.606
LVEDVi, per ml/m²	0.99 (0.97-1.01)	0.243
LVESVi, per mL/m²	1.01 (0.98-1.05)	0.579
LVEF, per %	0.97 (0.94-1.01)	0.112
LA diameter, per mm	1.09 (1.04-1.14)	0.001
LA volume, per mL/m²	1.05 (1.03-1.07)	<0.001
LA strain, per %	0.92 (0.89-0.96)	<0.001

Table 11.4
Multivariable Cox regression analysis to predict new onset atrial fibrillation for different left atrial parameters. Univariate predictors p<0.10 in univariable model were included in the multivariable model. Separate models were created for each left atrial parameter to avoid co-linearity. Abbreviations, see Tables 1 and 2.

	Multivariable LA diameter		Multivariable LA volume		Multivariable LA strain	
	HR (95% CI)	p-value	HR (95% CI)	p-value	HR (95% CI)	p-value
Age	1.03 (1.00-1.06)	0.071	1.01 (0.97-1.04)	0.635	1.01 (0.98-1.07)	0.732
Diabetes	1.70 (0.58-5.00)	0.332	1.78 (0.60-5.32)	0.302	1.17 (0.40-3.38)	0.779
E/e'	1.02 (0.99-1.06)	0.207	1.03 (1.00-1.07)	0.079	1.02 (0.98-1.05)	0.440
MR grade	1.66 (0.97-2.83)	0.063	1.40 (0.72-2.73)	0.322	1.67 (1.02-2.71)	0.041
LA diameter	1.07 (1.02-1.13)	0.011	-	-		
LA volume	-	-	1.03 (1.01-1.06)	0.007		
LA strain	-	-	-	-	0.91 (0.86-0.96)	<0.001

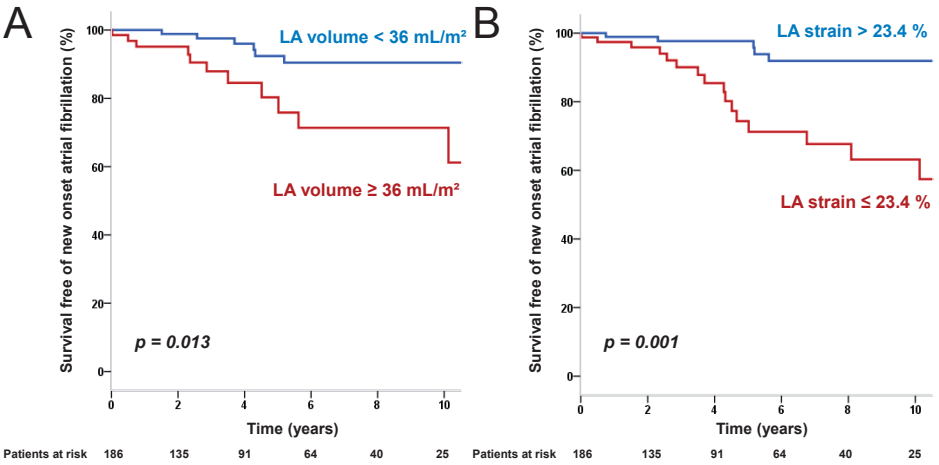

Figure 11.3
Kaplan-meier survival curves free of new onset atrial fibrillation in patients with left atrial diameter <45 mm (n=186). Patients are stratified according to median left atrial (LA) volume (Panel A) and LA strain (Panel B).

of 12% (23/186) versus 30% (17/57) in patients with LA diameter <45 mm versus ≥45 mm, respectively.[2]

Within the cohort of patients with LA diameter <45 mm, LA volume was larger and LA strain more impaired in patients that developed new onset atrial fibrillation compared with patients who remained in sinus rhythm (Table 1). Using ROC curve analysis, LA strain (AUC 0.74, p<0.001) provided greater predictive value for new onset atrial fibrillation compared to LA volume (AUC 0.70, p=0.004) in this subset of patients. Importantly, both LA parameters were able to further discriminate risk for new onset atrial fibrillation in patients with LA diameter <45 mm, as illustrated by the survival curves free of new onset atrial fibrillation in Figure 3. Patients with LA volume <36 versus ≥36 mL/m² and LA strain >23.4 versus ≤23.4 % (median values) had better survival free of atrial fibrillation with cumulative 5-year survival of 92% versus 80% (p=0.013) and 98% versus 74% (p=0.001), respectively. As shown in Table 2 and Figure 2, both LA parameters particularly yield high negative predictive value for new onset atrial fibrillation in this HCM sub-population.

Likelihood ratio test indicated significant incremental value of LA volume (p <0.001) on top of LA diameter to predict new onset atrial fibrillation in HCM patients with LA diameter <45 mm (Figure 4). Interestingly, addition of LA strain further increased the predictive value of the model containing LA diameter and LA volume (p =0.042).

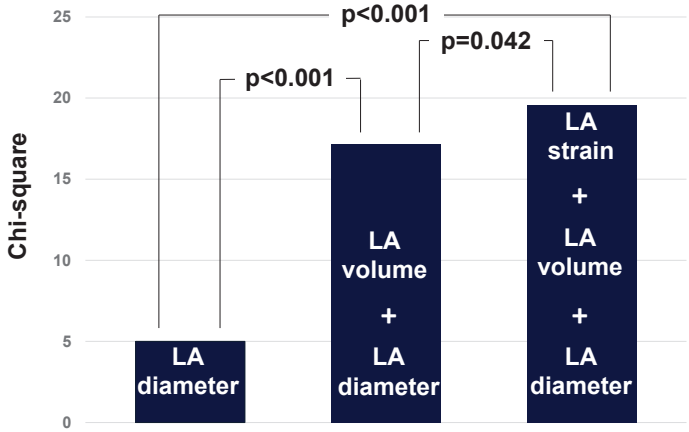

Figure 11.4
Likelihood ratio test in patients with left atrial diameter <45 mm (n=186). Subsequent addition of both left atrial (LA) volume and LA strain on top of diameter assessment provides incremental value for prediction of new onset atrial fibrillation.

DISCUSSION

The main study findings in this HCM population can be summarized as follows: 1) LA size (diameter and volume) and LA function (strain) are independently related to new onset atrial fibrillation, 2) the burden of new onset atrial fibrillation is significant despite the relative young age, even in patients with LA diameter <45 mm, and 3) adding LA volume and/or LA strain assessment on top of LA diameter improves prediction of new onset atrial fibrillation with both parameters yielding high negative predictive value in the subset of patients with LA diameter <45 mm.

Left atrial remodeling comprises structural and functional changes usually preceding atrial arrhythmias. In the current study, patients developing new onset atrial fibrillation had larger LA size (diameter and volume) and more impaired LA function (strain), compared to HCM patients free of atrial fibrillation. HCM patients are particularly prone to adverse atrial remodeling for several reasons. Increased filling pressures due to left ventricular diastolic dysfunction and hypertrophy, mitral regurgitation and outflow tract obstruction are well known determinants of increased LA size in HCM patients.[14,15] Moreover, increased atrial fibrosis contributes to atrial enlargement and functional impairment.[16] Although evidence is scarce, intrinsic atrial myopathy as part of the molecular disease has been suggested as well.[5] Specific sarcomeric gene mutations have recently been described in atypical forms of HCM that relate to juvenile onset of atrial fibrillation in these patients.[17] Even polymorphisms in non-sarcomeric genes, encoding for proteins involved in the renin-angiotensin-aldosterone system and collagen synthesis, have shown to

act as HCM disease modifiers, increasing the likelihood of atrial fibrillation development.[18] Therefore it is not unexpected that atrial fibrillation often complicates the natural course of HCM, translating into a significant morbidity and mortality burden.

Increased LA size, evaluated by uni-dimensional antero-posterior diameter assessment, has consistently been reported as one of the strongest correlates of atrial fibrillation in HCM patients.[3,5] Current guidelines recommend intensification of diagnostic arrhythmia surveillance with 48-hour Holter 6-monthly once LA diameter equals or exceeds 45 mm.[2] As atrial enlargement in the antero-posterior direction is restricted by the presence of the sternum and mediastinum (more specific), structural remodeling may be better described by evaluating atrial volume, often based on a 2-D approach (more sensitive).[8,19] Several reports demonstrate that increased LA volume heralds increased risk of atrial fibrillation and might be preferred over LA diameter.[7,8,20,21] The current study confirms this hypothesis, indicating higher sensitivity and negative predictive value of LA volume versus diameter to identify patients at risk for new onset atrial fibrillation.

Functional LA changes may coincide or even precede structural adaptations. Decreased LA ejection fraction, evaluated by echocardiography or cardiac magnetic resonance imaging, has been linked to the occurrence of atrial fibrillation in HCM patients.[7,20] Two-dimensional speckle tracking analysis allows angle independent assessment of LA function by measuring magnitude (strain) or rate (strain rate) of atrial deformation. In particular LA reservoir strain, referring to longitudinal deformation that occurs due to LA distention by pulmonary venous inflow during ventricular systole (reservoir phase) is a highly sensitive technique, able to identify atrial changes even in patients with normal LA size.[22,23] Hence, impaired LA reservoir strain is often noted in HCM patients.[24] A recent cross-sectional report in a limited number of patients indicated more impaired lateral reservoir Doppler-derived strain (rate) in HCM patients with versus without atrial fibrillation.[21] One study in 50 HCM patients indicated that LA reservoir speckle-tracking derived strain independently predicts occurrence of atrial fibrillation requiring hospitalization (odds ratio 0.85, 95% CI 0.75-0.97, p=0.017).[9] The present study, representing the largest cohort of HCM patients evaluated by LA strain so far, demonstrates higher sensitivity of LA strain compared to LA diameter to predict new onset atrial fibrillation and confirms its independent predictive value for this endpoint.

Importantly, 58% of new onset atrial fibrillation events in the HCM patients studied occurred despite a relatively preserved atrial diameter of <45 mm. This is of particular relevance as this subset of HCM patients is generally regarded as being at low risk to develop atrial fibrillation and no additional follow-up measures are recommended.[2] We showed that patients with LA diameter <45 mm who

actually do develop atrial fibrillation have larger LA volume and more impaired LA function compared to patients free of atrial arrhythmia. In particular patients with LA volume ≥36 mL/m² or LA strain ≤23.4 % had worse survival free of atrial fibrillation. Presence of relatively preserved LA volume <36 mL/m² or LA strain >23.4 % virtually excluded the risk of new onset atrial fibrillation (negative predictive value of 93% and 94%, respectively). Not unexpectedly, additional assessment of LA volume and LA strain therefore conveyed a higher predictive value for new onset atrial fibrillation in the subset of HCM patients with LA diameter <45 mm. These findings probably reflect the previously reported higher sensitivity of LA volume and LA strain assessment in comparison with LA diameter.

Clinical implications

Intensified monitoring to detect atrial fibrillation should indeed be offered to HCM patients with dilated LA ≥45 mm, as recommended.[2] Based on current findings, however, this strategy should not be restricted to those patients only, but LA volume and/or strain assessment should additionally be performed in order to rule out increased risk for atrial fibrillation. In those patients with LA volume >36 mL/² and/or LA strain <23.4 % it might therefore be prudent to intensify follow-up aiming for detection of subsequent atrial fibrillation occurrence. In addition, observational data have indicated that patients with only one atrial fibrillation episode have similar risk for thromboembolism versus those with repeated episodes and oral anticoagulation using warfarin significantly decreased that likelihood.[5,6] It has been suggested that prophylactic anticoagulation in HCM patients with increased LA size should be the focus of additional research. In light of current findings it might prove valuable to consider additional assessment of LA volume or strain to facilitate such clinical decision-making. Finally ablation for atrial fibrillation in HCM patients is increasingly reported although the results seem less compared to non-HCM patients.[25,26] The value of LA volume and strain rather than LA diameter to select candidates for ablation and predict success or recurrence of arrhythmia in HCM patients may be the scope of future investigation.

Limitations

Some limitations merit attention. First, this report is a retrospective longitudinal analysis of patients referred to a tertiary HCM center; therefore selection bias cannot be fully excluded. Second, ICD recipients are submitted to continuous heart rhythm monitoring, increasing the likelihood of atrial fibrillation detection. Other patients were followed by annual ECG or Holter monitoring (at discretion of treating physician). Therefore the true prevalence of new onset atrial fibrillation may have been underestimated in our study population.

CONCLUSION

Both LA size (diameter and volume) and function (strain) are independently related to new onset atrial fibrillation in HCM patients. A significant proportion of atrial fibrillation events, however, occurs in patients despite relatively preserved LA diameter <45 mm. Assessment of LA volume and strain have incremental predictive value in this patient subset, in particular to exclude increased risk for atrial fibrillation development based on high negative predictive value. These findings might impact on provision and intensity of follow-up surveillance to detect atrial fibrillation in HCM patients with preserved LA size.

REFERENCES

1. Gersh BJ, Maron BJ, Bonow RO et al. ACCF/AHA guideline for the diagnosis and treatment of hypertrophic cardiomyopathy: a report of the American College of Cardiology Foundation/American Heart Association Task Force on Practice Guidelines. *Circulation.* 2011, 124:e783-831.
2. Elliott PM, Anastasakis A, Borger MA et al. ESC Guidelines on diagnosis and management of hypertrophic cardiomyopathy: the Task Force for the Diagnosis and Management of Hypertrophic Cardiomyopathy of the European Society of Cardiology (ESC). *Eur Heart J.* 2014, 35:2733-2779.
3. Olivotto I, Cecchi F, Casey SA et al. Impact of atrial fibrillation on the clinical course of hypertrophic cardiomyopathy. *Circulation.* 2001, 104:2517-2524.
4. Siontis KC, Geske JB, Ong K et al. Atrial fibrillation in hypertrophic cardiomyopathy: prevalence, clinical correlations, and mortality in a large high-risk population. *J Am Heart Assoc.* 2014, 3:e001002.
5. Guttmann OP, Rahman MS, O'Mahony C et al. Atrial fibrillation and thromboembolism in patients with hypertrophic cardiomyopathy: systematic review. *Heart.* 2014;100:465-472.
6. Maron BJ, Olivotto I, Bellone P et al. Clinical profile of stroke in 900 patients with hypertrophic cardiomyopathy. *J Am Coll Cardiol.* 2002, 39:301-307.
7. Losi MA, Betocchi S, Aversa M et al. Determinants of atrial fibrillation development in patients with hypertrophic cardiomyopathy. *Am J Cardiol.* 2004, 94:895-900.
8. Tani T, Tanabe K, Ono M et al. Left atrial volume and the risk of paroxysmal atrial fibrillation in patients with hypertrophic cardiomyopathy. *J Am Soc Echocardiogr.* 2004, 17:644-648.
9. Paraskevaidis IA, Farmakis D, Papadopoulos C et al. Two-dimensional strain analysis in patients with hypertrophic cardiomyopathy and normal systolic function: a 12-month follow-up study. *Am Heart J.* 2009, 158:444-450.
10. Lang RM, Badano LP, Mor-Avi V et al. Recommendations for cardiac chamber quantification by echocardiography in adults: an update from the American Society of Echocardiography and the European Association of Cardiovascular Imaging. *Eur Heart J Cardiovasc Imaging.* 2015, 16:233-270.
11. Lancellotti P, Moura L, Pierard LA et al. European Association of Echocardiography recommendations for the assessment of valvular regurgitation. Part 2: mitral and tricuspid regurgitation (native valve disease). *Eur J Echocardiogr.* 2010, 11:307-332.
12. Debonnaire P, Leong DP, Witkowski TG et al. Left atrial function by two-dimensional speckle-tracking echocardiography in patients with severe organic mitral regurgitation: association with guidelines-based surgical indication and postoperative (long-term) survival. *J Am Soc Echocardiogr.* 2013, 26:1053-1062.
13. Camm AJ, Kirchhof P, Lip GY et al. Guidelines for the management of atrial fibrillation: the Task Force for the Management of Atrial Fibrillation of the European Society of Cardiology (ESC). *Eur Heart J.* 2010, 31:2369-2429.
14. Bauer F, Shiota T, White RD et al. Determinant of left atrial dilation in patients with hypertrophic cardiomyopathy: a real-time 3-dimensional echocardiographic study. *J Am Soc Echocardiogr.* 2004, 17:968-975.
15. Yang H, Woo A, Monakier D et al. Enlarged left atrial volume in hypertrophic cardiomyopathy: a marker for disease severity. *J Am Soc Echocardiogr.* 2005, 18:1074-1082.

16. Habibi M, Lima JA, Khurram IM et al. Association of left atrial function and left atrial enhancement in patients with atrial fibrillation: cardiac magnetic resonance study. *Circ Cardiovasc Imaging.* 2015, 8:e002769.
17. Girolami F, Iascone M, Tomberli B et al. Novel alpha-actinin 2 variant associated with familial hypertrophic cardiomyopathy and juvenile atrial arrhythmias: a massively parallel sequencing study. *Circ Cardiovasc Genet* .2014, 7:741-750.
18. Orenes-Pinero E, Hernandez-Romero D, Romero-Aniorte AI et al. Prognostic value of two polymorphisms in non-sarcomeric genes for the development of atrial fibrillation in patients with hypertrophic cardiomyopathy. *QJM.* 2014, 107:613-621.
19. Tsang TS, Abhayaratna WP, Barnes ME et al. Prediction of cardiovascular outcomes with left atrial size: is volume superior to area or diameter? *J Am Coll Cardiol.* 2006, 47:1018-1023.
20. Maron BJ, Haas TS, Maron MS et al. Left atrial remodeling in hypertrophic cardiomyopathy and susceptibility markers for atrial fibrillation identified by cardiovascular magnetic resonance. *Am J Cardiol.* 2014, 113:1394-1400.
21. Girasis C, Vassilikos V, Efthimiadis GK et al. Patients with hypertrophic cardiomyopathy at risk for paroxysmal atrial fibrillation: advanced echocardiographic evaluation of the left atrium combined with non-invasive P-wave analysis. *Eur Heart J Cardiovasc Imaging.* 2013, 14:425-434.
22. Kuppahally SS, Akoum N, Burgon NS et al. Left atrial strain and strain rate in patients with paroxysmal and persistent atrial fibrillation: relationship to left atrial structural remodeling detected by delayed-enhancement MRI. *Circ Cardiovasc Imaging.* 2010, 3:231-239.
23. Mondillo S, Cameli M, Caputo ML et al. Early detection of left atrial strain abnormalities by speckle-tracking in hypertensive and diabetic patients with normal left atrial size. *J Am Soc Echocardiogr.* 2011, 24:898-908.
24. Paraskevaidis IA, Panou F, Papadopoulos C et al. Evaluation of left atrial longitudinal function in patients with hypertrophic cardiomyopathy: a tissue Doppler imaging and two-dimensional strain study. *Heart.* 2009, 95:483-489.
25. Santangeli P, Di Biase L, Themistoclakis S et al. Catheter ablation of atrial fibrillation in hypertrophic cardiomyopathy: long-term outcomes and mechanisms of arrhythmia recurrence. *Circ Arrhythm Electrophysiol.* 2013, 6:1089-1094.
26. Contreras-Valdes FM, Buxton AE, Josephson ME et al. Atrial Fibrillation Ablation in Patients With Hypertrophic Cardiomyopathy: Long-Term Outcomes and Clinical Predictors. *J Am Coll Cardiol.* 2015, 65:1485-1487.

Summary, conclusions and future perspectives

SUMMARY

In this thesis we explored risk stratification and management of patients with structural heart disease, focusing on valvular heart disease and primary hypertrophic cardiomyopathy. In particular the potential clinical role of advanced echocardiography, including 3D-echocardiography and deformation imaging (strain), as well as clinical surrogates, were evaluated. The introduction of this thesis summarizes the rationale and background of our study.

The global burden of valvular heart disease such as aortic stenosis or mitral regurgitation is significant, and it is expected to increase due to Western population ageing. Left untreated, valvular heart disease is associated with poor prognosis. As older patients often present with several co-morbidities, interventional treatment tailored to their inherent high or prohibitive surgical risk is key and can nowadays be provided by less invasive percutaneous valve replacement or repair techniques, as indicated in the introduction of this thesis. Primary hypertrophic cardiomyopathy due to sarcomeric mutation(s), affecting about 1 out of 500 people, is associated with increased risk of sudden cardiac death, heart failure, arrhythmia and thrombo-embolism. Although the absolute sudden cardiac death risk is rather low, its impact is substantial as it tends to occur in young patients and gains significant media attention when it affects young athletes during sports, fueling debates about preventive sport participation screening. Risk stratification and adequate patient selection for interventions in patients with structural heart disease such as valvular heart disease or primary hypertrophic cardiomyopathy are critical to assess the need, timing and type of therapeutic intervention and assure beneficial outcomes. We elaborated how clinical risk scores or surrogates as well as advanced echocardiography techniques including 3-dimensional echocardiography and deformation imaging (strain) may be ideally suited for this purpose in patients with valvular heart disease and primary hypertrophic cardiomyopathy. In particular, the search for techniques or clinical surrogates that relate to the presence of fibrosis, a critical determinant of disease course in both forms of structural heart disease, is explained.

Part I: 3-Dimensional echocardiography

In the first part we explored the value of a novel clinical risk score to predict outcome after transcatheter aortic valve implantation and studied the potential role of non-invasive cardiac imaging in mitral valve disease, focusing on 3-dimensional echocardiography.

In Chapter 2 we present a clinical risk score, the *'$TAVI_2$-SCORe'*, that we developed to predict one year mortality after transcatheter aortic valve implantation

(TAVI), based on preprocedural clinical and echocardiographic characteristics of 511 patients that underwent this procedure. Porcelein *T*horacic aorta, *A*nemia, left *V*entricular dysfunction, recent myocardial *I*nfarction, male *S*ex, *C*ritical aortic valve stenosis, *O*ld age and *Re*nal dysfunction, were independently related to 1 year mortality after TAVI and comprised the constituents of the *'TAVI2-SCORe'*. Proportional to the hazard ratio, each constituent was assigned 1 point and 2 points for recent myocardial infarction. We indicated better discrimination and calibration performance of this novel risk score compared to conventional surgical risk scores to predict the endpoint. The *'$TAVI_2$-SCORe'* is an accurate, simple and bed-side available score that might assist to select those patients at high surgical risk that may ultimately benefit form TAVI treatment.

In Chapter 3 we provided an overview of contemporary non-invasive cardiac imaging techniques that can be applied to study mitral valve anatomy and function, in perspective to potential clinical applications. In particular we highlighted the role of 3-dimensional echocardiography for superior mitral valve morphological evaluation compared to 2-dimensional echocardiography, its potential for valve geometry assessment and its additive value to assess valve function comprising mitral stenosis or regurgitation. Multidetector row computed tomography offers mitral valve morphology and geometry evaluation with high spatial resolution in addition to providing anatomical imaging of the relationship of the valve with surrounding structures such as coronary sinus or circumflex artery. Such information may be critical when evaluating technical feasibility for indirect percutaneous annuloplasty techniques. The strength of cardiac magnetic resonance imaging in mitral valve disease involves being an accurate alternative for mitral regurgitation assessment, particularly in patients with poor acoustic window or contra-indication for transesophageal echocardiography.

Evidence is accumulating that mitral valve leaflets in patients with heart failure undergo active ultrastructural and structural remodeling, including larger leaflet area compared to normal controls. In Chapter 4 we showed, using advanced 3-dimensional echocardiography, that patients with functional mitral regurgitation indeed show larger leaflet area compared to normal subjects. More important, less leaflet remodeling was noted in patients with ≥ grade 3 versus < grade 3 functional mitral regurgitation, despite similar tethering degree. Lack of coaptation reserve (coaptation area ≤ 24% of the overall mitral valve leaflet area) was independently related to more severe mitral regurgitation. In addition we indicated that left ventricular function and sphericity as well as tenting volume and annulus dilatation are determinants of mitral leaflet remodeling. Such findings imply that the mitral valve leaflets are no innocent bystanders in functional mitral valve disease as larger leaflets for similar tethering degree might protect from significant mitral

regurgitation. Therefore the mitral leaflets in functional mitral valve disease might represent a biological or interventional therapeutic target.

In Chapter 5 we described the use of 3-dimensional transesophageal echocardiography (3D-TOE) for selecting and guiding in percutaneous mitral valve repair treatment using MitraClip. Evaluating technical feasibility for MitraClip therapy is a critical determinant of postprocedural success. 3D-TOE offers superior morphological characterization of the mitral valve and displays the presence and extent of morphological lesions. In addition it offers unique possibilities for evaluating coaptation length and depth in functional regurgitation as well as flail width and gap in organic disease. Furthermore, characterization of the origin and number of regurgitant jets as well as accurate quantification of regurgitation severity and leaflet area can be accomplished. During the percutaneous MitraClip procedure, 3D-TOE is indispensable for guiding transseptal puncture, steering of the guiding catheter in the left atrium, positioning and perpendicular alignment of the clip, mitral leaflet grasping and postprocedural evaluation, including regurgitation reduction and residual valve area. Finally, 3D-TOE provides a common and comprehensible communication platform between imagers, interventionalists and cardiac surgeons.

In Chapter 6 we aimed to assess the effect on mitral valve geometry in 42 patients that underwent percutaneous MitraClip therapy for functional mitral regurgitation. We showed that the mitral annulus becomes more elliptical with a tendency towards antero-posterior dimension reduction. Importantly, the coaptation area significantly increases after MitraClip by including mainly a larger part of the anterior mitral valve leaflet into the coaptation, bringing the coaptation point more anteriorly. These beneficial effects are noted, despite no increased leaflet stress as no change occurred in tenting volume or annular height to intercommissural width ratio. Therefore MitraClip therapy seems to affect mitral coaptation geometry similarly to surgical mitral annuloplasty, however, through a different mechanism. These geometric insights might fuel further design iterations and help understanding therapeutic efficacy and ultimately durability of percutaneous repair using MitraClip.

Part II: Echocardiographic deformation imaging

In the second part of this thesis we explored the role of risk stratification by ECG and myocardial deformation imaging (strain), as surrogate markers of fibrosis.

Chapter 7 comprises an evaluation of QRS fragmentation, a surrogate marker of fibrosis, and QTc duration on surface ECG in 195 primary hypertrophic cardiomyopathy patients without (in)complete bundle branch block. We showed that the presence of extensive QRS fragmentation in ≥ 3 territories (inferior, lateral,

septal and/or anterior) and/or QTc ≥ 460 ms independently related to malignant ventricular tachyarrhythmia and sudden cardiac death in these patients. Importantly, we indicated that both surface ECG markers provide incremental value on top of conventional sudden cardiac death risk factors to predict the combined endpoint, each yielding a positive predictive value of about 30%, which is higher than the usually reported 10 to 20% for conventional sudden death risk factors. These findings implicate that QRS fragmentation and QTc duration may serve as additional sudden death risk markers that might optimize selection of appropriate candidates for implantation of automated implantable cardioverter defibrillators (ICD).

In Chapter 8 we documented the potential role of imaging fibrosis in patients with severe left-sided valvular heart disease, focusing on aortic stenosis and mitral regurgitation. Focal and/or diffuse fibrosis formation is inherent to the natural disease course of severe valvular heart disease and relates to symptoms and dismal outcome. This renders imaging markers or surrogates of fibrosis a valuable potential tool to assist in risk stratification and decision making for the need and timing of valvular interventions. Delayed contrast-enhanced cardiac magnetic resonance imaging, T1 weighted cardiac magnetic resonance imaging, calibrated integrated backscatter echocardiography and several molecular nuclear imaging techniques provide direct fibrosis assessment. Indirect evaluation of ventricular fibrosis is offered by strain (rate) imaging using echocardiography or cardiac magnetic resonance as well as perfusable tissue fraction and index using positron emission tomography. Evidence for the use of imaging markers of fibrosis in left-sided valvular heart disease is rapidly accumulating as they hold great promise for early risk stratification in asymptomatic patients with severe left-sided valvular heart disease. Whether such an approach outperforms conventional risk factors in valvular heart disease and ultimately can improve outcome after valve intervention needs to be proven.

Volume overload in mitral regurgitation primarily affects the left atrium, making it an attractive potential subject for risk stratification. In Chapter 9 we explored the value of left atrial function assessment using 2-dimensional speckle tracking echocardiography in 121 patients with severe organic mitral regurgitation compared to 70 control subjects. We indicated that significant left atrial reservoir and contractile dysfunction was present in mitral regurgitation patients, particularly in those subjects with indication for mitral valve surgery based on current recommendations. Left atrial reservoir function (strain) independently predicted presence of surgical indication and proved to be more sensitive than left atrial diameter or volume. Left atrial strain ≤ 24% identified those patients with worse survival after mitral valve surgery, regardless the symptomatic status prior to

intervention. Impaired left atrial reservoir strain provided incremental value to predict mortality after surgery over current guidelines-based indications for mitral surgery. Therefore left atrial reservoir strain might be a valuable marker for follow-up and decision-making in patients with severe organic mitral regurgitation.

ICD device therapy improves outcome in selected primary hypertrophic cardiomyopathy patients, but accurate predictors of appropriate ICD therapy are poorly documented in this subgroup of patients. In Chapter 10, global longitudinal left ventricular strain (GLS) and left atrial volume index (LAVI) were evaluated in 92 primary hypertrophic cardiomyopathy patients that underwent ICD implantation. Both imaging markers related to appropriate ICD therapy, a combined endpoint of antitachycardia-pacing and/or shock for ventricular arrhythmia, independently of and incremental to conventional sudden cardiac death risk factors. Importantly, the combined presence of LAVI < 34 mL/m² and GLS < -14% adequately ruled out likelihood of appropriate ICD therapy, reflected by a 100% negative predictive value. Therefore both LAVI and GLS assessment on top of conventional sudden cardiac death risk factors might be helpful to optimize referral criteria and timing of ICD implantation in hypertrophic cardiomyopathy patients.

Hypertrophic cardiomyopathy patients with left atrial diameter ≥ 45 mm are considered to be at high risk for atrial fibrillation and are recommended to undergo at least 6-monthly arrhythmia surveillance using 24 hour Holter registration. In the final Chapter 11 of this thesis, we assessed left atrial diameter, volume and function (reservoir strain by 2-dimensional speckle tracking echocardiography) in relation to new onset atrial fibrillation in 243 primary hypertrophic cardiomyopathy patients. Although all 3 left atrial parameters were independent correlates of atrial fibrillation, 58% of atrial fibrillation events occurred despite left atrial diameter < 45 mm. In those patients, we showed high negative predictive values of 93% and 94% for left atrial volume < 36 mL/m² and strain > 23.4 %, respectively. In this group of patients, left atrial volume provided incremental predictive value over left atrial diameter, even further increased by left atrial strain. In primary hypertrophic cardiomyopathy patients with preserved left atrial diameter but increased left atrial volume (≥ 36 mL/m²) or impaired strain (≤ 23.4%), intensification of follow-up to detect subsequent atrial fibrillation might be warranted, in addition to current recommendations.

CONCLUSIONS AND FUTURE PERSPECTIVES

As risk is a continuum rather than a dichotomous event, risk stratification will not be perfect. Nevertheless risk stratification is key for optimal management of

patients with structural heart disease in daily clinical practice, including those with valvular heart disease or primary hypertrophic cardiomyopathy. Advanced echocardiographic techniques such as deformation imaging (strain) provide a very sensitive tool to assess early subclinical atrial or ventricular dysfunction, related to fibrosis, loading conditions, contractility and geometry in patients with valvular heart disease or primary hypertrophic cardiomyopathy, and offer a strong biological correlate to prognosis. In addition clinical markers, including surface ECG markers such as fragmented QRS, may yield prognostic clinical value. Whether early fibrosis imaging represents a hallmark for risk stratification needs to be proven, but ongoing research and scientific efforts in search for optimized risk stratification using advanced echocardiography and clinical surrogates will guarantee optimal outcome for patients with structural heart disease.

A clear tendency towards less invasive and more percutaneous therapies for valvular heart disease, including direct or indirect repair and valve replacement, is present and fueled by tremendous efforts of clinicians, scientists, engineers and medical industry. Non invasive cardiac imaging, including 3-dimensional echocardiography, offers unique pathophysiological insights as well as accurate anatomical, morphological and functional imaging of patients with valvular heart disease that aids in the optimal selection of candidates and procedural guiding of patients undergoing such percutaneous interventions. As we are just at the beginning of this intriguing era of percutaneous therapies for structural heart disease, it is crucial to confirm and further explore the indispensable role of 3-dimensional echocardiography and other imaging techniques for the management of these patients.

Samenvatting, conclusies en toekomstperspectieven

SAMENVATTING

In deze thesis bestudeerden we risico stratificatie en management van patiënten met structureel hartlijden, met focus op patiënten met hartklepaandoeningen en primaire hypertrofische cardiomyopathie. Meer bepaald werd de potentiële rol van geavanceerde echocardiografie, waaronder 3D-echocardiografie en deformatie beeldvorming (strain), evenals klinische surrogaat merkers, geëvalueerd. De introductie tot deze thesis vat de rationale en achtergrond van onze studie samen.

De globale belasting van hartklepaandoeningen zoals aortaklep stenose of mitralisklep lekkage is significant, wordt verwacht toe te nemen door vergrijzing van de Westerse populatie en impliceert een ongunstige prognose wanneer onbehandeld. Aangezien oudere patiënten zich vaak presenteren met verschillende co-morbiditeiten, is het primordiaal behandeling aan te bieden op maat van hun inherent hoog of prohibitief heelkundig risico. Dit kan tegenwoordig gerealiseerd worden door minder invasieve percutane klep vervanging of herstel technieken, zoals weergegeven in de introductie van deze thesis. Primaire hypertrofische cardiomyopathie secundair aan sarcomerische mutatie(s) treft ongeveer 1 op 500 mensen en is geassocieerd met plotse dood, hartfalen, arritmie en thromboembolische events. Hoewel het absolute plotse dood risico eerder beperkt is, is de impact substantieel aangezien dergelijke events de neiging hebben zich voor te doen bij jonge patiënten. Plotse dood bij jonge atleten tijdens sporten kan daarom vaak rekenen op belangrijke media aandacht en vormt steevast brandstof voor het maatschappelijk debat rond sport participatie screening. Risico stratificatie en adequate selectie van patiënten met structureel hartlijden zoals hartklep aandoeningen of primaire hypertrofische cardiomyopathie zijn dan ook kritisch om de nood, timing en het type therapeutische interventie te bepalen en gunstige uitkomsten te verzekeren. In deze thesis werkten we uit hoe klinische risico scores en hun surrogaten, zowel als geavanceerde echocardiografische technieken waaronder 3D-echocardiografie en deformatie beeldvorming (strain), ideale kandidaten kunnen zijn om dit doel te dienen bij patiënten met hartklep aandoeningen of primaire hypertrofische cardiomyopathie. Meer in het bijzonder werd de zoektocht naar technieken of klinische surrogaten die gerelateerd zijn aan de aanwezigheid van fibrose uitgelegd, een kritische determinant van de ziekte evolutie bij beide vormen van structureel hartlijden.

Deel I: 3-Dimensionele echocardiografie

In het eerste deel exploreerden we de waarde van een nieuwe klinische risico score om uitkomst te voorspellen na transcatheter aortaklep implantatie (TAVI) en

werd de potentiële rol van niet invasieve cardiale beeldvorming bij mitralisklep lijden bestudeerd, met focus op 3D-echocardiografie.

In Hoofdstuk 2 presenteren we een klinische risico score, de '*TAVI$_2$-SCORe*', die we ontwikkelden om 1-jaar overlijden na TAVI te voorspellen, gebaseerd op de pre-procedurale klinische en echocardiografische karakteristieken van 511 patiënten die deze interventie ondergingen. Porceleinen *T*horacale aorta, linker *V*entrikel dysfunctie, recent myocard *I*nfarct, mannelijk geslacht (*S*ex), *K*ritische aortaklep stenose, *A*nemie, *O*udere leeftijd en *Re*nale dysfunctie waren allen onafhankelijk gerelateerd aan 1-jaar overlijden na TAVI en omvatten de verschillende componenten van de '*TAVI$_2$-SCORe*'. Proportioneel aan de hazard ratio werd aan elke component 1 punt toegekend en 2 punten aan recent myocard infarct. We toonden aan dat deze nieuwe risico score beter presteerde betreffende discriminatie en calibratie dan conventionele heelkundige risico scores met betrekking tot het eindpunt. De '*TAVI$_2$-SCORe*' is een accurate, simpele en bed-side beschikbare score die zou kunnen assisteren om die patiënten te selecteren dewelke een hoog risico hebben voor heelkunde, maar uiteindelijk toch zouden kunnen baat hebben bij TAVI behandeling.

In Hoofdstuk 3 werd een overzicht geboden van hedendaagse niet invasieve cardiale beeldvormingstechnieken die aangewend kunnen worden om mitralisklep anatomie en functie te bestuderen en in perspectief geplaatst ten opzichte van potentiële klinische toepassingen. Meer bepaald stipten we de rol van 3D-echocardiografie aan met betrekking tot superieure morfologische evaluatie van de mitralisklep in vergelijking met 2D-echocardiografie, zijn potentiële waarde voor klep geometrie evaluatie en zijn toegevoegde waarde voor bepaling en kwantificatie van mitralisklep stenose en lekkage. Multidetector row computed tomography (MDCT) biedt eveneens de mogelijkheid tot geometrische en morfologische evaluatie van de mitralisklep met hoge spatiale resolutie, naast de gelegenheid om anatomische beeldvorming te verrichten van de relatie tussen de klep en zijn omliggende anatomische structuren zoals de coronaire sinus of de circumflex coronair arterie. Dit laatste kan van kritisch belang zijn bij het evalueren van de geschiktheid van patiënten voor het ondergaan van percutane annuloplastie technieken. De kracht van cardiale magnetische resonantie beeldvorming bij mitralisklep aandoeningen omvat een alternatief bieden voor bepaling van mitralisklep lekkage, voornamelijk bij patiënten met een beperkte echogeniciteit of contra-indicaties voor slokdarm echocardiografie.

Meer en meer evidentie stapelt zich op dat mitralisklepblaadjes in patiënten met hartfalen actieve structurele en ultra-structurele remodeling ondergaan, waaronder een groter klepblad oppervlakte vergeleken met controle patiënten. In Hoofdstuk 4 tonen we aan, gebruik makend van geavanceerde 3D-echocardio-

grafische evaluatie van mitralisklep geometrie, dat patiënten met functionele mitralisklep lekkage inderdaad een grotere klepblad oppervlakte hebben vergeleken met normale subjecten. Belangrijker nog, we stelden vast dat minder klepblad remodeling aanwezig was bij patiënten met ≥ graad 3 versus < graad 3 lekkage, ondanks eenzelfde graad van trekkrachten op de klepblaadjes (tethering). Dergelijk gebrek aan coaptatie reserve (coaptatie oppervlakte ≤ 24% van de totale klepblad oppervlakte) was onafhankelijk gerelateerd aan meer uitgesproken mitralisklep lekkage. Daarenboven toonden we aan dat linker ventrikel functie en sfericiteit naast tenting volume en annulus dilatatie determinanten zijn van mitralisklepblad remodeling. Deze bevindingen impliceren dat de mitralisklepblaadjes niet zomaar onschuldige 'bystanders' zijn bij functioneel mitraliskleplijden aangezien grotere klepblaadjes voor dezelfde graad van tethering protectief kunnen zijn ten aanzien van significante mitralisklep lekkage. Daarom is het niet uitgesloten dat de mitralisklepblaadjes in functioneel mitraliskleplijden een biologisch of interventioneel doel-op-zich zouden kunnen vormen.

In Hoodstuk 5 beschreven we het gebruik van 3D-slokdarm echocardiografie voor de selectie en het begeleiden van percutane mitralisklepherstel behandeling door middel van MitraClip. Het evalueren van de technische geschiktheid van een kandidaat voor MitraClip behandeling is een kritische determinant van post-procedureel succes. 3D-slokdarm echocardiografie biedt superieure morfologische karakterisatie van de mitralisklep en geeft adequaat de aanwezigheid en uitgebreidheid weer van morfologische laesies. Bovendien biedt het unieke mogelijkheden om de coaptatie lengte en diepte te bepalen bij functioneel mitraliskleplijden, alsook de opportuniteit om de breedte en de omvang van een flail klepbladsegment te bepalen bij organische klepziekte. Daarenboven kan de karakterisatie van de origine en het aantal lekkende jets bekomen worden, alsook accurate kwantificatie van de ernst van het kleplek en de klepblad oppervlakte. Tijdens de MitraClip procedure is 3D-slokdarm echocardiografie tevens onontbeerlijk voor begeleiding van de trans-septale punctie, sturing van de guiding-catheter in het linker atrium, positionering en loodrechte alignatie van de clip, grijpen van de klepblaadjes alsook de post-procedurele evaluatie, waaronder bepaling van de kleplek reductie en residuele klepoppervlakte. Tot slot biedt 3D-slokdarm echocardiografie een gemeenschappelijk en inzichtelijk communicatie platform tussen beeldvormers, interventie cardiologen en hartchirurgen.

In Hoofdstuk 6 streefden we ernaar om het effect op mitralisklep geometrie te evalueren bij 42 patiënten dewelke percutane MitraClip behandeling ondergingen voor functionele mitralisklep lekkage. We toonden aan dat de mitralis annulus meer elliptisch wordt met een trend tot reductie van de voor-achterwaartse diameter. Daarenboven was een belangrijke vaststelling dat de coaptatie oppervlakte

significant toenam na MitraClip, voornamelijk door inclusie van een groter deel van het voorste mitralisklepblad in de coaptatie, waardoor het coaptatie punt meer naar anterior komt te liggen. Deze gunstige veranderingen werden opgetekend ondanks afwezigheid van toename in klepblad stress, aangezien er geen wijziging was in tenting volume noch annulaire hoogte tot inter-commissurale breedte ratio. Daarom lijkt het zo dat MitraClip eenzelfde effect bekomt op mitralisklep coaptatie geometrie zoals bij heelkundige annuloplastie, zij het door een verschillend mechanisme. Deze geometrische inzichten kunnen brandstof vormen tot verdere design aanpassingen en helpen bij het begrip van therapeutische efficaciteit en uiteindelijk durabiliteit van percutaan herstel door middel van MitraClip.

Deel 2: Echocardiografische deformatie beeldvorming

In het tweede deel van deze thesis exploreerden we de rol van risico stratificatie door middel van ECG en myocardiale deformatie beeldvorming (strain), als surrogaat merkers van fibrose.

Hoofdstuk 7 omvat een evaluatie van QRS fragmentatie, een surrogaat fibrose merker, en QTc duur op oppervlakte ECG bij 195 primaire hypertrofische cardiomyopathie patiënten in afwezigheid van (on)volledig bundeltak blok. We toonden aan dat de aanwezigheid van uitgebreide QRS fragmentatie in ≥ 3 gebieden (inferior, lateraal, septaal en/of anterior) en/of een QTc duur van ≥ 460 ms onafhankelijk gerelateerd zijn aan maligne ventrikel tachy-aritmie en plotse cardiale dood bij deze patiënten. Belangrijker nog, we stelden vast dat beide oppervlakte ECG merkers meerwaarde bieden bovenop de conventionele plotse dood risicofactoren om het eindpunt te voorspellen. Beide merkers hebben een positieve predictieve waarde rond 30%, wat hoger is dan de meestal gerapporteerde 10 tot 20% voor conventionele plotse cardiale dood risico factoren. Deze bevindingen impliceren dat QRS fragmentatie en QTc duur additionele risico merkers zouden kunnen zijn dewelke de selectie van juiste kandidaten kan optimaliseren voor implantatie van een automatische defibrillator (ICD).

In Hoofdstuk 8 documenteerden we de potentiële rol van fibrose beeldvorming bij patiënten met ernstig linkszijdig kleplijden, met focus op aortaklep stenose en mitralisklep lekkage. Zowel focale als diffuse fibrose zijn inherent aan het natuurlijk verloop van ernstig kleplijden en zijn gerelateerd aan symptomen en ongunstige prognose. Daarom zijn fibrose beeldvorming merkers of surrogaten een waardevolle potentiële tool om te helpen bij risico stratificatie en besluitvorming betreffende de nood en timing van klepinterventies. Laattijdige contrast-versterkte cardiale magnetische resonantie, T1-gewogen cardiale magnetische resonantie, gecalibreerde geïntegreerde backscatter echocardiografie en verscheidene moleculaire nucleaire beeldvormingstechnieken maken directe bepaling van fibrose

mogelijk. Indirecte evaluatie van fibrose is op zijn beurt mogelijk door strain (rate) beeldvorming op basis van echocardiografie of cardiale magnetische resonantie, alsook door perfundeerbare weefsel fractie en index gebruik makende van positron emissie tomografie. Evidentie voor het gebruik van fibrose merkers bij linkszijdig kleplijden accumuleert snel, aangezien zij veelbelovend zijn betreffende de mogelijkheid tot vroegtijdige risico stratificatie in asymptomatische patiënten met ernstig linkszijdig kleplijden. Of een dergelijke aanpak daadwerkelijk conventionele risico factoren in kleplijden kan overtroeven en uiteindelijk zo de uitkomst kan helpen verbeteren na klep interventie dient nog te worden bewezen.

Volume overbelasting bij patiënten met mitralisklep lekkage treft in de eerste plaats het linker atrium dat daarom een attractieve potentiële kandidaat is voor risico stratificatie. In Hoofdstuk 9 verkenden we de waarde van linker atriale functie evaluatie op basis van 2D speckle-tracking echocardiografie in een groep van 121 patiënten met ernstige organische mitralisklep lekkage, vergeleken met 70 controle patiënten. We toonden aan dat significante linker atriale reservoir en contractiele dysfunctie aanwezig is in patiënten met mitralisklep lekkage, voornamelijk in patiënten die een indicatie vormen voor mitralisklep heelkunde, gebaseerd op de huidige richtlijnen. Linker atriale reservoir functie (strain) was niet alleen een onafhankelijke predictor van de aanwezigheid van een heelkundige indicatie, maar bleek eveneens sensitiever dan linker atriale diameter of volume. Linker atriale dysfunctie op basis van een strain waarde ≤24 % identificeerde patiënten met gedaalde overleving na mitralisklep heelkunde en dit, belangrijk, onafhankelijk van de symptomatische status voor de interventie. Verminderde linker atriale reservoir strain bood incrementele waarde om postoperatieve mortaliteit te voorspellen bovenop de huidige richtlijn-aanbevelingen voor mitralisklep heelkunde. Daarom zou linker atriale reservoir strain een waardevolle merker kunnen zijn voor follow-up en beslissingsvorming bij patiënten met ernstige organische mitralisklep lekkage.

ICD device therapie verbetert de uitkomst van geselecteerde patiënten met primaire hypertrofische cardiomyopathie. Desondanks bestaat er actueel slechts beperkte documentatie omtrent adequate predictoren van terechte ICD therapie in deze patiënten subgroep. In Hoofdstuk 10 werden globale longitudinale strain (GLS) en linker atriale volume geïndexeerd voor lichaamsoppervlakte (LAVI) bestudeerd in 92 primaire hypertrofische cardiomyopathie patiënten dewelke ICD implantatie ondergingen. Beide beeldvorming merkers waren gerelateerd aan terechte ICD therapie, gedefinieerd als een gecombineerd eindpunt bestaande uit anti-tachycardie pacing en/of shock voor ventriculaire aritmie, en dit onafhankelijk en incrementeel ten opzichte van conventionele risicofactoren voor plotse dood. Belangrijk, de gecombineerde aanwezigheid van LAVI < 34 ml/m² en GLS < -14 %

sloten adequaat de waarschijnlijkheid voor terechte ICD therapie uit, weerspiegeld door de 100% negatieve predictieve waarde. Aldus zouden beiden LAVI en GLS evaluatie, bovenop evaluatie van de conventionele risicofactoren voor plotse dood, een hulp kunnen bieden ter optimalisatie van criteria voor verwijzing alsook timing van ICD implantatie bij patiënten met primaire hypertrofische cardiomyopathie.

Primaire hypertrofische cardiomyopathie patiënten met een linker atriale diameter ≥ 45 mm worden als hoog risico patiënten beschouwd voor boezemfibrillatie. Dergelijke patiënten dienen daarom, op basis van de huidige richtlijnaanbevelingen, 6-maandelijks 24 uur Holter ritme registratie te ondergaan. In het laatste Hoofdstuk 11 van dit proefschrift evalueerden we linker atriale diameter, volume en functie (reservoir strain op basis van speckle-tracking echocardiografie) in relatie tot de novo boezemfibrillatie in 243 patiënten met primaire hypertrofische cardiomyopathie. Hoewel alle 3 atriale parameters onafhankelijk gerelateerd waren met boezemfibrilleren, noteerden we 58% van de boezemfibrillatie events bij patiënten ondanks een linker atrium diameter < 45 mm. In die patiënten subgroep toonden we aan dat een linker atrium volume (geïndexeerd voor lichaamsoppervlakte) < 36 ml/m² een negatieve predictieve waarde had voor het eindpunt van 93%, en gelijkaardig 94% voor een linker atriale strain waarde > 23.4 %. In deze groep bood linker atriale volume incrementele predictieve waarde voor de novo boezemfibrilleren bovenop linker atriale diameter. Toevoegen van linker atriale strain evaluatie verbeterde het predictief model verder significant. Bij patiënten met primaire hypertrofische cardiomyopathie en relatief bewaarde atriale diameter (< 45 mm), lijkt het dus aangewezen dat wanneer er een vergroot linker atriaal volume aanwezig is ≥ 36 ml/m² of een gedaalde linker atriale strain functie ≤ 23.4 %, intensificatie van follow-up ter detectie van boezemfibrillatie wordt aangeraden, aanvullend op de huidige aanbevelingen.

CONCLUSIES EN TOEKOMSTPERSPECTIEVEN

Aangezien risico een continuüm is eerder dan een dichotome gebeurtenis, zal beslissingsvorming op basis van risico stratificatie nooit perfect zijn. Desalniettemin speelt risico stratificatie een sleutelrol bij optimaal management van patiënten met structureel hartlijden in de dagelijks praktijk, inclusief patiënten met kleplijden of primaire hypertrofische cardiomyopathie. Geavanceerde echocardiografische technieken zoals deformatie beeldvorming (strain) bieden bij dergelijke patiënten een ongeziene mogelijkheid om vroegtijdige atriale of ventriculaire dysfunctie op te sporen, gerelateerd aan fibrose, lading condities, contractiliteit en geometrie,

dewelke biologisch sterk gerelateerd is aan de prognose. Bovendien kunnen klinische merkers zoals gefragmenteerde QRS complexen op een oppervlakte ECG voor eenzelfde doel worden gebruikt. Of vroegtijdige fibrose beeldvorming daadwerkelijk de heilige graal van risico stratificatie vertegenwoordigt, dient nog te worden bewezen. Wel staat het reeds vast dat doorgedreven onderzoek en wetenschappelijke inspanningen op zoek naar optimalisatie van risico stratificatie en dus therapeutische besluitvorming op basis van geavanceerde echocardiografie en klinische merkers mede een garantie zullen bieden om de uitkomst te verbeteren van patiënten met structureel hartlijden.

Een duidelijk trend tot minder invasieve en meer percutane therapieën ter behandeling van hartklep aandoeningen heeft zich afgetekend, waaronder direct of indirect klepherstel en klep vervanging. Deze evolutie wordt verder gevoed vanuit enorme inspanningen door clinici, wetenschappers, ingenieurs en de medische industrie. Niet invasieve cardiale beeldvorming, waaronder 3D-echocardiografie, vormt een uniek platform om fysio-pathologische inzichten te verwerven, alsook accurate anatomische, morfologische en functionele beeldvorming te verrichten bij patiënten met hartklep aandoeningen. Hierdoor kan optimale patiënten selectie en procedurele begeleiding verzorgd worden van patiënten die een dergelijke percutane interventie ondergaan. Aangezien we nog maar aan de wieg staan van dit intrigerend tijdperk van percutane therapieën voor structureel hartlijden, is het cruciaal om de onmisbare rol van 3D-echocardiografie en overige beeldvormingstechnieken te bevestigen en verder te exploreren bij het management van deze patiënten.

List of publications

LIST OF PUBLICATIONS

1. **Debonnaire P**, Van Rillaer O, Arts J, Ramboer K, Tubbax H, Van Hootegem P. Primary aorto enteric fistula: report of 18 Belgian cases and literature review. *Acta Gastroenterol Belg.* 2008 Apr-Jun;71(2):250-258.
2. Van Rillaer O, **Debonnaire P**, Ramboer K. Primary iliac arterioenteric fistula. *JBR-BTR.* 2009 May-Jun;92(3):176-177.
3. **Debonnaire P**, Coussement P, Schepens M. A vascular tangle on coronary angiography. *Acta Cardiol.* 2010 Aug;65(4):481-482.
4. **Debonnaire P**, De Backer O, De Geeter F, Delanote J, Vandekerckhove Y, Muyldermans L. Multimodality imaging of cardiac involvement in neurofibromatosis. *J Am Coll Cardiol.* 2011 Apr 26;57(17):e209.
5. **Debonnaire P**, Onsea K, Desmet W. Straddling thrombus through a patent foramen ovale secondary to saddle embolism. *Acta Clin Belg.* 2011 May-Jun;66(3):243.
6. De Backer O, **Debonnaire P**, Muyldermans L, Missault L. Tako-tsubo cardiomyopathy with left ventricular outflow tract (LVOT) obstruction: case report and review of the literature. *Acta Clin Belg.* 2011 Jul-Aug;66(4):298-301.
7. **Debonnaire P**, Bammens B, Blockmans D, Herregods MC, Dubois C, Voigt JU. Multimodality imaging of giant coronary artery aneurysms in immunoglobulin G4-related sclerosing disease. *J Am Coll Cardiol.* 2012 Apr 3;59(14):e27.
8. **Debonnaire P**, Palmen M, Marsan NA, Delgado V. Contemporary imaging of normal mitral valve anatomy and function. *Curr Opin Cardiol.* 2012 Sep;27(5):455-464.
9. Witkowski TG, Thomas JD, **Debonnaire P**, Delgado V, Hoke U, Ewe SH, Versteegh MI, Holman ER, Schalij MJ, Bax JJ, Klautz RJ, Marsan NA. Global longitudinal strain predicts left ventricular dysfunction after mitral valve repair. *Eur Heart J Cardiovasc Imaging.* 2013 Jan;14(1):69-76.
10. **Debonnaire P**, Katsanos S, Delgado V. Computed tomography to improve TAVI outcomes. *EuroIntervention.* 2012 Sep;8(5):531-533.
11. **Debonnaire P**, De Backer O, Orlent H, Vandevelde K. One for the road... *Eur Heart J.* 2013 Aug;34(32):2500.
12. **Debonnaire P**, Van Herck PL, Katsanos S, van der Kley F, de Weger A, Palmen M, Marsan NA, Schalij MJ, Delgado V. How should I treat acute aortic annulus rupture during transcatheter aortic valve implantation? *EuroIntervention.* 2013 Jan 22;8(9):1103-1109.
13. Al Amri I, **Debonnaire P**, Witkowski T, van der Kley F, Palmen M, de Weger A, Klautz RJ, Bax JJ, Schalij MJ, Ajmone Marsan N, Delgado V. Mitral valve geometry and hemodynamics after surgical mitral valve annuloplasty and implications for percutaneous treatment of patients with recurrent mitral regurgitation. *Am J Cardiol.* 2013 Sep 1;112(5):714-719.
14. **Debonnaire P**, Leong DP, Witkowski TG, Al Amri I, Joyce E, Katsanos S, Schalij MJ, Bax JJ, Delgado V, Marsan NA. Left atrial function by two-dimensional speckle-tracking echocardiography in patients with severe organic mitral regurgitation: association with guidelines-based surgical indication and postoperative (long-term) survival. *J Am Soc Echocardiogr.* 2013 Sep;26(9):1053-1062.
15. Katsanos S, Ewe SH, **Debonnaire P**, van der Kley F, de Weger A, Palmen M, Scholte AJ, Schalij MJ, Bax JJ, Marsan NA, Delgado V. Multidetector row computed tomography parameters associated with paravalvular regurgitation after transcatheter aortic valve implantation. *Am J Cardiol.* 2013 Dec 1;112(11):1800-1806.

16. Hoogslag GE, Thijssen J, Höke U, Boden H, Antoni ML, **Debonnaire P**, Haeck ML, Holman ER, Bax JJ, Ajmone Marsan N, Schalij MJ, Delgado V. Prognostic implications of left ventricular regional function heterogeneity assessed with two-dimensional speckle tracking in patients with ST-segment elevation myocardial infarction and depressed left ventricular ejection fraction. *Heart Vessels.* 2014 Sep;29(5):619-628.
17. Nazeri I, Abdi S, Mandegar MH, Naemi S, Roshanali F, Tehrai M, Shahabi P, **Debonnaire P**, van der Kley F, Katsanos S, Delgado V, Van Mieghem NM. How should I treat acute left main coronary obstruction after transapical aortic valve implantation? *EuroIntervention.* 2013 Oct;9(6):761-764.
18. Joyce E, Hoogslag GE, Leong DP, **Debonnaire P**, Katsanos S, Boden H, Schalij MJ, Marsan NA, Bax JJ, Delgado V. Association between left ventricular global longitudinal strain and adverse left ventricular dilatation after ST-segment-elevation myocardial infarction. *Circ Cardiovasc Imaging.* 2014 Jan;7(1):74-81.
19. Joyce E, Leong DP, Hoogslag GE, van Herck PL, **Debonnaire P**, Abate E, Holman ER, Schalij MJ, Bax JJ, Delgado V, Marsan NA. Left ventricular twist during dobutamine stress echocardiography after acute myocardial infarction: association with reverse remodeling. *Int J Cardiovasc Imaging.* 2014 Feb;30(2):313-322.
20. **Debonnaire P**, Thijssen J, Leong DP, Joyce E, Katsanos S, Hoogslag GE, Schalij MJ, Atsma DE, Bax JJ, Delgado V, Marsan NA. Global longitudinal strain and left atrial volume index improve prediction of appropriate implantable cardioverter defibrillator therapy in hypertrophic cardiomyopathy patients. *Int J Cardiovasc Imaging.* 2014 Mar;30(3):549-558.
21. Kamperidis V, Joyce E, **Debonnaire P**, Katsanos S, van Rosendael PJ, van der Kley F, Sianos G, Bax JJ, Ajmone Marsan N, Delgado V. Left ventricular functional recovery and remodeling in low-flow low-gradient severe aortic stenosis after transcatheter aortic valve implantation. *J Am Soc Echocardiogr.* 2014 Aug;27(8):817-825.
22. **Debonnaire P**, Delgado V, Bax JJ. Potential role of fibrosis imaging in severe valvular heart disease. *Heart.* 2015 Mar;101(5):397-407.
23. Cottens D, Corteville B, Vanvinckenroye A, Schepens M, Missault L, **Debonnaire P**. Moderate gradient with disproportional dyspnoea: multimodality imaging of funnel-shaped subaortic membrane. *Eur Heart J.* 2015 Mar 7;36(10):583.
24. Katsanos S, van Rosendael P, Kamperidis V, van der Kley F, Joyce E, **Debonnaire P**, Karalis I, Bax JJ, Marsan NA, Delgado V. Insights into new-onset rhythm conduction disorders detected by multi-detector row computed tomography after transcatheter aortic valve implantation. *Am J Cardiol.* 2014 Nov 15;114(10):1556-1561.
25. De Backer O, **Debonnaire P**, Gevaert S, Missault L, Gheeraert P, Muyldermans L. Prevalence, associated factors and management implications of left ventricular outflow tract obstruction in takotsubo cardiomyopathy: a two-year, two-center experience. *BMC Cardiovasc Disord.* 2014 Oct 22;14:147.
26. Katsanos S, **Debonnaire P**, van der Kley F, van Rosendael PJ, Joyce E, de Graaf MA, Schalij MJ, Scholte AJ, Bax JJ, Ajmone Marsan N, Delgado V. Position of Edwards SAPIEN transcatheter valve in the aortic root in relation with the coronary ostia: implications for percutaneous coronary interventions. *Catheter Cardiovasc Interv.* 2015 Feb 15;85(3):480-487.
27. **Debonnaire P**, Al Amri I, Leong DP, Joyce E, Katsanos S, Kamperidis V, Schalij MJ, Bax JJ, Marsan NA, Delgado V. Leaflet remodelling in functional mitral valve regurgitation: characteristics, determinants, and relation to regurgitation severity. *Eur Heart J Cardiovasc Imaging.* 2015 Mar;16(3):290-299.

28. **Debonnaire P**, Delgado V, Bax JJ, Marsan NA. Tools & Techniques - Clinical: 3D transoesophageal echocardiography for selecting and guiding in percutaneous mitral valve repair using MitraClip. *EuroIntervention*. 2014 Nov;10(7):884-886.
29. Joyce E, Ninaber MK, Katsanos S, **Debonnaire P**, Kamperidis V, Bax JJ, Taube C, Delgado V, Ajmone Marsan N. Subclinical left ventricular dysfunction by echocardiographic speckle-tracking strain analysis relates to outcome in sarcoidosis. *Eur J Heart Fail*. 2015 Jan;17(1):51-62.
30. **Debonnaire P**, Fusini L, Wolterbeek R, Kamperidis V, van Rosendael P, van der Kley F, Katsanos S, Joyce E, Tamborini G, Muratori M, Gripari P, Bax JJ, Marsan NA, Pepi M, Delgado V. Value of the "TAVI2-SCORe" versus surgical risk scores for prediction of one year mortality in 511 patients who underwent transcatheter aortic valve implantation. *Am J Cardiol*. 2015 Jan 15;115(2):234-242.
31. Kamperidis V, van Rosendael PJ, Ng AC, Katsanos S, van der Kley F, **Debonnaire P**, Joyce E, Sianos G, Marsan NA, Bax JJ, Delgado V. Impact of flow and left ventricular strain on outcome of patients with preserved left ventricular ejection fraction and low gradient severe aortic stenosis undergoing aortic valve replacement. *Am J Cardiol*. 2014 Dec 15;114(12):1875-1881.
32. **Debonnaire P**, Katsanos S, Joyce E, van den Brink OV, Atsma DE, Schalij MJ, Bax JJ, Delgado V, Marsan NA. QRS Fragmentation and QTc Duration Relate to Malignant Ventricular Tachyarrhythmias and Sudden Cardiac Death in Patients with Hypertrophic Cardiomyopathy. *J Cardiovasc Electrophysiol*. 2015 May;26(5):547-555.
33. van Rosendael PJ, Joyce E, Katsanos S, **Debonnaire P**, Kamperidis V, van der Kley F, Schalij MJ, Bax JJ, Ajmone Marsan N, Delgado V. Tricuspid valve remodelling in functional tricuspid regurgitation: multidetector row computed tomography insights. *Eur Heart J Cardiovasc Imaging*. 2015 Jun. *E-Pub ahead of print.*
34. Joyce E, **Debonnaire P**, Leong DP, Abate E, Katsanos S, Bax JJ, Delgado V, Ajmone Marsan N. Differential response of LV sublayer twist during dobutamine stress echocardiography as a novel marker of contractile reserve after acute myocardial infarction: relationship with follow-up LVEF improvement. *Eur Heart J Cardiovasc Imaging*. 2015 Jul. *E-Pub ahead of print.*
35. Joyce E, Hoogslag GE, Al Amri I, **Debonnaire P**, Katsanos S, Bax JJ, Delgado V, Marsan NA. Quantitative Dobutamine Stress Echocardiography Using Speckle-Tracking Analysis versus Conventional Visual Analysis for Detection of Significant Coronary Artery Disease after ST-Segment Elevation MyocardialInfarction. *J Am Soc Echocardiogr*. 2015 Aug. *E-Pub ahead of print.*
36. Al Amri I, **Debonnaire P**, van der Kley F, Schalij MJ, Bax JJ, Marsan NA, Delgado V. Acute effect of MitraClip implantation on mitral valve geometry in patients with functional mitral regurgitation: insights from three-dimensional transoesophageal echocardiography. *EuroIntervention*. 2015 Sep. *E-Pub ahead of print.*
37. Gheorghiade M, Greene SJ, Butler J, Filippatos G, Lam CS, Maggioni AP, Ponikowski P, Shah SJ, Solomon SD, Kraigher-Krainer E, Samano ET, Müller K, Roessig L, Pieske B; SOCRATES-REDUCED Investigators and Coordinators. Collaborators: ..., **Debonnaire P**, et al. Effect of Vericiguat, a Soluble Guanylate Cyclase Stimulator, on Natriuretic Peptide Levels in Patients With Worsening Chronic Heart Failure and Reduced Ejection Fraction: The SOCRATES-REDUCED Randomized Trial. *JAMA*. 2015 Dec;314(21):2251-2262.

38. Haeck MLA, Hoogslag GE, Boden H, Velders MA, Katsanos S, al Amri I, **Debonnaire P**, Schalij MJ, Bax JJ, Ajmone Marsan N, Delgado V. Prognostic implications of elevated pulmonary artery pressure after ST-segment elevation myocardial infarction. *Submitted.*

39. Joyce E, Kamperidis V, Ninaber MK, Katsanos S, **Debonnaire P**, Schalij MJ, Taube C, Bax JJ, Delgado V, Ajmone Marsan N. Diagnosis of Early Right Ventricular Dysfunction in Sarcoidosis: Prevalence, Correlates and Association with Clinical Outcome. *Submitted.*

40. Joyce E, Hoogslag GE, Kamperidis V, **Debonnaire P**, Katsanos S, Ajmone Marsan N, Bax JJ, Delgado V. Relationship between Myocardial Function, Body Mass Index and Outcome after ST-segment Elevation Myocardial Infarction: Insights into the Obesity Paradox from Longitudinal Strain. *Submitted.*

41. Joyce E, Katsanos S, Kamperidis V, Ninaber MK, **Debonnaire P**, Schalij MJ, Taube C, Bax JJ, Delgado V, Ajmone Marsan N. Left Ventricular Function in Sarcoidosis as assessed by Speckle Tracking Strain Echocardiography: Relationship to Disease Severity and Evolution over Time. *Submitted.*

42. Abate E, Hoogslag GE, Al Amri I, **Debonnaire P**, Wolterbeek R, Bax JJ, Delgado V, Ajmone Marsan N. Time Course, Predictors and Prognostic Implications of Significant Mitral Regurgitation After ST-Segment Elevation Myocardial Infarction. *Submitted.*

43. Katsanos S, van Rosendael P, **Debonnaire P**, Kamperidis V, van der Kley F, Joyce E, Karalis I, Palmen M, Bax JJ, Ajmone Marsan N, Delgado V. Quantitative analysis of changes in mitral regurgitation after transcatheter aortic valve implantation. *Submitted.*

44. Katsanos S, van Rosendael P, van den Brink O, **Debonnaire P**, Joyce E, van der Kley F, Ajmone Marsan N, Bax JJ, Delgado V. Fate of transcatheter valve-in-valve implantation and redo cardiac surgery for failing bioprosthetic valves in patients with high operative risk. *Submitted.*

45. **Debonnaire P**, Joyce E, Atsma DE, Schalij MJ, Bax JJ, Delgado V, Ajmone Marsan N. Left atrial size and function in hypertrophic cardiomyopathy patients and risk of new onset atrial fibrillation. *Submitted.*

46. Van De Heyning CM, Bertrand PB, **Debonnaire P**, De Maeyer C, Vandervoort PM, Coussement P, Paelinck BP, De Bock D, Vrints CJ, Claeys MJ. Mechanism of symptomatic improvement after MitraClip therapy for secondary mitral regurgitation: the role of improved resting and exercise hemodynamics. *Submitted.*

Curriculum vitae

CURRICULUM VITAE

Philippe Debonnaire was born on October 2nd 1980 in Turnhout (Belgium). He graduated from Sint-Jozefcollege high school in 1998 and subsequently studied Medicine at the Catholic University of Leuven in Belgium. In 2005 he obtained his Medical Degree, magna cum laude. After a period of 6 years training in internal medicine and cardiology at the University Hospital of Leuven, he became cardiologist in 2011. During that period he obtained an additional degree in Sports Medicine, magna cum laude, at the Catholic University of Leuven.

In 2011 he moved with his family to Leiden where he completed a 2-year research fellowship in advanced non invasive cardiac imaging (3D and deformation echocardiography, computed tomography, magnetic resonance imaging) for structural heart disease at the Leiden University Medical Center (LUMC) in Leiden, the Netherlands, promoted by Prof. dr. Jeroen J. Bax and co-promoted by dr. Victoria Delgado and dr. Nina Ajmone Marsan. His research was supported by a Research Grant of the European Association of Cardiovascular Imaging (EACVI), obtained in 2013. He received EACVI accreditation for echocardiography in 2012 and won the Meda Pharma best abstract presentation award at the Belgian Heart Rhythm Association congress in 2013.

In October 2013 he joined the cardiology faculty of Sint-Jan Hospital in Bruges, Belgium, where he is working as staff cardiologist since. His main field of interest lies in advanced echocardiographic imaging (3-dimensional, deformation, stress) in patients with valvular heart disease, various cardiomyopathies and structural heart interventions. Philippe Debonnaire is faculty member of Crossroads (Abott Vascular), an educational network to train centers for Mitra-Clip therapy, imaging proctor for MitraClip therapy (Abbott Vascular), board member of the Belgian Working Group of Non Invasive Cardiac Imaging (BWGNICI) and was awarded Scientific Fellow of the European Society of Cardiology (FESC) in 2015.

Acknowledgements

ACKNOWLEDGEMENTS

At first, I would like to express my sincere gratitude to Prof. Jeroen J. Bax, my promotor, and Dr. Victoria Delgado and Dr. Nina Ajmone Marsan, my co-promotors. I have lived a unique journey by performing a 2-year doctoral research fellowship, indebted to the art of motivation, guidance and perseverance to obtain preset scientific and personal goals, which they perfectly master. In addition I thank the European Association of Cardiovascular Imaging for awarding me a Scientific Research Grant.

Second, to the *'over-seas'* co-fellows I worked with and that became unique friends for life: Darryl, Dominique, Ewe, Tomasz, Robert, Emer, Spiros, Vasilis and Olivier. Many characters, different personalities, endless humour and tons of intelligence that were a daily inspiration during the good and the bad times and that made the whole experience an enrichment to life, transcending the scientific merits.

Third, I will not forget the support and many laughters we had with the structural heart intervention team including Prof. Martin J. Schalij and Frank van der Kley in particular. I am also grateful for the support of the *'Dutch-students'*: Georgette, Ibtihal, Philippe, Ülas and all the others. In addition I thank the the secretary team, study-nurses and the echocardiographers who made may stay most enjoyable and memorable.

Lastly, my deepest gratitude and love goes to my family. To my lovely wife, Charlotte, who has made immense sacrifice during many years for me to pursue my ambitions and never failed on supporting, encouraging and believing in me. To my wonderful kids Ralph, Anaïs and James that are a constant joy to life and had to miss me on many occasions. To my parents and parents-in-law, brothers and sisters (in-law), Knokke-Marraine, who have always expressed their sincere interest in my work and for being the most important in life: family. This thesis is dedicated to them.